Fall 2010

Intelligent power system operation in an uncertain environment

Yusuf Yare

Department: Electrical and Computer Engineering

INTELLIGENT POWER SYSTEM OPERATION

IN AN UNCERTAIN ENVIRONMENT

by

YUSUF YARE

A DISSERTATION

Presented to the Faculty of the Graduate School of the

MISSOURI UNIVERSITY OF SCIENCE AND TECHNOLOGY

In Partial Fulfillment of the Requirements for the Degree

DOCTOR OF PHILOSOPHY

in

ELECTRICAL ENGINEERING

2010

Approved by:

Ganesh Kumar Venayagamoorthy, Advisor
Keith A. Corzine
Cihan H. Dagli
Jagannathan Sarangapani
Donald C. Wunsch II

PUBLICATION DISSERTATION OPTION

This dissertation has been prepared in the style utilized by the following journals:

PAPER I

IET Journal on Generation, Transmission & Distribution (http://www.ietdl.org/IET-GTD). Pages 31-58 are published in that journal.

PAPER II

Elsevier Journal on Engineering Application of Artificial Intelligence (http://www.elsevier.com/locate/engappai). Pages 59-100 are published in that journal.

PAPER II

Elsevier Journal on Engineering Application of Artificial Intelligence (http://www.elsevier.com/locate/engappai). Pages 101-132 are revised submission/in review process for publication in that journal.

PAPER IV

IET Journal on Generation, Transmission & Distribution (http://www.ietdl.org/IET-GTD). Pages 133-160 are in review process for publication in that journal.

PAPER V

IEEE Transactions on Smart Grid (http://www.ieee-pes.org/publications/transactions). Pages 161-194 are revised submission/in review process for publication in that journal.

PAPER VI

IEEE Transactions on Power Systems (http://www.ieee-pes.org/publications/transactions). Pages 195-235 are in review process for publication in that journal.

ABSTRACT

This dissertation presents some challenging problems in power system operations. The efficacy of a heuristic method, namely, modified discrete particle swarm optimization (MDPSO) algorithm is illustrated and compared with other methods by solving the reliability based generator maintenance scheduling (GMS) optimization problem of a practical hydrothermal power system. The concept of multiple swarms is incorporated into the MDPSO algorithm to form a robust multiple swarms-modified particle swarm optimization (MS-MDPSO) algorithm and applied to solving the GMS problem on two power systems. Heuristic methods are proposed to circumvent the problems of imposed non-smooth assumptions common with the classical approaches in solving the challenging dynamic economic dispatch problem. The multi-objective combined economic and emission dispatch (MO-CEED) optimization problem for a wind-hydrothermal power system is formulated and solved in this dissertation. This MO-CEED problem formulation becomes a challenging problem because of the presence of uncertainty in wind power. A family of distributed optimal Pareto fronts for the MO-CEED problem has been generated for different scenarios of capacity credit of wind power. A real-time (RT) network stability index is formulated for determining a power system's ability to continue to provide service (electric energy) in a RT manner in case of an unforeseen catastrophic contingency. Cascading stages of fuzzy inference system is applied to combine non real-time (NRT) and RT power system assessments. NRT analysis involves eigenvalue and transient energy analysis. RT analysis involves angle, voltage and frequency stability indices. RT Network status index is implemented in real-time on a practical power system.

ACKNOWLEDGMENTS

I would like to express my profound thanks to my advisor, Dr. Ganesh Kumar Venayagamoorthy, for guiding me through my PhD studies. I particularly want to express my gratitude to him for his motivation and dedicated supervision towards the completion of this dissertation. I would like to thank my committee members, Dr. Keith A. Corzine, Dr. Cihan H. Dagli, Dr. Jagannathan Sarangapani and Dr. Donald C. Wunsch II, for their interest and willingness to help me during the period of my PhD studies and dissertation work.

I would like to gratefully acknowledge the financial support given to me during my PhD studies by the National Science Foundation (NSF), USA. I would also like to thank Prof. U. O. Aliyu from Abubakar Tafawa Balewa University, Bauchi, Nigeria for providing some relevant data for the studies carried out.

My wife, Stella E. C. Yare, and children, John S. Yare and Anita R. Yare, provided immense loving support, sacrifice and understanding during my PhD studies. They stood by me with endless patience and strength during my PhD years. I am grateful to my mother, Saratu Yare, for her prayers and encouragement throughout my PhD days.

This work is dedicated to God, from whom I draw strength and inspiration to face each day.

TABLE OF CONTENTS

Page

LIST OF ILLUSTRATIONS

LIST OF TABLES

PAPER III

PAPER IV

PAPER V

PAPER VI

SECTION
1. INTRODUCTION

1.1. OVERVIEW

An overview of issues addressed in this dissertation leading towards obtaining a secured power system operation is shown in Fig. 1.1. The benefits resulting from addressing these issues for a modern power system (consisting of thermal, hydro and wind generation sources) include:

- Secured maintenance schedules and generation dispatch.
- Feasible maintenance schedules and dispatch for practical implementation.
- Increased power system efficiency and reliability.
- Optimal power system operation.
- Efficient dynamic optimization.
- Better power quality and reduction in transmission line losses.
- Saving in fuel cost needed for power system operation.
- Emission reduction.

1.2. POWER SYSTEM MAINTENANCE

The purpose of maintenance is to extend equipment lifetime, or at least the mean time to the next failure whose repair may be costly. It is expected that effective maintenance policies can reduce the frequency of service interruptions and the many undesirable consequences of such interruptions. Maintenance clearly affects components and system reliability: if too little is done, this may result in an excessive number of costly failures and poor system performance, and hence reliability is degraded, when done too often, reliability may improve but the cost of maintenance will sharply increase. In a cost-effective scheme, the two expenditures must be balanced. Maintenance is just one of the tools for ensuring satisfactory component and system reliability, others include system capacity, reinforcing redundancy and employing more reliable components.

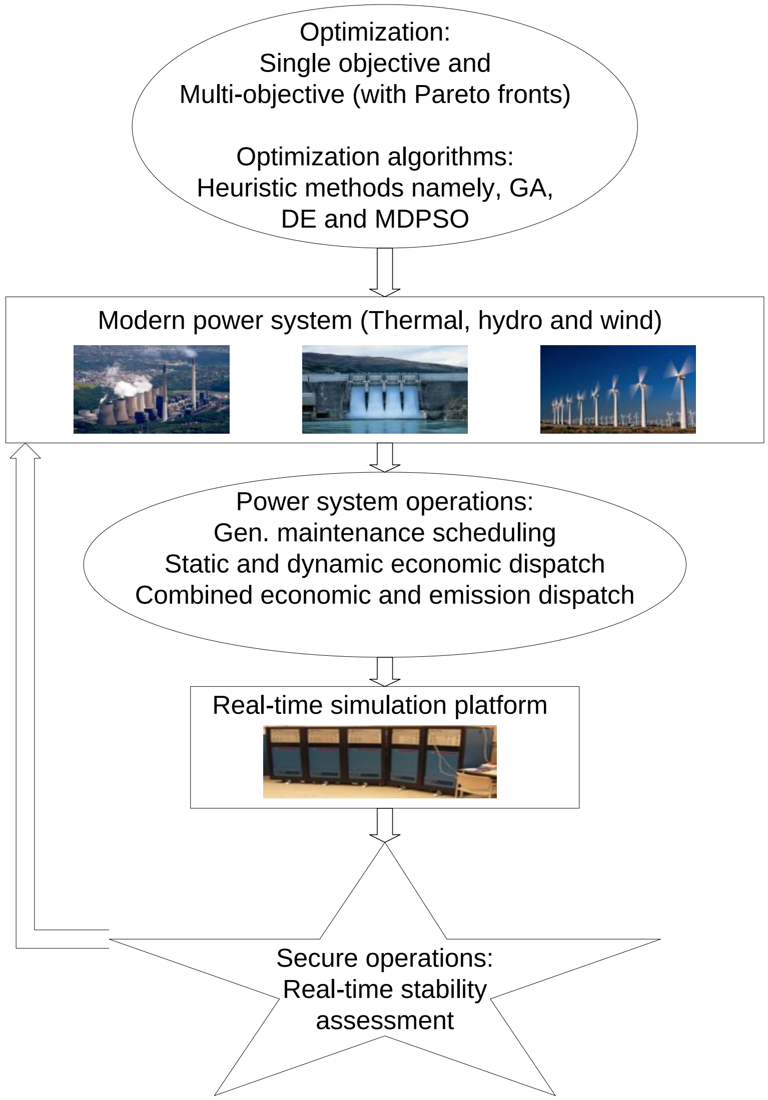

Fig. 1.1. An Overview of Issues Addressed in this Dissertation

However, **w**hen these approaches are heavily constrained, electric utilities are forced to get the most out of the devices they already own through more effective operating policies, including an improved maintenance program [1].

Figure 1.2 shows maintenance as part of the overall asset management effort [1]. Maintenance policy is part of the operating policies and, in a given setting, it is selected to satisfy both technical requirements and financial constraints. Maintenance programs range from the very simple to the quite sophisticated, the oldest replacement schemes been the age and bulk replacement policies. Within the age maintenance policy, components are replaced at a certain age or when they fail while the bulk replacement program ensures that all devices in a given class are replaced at predetermined intervals, or when the fail.

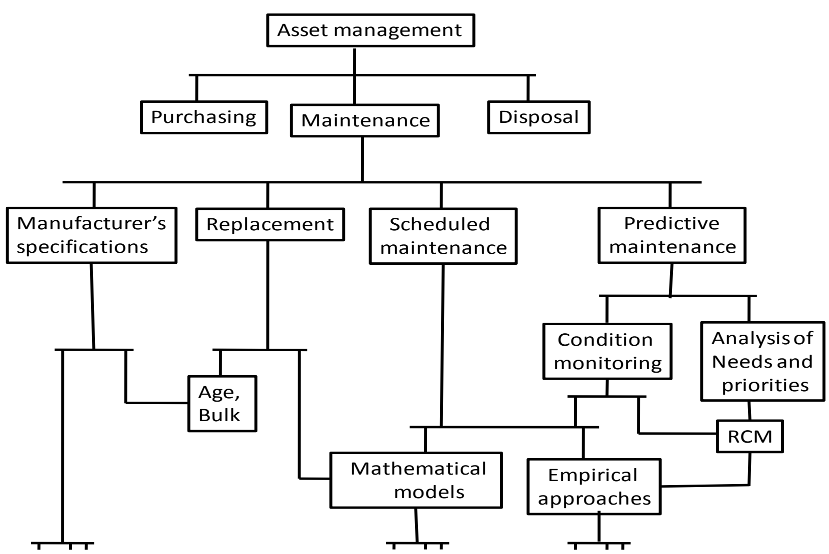

Fig. 1.2. Classification of the Various Maintenance Approaches

Rigid maintenance schedule schemes are pre-defined activities carried out at fixed time intervals. Whenever the component fails, it is repaired or replaced. Both repair and replacement are assumed to be much more costly than a single maintenance job. The maintenance intervals are selected on the basis of long-time experience (not necessarily an inferior alternative to mathematical models). To this day, this is the approach most frequently used.

The reliability-centered maintenance (RCM) is a program under the predictive maintenance routines. In RCM approach, various alternative maintenance policies can be compared and the one most cost-effective for sustaining equipment reliability is selected. RCM programs have been installed by several electric utilities as a useful management tool, and those utilities using the RCM are expecting to gain the following benefits: longer up-times, lower costs, better control and decisions, and better use of labor. Preventive maintenance optimization (PREMO) is claimed to be more efficient than RCM. It is based on extensive task analysis rather than system analysis and has the capability of drastically reducing the required number of maintenance tasks in a plant. RCM and PREMO have been very useful in ensuring economic operation of power stations, but do not provide the full benefits and flexibility of programs based on mathematical models. For a complete evaluation of the effects of a maintenance policy, one had to know by how much its application would extend the life of a component. To find this out, a mathematical model (MM) of the component deterioration process is required, which is then combined with a model describing the effects of maintenance. The MM provides a quantitative link between the reliability and maintenance. This connection is missing in earlier approaches of RCM and PREMO. Once MM is constructed, the process can be optimized with regard to changes in one or more of the variables. The simpler mathematical models are essentially still based on fixed maintenance intervals, and the optimization will result in identifying the least costly maintenance frequency. More complex models incorporate the idea of condition monitoring, where decisions with regard to the timing and amount of maintenance are dependent on the actual condition (stage of deterioration) of the device. MMs may be deterministic or probabilistic.

The most often used device to establish the need for maintenance is periodic inspection. This is known as the predictive (as needed) maintenance. The inspection intervals vary widely and are also different for different tasks. Another device for detecting maintenance needs is continuous monitoring (such as oil leakage, vibration, bearing temperature, tap changer condition, corrosion and discharge voltage). Most effective diagnostic tools are gas and oil analysis, power factor test, surge testing, vibration monitoring and contact resistance.

Probabilistic models probabilistic approaches are not used in maintenance planning by most utilities. However, many do wish to compute such indices as unavailability, failure frequency and duration (or MTTF).

Present maintenance policies are primarily based on historical records and data requirements. These may include inspection records and maintenance data, generator manuals, together with experience and memory. Data such as test reports, failure statistics, maintenance protocols and history and operational logs are also used. Contracting out maintenance work is also been practiced by most utilities. Some do it on an “as needed” basis or only for special tests, others contract out major maintenance work. Scheduled maintenance scheme considers both the intervals and durations for scheduled maintenance tasks, with typical maintenance data shown in Table 1.1 below [1].

Table 1.1: Typical Maintenance Interval and Duration
for some Power System Equipment

	Generators		Transformers		Breakers	
	Interval	Duration	Interval	Duration	Interval	Duration
Minor maintenance	1 yr	1 - 2 wks	1 yr	1 day	1 yr	1 day
Minor overhaul	5 yrs	4 - 5 wks	5 yrs	3 days	5 yrs	3 days
Major overhaul	8 - 10 yrs	6 - 8 wks	7 yrs	4 - 8 wks	8 - 10 yrs	2 wks

The simplest maintenance policies consist of a set of instructions taken from equipment manuals or based on long-standing experience. There are no quantitative relationships involved and the possibilities are very limited for making predictions about effectiveness of the policy or carrying out any sort of optimization. To make numerical predictions and carry out optimizations, mathematical models are needed which can represent the effects of maintenance on reliability and cost. Mathematical models can be deterministic or probabilistic. Both can be put to good use in appropriate maintenance studies [1].

In modern power systems, the demand for electricity has greatly increased with related expansions in system size, which has resulted in higher number of generators and lower reserve margins. Consequently, the generator maintenance scheduling (GMS) for a large power system has become a complex multi-objective constrained optimization problem. Within the last three decades, several techniques have appeared in the literature that addressed such optimization problem under different scenarios. Optimization methods such as branch and bound technique, dynamic programming and integer programming were few early techniques that were used to solve simple optimization problems. The primary goal of the GMS is the effective allocation of generating units for maintenance while ensuring high system reliability, reducing production cost, prolonging generator life time subject to some unit and system constraints [2] - [3].

Power system equipment are made to remain in good operating conditions by regular preventive maintenance. The task of generator maintenance is often performed manually by human experts who generate the schedule based on their experience and knowledge of the system, and in such cases there is no guarantee that the optimal or near optimal schedule is found. The purpose of maintenance scheduling is to find the sequence of scheduled outages of generating units over a given period of time such that the level of energy reserve is maintained. This type of schedule is important mainly because other planning activities are directly affected by such decisions.

1.3. ECONOMIC DISPATCH

One of the options available to the utilities in order to maintain a high level of reliability and economy of the power system is economic dispatch (ED), and is considered to be one of the key functions in electric power system operations. The ED is essentially an optimization problem, formulated with the aim of minimizing the total generation cost of units while satisfying important system constraints. Previous efforts on solving ED problems have employed various mathematical programming methods and optimization techniques. These conventional methods include the lambda-iteration, the base point and participation factors and the gradient methods [2]. In these numerical methods for solution of ED problems, an essential assumption is that the incremental fuel cost curves of the units are monotonically increasing piecewise-linear functions. Unfortunately, the input-output characteristics of modern generating units are inherently highly nonlinear due to valve-point loading effects, ramp-rate limits, prohibited operating zones and so on, which tend to generate multiple local minima points in the cost function. Classical dispatch algorithms require that these characteristics be approximated, however such approximations may lead to suboptimal operation of the generator and results in heavy revenue losses. Furthermore, for a large-scale mixed-generating system, the conventional method has oscillatory problem resulting in a large solution time [3]. A dynamic programming (DP) method for solving the ED problem with valve-point modeling has been presented in [2]. However, the DP method may cause the dimensions of the ED problem to become extremely large, thus requiring enormous computational efforts.

Dynamic economic dispatch (DED) is a method of scheduling generator outputs to meet the anticipated and predicted load demand over a certain period of time in order to operate the power system most economically. It is therefore the most accurate formulation of the economic dispatch problem and also the most difficult to solve. The DED is a dynamic optimization problem taking into accounts the constraints imposed on system operation by generator ramping-rate limits. The DED is normally solved by dividing the entire dispatch period into a number of small time intervals, then a static economic dispatch (SED) generally referred to as the ED, is employed to solve the problem in each interval [2] - [3].

1.4. INTELLIGENT OPTIMIZATION ALGORITHMS

Most of power system optimization, problems including GMS, ED and multi-objective combined economic and emission dispatch (MO-CEED), have complex nonlinear characteristics with stringent equality and inequality constraints to be satisfied. Solving such nonlinear optimization problems for most cases may not be feasible because their numerical solutions require extensive computational efforts, which increase exponentially with the problem complexities. Even though deterministic optimization problems are formulated with known parameters, practical problems almost invariably include some unknown parameters. The inclusion of wind generation into the GMS, ED and MO-CEED problems has further added degrees of nonlinearities to the optimization problem due to the variability and intermittency of wind energy resources. This nonlinear optimization problem becomes difficult to be solved by classical methods, hence the need for intelligent heuristic optimization techniques. Advanced optimization techniques and simulation capabilities are needed to support the future modern power system planning, operation and real-time implementation of the inherent dynamic optimization problems involving variable and intermittent wind energy resources. Intelligent optimization techniques are computationally fast approaches that yield optimal or near optimal solutions in many practical power system optimization problems.

In order to make numerical methods more convenient for solving GMS, ED and MO-CEED problems, artificial intelligent techniques, such as the Hopfield neural networks, genetic algorithm (GA), simulated annealing (SA), differential evolution (DE) and particle swarm optimization (PSO) have been successfully employed to solve power system optimization problems [3].

In the past decade, a global optimization technique known as GA or SA, which is a form of probabilistic heuristic algorithm, has been successfully used to solve power system optimization problems such as feeder reconfiguration and capacitor placement in a distribution system [3]. The GA method is usually faster than the SA method because the GA has parallel search techniques, which emulate natural genetic operations. Due to its high potential for global optimization, GA has received great attention in solving unit commitment and ED problems. Though the GA methods have been employed successfully to solve complex optimization problems, recent research has identified some deficiencies in GA performance. This degradation in efficiency is apparent in applications with highly *epistatic* objective functions (i.e., where the parameters being optimized are highly correlated). The crossover and mutation operations cannot ensure better fitness of offspring because chromosomes in the population have similar structures and their average fitness is high toward the end of the evolutionary process [3]. Also the premature convergence of GA degrades its performance and reduces its search capability that leads to a higher probability toward obtaining a local optimum.

PSO, first introduced by Kennedy and Eberhart, is one of the modern heuristic algorithms. It was developed through simulation of a simplified social system, and has been found to be robust in solving discrete and continuous nonlinear optimization problems [3], such as the GMS, ED and MO-CEED problems.

1.5. STABILITY ASSESSMENT AND IMPROVED CONTROLS FOR A POWER SYSTEM

Stability assessment (SA) deals with the analysis of a power system assuming credible system contingencies or sequence of events had occurred [3] - [4]. If the analysis indicates that a system is unstable, the stability control should provide preventive strategies by changing system operating conditions to a more viable and stable status, hence forestalling the possibility of cascading outages. A power system is said to be stable if it can withstand all credible contingencies without violating any of the system constraints. If there is at least one contingency, or sequence of probable events, which violates the system constraints, the system is judged to be unstable or insecure. Therefore the goal of SA is to determine when disruptions of service are likely to occur. The reason for undertaking a SA therefore is to determine the ability of the power system to continue providing service in case of an unforeseen, but probable, catastrophic contingency.

A power system can become unstable for various reasons such as, major component failures, communication interruptions, human errors, unfavorable weather conditions, and sometimes sabotage.

1.6. OBJECTIVES OF RESEARCH

The objectives of this research can be classified as follows:

- Solve the GMS problem for an interconnected power system while meeting practical generator and system constraints.
- Framework developments and their application to solving the GMS and ED problems.
- Illustrate and solve the challenging problem of economic dispatch for systems with dynamic load, and characterized by smooth and nonsmooth fuel cost functions.
- Formulation and application of economic cost function based GMS and ED problems for hydrothermal power system while satisfying practical system constraints.
- Formulation and solving the multi-objective combined economic and emission dispatch optimization problem for a wind-hydrothermal power system.
- Formulation of the real-time network status index for a power system.
- Demonstration of real-time stability assessment for a practical power system using the real-time digital simulator (RTDS).

1.7. CONTRIBUTIONS OF THIS DISSERTATION

The following key contributions have been accomplished in this dissertation:

- Developed modified particle swarm optimization (MDPSO) algorithm to achieve fast convergence and better quality solutions [5].
- Developed multiple-swarms MDPSO framework to achieve faster convergence and better quality solutions [6].
- Illustrated and applied the MDPSO to solve the reliability based GMS optimization problem of a practical hydrothermal power system [5].
- Illustrated and applied the multiple-swarms MDPSO framework to solve the reliability based GMS optimization problem of a hydrothermal power system [6].
- Illustrated the smooth and nonsmooth economic cost function formulation of the GMS optimization problem with practical generator constraints using both the classical and heuristic methods [8], [9].
- Applied heuristic methods, namely, GA, DE and MDPSO to solve the static and dynamic ED for generators with smooth and nonsmooth economic cost functions with practical constraints and transmission line losses [10].
- Incorporated additional practical generator constraints such as the generator prohibited zones and ramp-rate limits, system power loss and increased the dimensionality of the problem in solving the ED problem [10].
- Formulated stochastic MO-CEED optimization problem for a wind-hydrothermal power system [11]. Uncertainty in wind power was incorporated in this formulation.
- Solved the stochastic MO-CEED problem for wind-hydrothermal power system using a family of optimal Pareto fronts [11].
- Presented platforms for which optimized energy and generation cost management in the presence of wind energy penetration is made possible [8], [9], [11].
- Quantified emission reductions as a consequence of increased capacity credit of wind power during GMS [8], [9], as well as after solving the MO-CEED [11].
- Demonstrated the potential for increased daily cost saving and emission reduction for a practical Nigerian power system [11].
- Formulated the network status index for a power system and implemented in real time platform [12].

- Demonstrated on the Nigerian hydrothermal power system for *N-1*, *N-2*, ..., *N-k* generator outages and *N-1* permanent transmission line outage (topology change).

1.8. DISSERTATION OUTLINE

A brief introduction and the objectives of this research are described in this section. The rest of the dissertation present articles one to six that have been published/submitted for journal publications. Paper 1 presents a modified discrete particle swarm optimization (MDPSO) algorithm and its application to reliability based GMS problem. The paper also shows pragmatic maintenance unit scheduling framework for a power utility that achieved better utilization of available energy generation with improved reliability and reduction in energy cost. Paper 2 introduces the concept of multiple-swarms of particle swarm optimization (MS-PSO) and the evolution of a single best solution from many best solutions for solving the complex GMS constrained optimization problem. Paper 3 describes three heuristic methods for solving both the static economic dispatch (SED) and dynamic economic dispatch (DED). Multi-objective combined economic and emission dispatch (MO-CEED) optimization problem for a wind-hydrothermal power system is presented in Paper 4. In pursuance of the smart grid initiative, Paper 5 presents an optimal preventive generator maintenance scheduling (GMS) for a wind-hydrothermal power system. Paper 6 presents real-time (RT) stability assessment (SA) of a power system, with detail formulation of network status index for smart grid development. A conclusions section is provided that summarizes the work presented in this dissertation, including a subsection that enumerates areas of future research.

1.9. REFERENCES

[1] J. Endrenyi, S. Aboresheid, R. N. Allan, G. J. Anders, S. Asgarpoor, R. Billinton, N. Chowdhury, E. N. Dialynas, M. Fipper, R. H. Fletcher, C. Grigg, J. McCalley, S. Meliopoulos, T. C. Mielnik, P. Nitu, N. Rau, N. D. Reppen, L. Salvaderi, A. Schneider and Ch. Singh, “The present status of maintenance strategies and the impact of maintenance on reliability,” *IEEE Transactions on Power Systems,* vol. 16, no. 4, pp. 638-646, November 2001.

[2] A. J. Wood and B. F. Wollenberg, *Power generation operation and control*. New York, NY: John Wiley and Sons, 2004.

[3] K. Y. Lee and M. A. El-Sharkawi, *Modern Heuristic Optimization Techniques: Theory and Applications to Power Systems*. ISBN: 978-0471-45711-4, IEEE Press, 445 Hoes Lane, Piscataway, New Jersey, 2008.

[4] P. Kundur, *Power System Stability and Control*. The EPRI Power System Engineering Series, McGraw-Hill, Inc, USA, 1994.

[5] Y. Yare, G. K. Venayagamoorthy and U. O. Aliyu, "Optimal generator maintenance scheduling using a modified discrete PSO," *IET Generation, Transmission & Distribution,* vol. 2, no. 6, pp. 834-846, November 2008.

[6] Y. Yare and G. K. Venayagamoorthy, "Optimal maintenance scheduling of generators using multiple swarms-MDPSO framework," *ScienceDirect/Elsevier Journal-Engineering Application of Artificial Intelligence*, vol. 23, (6), pp. 895-910, 2010.

[7] Y. Yare, G. K. Venayagamoorthy and U. O. Aliyu, "Optimal generator maintenance scheduling of the Nigerian power system," *Accepted book chapter,* in press.

[8] Y. Yare and G. K. Venayagamoorthy, "Wind-hydrothermal GMS of a modern power system with uncertainty in wind generation," *IEEE Power and Energy Society (PES) General Meeting,* Minneapolis, Minnesota, USA, July 2010.

[9] Y. Yare, G. K. Venayagamoorthy and A. Y. Saber, "Generator maintenance scheduling for a wind-hydrothermal power system with uncertainty in wind energy generation," *IEEE Transactions on Smart Grid,* 2010: *Submitted (In review process).*

[10] Y. Yare, G. K. Venayagamoorthy and A. Y. Saber, "Heuristic methods for static and dynamic economic dispatch with practical generator constraints," *ScienceDirect/Elsevier Journal-Engineering Application of Artificial Intelligence,* 2010: *Accepted for publication*.

[11] Y. Yare and G. K. Venayagamoorthy, "Multi-objective combined economic and emission dispatch with uncertainty in wind power for a wind-hydrothermal system," *IET Journal Generation, Transmission & Distribution,* 2010: *Submitted (In review process).*

[12] Y. Yare and G. K. Venayagamoorthy, "Real-time stability assessment of a power system," *IEEE Transactions on Power Systems,* 2010*: Submitted (In review process).*

I. OPTIMAL GENERATOR MAINTENANCE SCHEDULING USING A MODIFIED DISCRETE PSO

Y. Yare[1], G. K. Venayagamoorthy[1] and U. O. Aliyu[2]

[1]Real-Time Power and Intelligent Systems Laboratory, Department of Electrical and Computer Engineering, Missouri University of Science and Technology Rolla, MO 65409-0249 USA (E-mail: yyqh3@umr.edu & gkumar@ieee.org)

[2]Electrical Engineering Programme, Abubakar Tafawa Balewa University, PMB 0248, Bauchi, Nigeria (E-mail: uoaliyu@yahoo.com)

ABSTRACT: This paper presents a modified discrete particle swarm optimization (MDPSO) algorithm for generating optimal preventive maintenance schedule of generating units for economical and reliable operation of a power system, while satisfying system load demand and crew constraints. Discrete particle swarm optimization (DPSO) is known to effectively solve large scale multi-objective optimization problems and has been widely applied in power system. Here, the MDPSO proposed for the generator maintenance scheduling (GMS) optimization problem generates optimal and feasible solutions and overcomes the limitations, of the conventional methods, such as extensive computational effort, which increases exponentially as the size of the problem increases. The efficacy of the proposed algorithm is illustrated and compared with the genetic algorithm (GA) and DPSO in two case studies – a 21-unit test system and a 49-unit system feeding the Nigerian national grid. The MDPSO algorithm is found to generate schedules with comparatively higher system reliability indices than those obtained with GA and DPSO.

INDEX TERMS: Cost, discrete optimization, generator maintenance, genetic algorithm, Nigerian power system, optimal scheduling and particle swarm optimization.

NOMENCLATURE

AM_t Available manpower at period t

c_1 & c_2 Cognitive and social acceleration constants respectively

d	Particle's dimension
d_i	Duration of maintenance for unit i
DPSO	Discrete particle swarm optimization
e_i	Earliest period for maintenance of unit i to begin
ES	Evolutionary strategy
GA	Genetic algorithm
GMS	Generator maintenance scheduling
i	Index of generating units
k	Discrete time step
I	Set of generating unit indices
l_i	Latest period for maintenance of unit i to end
L_t	Anticipated load demand for period t
MDPSO	Modified discrete particle swarm optimization
M_{it}	Manpower needed by unit i at period t
N	Total number of generating units
P_{ibd}	*i-th* Particle best position for dimension d
P_{gd}	Swarm's best position for dimension d
P_{gn}	*n-th* dimension coordinate of the global best position (P_g)
P_{it}	Generating capacity of unit i in period t
PSO	Particle swarm optimization
$rand_1$ & $rand_2$	Random numbers with uniform distribution in the range of [0, 1]
randn()	Gaussian distributed random number with a zero mean and a variance of 1
t	Index of period
T	Set of indices of periods in planning horizon
$\|V_1\|$, $\|V_2\|$ & $\|V_3\|$	Amount of violations of maintenance window, crew and load constraints respectively
$\|V_c\|$	Amount of violation of constraint c
V_{id}	*i-th* Particle velocity in dimension d
w	Inertia weight constant

ω_1, ω_2 & ω_3 Weighting coefficients of maintenance window, crew and load constraints respectively

ω_c Weighting coefficient

X_{id} *i-th* Particle position in dimension *d*

1. INTRODUCTION

In modern power systems, the demand for electricity has greatly increased with related expansions in system size, which has resulted in higher number of generators and lower reserve margins. Consequently, the generator maintenance scheduling (GMS) for a large power system has become a complex multi-objective constrained optimization problem. Within the last three decades, several techniques have appeared in the literature that addressed such optimization problem under different scenarios [1-14]. The primary goal of the GMS is the effective allocation of generating units for maintenance while ensuring high system reliability, reducing production cost, prolonging generator life time subject to some unit and system constraints.

Basically, different optimization techniques applied so far to solving GMS can be classified according to the type of the search space and/or the objective function [1-13]. Thus, much earlier work relied on methods such as branch and bound technique [4], dynamic programming [5] and integer programming [6] with their performances demonstrated with respect to simple case studies. Depending on the problem formulation, the objective function could be minimization of the unit maintenance costs or some predefined reliability risks subject to some constraints resulting in nonlinear optimization as proposed in [8-11]. Solving such nonlinear optimization problems for most cases may not be feasible because their numerical solutions require extensive computational efforts, which increase exponentially with the problem complexities. Even though deterministic optimization problems are formulated with known parameters, real world problems almost invariably include some unknown parameters.

In order to obtain approximate solution of a complex GMS, new concepts have emerged in recent years [12-15]. They include applications of probabilistic approach [12], simulated annealing [13], decomposition technique [14] and genetic algorithm (GA) [15]. A flexible GMS that considered uncertainties is proposed with a fuzzy 0-1 integer programming technique adopted and applied to Taiwan power system [15]. The application of GA to GMS presented in [15] have been compared with, and confirmed to be superior to other conventional algorithms such as heuristic approaches and branch-and-bound (B&B) in the quality of solutions. However, the application of particle swarm optimization (PSO) and their variants to GMS have not been fully explored in the literature and this constitutes the main focus of this research effort.

In this paper, we propose a modified discrete particle swarm optimization (MDPSO) algorithm that is not overly affected by the size and nonlinearity of the GMS problem, and can converge to the optimal solution in many problems where most analytical methods fail to converge [16, 17].

The primary contributions of this paper are:

- Enhancement of discrete particle swarm optimization (DPSO) capabilities with evolutionary computation techniques such as the evolutionary strategies (ESs), to solve complex GMS optimization problem.
- Comparison of three algorithms – DPSO, MDPSO and GA for solving the GMS problem on a 21-unit test system [5].
- Application of MDPSO to solving the GMS problem for the Nigerian power system which operates the traditional utility market, and where load frequently exceeds generation.

2. PROBLEM FORMULATION

Generally, there are two main categories of objective functions in GMS, namely, based on reliability and economic cost [2]. The reliability criteria of leveling reserve generation for the entire period of study is considered in this paper [18, 19]. The problem studied here is solved by minimizing the sum of squares of the reserve over the entire operational planning period [18, 19]. The problem has a number of unit and system constraints to be satisfied. The constraints include the following:

- Maintenance window and sequence constraints - defines the starting of maintenance at the beginning of an interval and finishing at the end of the same interval. The maintenance cannot be aborted or finished earlier than scheduled.

- Crew and resource constraints - for each period, number of people to perform maintenance schedule cannot exceed the available crew. It defines manpower availability and the limits on the resources/tools needed for maintenance activity at each time period.
- Load and spinning reserve constraints - total capacity of the units running at any interval should be not less than predicted load at that interval.

Suppose $T_i \subset T$ is the set of periods when maintenance of unit i may start, $T_i = \{t \in T : e_i \le t \le l_i - d_i + 1\}$ for each i.

Define

$$X_{it} = \begin{cases} 1 & \text{if unit } i \text{ starts maintenance in period } t \\ 0 & \text{otherwise} \end{cases} \tag{1}$$

to be the maintenance start indicator for unit i in period t. Let S_{it} be the set of start time periods k such that if the maintenance of unit i starts at period k that unit will be in maintenance at period t, $S_{it} = \{k \in T_i : t - d_i + 1 \le k \le t\}$. Let I_t be the set of units which are allowed to be in maintenance in period t, $I_t = \{i : t \in T_i\}$.

The objective function to be minimized is given by (2) subject to the constraints given by (3), (4) and (5).

$$\underset{X_{it}}{Min} \left\{ \sum_t \left(\sum_i P_{it} - \sum_{i \in I_t} \sum_{k \in S_{it}} X_{ik} \cdot P_{ik} - L_t \right)^2 \right\} \tag{2}$$

subject to the maintenance window constraint

$$\sum_{t \in T_i} X_{it} = 1 \qquad \forall i \, , \tag{3}$$

the crew constraint

$$\sum_{i \in T_t} \sum_{k \in S_{it}} X_{ik} \cdot M_{ik} \leq AM_t \qquad \forall t, \tag{4}$$

and the load constraint

$$\sum_{i} P_{it} - \sum_{i \in I_t} \sum_{k \in S_{it}} X_{ik} \cdot P_{ik} \geq L_t \qquad \forall t, \tag{5}$$

Penalty cost given by (6) is added to the objective function in (2) if the schedule cannot satisfy the maintenance window, crew and load constraints. The penalty value for each constraint violation is proportional to the amount by which the constraint is violated.

$$Penalty\ \mathrm{cost} = \sum_{c=1}^{3} \omega_c |V_c| = \omega_1 |V_1| + \omega_2 |V_2| + \omega_3 |V_3| \tag{6}$$

3. MODIFIED DISCRETE PSO

Particle swarm optimization (PSO) is an algorithm inspired by the social behavior of bird flocking or fish schooling which is used for finding optimal regions of complex search spaces through the interaction of individuals in a population of particles [16]. The following subsections describe the DPSO and enhanced modified DPSO (MDPSO) algorithm.

3.1. Discrete PSO

The general concepts behind optimization techniques initially developed for problems defined over real-valued vector spaces, such as PSO, can also be applied to discrete-valued search spaces where either binary or integer variables have to be arranged into particles [17]. When integer solutions (not necessarily 0 or 1) are needed, the optimal solution can be determined by rounding off the real optimum values to the nearest integer [17]. Discrete particle swarm optimization has been developed specifically for solving discrete problems. DPSO allows discrete steps in velocity and thus in position. In this version of PSO, the velocity is limited to a certain range [- V_{max}, V_{max}] such that V_{id} always lies in that range.

The new velocity and position for each particle *i* in dimension *d* is determined according to the velocity and position update equations given by (7) and (8).

$$V_{id}(k) = round\ (w \cdot V_{id}(k-1) + c_1 \cdot rand_1 \cdot (P_{ibd} - X_{id}(k-1)) + c_2 \cdot rand_2 \cdot (P_{gd} - X_{id}(k-1))) \quad (7)$$

$$X_{id}(k) = X_{id}(k-1) + V_{id}(k) \quad (8)$$

DPSO has some advantages over other similar optimization techniques such as GA. In DPSO, every particle remembers its own previous best value as well as the neighborhood best; therefore, it has a more effective memory capability than the GA. DPSO is also more efficient in maintaining the diversity of the swarm, since all the particles use some information related to the most successful particle in order to improve themselves, whereas in GA, the worse solutions at every generation are discarded and only the good ones are saved for next generation. Therefore, in GA the population evolves around a set of best individuals in every generation. In addition, DPSO is easier to implement and there are fewer parameters to adjust compared to GA [17].

3.2. Modified DPSO

The modified discrete particle swarm optimization is a combination of DPSO and an evolutionary strategy enhancing the algorithm to perform optimal search under complex environments such as the case of the constrained GMS optimization problem considered in this paper. This version of MDPSO is a variant of the original formulation of the DPSO to solve discrete optimization problems. Supposing $X = (X_1, X_2, \ldots X_N)$ is the particle chosen with a random number less than a predefined mutation rate (for 0 < mutation rate < 0.3) then the mutation result of this particle is given by (9).

$$X_{id} = P_{gd} + (randn() \cdot P_{gd} / 2) \qquad d = 1, 2, \ldots N \quad (9)$$

Herein, the mutation operator is introduced into the DPSO algorithm. The main goal is to increase the diversity of the population by preventing the particles from moving too close to each other, thus converging prematurely to local optima. This in turn improves the DPSO's search performance. The flowchart for the MDPSO algorithm applied to GMS problem is illustrated in Fig. 1.

4. CASE STUDIES AND RESULTS

Two case studies are considered to illustrate the effectiveness of the MDPSO algorithm for solving the GMS problem. First, the three algorithms are applied and compared on a 21 unit test system [5]. The second case study is specific to GMS for a 49-unit system of the Nigerian power system. These case studies are described below and implemented in MATLAB environment.

4.1. Case I: 21 Units Test System

In order to investigate the performance of MDPSO for the GMS, a test system comprising 21 units over a planning period of 52 weeks is used, which is obtained from the example presented in [2, 5]. During this period, 21 units need to undergo maintenance, and Table 1 lists the generator ratings, allowed maintenance period, maintenance duration of each unit and crew required weekly for each unit.

TABLE 1

Data for the 21 Units Test System

Unit	Capacity (MW)	Allowed period	Maintenance duration (weeks)	Manpower required for each week
1	555	1-26 weeks	7	10+10+5+5+5+5+3
2	180		2	15+15
3	180		1	20
4	640		3	15+15+15
5	640		3	15+15+15
6	276		10	3+2+2+2+2+2+2+2+2+3
7	140		4	10+10+5+5
8	90		1	20
9	76		2	15+15
10	94		4	10+10+10+10
11	39		2	15+15
12	188		2	15+15
13	52		3	10+10+10
14	555	27-52 weeks	5	10+10+10+5+5
15	640		5	10+10+10+10+10
16	555		6	10+10+10+5+5+5
17	76		3	10+15+15
18	58		1	20
19	48		2	15+15
20	137		1	15
21	469		4	10+10+10+10

The maintenance outages for the generating units are scheduled to minimize the sum of squares of reserves and satisfy the following constraints:

- Maintenance window - each unit must be maintained exactly once every 52 weeks without interruption.
- Load constraint and spinning reserve - the system's peak load including 6.5% spinning reserve [20] is 5047MW.
- Crew constraint - there are only 40 crew available each week for the maintenance work.

4.1.1. GMS with GA

In GA, real numbers are often encoded using binary numbers [21]. The GA domain in this study is set with 50 individuals (chromosomes) representing all possible schedules. The GA for this GMS problem is encoded by grouping the units for maintenance according to their allowed periods shown in Table 1. 13 units are scheduled in the first 26 weeks while the remaining 8 units are scheduled within the last 26 weeks. With the former, each chromosome consists of 13 unit genes, with each gene encoded as 5 bits representing the maintenance starting period, and the length of each chromosome is 65 bits. Similar encoding procedure is done on the 8 units resulting in chromosome length of 40 bits. Fig. 2 shows the chromosome representation for the 13 and 8 units according to the allowed maintenance periods of Table 1. Though the schedule in Fig. 2 (b) shows week numbers within 1 to 26, this translates to weeks within 27 to 52.

4.1.2. GMS with DPSO and MDPSO

The integer encoding approach consists of a string of integers, each of which indicates the maintenance start period of a unit and the string length or particle dimension is equal to the number of units. Since, the maintenance period varies for every unit; the start period is selected within the specified maintenance window of 52 weeks.

To implement the DPSO and MDPSO, a population size of 30 particles is chosen to provide sufficient diversity into the population taking into account the dimensionality and complexity of the problem. This population size ensured that the domain is examined in full but at the expense of increase in execution time.

4.1.3. Results

Figure 3 (a) shows fitness values, given by (2), averaged over 5000 trials for three different DPSO/MDPSO parameters. Cases A, B and C in Fig. 3 denotes three DPSO/MDPSO parameter settings, w=0.8 and c_1=c_2=2, w=linearly decreasing and

$c_1=c_2=2$, lastly $w=0.729$ and $c_1=c_2=1.49$ (constriction factor based PSO) [22] respectively. The MDPSO performs better than the DPSO. The MDPSO and DPSO algorithms produced best results in case A, and the worst result is in case C. In all cases, the MDPSO yields better fitness values compared to the DPSO and GA. The DPSO however, showed better fitness values than the GA. Fig. 3 (b) shows the percentage of feasible optimal maintenance schedules obtained for 5000 iterations over 5000 trials. The MDPSO is seen to produce more number of feasible solutions than the DPSO and the GA. Its performance can be further improved with increased number of iterations. The result shows the efficiency and better performance of MDPSO over the DPSO and GA. Both MDPSO and DPSO algorithms performed best for case A ($w=0.8$ and $c_1=c_2=2$) and worst for the case C (constriction factor based PSO) for this GMS problem.

Figure 4 shows available generation and crew requirements for optimal maintenance schedules obtained from the results in Table A.1 using $w=0.8$ and $c_1=c_2=2$. Within the maintenance window, a minimum of 5047MW (with spinning reserve) is sustained to meet the peak demand, while the crew is limited to maximum of 40. The maximum generation is 5688MW.

It is important to note from Fig. 4 that the crew demand is inversely related with the availability generation over the entire maintenance period. When maintenance activities increase in a particular week, more generators are shut down which translate to reduced generation. It is worthy of note also that there is maintenance activity in every week throughout the 52 weeks without any interruption. All the three algorithms considered were able to generate optimal schedules that met all constraints.

The ‘reliability index’ (RI) given by (10) describes the degree of performance of the algorithms that results in optimal maintenance schedules. It is computed by taking the minimum of the ratio of available generation to load demand over 5000 trials and the entire operational period. The functional aspect of the reliability indices is that they show the generation adequacy and the ability of the system to supply the aggregate electrical energy and meet demand requirements of the customers at all times during maintenance period.

$$RI = \underset{\substack{(over\,5000\\ trials)}}{Min}\left(\underset{\substack{(over\,52\\ weeks)}}{Min}\left(\begin{array}{cc}\dfrac{Avail.Gen.}{Load} & if\ Avail.Gen. \leq Load\\ 1 & otherwise\end{array}\right)\right) \tag{10}$$

Figure 5 (a) shows the reliability indices of the maintenance scheduling problem for the three algorithms considered in this study. The MDPSO is seen to produce the most reliable schedule compared with DPSO and GA over 5000 trials. Figure 5 (b) shows the computational time for off-line execution of the DPSO, MDPSO and GA algorithms, set under the same conditions with w=0.8 and c_1=c_2=2. Each experiment is run for 5000 iterations/ generations over 5000 trials. The result reveals that MDPSO has faster execution time than the DPSO, and much faster compared to the GA.

4.2. Case II: Nigerian Power System

The Nigerian power system consists of a total of 49 functional units distributed among 7 generating stations at the following locations: AFAM, DELTA, EGBIN, SAPELE, JEBBA, KAINJI and SHIRORO. Table 2 summarizes the units' base case ratings. Note that all the units at AFAM and DELTA stations as well as 8 units at EGBIN station are gas turbines, whilst all units at SAPELE station and other 6 units at EGBIN station are steam driven. The JEBBA, KAINJI and SHIRORO hydro stations are all sited in Northwestern Nigeria. Over 25 years of operational experience and available historical data on hydrological conditions reveal that inflow variation profile at each hydro station location, significantly impacts the generated power output of each hydro plant. This inflow profile also dictates the allowed periods for the maintenance of the three hydro plants.

These scenarios have been taken into consideration in solving this GMS problem using the MDPSO-a and MDPSO-b case studies described below. MDPSO-a and MDPSO-b represent two case studies having different schedules for maintenance. A detailed description of these case studies is presented below.

4.2.1. MDPSO-a

Table 2 present the data for the Nigerian power system used to investigate the performance of the proposed MDPSO algorithm. All the hydrothermal units feeding the Nigerian national grid are to be scheduled for maintenance over a planning horizon of 52 weeks. The table shows the allowed periods for which planned preventive maintenance of generating units should be carried out. In this case study, GTs and steam turbines are to be shut down for maintenance only when the hydro plants are operating at their maximum generation. This corresponds to the months of January to April and November to December each year. The hydro plants can then be scheduled for maintenance during low inflow period corresponding to the months of May to October of each year. Within these months no thermal plant is allowed to be shut down for maintenance. The maintenance duration of each unit and crew required weekly for each unit are shown in Table 2. A maximum power demand of 3625MW plus 5% load increase is considered during the hot season of March to July every year.

4.2.2. MDPSO-b

In this case study, the advantage and cost benefits of appropriate combination of thermal and hydro plants for maintenance within the period of low water level from May to October is investigated. Five thermal plants, namely AFAMG 19, AFAMG 20, EGBINST 1, EGBINST 2 and SAPELEST 6 are scheduled for maintenance along with the hydro plants within the period of low water level. The remaining thermal plants are maintained in the months of January to April and November to December each year. There is 5% load variation between the months of March and July. Though the proposed maintenance scenario in MDPSO-b deviates from the current practice of the Nigerian power utility, wherein the thermal plants are expected to be operated at optimum generation during low inflows at all the hydro stations, the results of this comparison are noteworthy for good energy management and planning.

4.2.3. Results

Table 3 shows yearly summary of the load availability (with and without maintenance), load demand and the cost in Nigerian Naira to purchase energy from Independent Power Producers (IPPs) or possibly the West African Power Pool (WAPP) to supply loads that would have been suppressed as a result of maintenance activities. As seen from the Table 3, the annual base case generation for Nigeria cannot meet the yearly load demand due to inadequate generation from some generating units. Some of these units' contributions to the national grid are marginally low and are represented by a zero generation output. This means that there will be persistent load shedding to be carried out by the utility throughout the year.

TABLE 2

Outage and Manpower Data for the 49 Units of the Nigerian Power System

	S/N	Plant number	Name of turbine	Type of turbine	Base case rating (MW)	Allowed period	Maintenance duration (Weeks)	Manpower required for each week
I	1	3	EGBINST1	ST	190	January - April (1 - 17 weeks)	5	6+5+5+4+2
	2	3	EGBINST2	ST	190		5	6+5+5+4+2
	3	3	EGBINST3	ST	190		5	6+5+5+4+2
	4	3	EGBINST4	ST	190		5	6+5+5+4+2
	5	3	EGBINST5	ST	190		5	6+5+5+4+2
	6	3	EGBINST6	ST	190		5	6+5+5+4+2
	7	4	EGBINGT1	GT	30		2	4+3
	8	4	EGBINGT2	GT	30		2	4+3
	9	4	EGBINGT3	GT	30		2	4+3
	10	4	EGBINGT4	GT	30		2	4+3
	11	4	EGBINGT5	GT	30		2	4+3
	12	4	EGBINGT6	GT	30		2	4+3
	13	4	EGBINGT7	GT	30		2	4+3
	14	4	EGBINGT8	GT	30		2	4+3
	15	5	SAPELST1	ST	0		4	4+3+3+2
	16	5	SAPELST2	ST	0		4	4+3+3+2
	17	5	SAPELST3	ST	0		4	4+3+3+2
	18	5	SAPELST4	ST	0		4	4+3+3+2
	19	5	SAPELST5	ST	0		4	4+3+3+2
	20	5	SAPELST6	ST	85.3		4	4+3+3+2
II	21	6	JEBBGH1	H	88.3	May - October (18 - 43 weeks)	4	5+4+3+2
	22	6	JEBBGH2	H	88.3		4	5+4+3+2
	23	6	JEBBGH3	H	88.3		4	5+4+3+2
	24	6	JEBBGH4	H	88.3		4	5+4+3+2
	25	6	JEBBGH5	H	88.3		4	5+4+3+2
	26	6	JEBBGH6	H	88.3		4	5+4+3+2
	27	7	KAING05	H	112.5		4	5+5+4+3
	28	7	KAING06	H	0		4	5+5+4+3
	29	7	KAING07	H	0		3	4+3+2
	30	7	KAING08	H	0		3	4+3+2
	31	7	KAING09	H	0		3	4+3+2
	32	7	KAING10	H	76.5		3	4+3+2
	33	7	KAING11	H	90		4	5+4+3+3
	34	7	KAING12	H	0		4	5+4+3+3
	35	8	SHIRGH1	H	140		2	4+3
	36	8	SHIRGH2	H	140		2	4+3
	37	8	SHIRGH3	H	140		2	4+3
	38	8	SHIRGH4	H	0		2	4+3
III	39	1	AFAMGT19	GT	138	November - December (44 - 52 weeks)	5	5+5+4+3+3
	40	1	AFAMGT20	GT	138		5	5+5+4+3+3
	41	2	DELTAG03	GT	19.6		2	4+3
	42	2	DELTAG04	GT	19.6		2	4+3
	43	2	DELTAG06	GT	19.6		2	4+3
	44	2	DELTAG07	GT	19.6		2	4+3
	45	2	DELTAG08	GT	0		4	4+4+3+3
	46	2	DELTAG15	GT	85		4	4+4+3+3
	47	2	DELTAG16	GT	85		4	4+4+3+3
	48	2	DELTAG17	GT	85		4	4+4+3+3
	49	2	DELTAG18	GT	85		4	4+4+3+3

*GT- Gas turbine, ST- Steam turbine, H- Hydro.

The effect of scheduling thermal units for maintenance along with the hydro units within the months of May to October is shown in Table 3. The MDPSO-b produced optimal result that shows not only an even annual generation as seen in Fig. 6 (a), but also an improved energy management as there is 0.03% decline in suppressed load during maintenance due to 0.03% increase in annual generation, and an equivalent reduction in the cost of energy to be purchased when compared to the results obtained by MDPSO-a. Though this percentage is small, it shows that better energy management is achievable with proper scheduling of the generating units.

TABLE 3

Annual Load Availability, Demand and Cost of Purchasing Energy

	Annual generation - without maintenance	Annual generation - with maintenance	Annual load demand	Annual suppressed load - without maintenance	Annual suppressed load - with maintenance	Increase in suppressed load due to maintenance
MDPSO-a						
Mega watt hour (MWh)	29,601,936.00	27,347,930.40	31,990,896.00	2,388,960.00	4,642,965.60	94.35%
Cost of purchasing energy (X 1000 Naira/year)			191,945,376.00	14,333,760.00	27,857,793.60	13,524,033.60
MDPSO-b						
Mega watt hour (MWh)	29,601,936.00	27,348,720.00	31,990,896.00	2,388,960.00	4,642,176.00	94.32%
Cost of purchasing energy (X 1000 Naira/year)			191,945,376.00	14,333,760.00	27,853,056.00	13,519,296.00

*Cost of energy in Nigeria: 6 Naira/kWh and 234 Naira is equivalent to 1 Pound Sterling

Table 4 shows the cost of improving system reliability index for MDPSO-a and MDPSO-b with and without maintenance. Without maintenance for the two cases, there is 14,333,760,000.00 Naira to be expended on purchase of energy if a ‘reliability index’ of 1 is required. For zero cost, there is slight improvement in system reliability for MDPSO-b than for MDPSO-a with maintenance. The costs for 0.89 and 1 reliability indices with maintenance is seen to be higher for MDPSO-a than for MDPSO-b.

TABLE 4

Cost of Improving the Reliability Index (10)

	Without maintenance		With maintenance		
	MDPSO-a				
Reliability index	0.89	1	0.76	0.89	1
Cost (x1000 Naira)	0	14,333,760.00	0	13,524,033.60	27,857,793.60
	MDPSO-b				
Reliability index	0.89	1	0.78	0.89	1
Cost (x1000 Naira)	0	14,333,760.00	0	13,519,296.00	27,853,056.00

Table A.2 of the Appendix presents the generator schedules obtained by MDPSO-a and MDPSO-b, whilst Fig. 6 (a) shows the available generation for MDPSO-a and MDPSO-b during maintenance, the maximum generation plus a 5% load increase within the hot season of March to July each year. For MDPSO-a, between the months of May and October when the hydro plants are undergoing maintenance, the bulk of the generation is entirely from the thermal plants as they are prevented from maintenance during this period. This leads to an uneven generation over the entire maintenance period, resulting to an unpredictable energy profile, sharp and large variations in load shedding. MDPSO-b however, produced better and more even generation throughout the year under maintenance, with an average generation and standard deviation of 3130.5800±68.2985MW, while MDPSO-a produces average generation and standard deviation of 3130.4900±117.3519MW.

Figure 6 (b) shows the corresponding crew availability for MDPSO-a and MDPSO-b during maintenance. MDPSO-b scheduling produced better crew distribution over the maintenance period than MDPSO-a. Both cases are seen to have satisfied the crew constraint. MDPSO-a generates average crew requirement and standard deviation of 12±4.9074, while MDPSO-b produces 11±4.9670.

Figure 7 (a) presents the reliability indices for MDPSO-a and MDPSO-b during maintenance period, compared against the system reliability indices without maintenance. MDPSO-b produces better system reliability than MDPSO-a after 5000 iterations. Figure 7 (b) shows the plots of costs of purchasing energy versus the reliability indices with the solutions obtained for MDPSO-a and MDPSO-b. It can be seen from the figure that at any system reliability index, the corresponding energy cost for MDPSO-a solution is higher than that for MDPSO-b solution. Similarly, at any energy cost, MDPSO-b gives better reliability index than MDPSO-a. Without maintenance, the system has much higher reliability index than the two cases considered with maintenance, and there is no need to purchase energy as a result of maintenance activities. Fig. 7 (c) presents the elapsed computational time for the off-line execution of the MDPSO for case study I and, MDPSO-a and MDPSO-b for case study II. The result shows that as the number of generating units increased from 21 to 49 (i.e. by a factor of 2.33), the elapsed computational time also increased from 18250 seconds for case study I to 41975 seconds for case study II on Intel Pentium D personal computer with 3.4GHz speed. This implies a computational time increase by factor of 2.3. It is extrapolated that computational time is in the order of 85000 seconds for 100 generating units on the same computer platform.

5. CONCLUSIONS

The problem of generating optimal preventive maintenance schedule of generating units for economical and reliable operation of a power system while satisfying system load demand and crew constraints over one year period, has been presented for a 21-unit test system and the Nigerian power system comprising 49 units. Three algorithms, namely the DPSO, MDPSO and GA were applied and compared on the 21-unit test system. The results obtained, showed that the MDPSO performed better than DPSO and GA algorithms. The incorporation of the mutation operator in the MDPSO algorithm significantly improved the diversity of the PSO’s population and ensured convergence towards satisfactory solutions. The results offered a feasible and practical optimal solution that can be implemented in real time.

Two case studies on the Nigerian electric utility hydrothermal unit system, to investigate and characterize the desirability of scheduling some thermal units for maintenance along with the hydro plants during low inflow period, were studied extensively via MDPSO. Several results obtained and analyses carried out were presented from the standpoints of their practical applications. The proposed method has evolved pragmatic maintenance unit scheduling framework for the Nigerian power utility that achieved better utilization of available energy generation with improved reliability and reduction in energy cost. The proposed method can be flexibly modified to accommodate the maintenance unit requirements of emerging independent power producers and future generation additions as well as network constraints not considered in this paper.

ACKNOWLEDGMENT

The financial support from the National Science Foundation (NSF), USA under the grant ECCS # 0348221 is gratefully acknowledged by the authors.

REFERENCES

1 Marwali, M. K. C. and Shahidehpour, S. M.: 'Coordination between long – term and short – term generation scheduling with network constraints', *IEEE Transactions on Power Systems*, August 2000, 15, pp. 1161-1167.

2 Dahal, K. P. and McDonald, J. R.: 'Generator maintenance scheduling of electric power systems using genetic algorithms with integer representation', *IEE Conference on Genetic Algorithms in Engineering Systems: Innovations and Applications*, September 2-4 1997, pp. 456-461.

3 Negnevisky, M. and Kelareva, G.: 'Application of genetic algorithms for maintenance scheduling in power systems', *IEEE Transactions on Power Systems*, 1999, pp. 447-451.

4 Edwin, K. W. and Curtius, F.: 'New maintenance scheduling method with production cost minimization via integer linear programming', *International Journal of Electrical Power and Energy Systems,* 1990, 12, pp. 165-170.

5 Yamayee, Z. and Sidenblad, K.: 'A computationally efficient optimal maintenance scheduling method', *IEEE Transactions on Power Apparatus and Systems*, February 1983, PAS-102, (2), pp. 330-338.

6 Dopaz, J. F. and Merrill, H. M.: 'Optimal generator scheduling using integer programming', *IEEE Transactions on Power Apparatus and Systems*, 1975, PAS-94, pp. 1537-1545.

7 Zurn, H. H. and Quintana, V. H.: 'Generator maintenance scheduling via successive approximations dynamic programming', *IEEE Transactions on Power Apparatus and Systems*, 1975, PAS-94, pp. 667-671.

8 Yamayee, Z. A.: 'Maintenance scheduling: description, literature survey, and interface with overall operations scheduling', *IEEE Transactions on Power Apparatus and Systems*, 1982, PAS-101, pp. 2770-2779.

9 Kim, H., Hayashi, Y. and Nara, K.: 'An algorithm for thermal unit maintenance scheduling through combined GA, SA, and TS', *IEEE Transactions on Power Systems*, February 1997, 12, (1), pp. 329-335.

10 Chen, L. and Toyoda, J.: 'Optimal generating unit maintenance scheduling for multi-area system with network constraints', *IEEE Transactions on Power Systems,* August 1991, 6, (3), pp. 1168-1174.

11 Leou, R. C.: 'A flexible unit maintenance scheduling considering uncertainties', *IEEE Transactions on Power Systems,* August 2001, 16, (3), pp. 553-559.

12 Billinton, R. and Abdulwhab, A.: 'Short-term generating unit maintenance in a deregulated power system using a probabilistic approach', *IEE Proceedings - Generation, Transmission and Distribution,* July 2003, 150, (4), pp. 463-468.

13 Satoh, T. and Nara, K.: 'Maintenance scheduling by using simulated annealing method', *IEEE Transactions on Power Systems,* 1991, 6, pp. 850-857.

14 Yellen, J., Al-khamis, T. M., Vermuri, S. and Lemonidis,. L.: 'A decomposition approach to unit maintenance scheduling', *IEEE Transactions on Power Systems,* 1992, 7, pp. 726-733.

15 Firma, H. T. and Legey, L. F. L.: 'Generation expansion: an iterative genetic algorithm approach', *IEEE Transactions on Power Systems*, August 2002, 17, (3), pp. 901-906.

16 Kennedy, J. and Eberhart, R.: 'Particle swarm optimization', *IEEE International Conference on Neural Networks,* November 1995, 4, pp. 1942-1948.

17 del Valle, Y., Venayagamoorthy, G. K., Mohagheghi, S., Hernandez, J. and Harley, R. G.: 'Particle swarm optimization: Basic concepts, variants and applications in power system', *IEEE Transactions on Evolutionary Computation,* April 2008, 12, (2), pp. 171-195.

18 Dahal, K. P., McDonald, J. R. and Burt, G. M.: 'Modern heuristic techniques for scheduling generator maintenance in power systems', *Transactions of Institute of Measurement and Control,* 2000, 22.

19 Wang, X. and McDonald, J. R.: 'Modern power system planning', McGraw-Hill, London, 1994, pp. 247-307.

20 Kirby, B. J.: 'Spinning reserve from responsive loads', *OAK Ridge National Laboratory-Department of Energy,* 2003, ORNL/TM-2003/19.

21 Davis, L.: 'Handbook on genetic algorithms', Van Nostrand Reinhold, New York, 1991.

22 Clerc, M. and Kennedy, J.: 'The particle swarm – explosion, stability, and convergence in a multidimensional complex space', *IEEE Transactions on Evolutionary Computation*, 2002, 6, (1), pp. 58-873.

APPENDIX

TABLE A.1

Typical Generator Maintenance Schedules Obtained by
DPSO, MDPSO and GA after 5000 Iterations for Case Study I

Week no.	Generating units scheduled for maintenance				Week no.	Generating units scheduled for maintenance		
	DPSO	MDPSO	GA			DPSO	MDPSO	GA
1	5	3,12	1,7,13		27	16	20	14
2	5	2,12	1,7,13		28	16,18	16	14
3	5	2	1,7,13		29	16	16	14
4	4	6	1,7		30	16	16	14
5	4	6,9,13	1		31	16	16	14,16,18
6	4	6,9,13	1		32	16	16	16
7	3,6	6,13	1		33	-	16	16
8	6,10,13	6,7	2		34	20	19	16
9	6,10,13	6,7,10	2		35	21	17,19	16
10	6,10,13	6,7,10	-		36	21	17	16
11	6,9,10	6,7,10	6		37	21	17	-
12	6,9	6,7,11	6		38	21	14	-
13	6	6,8,11	6		39	19	14	15
14	6,7	5	5,6		40	19	14	15
15	6,7	5	4,5,6,12		41	15	14	15
16	6,7	5	4,5,6,12		42	15	14	15
17	2,7	1	4,6		43	15	-	15
18	2,12	1	6		44	15	15	-
19	8,12	1	6		45	15	15	19,20
20	1	1	6		46	17	15	19
21	1	1	-		47	17	15	17
22	1	1	9,10		48	14,17	15	17
23	1	1	9,10,11		49	14	21	17,21
24	1	4	8,10,11		50	14	21	21
25	1	4	3,10		51	14	21	21
26	1	4	-		52	14	18,21	21

TABLE A.2

Typical Generator Maintenance Schedules Obtained by
MDPSO-a and MDPSO-b after 5000 Iterations for Case Study II

Week no.	Generating units scheduled for maintenance			Week no.	Generating units scheduled for maintenance	
	MDPSO-a	MDPSO-b			MDPSO-a	MDPSO-b
1	2,14,15,17	4,9,15		27	22	24,25,30
2	2,6,14,15,17	4,7,9,15		28	22	22,24,25,30,38
3	2,6,15,17,18	4,7,8,15		29	22,37,38	22,25,38,40
4	2,6,15,17,18,20	4,6,8,10,11,15		30	37,38	22,23,38,40
5	2,6,18,20	6,10,11,16		31	25,36	22,23,38,40
6	4,6,12,18,20	1,5,16		32	25,28,36	23,40
7	4,12,19,20	1,5,12,16		33	25,28	23,40
8	4,5,19	1,12,16		34	21,25,28	31,32,37
9	4,5,9,19	1,3		35	21,28,32	18,31,32,37
10	4,5,9,19	1,3		36	21,32,34	18,28,31,37
11	1,5,13	3,13		37	21,32,34	18,28,31,37
12	1,5,13	3,13		38	23,34,35	18,28,37
13	1,3,8	2,3,13		39	23,34,35	20,36
14	1,3,8,16	2,13,14,17		40	23,27	19,20,36
15	1,3,16	2,14,17		41	23,27,31	19,20,26,36
16	3,7,10,11,16	2,14,17		42	27,31	19,20,26,33,36
17	3,7,10,11,16	2,14,17		43	27,31	19,26,33,36
18	33	34		44	46,47,48,49	41,44,49
19	29,33	21,34		45	46,47,48,49	41,44,45,47,49
20	29,30,33	21,27,39		46	46,47,48,49	45,47,49
21	24,30,33	21,27,39		47	46,47,48,49	45,47,49
22	24,30	21,27,35,39		48	39,40,41	45,46,47
23	24,26	35,39		49	39,40,41,44,45	46,48
24	24,26	29,39		50	39,40,44,45	46,48
25	26	24,29,30		51	39,40,42,43	42,43,46,48
26	22,26	24,25,29,30		52	39,40,42,43	42,43,48

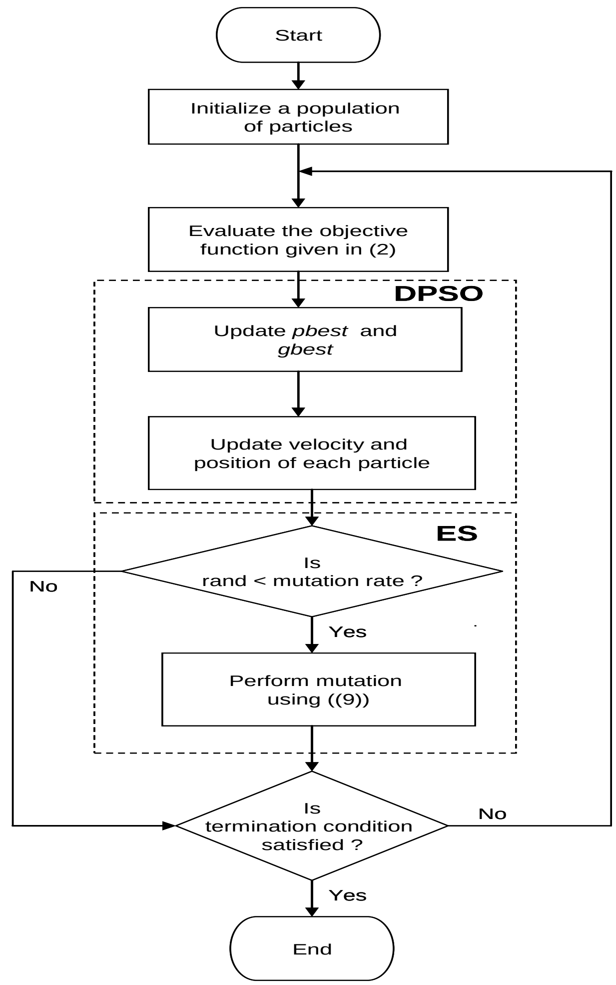

Fig. 1. Flowchart of MDPSO Algorithm for GMS Problem

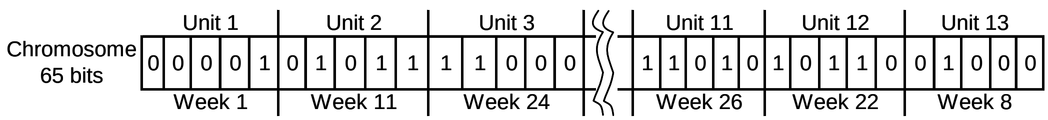

(a) 13 Units (First Six Months)

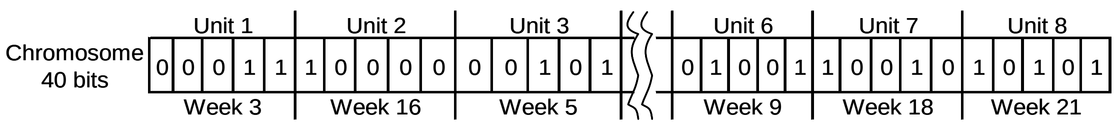

(b) 8 Units (Second Six Months)

Fig. 2. Example of a Chromosome Representation

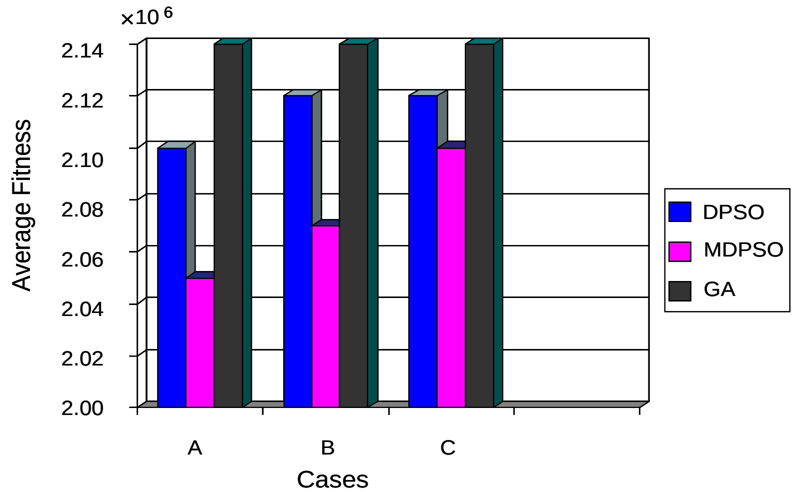

(a) Average Fitness

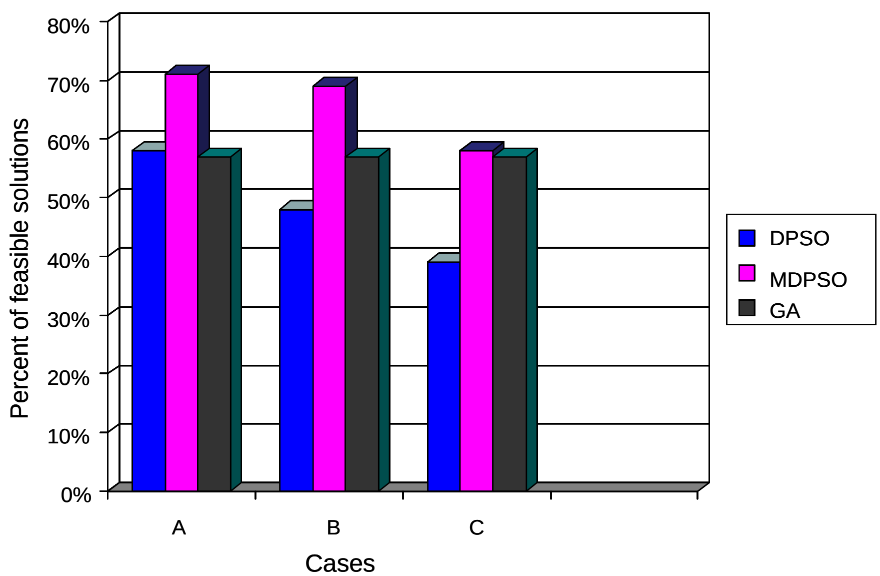

(b) Percent of Feasible Solutions

Fig. 3. Average Fitness and Percent of Feasible Solutions Produced by DPSO, MDPSO and GA for Case Study I

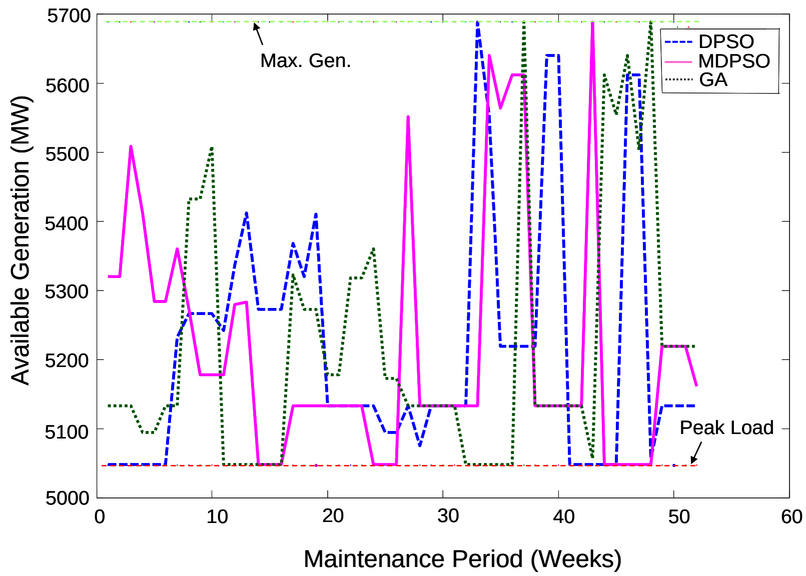

(a) Generation Plots

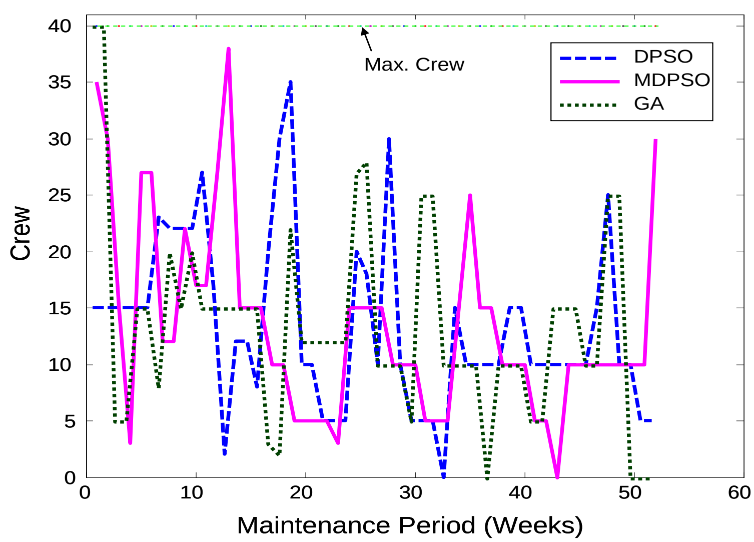

(b) Crew Plots

Fig. 4. Generation and Crew Plots during Maintenance Period for Case Study I

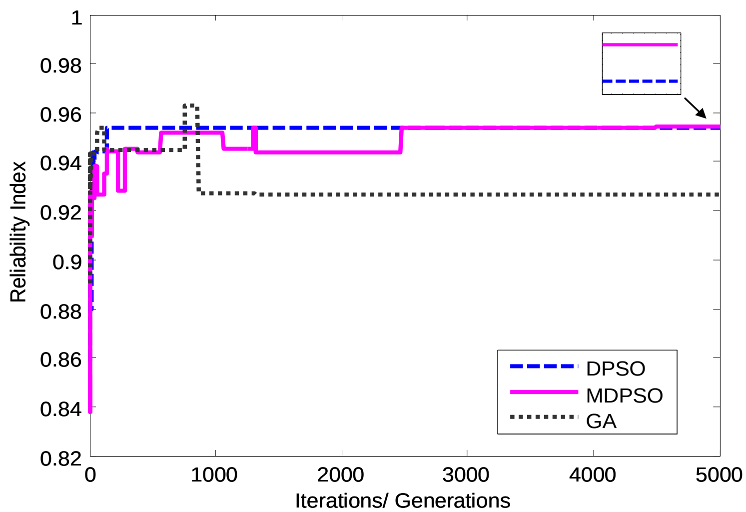

(a) Reliability Indices

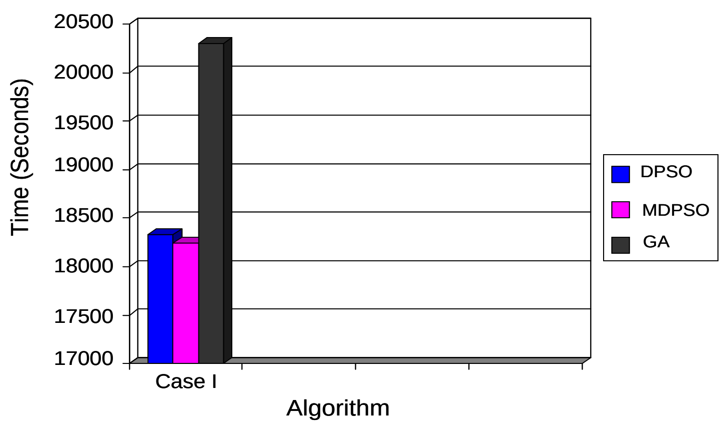

(b) Off-line Execution Time

Fig. 5. Reliability Indices and Off-line Execution Time Plots for DPSO, MDPSO and GA for Fixed Number of 5000 Iterations Over 5000 Trials for Case Study I

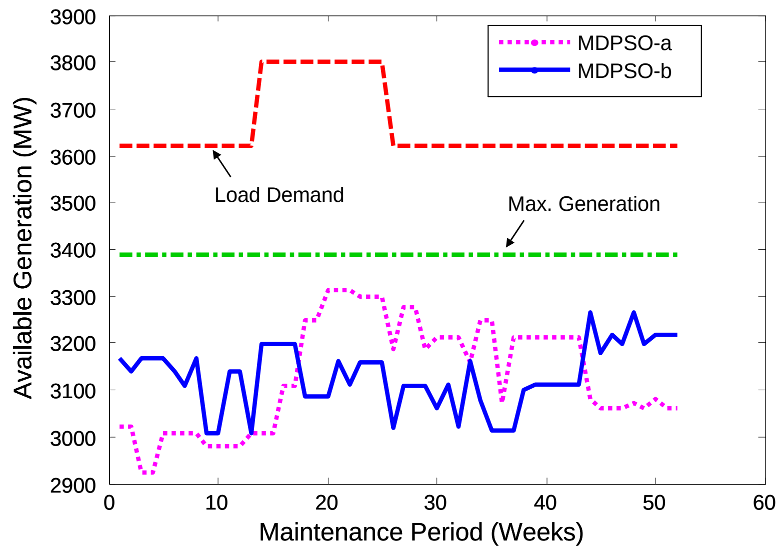

(a) Generation Plots

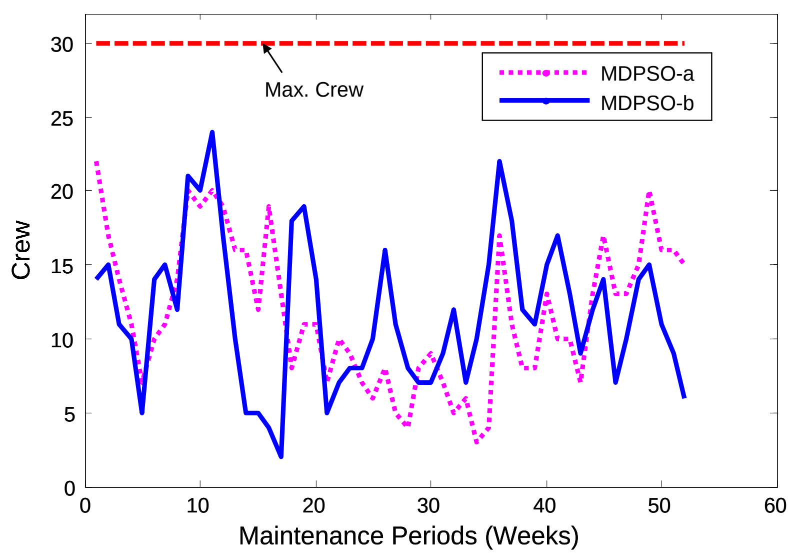

(b) Maintenance crew Plots

Fig. 6. Generation and Crew Plots during Maintenance for Case Study II

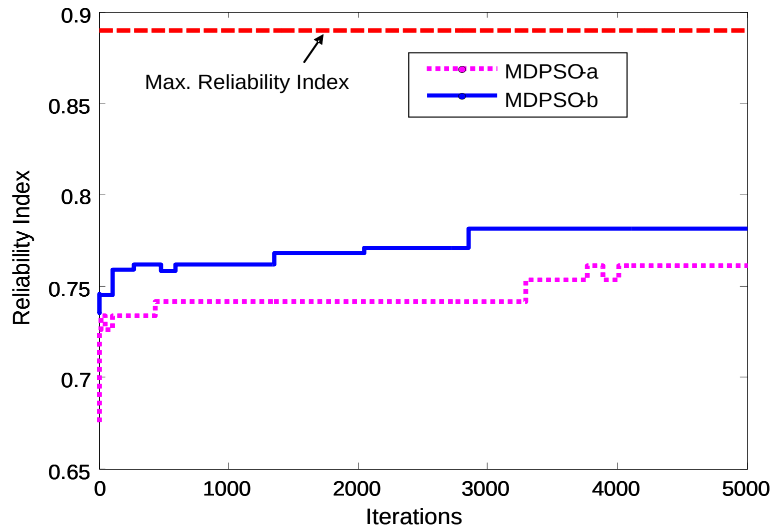

(a) Reliability Index Plots

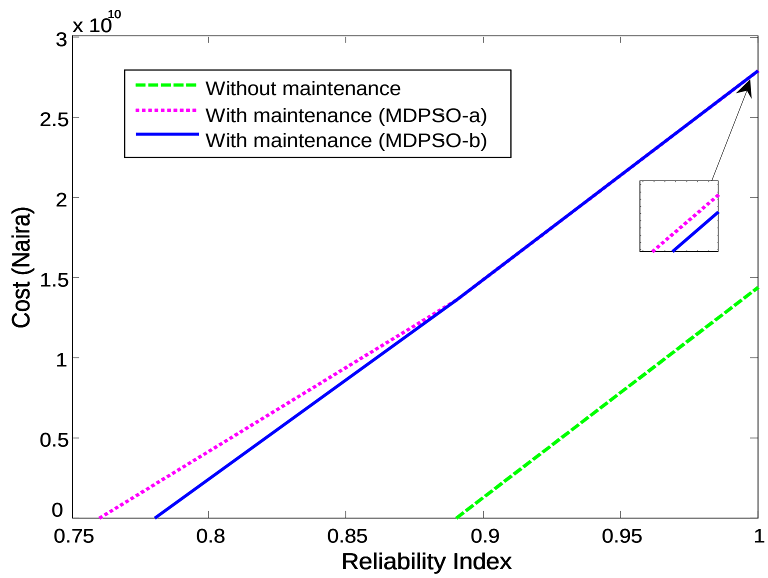

(b) Cost versus Reliability Index Plots

Fig. 7. Reliability Index, Cost versus Reliability Index Plots for MDPSO-a and MDPSO-b for Case Study II and Off-line Execution Time Plot for MDPSO of Case Study I, MDPSO-a and MDPSO-b of Case Study II

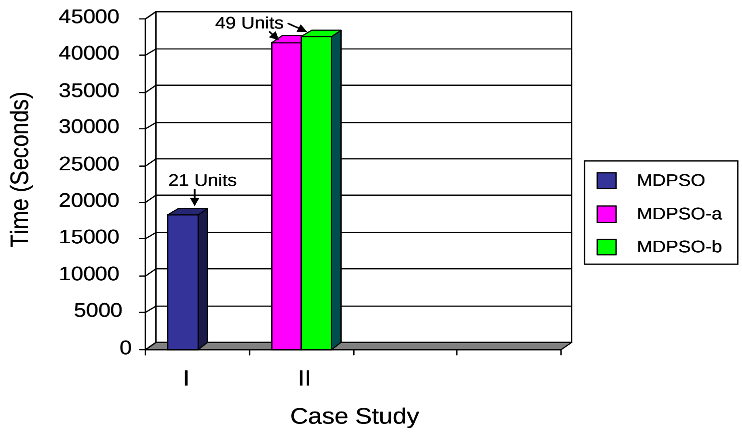

(c) Off-line Execution Time

Fig. 7. Reliability Index, Cost versus Reliability Index Plots for MDPSO-a and MDPSO-b for Case Study II and Off-line Execution Time Plot for MDPSO of Case Study I, MDPSO-a and MDPSO-b of Case Study II (cont.)

II. OPTIMAL MAINTENANCE SCHEDULING OF GENERATORS USING MULTIPLE SWARMS-MDPSO FRAMEWORK

Y. Yare and G. K. Venayagamoorthy

Real-Time Power and Intelligent Systems Laboratory, Department of Electrical and Computer Engineering, Missouri University of Science and Technology,
Rolla, MO 65409-0249 USA
(E-mail: yyqh3@mst.edu & gkumar@ieee.org)

ABSTRACT: In this paper, a challenging power system problem of effectively scheduling generating units for maintenance is presented and solved. The problem of generator maintenance scheduling (GMS) is solved in order to generate optimal preventive maintenance schedules of generators that guarantee improved economic benefits and reliable operation of a power system, subject to satisfying system load demand, allowable maintenance window, and crew and resource constraints. Multiple swarms concept is incorporated into the modified discrete particle swarm optimization (MDPSO) algorithm to form a robust multiple swarms-modified particle swarm optimization (MS-MDPSO) algorithm and is suitably applied to solve this GMS problem. The performance and effectiveness of the MS-MDPSO algorithm in solving the GMS problem is illustrated and compared with the MDPSO algorithm on two power systems, the 21-unit test system and 49-unit Nigerian hydrothermal power system. The GMS of the two power systems are considered and the results presented shows great potential for utility application in their area control centers for effective energy management, short and long term generation scheduling, system planning and operation.

INDEX TERMS: Generator maintenance, multiple swarms-modified discrete particle swarm optimization, optimal scheduling, reliability index.

NOMENCLATURE

AM_t Available manpower at period t

c_1 & c_2 Cognitive constant and social acceleration constants respectively

d	Dimension of the problem
D_i	Duration of maintenance for unit i
DPSO	Discrete particle swarm optimization
e_i	Earliest period for maintenance of unit i to begin
ES	Evolutionary strategy
GA	Genetic algorithm
GMS	Generator maintenance scheduling
i	Index of generating units
I	Set of generating unit indices
l_i	Latest period for maintenance of unit i to end
j	Index of n multiple swarms
k	Discrete time step
l	Index of particle in a swarm
L_t	Anticipated load demand for period t
m	Population size of each swarm
MDPSO	Modified discrete particle swarm optimization
MS-MDPSO	Multiple swarms–modified discrete particle swarm optimization
M_{it}	Manpower needed by unit i at period t
M_r	Mutation rate
N	Total number of generating units
N_c	Number of constraint violation
n	Number of multiple swarms
P_j^t	*j-th* swarm population in time t
P_{jgd}	*j-th* swarm global best position for dimension d
P_{jlbd}	*l-th* particle best position in *j-th* swarm for dimension d
P_{ik}	Generating capacity for unit i in start time period k
P_{it}	Generating capacity of unit i in period t
PSO	Particle swarm optimization
R	Spinning reserve

rand, $rand_1$ *and* $rand_2$ Random numbers for a uniform distribution in the range of [0, 1]

randn() Gaussian distributed random number with a zero mean and a variance of 1

S_{it} Set of start time period

t Index of period

T Set of indices of periods in planning horizon

T_i Set of periods when maintenance of unit *i* may start

$|V_1|$, $|V_2|$ & $|V_3|$ Amount of violations of load, maintenance window and crew constraints respectively

V_c Amount of violation of constraint *c*

V_{jld} *l-th* particle velocity in *j-th* swarm for dimension *d*

w_{iner} Inertia weight constant which is a fixed value, linearly decreasing or dynamically changing

ω_c Weighting coefficient

ω_1, ω_2 & ω_3 Weighting coefficients of load, maintenance window and crew constraints respectively

X_{ik} Maintenance start indicator for unit *i* in start time period *k*

X_{it} Maintenance start indicator for unit *i* in period *t*

X_{jld} *l-th* particle position in *j-th* swarm for dimension *d*

1. INTRODUCTION

Maintenance scheduling of generating units is an important task in power system and plays important role in the operation and planning activities of the electric power utility. The simultaneous solution of all aspects of the operation and planning scheduling problems in the presence of system complexity at different time-scales, different order of uncertainties and problems dimensionality is required for the efficient economic operation of the utility system.

Power system equipment are made to remain in good operating conditions by regular preventive maintenance. The task of generator maintenance is often performed manually by human experts who generate the schedule based on their experience and knowledge of the system, and in such cases there is no guarantee that the optimal or near optimal schedule is found. The purpose of maintenance scheduling is to find the sequence of scheduled outages of generating units over a given period of time such that the level of energy reserve is maintained. This type of schedule is important mainly because other planning activities are directly affected by such decisions. Modern power systems have witnessed increased demand for electrical energy with a related expansion in system size, which leads to higher number of generators and lower reserve margins. The resultant effect is the increased complexity of the constrained generator maintenance scheduling **(**GMS) optimization problem for such large power system. Present research efforts toward solving the GMS constrained optimization problem can be categorized based on the objective function and the type of the problem hyper space [1-10]. Optimization methods such as branch and bound technique [3], dynamic programming [4] and integer programming [5] were few early techniques that were used to solve simple optimization problems. Approximate solution to the constrained GMS problem can be obtained using new problem optimization concepts [9-12]. Some of these optimization methods include but not limited to applications of probabilistic approach [9], simulated annealing [10], decomposition technique [11] and genetic algorithm (GA) [12].

Bio-inspired and evolutionary techniques have been shown to be very effective optimization tools in solving power system problems [13]. Hence their application in solving power system optimization problems, such as GMS, unit commitment and economic dispatch problems. The multi-species particle swarm optimizer presented in [14] extends the original PSO by dividing the particle swarm spatially into a multiple cluster called a species in a multi-dimensional search space. Each species explores a different area of the search space and tries to find out the global or local optima of that area, hence can be used to locate all the global minima of multi-modal functions in parallel [14]. Particle population is split into a set of interacting swarms [15]. These swarms interact locally by an exclusion parameter and globally through a new anti-convergence operator [15]. Cooperative particle swarm optimizer is presented in [16] where cooperative behavior is used to significantly improve the performance of the original PSO algorithm, achieved by using multiple swarms to optimize different components of the solution vector cooperatively. Three sub-swarm discrete particle swarm optimization algorithm is presented in [17], where particles are divided into three sub-swarms. One sub-swarm flies toward global best position, the second sub-swarm flies in the opposite direction, while the third sub-swarm flies randomly around the global best position [17]. A strategy that allocates an appropriate number of swarms as required to support convergence and diversity criteria among the swarms is presented in [18]. The multiple swarms in [18] are encouraged to explore different regions, and their collective efforts and knowledge are shared among the swarms, thus the diversity is preserved. PSO approaches based on some form of implicit or explicit grouping of particles into sub-swarms is presented in [19]. Two main approaches of sub-swarms PSO algorithms in [19] are the cooperative and competitive PSO algorithms. The cooperative PSO algorithm has some form of cooperation existing between sub-swarms. The cooperation is mainly in terms of exchanging information about best positions found by the different groups. On the other hand, the competitive PSO algorithm is where the particles are in direct competition with other particles. Multi-phase PSO algorithm presented in [20-21] divides the main swarm of particles into subgroups, where each subgroup performs a different task, or exhibits a different behavior. The behavior of a group, or a task performed by a group usually changes over time in response to the group’s interaction with the environment, different groups of particles have trajectories that proceed along trajectories with different goals in different phases of the algorithm [20-21]

Capabilities of discrete particle swarm optimization (DPSO) algorithm have been enhanced with evolutionary strategies (ESs) to produce a modified discrete particle swarm optimization (MDPSO) in [22]. Detail comparison of three algorithms – DPSO, MDPSO and GA and their application to solving the power system GMS problem are also presented in [22], which showed that MDPSO produced better results compared with DPSO and GA on similar benchmark test systems.

The primary contributions of this paper are:

- Solving the challenging GMS problem for 21-unit test system and 49-unit Nigerian hydrothermal power system using enhanced evolutionary algorithms.
- Improving the quality of the maintenance schedules generated during GMS in terms of reliability and energy cost over what was achieved by MDPSO [22] algorithm. This improvement is achieved through the use of the multiple swarms concept on the

MDPSO algorithm referred to by the authors as the multiple swarms-modified discrete particle swarm optimization (MS-MDPSO). The MS-MDPSO algorithm takes advantage of maximizing benefits arising from a balanced trade-off of both the exploitation abilities of each n multiple swarms of population sizes m_1, $m_2, \ldots, m_j, \ldots, m_n$ (where $m_1 = m_2 = \ldots = m_j = \ldots = m_n = m$ is been used for this study) and the exploration of the n multiple swarms put together, and then evolving a single global best solution from a set of n global best solutions obtained from n multiple swarms.

- The performance of the MS-MDPSO algorithm is illustrated and compared with the MDPSO [22] algorithm for solving the GMS problem of the two practical power systems.

The rest of the paper is organized as follows: The mathematical problem formulation is presented in Section 2. Section 3 describes the concept of the multiple swarms-MDPSO algorithm. Implementation of MS-MDPSO for GMS and typical results are presented in Section 4. Finally, the conclusions are presented in Section 5.

2. PROBLEM FORMULATION

The purpose of maintenance operation is to extend equipment lifetime, or at least the mean time to the next failure whose repair may be costly. It is expected that effective maintenance policies can reduce the frequency of service interruptions and the many undesirable consequences of such interruptions. Maintenance clearly affects components and system reliability: if too little is done, this may result in an excessive number of costly failures and poor system performance, and hence reliability is degraded, when done too often, reliability may improve but the cost of maintenance will sharply increase. In a cost-effective scheme, reliability and cost of maintenance must be balanced.

Suppose $T_i \subset T$ is the set of periods when maintenance of unit i may start, $T_i = \{t \in T : e_i \le t \le l_i - D_i + 1\}$ for each i.

Define

$$X_{it} = \begin{cases} 1 & \text{if unit } i \text{ starts maintenance in period } t \\ 0 & \text{otherwise} \end{cases} \tag{1}$$

to be the maintenance start indicator for unit *i* in period *t*. Let S_{it} be the set of start time periods *k* such that if the maintenance of unit *i* starts at period *k* that unit will be in maintenance at period *t*, $S_{it} = \{k \in T_i : t - D_i + 1 \le k \le t\}$. Let I_t be the set of units which are allowed to be in maintenance in period t, $I_t = \{i : t \in T_i\}$.

The two main categories of objective functions in solving GMS problem are based on reliability and economic cost [2], [22-24]. The reliability criterion of optimizing generation over the entire operational period of study is considered for solving the GMS problem in this paper. The net reserve of the system during any period *t* is the total installed capacity from all generating units $\left(\sum_{i \in I_t} P_{it}\right)$ minus the reserve loss due to the pre-scheduled outages as a result of planned generator maintenance $\left(\sum_{i \in I_t} \sum_{k \in S_{it}} X_{ik} \cdot P_{ik}\right)$ and the peak load forecast for that maintenance period (L_t). Hence the component $\left(\sum_{i \in I_t} P_{it} - \sum_{i \in I_t} \sum_{k \in S_{it}} X_{ik} \cdot P_{ik} - L_t\right)$ represents the net reserve level in time period *t*. Minimizing the sum of the squares of the reserves over the entire operational planning period enhances reduction in large variations of reserve and better long-term reserve capacity planning in the presence of unit maintenance. Therefore, the objective function to be minimized can be expressed by (2).

$$\min_{X_{it}} \left\{ \sum_t \left(\sum_i P_{it} - \sum_{i \in I_t} \sum_{k \in S_{it}} X_{ik} \cdot P_{ik} - L_t \right)^2 \right\} \tag{2}$$

The objective function in (2) is minimized subject to the following unit and system constraints given by (3), (4) and (5). Transmission loss and network limitations constraints are not considered for simplicity, but could be flexibly incorporated.

- Load and spinning reserve constraints – this specifies that the total capacity of the units running at any interval should not be less than forecasted load and spinning reserve for that interval.

$$\sum_{i} P_{it} - \sum_{i \in I_t} \sum_{k \in S_{it}} X_{ik} \cdot P_{ik} \geq L_t \qquad \forall t, \tag{3}$$

- Maintenance window and sequence constraints – this defines the starting of maintenance at the beginning of an interval and finishing at the end of the same interval. The maintenance cannot be aborted or finished earlier than scheduled.

$$\sum_{t \in T_i} X_{it} = 1 \qquad \forall i \, , \tag{4}$$

- Crew and resource constraints – this specifies that for each maintenance period, the number of people to perform maintenance schedule cannot exceed the available crew. It also defines manpower availability and the limits on the resources/tools needed for maintenance activity at each time period.

$$\sum_{i \in T_t} \sum_{k \in S_{it}} X_{ik} \cdot M_{ik} \leq AM_t \qquad \forall t, \tag{5}$$

Penalty cost given by (6) is added to the objective function in (2) if the schedule cannot satisfy the load, maintenance window and crew constraints. The penalty value for each constraint violation $|V_1|$, $|V_2|$ *and* $|V_3|$ is proportional to the amount by which the constraint is violated.

$$Penalty\mathrm{cost} = \sum_{c=1}^{N_c} \omega_c |V_c| = \omega_1 |V_1| + \omega_2 |V_2| + \omega_3 |V_3| \tag{6}$$

The weighting coefficients ω_1, ω_2 & ω_3 are chosen in such a way that the violation of harder constraints gives a greater penalty value than for softer constraints. Typically the weighting coefficients are in the range 0.2 to 1.2.

3. MULTIPLE SWARMS-MDPSO ALGORITHM

Subsection 3.1 presents the MDPSO algorithm, while subsection 3.2 presents the design details of the MS-MDPSO algorithm whose flowchart is shown in Fig. 1 (a) and (b).

3.1. MDPSO

The modified discrete particle swarm optimization (MDPSO) algorithm presented in [19], [22] is an enhancement of DPSO algorithm with the inclusion of an evolutionary strategy based mutation operator similar to the one used in genetic algorithm. The MDPSO algorithm is applied in the update procedure of the velocities and positions of the particles [22].

Let X and V denote a particle's coordinates (position) and its corresponding flight speed (velocity) in a search space, respectively. Therefore, the lth particle is represented as $X_{ld} = (X_{l1}, X_{l2}, \ldots, X_{lN})$ in the d-dimensional space. The best previous position of the lth particle, referred to as *pbest*, is recorded and represented as $P_{lbd} = (P_{lb1}, P_{lb2}, \ldots, P_{lbN})$. The index of the best particle among all the *pbest* in the swarm is referred to as the *gbest* and is represented by P_{gd}. The rate of the velocity for particle lth is represented as $V_{ld} = (V_{l1}, V_{l2}, \ldots, V_{lN})$. The new velocity and position for each particle i in dimension d is determined according to the velocity and position update equations given by (7) and (8) respectively. The inertia weight w_{iner} is updated according to (9).

$$V_{ld}(t) = round\left(w_{iner} \cdot V_{ld}(t-1) + c_1 \cdot rand_1 \cdot \left(P_{lbd}(t-1) - X_{ld}(t-1)\right) + c_2 \cdot rand_2 \cdot \left(P^*_{gb}(t-1) - X_{ld}(t-1)\right)\right) \tag{7}$$

$$X_{ld}(t) = X_{ld}(t-1) + V_{ld}(t) \tag{8}$$

$$w_{iner} = w_{iner}^{\max} - \left(\frac{w_{iner}^{\max} - w_{iner}^{\min}}{iter_{\max}}\right) \times iter \tag{9}$$

A mutation operator is introduced into the DPSO algorithm above, so that the swarm's best position in dimension d is updated according to (10). Supposing P^*_{gd} is the particle chosen with a random number less than a predefined mutation rate (for 0<mutation rate<0.3), then the mutation equation is given by (10).

$$P_{gd}^{*} = P_{gd} + (randn() \times P_{gd} / 2) \tag{10}$$

where d = 1, 2, …, N is the problem dimension.

3.2. MS-MDPSO

The concept of multiple swarms in modified discrete particle swarm optimization (MDPSO) to explore the problem space together for the purpose of finding optimal solutions is considered in this paper. Multiple swarms in MDPSO select their own global best leaders to lead and influence their movement toward the best solution found so far. Information shared within a swarm and among swarms is portrayed in the multiple swarms' movement. This concepts produce an improved and efficient hybrid algorithm referred to in this paper, as the multiple swarms-modified discrete particle swarm optimization (MS-MDPSO) algorithm and is applied to solving the GMS problem as illustrated in the flowchart of Fig. 1 (a) and (b).

The MS-MDPSO algorithm takes advantage of maximizing benefits arising from a balanced trade-off of both the exploitation abilities of each n multiple swarms of population sizes $m_1, m_2, \ldots, m_j, \ldots, m_n$ (where $m_1 = m_2 = \ldots = m_j = \ldots = m_n = m$ is been used for this study) and the exploration of the n multiple swarms put together, and then evolving a single global best solution from a set of n global best solutions obtained from n multiple swarms. It is this newly found single global best solution that is used to generate the optimal solution (optimal maintenance schedules) for this GMS problem as depicted in Fig. 1 (a) and (b).

Particle X_{jl}^{k} (where j=1, 2,…, n, and l=1, 2,…, m) in each of the n multiple swarms of population P_1^k, P_2^k, …, P_j^k, …, P_n^k with sizes $m_1, m_2, \ldots, m_j, \ldots, m_n$ respectively can be modeled at discrete time k by (11).

$$\begin{gathered} P_1^k = \left[X_{11}^k \middle| X_{12}^k \middle| \cdots \middle| X_{1m_1}^k\right], P_2^k = \left[X_{21}^k \middle| X_{22}^k \middle| \cdots \middle| X_{2m_2}^k\right], \ldots, \\ P_j^k = \left[X_{j1}^k \middle| X_{j2}^k \middle| \cdots \middle| X_{jm_j}^k\right], \ldots, P_n^k = \left[X_{n1}^k \middle| X_{n2}^k \middle| \cdots \middle| X_{nm_n}^k\right] \end{gathered} \tag{11}$$

where $m_1 = m_2 = \ldots = m_j = \ldots = m_n = m$ for this study.

The MDPSO velocity and position update equations given by (7) and (8) respectively are modified and used in the MS-MDPSO algorithm to update the particles' velocities and positions in each n multiple swarms as shown in (12)-(13).

$$\begin{aligned} V_{jld}(k) = round\ (w \cdot V_{jld}(k-1) + c_1 \cdot rand_1 \cdot (P_{jlbd}(k-1) - X_{jld}(k-1)) \\ + c_2 \cdot rand_2 \cdot (P_{jgd}(k-1) - X_{jld}(k-1))) \end{aligned} \tag{12}$$

$$X_{jld}(k) = X_{jld}(k-1) + V_{jld}(k) \tag{13}$$

With w =0.8, c_1=2 and c_2=2, the particles have good global searching abilities and converge to the global optimal position.

For mutation rate that lies within the range ($0 < M_r < 0.3$), the mutation equation of the chosen particle is modified from (10) and given by (14)-(15).

$If\ \ rand < M_r$

$$P^*_{jgd}(k-1) = P_{jgd}(k-1) + ceil\ (randn\ \times P_{jgd}(k-1) / \beta_{gb}) \tag{14}$$

$else$

$$P^*_{jgd}(k-1) = P_{jgd}(k-1)` \tag{15}$$

end

Where β_{gb} can be either dynamically changing or fixed, and controls the mutation process. The mutation operation increases the diversity of the population by preventing the particles from moving too close to each other, thus converging prematurely to local optima.

4. IMPLEMENTATION OF MS-MDPSO FOR GMS AND RESULTS

Two case studies are presented in this section to demonstrate the application and performance of the MS-MDPSO algorithm compared with MDPSO algorithm for solving the GMS problem of two practical power systems.

4.1. GMS Implementation with MS-MDPSO

The global best solution is the evolved single best solution from a set of *n* global best solutions of the *n* multiple swarms. The performances of the *n* global best solutions are measured by comparing their fitness evaluations against each other. The resultant solution with the best fitness emerges as the single global best solution of the *n* multiple swarms. The global best solution is then used to generate the optimal maintenance schedules for all the generating units. It is also used to determine the optimal maintenance start period X_{ik} for each generating unit *i*, and when applied to (3) and (5) it produces the optimal available generation from all running units during maintenance and crew requirement for generators undergoing maintenance respectively over a maintenance period of fifty two weeks.

4.2. 21-Unit Test System

A test system comprising twenty one generating units [2], [4], [22-24] with installed capacity, units' maintenance duration (weeks) and anticipated manpower requirement over a maintenance planning period of fifty two weeks is used to demonstrate the performance of the MS-MSPSO algorithm for the GMS problem. Table 1 shows the unit rating, allowed maintenance period, maintenance duration and technical manpower/crew requirement by generating units during each maintenance week. The maintenance outages for the generating units are scheduled to minimize the sum of squares of reserves and meet the maintenance window constraint (each unit must be maintained exactly once every fifty two weeks without interruption), the system peak load demand (4739MW), and manpower/crew requirements to carry out maintenance tasks (there is maximum of thirty five in total of technical manpower/crews available each week for the maintenance work).

4.2.1. Test, Results and Discussion

Figures 2 (a) and (b) show typical available generation and maintenance crew plots respectively for the 21-unit test system using the MDPSO and MS-MDPSO algorithms.

TABLE 1

Data for the 21-Unit Test System

Unit	Capacity (MW)	Allowed maintenance period	Maintenance duration (weeks)	Manpower required by units for each maintenance week
1	555	1-26 weeks	7	10+10+5+5+5+5+3
2	180		2	15+15
3	180		1	20
4	640		3	15+15+15
5	640		3	15+15+15
6	276		10	3+2+2+2+2+2+2+2+2+3
7	140		4	10+10+5+5
8	90		1	20
9	76		2	15+15
10	94		4	10+10+10+10
11	39		2	15+15
12	188		2	15+15
13	52		3	10+10+10
14	555	27-52 weeks	5	10+10+10+5+5
15	640		5	10+10+10+10+10
16	555		6	10+10+10+5+5+5
17	76		3	10+15+15
18	58		1	20
19	48		2	15+15
20	137		1	15
21	469		4	10+10+10+10

It can be deduced from these figures and the typical maintenance schedules presented in Table A.1 of the Appendix that using the MDPSO algorithm, weeks 23 and 35 indicate periods with low maintenance task (no unit is scheduled for maintenance) resulting in comparatively high available generation on same weeks 23 and 35. Similarly, using the MS-MDPSO algorithm, weeks 30 and 36 indicate periods with low maintenance activity (no unit is scheduled for maintenance) resulting in comparatively high available generation on same weeks 30 and 36. The weekly manpower requirement depicted in Fig. 2 (b) using the MS-MDPSO algorithm clearly satisfies the crew constraint expressed in (5). This is not the case with the MDPSO algorithm, the 8*th* week experienced lowest drop in available generation (shown in Fig. 2(a)) due to heightened maintenance activities carried out simultaneously on units 3, 6 and 11 (shown in Table A.1 of the Appendix), which also violated the manpower/crew constraint in (5). However, both the MDPSO and MS-MDPSO algorithms produced available generation that satisfies the constraint given by (3) as shown in Fig. 2 (a).

Figure 2 (c) shows typical convergence of the objective function given in (2) for the 21-unit test system using MDPSO and MS-MDPSO algorithms, obtained after 100 iterations. The figure shows that the minimization of the objective function converged to 13863021.02 and 13749264.32 using the MDPSO and MS-MDPSO algorithms respectively. A lower value of the objective function is preferable for better economic benefit, and is also a guarantee for more effective maintenance schedules produced by the MS-MDPSO algorithm.

Table 2 presents the statistical comparison of convergence of the objective function for the 21-unit test system using the MDPSO and MS-MDPSO algorithms, obtained after 100 iterations of 5000 trials. The table shows optimal numerical values of the objective function produced by MDPSO and MS-MDPSO to be 13863021.02 and 13749264.32 respectively, representing 113756.70 (0.82%) reduction. This indicates improvement in minimizing the objective function given by (2) using MS-MDPSO compared with MDPSO algorithm, especially in cases with large variations of system net reserve. It also represents improvement in the quality of maintenance schedules generated by the MS-MDPSO algorithm compared with the MDPSO algorithm. The statistical results presented in Table 2 for the 21-unit test system shows, generally, that the MS-MDPSO algorithm produced better maintenance schedules compared with the MDPSO algorithm for the same GMS problem.

TABLE 2

Statistical Comparison of Convergence of the
Objective Function for the 21-Unit Test System

	Algorithm	
	MDPSO	MS-MDPSO
Minimum	13863021.02	13749264.32
Maximum	14132336.49	14015289.69
Mean	13984883.84	13870778.81
Standard deviation	±11943	±11429

Table 3 and Fig. 2 (d), (e), and (f) further illustrates the design and application of MS-MDPSO algorithm for solving the GMS problem by presenting typical evolution of single global best solution (*Gbest*) from a set of five global best solutions ($gbest_1$, $gbest_2$, *gbest*$_3$, *gbest*$_4$ and *gbest*$_5$) obtained from five multiple swarms (n=5) over five trials for the 21-unit test system presented in subsection 4.2. Table 3 and Fig. 2 (e) shows that for the 21-unit test system, the *Gbest* (consisting of an array of 100 global best solutions) obtained for 100 iterations over the first trial is primarily composed of *gbest*$_1$ (33 global best solutions from swarm #1), *gbest*$_2$ (28 global best solutions from swarm #2), *gbest*$_3$ (22 global best solutions from swarm #3), *gbest*$_4$ (14 global best solutions from swarm #4) and *gbest*$_5$ (2 global best solutions from swarm #5). Further, Gbest feasible solutions obtained over five trials are presented in Table 3 and depicted in Fig. 2 (f).

TABLE 3

Gbest Solution for the 21-Unit Test System using MS-MDPSO

	21-unit test system					
	Number of trials					
	#1 (Iterations)	#2 (Iterations)	#3 (Iterations)	#4 (Iterations)	#5 (Iterations)	Total (%)
gbest$_1$	33	2	4	48	8	95 (19.0%)
gbest$_2$	28	55	19	24	61	187 (37.4%)
gbest$_3$	22	40	4	14	16	96 (19.2%)
gbest$_4$	15	2	2	10	12	41 (8.2%)
gbest$_5$	2	1	71	4	3	81 (16.2%)
Gbest	100	100	100	100	100	500 (100%)

4.3. Nigerian Grid System

Table 4 presents data of the Nigerian grid system comprising a total of forty nine functional generating units spread across seven generating stations located at: AFAM, DELTA, EGBIN, SAPELE, JEBBA, KAINJI and SHIRORO [22] as depicted in Fig. 3. The table shows the type of power station, name of power station, plant number, name of turbine unit, type of turbine, unit's actual base case rating, allowed maintenance period, maintenance duration and technical manpower/crew requirement by generating unit for each maintenance week. All the generating units at AFAM and DELTA stations as well as eight generating units at EGBIN station are gas turbines (GTs), while all generating units at SAPELE station and other six generating units at EGBIN station are steam turbines (STs). Also the four thermal plants utilize natural gas supplied from the Nigerian Gas Company (NGC) as their raw material input. The three hydro stations (Hs) namely JEBBA, KAINJI and SHIRORO are located in Northwestern Nigeria. Well over two decades of operational experience and available historical data on hydrological conditions reveal that inflow variation profile at each hydro station location, by and large affects the generated power output of each hydro plant [22]. The maintenance window and sequence constraints of the three hydro plants are greatly influenced by the trend of the inflow into these hydrological areas. This result in two distinct case studies namely, case a: MDPSO-a and MS-MDPSO-a and case b: MDPSO-b and MS-MDPSO-b described below.

4.3.1. Case a: MDPSO-a and MS-MDPSO-a

The operational data for the Nigerian grid system used to illustrate the effectiveness and performance of the proposed MS-MDPSO algorithm and compared with MDPSO algorithm is shown in Table 1. The 49 generating units of the Nigerian data need to be scheduled for maintenance over a 52 week maintenance planning period. The allowed period for maintenance, maintenance duration and the manpower required for each maintenance week are also shown in Table 1. Thermal and steam turbines could be shut down for maintenance only when the hydro plants are operating at their maximum generation, which tallies with the months of January to April and November to December each operational year. On the other hand, the hydro plants can be scheduled for maintenance during low water level corresponding to the months of May to October, the thermal plants supports the hydro generation within these periods and should therefore not be scheduled for shutdown maintenance. 5% increased load variation is allowed during the hot season of March to July each operational year.

4.3.2. Case b: MDPSO-b and MS-MDPSO-b

The economic implication in terms of reduced energy cost and increased reliability is enhanced by a logical and appropriate combination of thermal and hydro plants for maintenance within the period of low water level from May to October.

TABLE 4

Power Station, Maintenance and Manpower Data for the 49 Generating Units in the Nigerian Grid System

Type of power station	Power station						Allowed maintenance period	Maintenance duration (Weeks)	Manpower required by units for each maintenance week
	Name of power station	S/N	Plant number	Name of turbine unit	Type of turbine	Base case rating (MW)			
Thermal	Egbin PS	1	3	EGBINST1	ST	190.0	January - April (1 - 17 weeks)	5	6+5+5+4+2
		2	3	EGBINST2	ST	190.0		5	6+5+5+4+2
		3	3	EGBINST3	ST	190.0		5	6+5+5+4+2
		4	3	EGBINST4	ST	190.0		5	6+5+5+4+2
		5	3	EGBINST5	ST	190.0		5	6+5+5+4+2
		6	3	EGBINST6	ST	190.0		5	6+5+5+4+2
		7	4	EGBINGT1	GT	220.0		2	4+3
		8	4	EGBINGT2	GT	30.0		2	4+3
		9	4	EGBINGT3	GT	30.0		2	4+3
		10	4	EGBINGT4	GT	30.0		2	4+3
		11	4	EGBINGT5	GT	30.0		2	4+3
		12	4	EGBINGT6	GT	30.0		2	4+3
		13	4	EGBINGT7	GT	30.0		2	4+3
		14	4	EGBINGT8	GT	30.0		2	4+3
	Sapele PS	15	5	SAPELST1	ST	0.0		4	4+3+3+2
		16	5	SAPELST2	ST	0.0		4	4+3+3+2
		17	5	SAPELST3	ST	0.0		4	4+3+3+2
		18	5	SAPELST4	ST	0.0		4	4+3+3+2
		19	5	SAPELST5	ST	0.0		4	4+3+3+2
		20	5	SAPELST6	ST	85.3		4	4+3+3+2
Hydro	Jebba PS	21	6	JEBBGH1	H	88.3	May - October (18 - 43 weeks)	4	5+4+3+2
		22	6	JEBBGH2	H	88.3		4	5+4+3+2
		23	6	JEBBGH3	H	88.3		4	5+4+3+2
		24	6	JEBBGH4	H	88.3		4	5+4+3+2
		25	6	JEBBGH5	H	88.3		4	5+4+3+2
		26	6	JEBBGH6	H	88.3		4	5+4+3+2
	Kainji PS	27	7	KAING05	H	112.5		4	5+5+4+3
		28	7	KAING06	H	0.0		4	5+5+4+3
		29	7	KAING07	H	0.0		3	4+3+2
		30	7	KAING08	H	0.0		3	4+3+2
		31	7	KAING09	H	0.0		3	4+3+2
		32	7	KAING10	H	76.5		3	4+3+2
		33	7	KAING11	H	90.0		4	5+4+3+3
		34	7	KAING12	H	0.0		4	5+4+3+3
	Shiroro PS	35	8	SHIRGH1	H	249.0		2	4+3
		36	8	SHIRGH2	H	249.0		2	4+3
		37	8	SHIRGH3	H	140.0		2	4+3
		38	8	SHIRGH4	H	249.0		2	4+3
Thermal	Afam PS	39	1	AFAMGT19	GT	138.0	November - December (44 - 52 weeks)	5	5+5+4+3+3
		40	1	AFAMGT20	GT	138.0		5	5+5+4+3+3
	Delta PS	41	2	DELTAG03	GT	19.6		2	4+3
		42	2	DELTAG04	GT	19.6		2	4+3
		43	2	DELTAG06	GT	19.6		2	4+3
		44	2	DELTAG07	GT	19.6		2	4+3
		45	2	DELTAG08	GT	0.0		4	4+4+3+3
		46	2	DELTAG15	GT	85.0		4	4+4+3+3
		47	2	DELTAG16	GT	85.0		4	4+4+3+3
		48	2	DELTAG17	GT	85.0		4	4+4+3+3
		49	2	DELTAG18	GT	85.0		4	4+4+3+3

*PS- Power station, GT- Gas turbine, ST- Steam turbine, H- Hydro.

These are investigated in this case study. Only five of the thermal plants, namely AFAMG 19, AFAMG 20, EGBINST 1, EGBINST 2 and SAPELEST 6 are allowed to be scheduled for maintenance along with the hydro plants within the period of low water level. There is 5% increased load variation allowed during the hot season of March to July each operational year

4.3.3. Test, Results and Discussion

Table A.2 in the Appendix presents the generator schedules obtained by case a: MDPSO-a and MS-MDPSO-a, while the schedules produced by case b: MDPSO-b and MS-MDPSO-b are shown in Table A.3. Notice that both MDPSO-b and MS-MDPSO-b of case b in Table A.3 generate similar maintenance schedules for weeks 14, 15, 16 and 17.

Table 5 presents the annual generation, load demand and the cost in Nigerian Naira for purchasing energy form Independent Power Producers (IPPs). The resultant suppressed loads as a consequence of scheduled maintenance work are also shown in Table 5. The suppressed loads can be catered for by purchase of additional energy from IPPs, or other sources. The annual base case generation for Nigeria cannot meet the annual load demand due to inadequate generation from some generating units. These units' energy contributions to the national grid are marginally low and are represented with a zero generation as shown in Table 4. This scenario translates to frequent load shedding over the entire maintenance planning period of fifty two weeks. Table 5 shows 94.35% and 94.30% increases in suppressed loads due to scheduled maintenance planning using MDPSO-a and MS-MDPSO-a respectively. These translates to 13,524,336,000.00Naira/year and 13,517,280,000.00Naira/year as costs of purchasing additional energy from IPPs to supplement and meet the rising energy demand occasioned by the increases in suppressed loads due to scheduled maintenance. Table 5 shows that case MS-MDPSO-a produces a 0.05% reduction in suppressed load increase compared to case MDPSO-a under scheduled shutdown maintenance.

Similarly, Table 5 also shows 94.32% and 94.27% increases in suppressed load occasioned by scheduled maintenance planning using MDPSO-b and MS-MDPSO-b respectively. These infer 13,520,304,000.00Naira/year and 13,513,248,000.00Naira/year as costs of purchasing additional energy from IPPs to satisfy the rising energy demand caused by increases in suppressed loads due to scheduled maintenance. Case MS-MDPSO-b produces a 0.05% reduction in suppressed load increase compared to case MDPSO-b under scheduled maintenance. These reductions translate to a huge annual savings of energy to be purchased in order to service the suppressed loads. The percentages may be small, but they are worth noting considering their impacts over an entire operational year, and could form basis for good planning and better energy management. Saved cost of fuel for units scheduled for maintenance was not considered in this study.

TABLE 5

Annual Generation, Load Demand and Cost of Purchasing Energy

	Annual generation - without maintenance	Annual generation - with scheduled shutdown maintenance	Annual load demand	Annual suppressed load - without maintenance	Annual suppressed load - with scheduled shutdown maintenance	Increase in suppressed load due to maintenance
Case MDPSO-a						
Mega watt hour (MWh)	29,601,936.00	27,348,048.00	31,990,896.00	2,388,960.00	4,643,016.00	94.35%
Cost of purchasing energy (X 1000 Naira/year)			191,945,376.00	14,333,760.00	27,858,096.00	13,524,336.00
Case MS-MDPSO-a						
Mega watt hour (MWh)	29,601,936.00	27,349,056.00	31,990,896.00	2,388,960.00	4,641,840.00	94.30%
Cost of purchasing energy (X 1000 Naira/year)			191,945,376.00	14,333,760.00	27,851,040.00	13,517,280.00
Case MDPSO-b						
Mega watt hour (MWh)	29,601,936.00	27,348,552.00	31,990,896.00	2,388,960.00	4,642,344.00	94.32%
Cost of purchasing energy (X 1000 Naira/year)			191,945,376.00	14,333,760.00	27,854,064.00	13,520,304.00
Case MS-MDPSO-b						
Mega watt hour (MWh)	29,601,936.00	27,349,728.00	31,990,896.00	2,388,960.00	4,641,168.00	94.27%
Cost of purchasing energy (X 1000 Naira/year)			191,945,376.00	14,333,760.00	27,847,008.00	13,513,248.00

*Cost of energy in Nigeria: 6 Naira/kWh and 150 Naira is equivalent to 1 US Dollar

Figure 4 (a) shows the available generation for case a: MDPSO-a and MS-MDPSO-a, while the available generation for case b: MDPSO-b and MS-MDPSO-b are presented in Fig. 4 (b). Presented in the two figures are also the maximum generation of 3388MW and a 5% load variation within the hot season of March to July each year. For cases MDPSO-a and MS-MDPSO-a, between the months of May and October when the hydro plants are undergoing maintenance, the major energy generation is supplied from the thermal plants since they are not scheduled for maintenance within this period. Their energy generation curves are not spread evenly over the entire maintenance period, which is interpreted as resulting to an unpredictable energy profile which causes large and sudden variations in loads requiring shedding. Cases MDPSO-b and MS-MDPSO-b however, generate evenly distributed generation throughout the year under maintenance, with an average generation and standard deviation of 3130.557±79.781MW and 3130.692±78.125MW respectively. While cases MDPSO-a and MS-MDPSO-a produce average generation and standard deviation of 3130.500±121.075MW and 3130.610±119.559MW respectively.

Figures 4 (c) and (d) presents the corresponding crew availability needed to carryout the scheduled shutdown maintenance of the generating units for case a: MDPSO-a and MS-MDPSO-a, and case b: MDPSO-b and MS-MDPSO-b respectively. Case b: MDPSO-b and MS-MDPSO-b scheduling generate more even crew distribution over the maintenance period compared with case a: MDPSO-a and MS-MDPSO-a. Both cases however satisfied the crew constraint placed at thirty. Cases MDPSO-a and MS-MDPSO-a have an average crew requirement and standard deviation of 12±5.438 and 12±4.769 respectively, while cases MDPSO-b and MS-MDPSO-b require 12±3.658 and 12±3.567 respectively.

Table 6 presents the cost of improving 'reliability index' (RI) for case a: MDPSO-a and MS-MDPSO-a and case b: MDPSO-b and MS-MDPSO-b without maintenance and with scheduled shutdown maintenance. The RI is computed by taking the minimum of the ratio of available generation to load demand over 5000 trials and the entire operational period [22] as given by (16).

$$RI = \underset{\substack{(over\ 5000\\ trials)}}{Min}\left(\underset{\substack{(over\ 52\\ weeks)}}{Min}\left(\begin{matrix}\frac{Avail.Gen.}{Load} & if\ Avail.Gen. \leq Load\\ 1 & otherwise\end{matrix}\right)\right) \tag{16}$$

Table 6 shows that case MS-MDPSO-a produces schedules with better RI compared with case MDPSO-a, while case MS-MDPSO-b produces improved RI over case MDPSO-b under scheduled shutdown maintenance for 100 iterations of 5000 trials. Further experiments for 5000 iterations of 5000 trials reveals RIs of 0.76, 0.769, 0.78 and 0.786 for cases MDPSO-a, MS-MDPSO-a, MDPSO-b and MS-MDPSO-b respectively. The costs for 0.89 and 1 RIs under maintenance is seen to be the least for case MS-MDPSO-b and the highest for case MDPSO-a. These numerical RIs suggest that the

Nigerian power system is more reliable when this long-term maintenance planning is based on MS-MDPSO algorithm compared with MDPSO algorithm. It also imply enhanced capability of long-term predictability of generation and manpower/crew requirement needed for maintenance over the entire maintenance horizon using MS-MDPSO algorithm compared with MDPSO algorithm.

TABLE 6

Cost of Improving the Reliability Index

	Without maintenance		With scheduled shutdown maintenance		
	Case MDPSO-a				
Reliability index	0.89	1	0.752	0.89	1
Cost (x1000 Naira)	0	14,333,760.00	0	13,524,336.00	27,858,096.00
	Case MS-MDPSO-a				
Reliability index	0.89	1	0.761	0.89	1
Cost (x1000 Naira)	0	14,333,760.00	0	13,517,280.00	27,851,040.00
	Case MDPSO-b				
Reliability index	0.89	1	0.766	0.89	1
Cost (x1000 Naira)	0	14,333,760.00	0	13,520,304.00	27,854,064.00
	Case MS-MDPSO-b				
Reliability index	0.89	1	0.772	0.89	1
Cost (x1000 Naira)	0	14,333,760.00	0	13,513,248.00	27,847,008.00

Figures 5 (a) and (b) show the plots of RIs versus iterations for case a: MDPSO-a and MS-MDPSO-a, and case b: MDPSO-b and MS-MDPSO-b respectively during shutdown maintenance period, compared against the maximum RI of 0.89 representing a case without any ongoing maintenance work taking place over a period of fifty two weeks. The plots show that case MS-MDPSO-b generate the best RI of 0.772 while case MDPSO-a produce the worst RI of 0.752 after 100 iterations of 5000 trials.

Figures 5 (c) and (d) present the plots of cost of purchasing energy versus the RI for case a: MDPSO-a and MS-MDPSO-a, and case b: MDPSO-b and MS-MDPSO-b respectively. It can be seen from the figure that at any RI, the corresponding energy cost for case MS-MDPSO-a is lower compared with case MDPSO-a, and similarly case MS-MDPSO-b produce lower energy cost to be purchased compared with case MDPSO-b. On the overall, at any energy cost case MS-MDPSO -b gives the best RI compared with either MDPSO-b, MS-MDPSO-a or MDPSO-a. Without maintenance for the two cases, there is 14,333,760,000.00 Naira to be spent on purchase of energy if a RI of 1 is desirable, otherwise the RI simply remains at 0.89 with zero cost with no purchase of energy as shown in Table 6. In the absence of any ongoing maintenance work, the system has higher RI than the two cases considered during scheduled shutdown maintenance, and there may not be need to spend financial resources on energy purchases as a consequence of maintenance actions.

Figs. 6 (a) and (b) shows typical convergence of the objective function for the Nigerian power system obtained after 100 iterations of 5000 trials. The converged results clearly present minimization of the objective function given by (2). The minimized objective function produced using Case a: MDPSO-a and MS-MDPSO-a are 33000504.15 and 32913169.25, respectively, as shown in Fig. 6 (a). Similarly, the minimized objective function produced using Case b: MDPSO-b and MS-MDPSO-b are 31550689.31 and 31416025.42 respectively as shown in Fig. 6 (b). The optimization process demonstrates the capabilities of the MDPSO and MS-MDPSO algorithms in minimizing large variations of system net reserve in case they occur.

Table 7 shows the statistical comparison of convergence of the objective function given by (2) for the Nigerian power system using Case a: MDPSO-a and MS-MDPSO-a and Case b: MDPSO-b and MS-MDPSO-b described in subsections 4.3.1 and 4.3.2, respectively, obtained after 100 iterations of 5000 trials. The table shows that for Case a, the minimized numerical values of the objective function produced by MDPSO-a and MS-MDPSO-a are 33000504.15 and 32913169.25, respectively, representing 87334.90 (0.26%) reduction. Similarly, for Case b, the minimized numerical values of the objective function produced by MDPSO-b and MS-MDPSO-b are 31550689.31 and 31416025.42 respectively, representing 134663.89 (0.42%) reduction. The results indicate that better and enhanced optimization is achieved with the MS-MDPSO compared with MDPSO for both Cases a and b. The best optimization result of 31416025.00 is obtained with the MS-MDPSO-b while the worst optimization result of 33000504.00 is obtained with the MDPSO-a. The results also imply that better maintenance schedules are generated by the MS-MDPSO-b. Both MDPSO and MS-MDPSO algorithms however, produce optimal schedules that utilizes every allowable maintenance week of the entire fifty two weeks as shown in Tables A.2 and A.3 of the Appendix.

The results presented for this 49-unit Nigerian hydrothermal power system shows, generally, that the MS-MDPSO algorithm produces better maintenance schedules compared with the MDPSO algorithm for this GMS problem.

TABLE 7

Statistical Comparison of Convergence of the Objective Function for the Nigerian Power System

	Algorithm			
	Case a		Case b	
	MDPSO-a	MS-MDPSO-a	MDPSO-b	MS-MDPSO-b
Minimum	33000504.15	32913169.25	31550689.31	31416025.42
Maximum	33163777.44	33068250.25	31686766.81	31591144.36
Mean	33106214.39	32996982.49	31597889.45	31477710.25
Standard deviation	±45580	±42710	±42630	±41890

Table 8, Fig. 2 (d), Fig. 6 (c) and (d) further illustrates the design and application of MS-MDPSO algorithm for solving the GMS problem by presenting typical evolution of single global best solution (*Gbest*) from a set of five global best solutions ($gbest_1$, $gbest_2$, $gbest_3$, $gbest_4$ and $gbest_5$) obtained from five multiple swarms (n=5) over five trials for the 49-unit Nigerian power system presented in subsection 4.3. Table 8 and Fig. 6 (c) shows that for the 49-unit Nigerian power system, the *Gbest* (consisting of an array of 100 global best solutions) obtained for 100 iterations over the first trial is composed of $gbest_1$ (34 global best solutions from swarm #1), $gbest_2$ (11 global best solutions from swarm #2), $gbest_3$ (9 global best solutions from swarm #3), $gbest_4$ (5 global best solutions from swarm #4) and $gbest_5$ (41 global best solutions from swarm #5). Gbest feasible solutions obtained over five trials are also presented in Table 8 and depicted in Fig. 6 (d).

TABLE 8

Gbest Solution for the 49-Unit Nigerian Power System using MS-MDPSO

	49-unit Nigerian hydrothermal power system					
	Number of trials					
	#1 (Iterations)	#2 (Iterations)	#3 (Iterations)	#4 (Iterations)	#5 (Iterations)	Total (%)
$gbest_1$	34	45	1	46	49	175 (35%)
$gbest_2$	11	9	24	5	35	84 (16.8%)
$gbest_3$	9	29	2	32	13	85 (17.0%)
$gbest_4$	5	6	48	9	1	69 (13.8%)
$gbest_5$	41	11	25	8	2	87 (17.4%)
Gbest	100	100	100	100	100	500 (100%)

5. CONCLUSIONS

The problem of generating optimal preventive maintenance schedules of generating units for the purpose of maximizing economic benefits and improving reliable operation of a power system, subject to satisfying system load demand, allowable maintenance window, and crew and resource constraints over fifty two weeks maintenance and operational period has been presented for 21-unit test system and 49-unit Nigerian hydrothermal grid system.

Improvement in the quality of the maintenance schedules generated by MS-MDPSO algorithm in terms of reliability and energy cost curtailment over what was achieved by MDPSO algorithm has been presented. This improvement is achieved through the use of the multiple swarms' idea on the MDPSO algorithm. The eventual evolution of a single best solution forms the optimal maintenance schedules as applied to the respective two power systems considered in this paper. The better solutions obtained by the MS-MDPSO algorithm for the two GMS problems are achieved at the expense of more computational time, which is not a problem since the simulation is done off-line.

With respect to the 49-unit Nigerian hydrothermal power system, two possible case studies have been investigated and compared. The logical and optimal placements of some thermal plants for maintenance along with hydro plants during low water level have been illustrated using the MDPSO and the proposed MS-MDPSO algorithms, and their results compared. The MS-MDPSO algorithm demonstrates better performance over the MDPSO algorithm for this GMS problem, and produce optimal maintenance unit scheduling framework for the Nigerian power utility that achieved better utilization of available energy generation with improved reliability and reduction in energy cost.

The studies and analysis presented in this paper provides potential for practical implementation and enhancement of effective planning strategies that incorporates other short-term generation scheduling measures, such as unit commitment and economic load dispatch, and the integration of renewable energy resources.

ACKNOWLEDGMENT

The financial support from the National Science Foundation (NSF), USA under the grant ECCS # 0348221 is gratefully acknowledged by the authors.

REFERENCES

1 Marwali, M. K. C. and Shahidehpour, S. M.: ‘Coordination between long – term and short – term generation scheduling with network constraints’, *IEEE Transactions on Power Systems*, August 2000, 15, pp. 1161-1167.

2 Dahal, K. P. and Chakpitak, N.: ‘Generator maintenance scheduling in power systems using metaheuristic-based hybrid approaches’, *Electric Power Systems Research*, May 2007, 77, pp. 771-779.

3 Edwin, K. W. and Curtius, F.: ‘New maintenance scheduling method with production cost minimization via integer linear programming’, *International Journal of Electrical Power and Energy Systems,* 1990, 12, pp. 165-170.

4 Yamayee, Z. and Sidenblad, K.: ‘A computationally efficient optimal maintenance scheduling method’, *IEEE Transactions on Power Apparatus and Systems*, February 1983, PAS-102, (2), pp. 330-338.

5 Dopaz, J. F. and Merrill, H. M.: ‘Optimal generator scheduling using integer programming’, *IEEE Transactions on Power Apparatus and Systems*, 1975, PAS-94, pp. 1537-1545.

6 Yamayee, Z. A.: ‘Maintenance scheduling: description, literature survey, and interface with overall operations scheduling’, *IEEE Transactions on Power Apparatus and Systems*, 1982, PAS-101, pp. 2770-2779.

7 Kim, H., Hayashi, Y. and Nara, K.: ‘An algorithm for thermal unit maintenance scheduling through combined GA, SA, and TS’, *IEEE Transactions on Power Systems*, February 1997, 12, (1), pp. 329-335.

8 Chen, L. and Toyoda, J.: 'Optimal generating unit maintenance scheduling for multi-area system with network constraints', *IEEE Transactions on Power Systems,* August 1991, 6, (3), pp. 1168-1174.

9 Billinton, R. and Abdulwhab, A.: 'Short-term generating unit maintenance in a deregulated power system using a probabilistic approach', *IET Proceedings - Generation, Transmission and Distribution,* July 2003, 150, (4), pp. 463-468.

10 Satoh, T. and Nara, K.: 'Maintenance scheduling by using simulated annealing method', *IEEE Transactions on Power Systems,* 1991, 6, pp. 850-857.

11 Yellen, J., Al-khamis, T. M., Vermuri, S. and Lemonidis, L.: 'A decomposition approach to unit maintenance scheduling', *IEEE Transactions on Power Systems*, 1992, 7, pp. 726-733.

12 Firma, H. T. and Legey, L. F. L.: 'Generation expansion: an iterative genetic algorithm approach', *IEEE Transactions on Power Systems*, August 2002, 17, (3), pp. 901-906.

13 Lee, K. Y. and El-Sharkawa, M. A.: 'Modern heuristic optimization techniques: theory and applications to power systems', IEEE Press, 445 Hoes Lane, Piscataway, New Jersey, 2008, pp. 354-359

14 Iwamatsu, M.: 'Multi-species particle swarm optimizer for multimodal function optimization', *IEICE Transactions on Information Systems,* E89D, (3), 2006, pp. 1181-1187.

15 Blackwell, T. and Branke, J.: 'Multiswarms, exclusion, and anti-convergence in dynamic environments', *IEEE Transactions on Evolutionary Computation*, 10, (4), August 2006, pp. 459-472.

16 Van den Bergh, F. and Engelbrecht, A. P.: 'A cooperative approach to particle swarm optimization', *IEEE Transactions on Evolutionary Computation*, 8, (3), June 2004, pp. 225-239.

17 Xu, Y., Chen, G. and Yu, J.: 'Three sub-swarms discrete particle swarm optimization algorithm', *IEEE Proceedings on International Conference on Information Acquisition*, Welhai, Shandong, China, August 2006, pp. 1224-1228.

18 Yen, G. G. and Leong, W. F.: 'Dynamic multiple swarms in multiobjective particle swarm optimization', *IEEE Transactions on Systems, Man, and Cybernetics*, 39, (4), July 2009, pp. 890-911.

19 Engelbrecht, A. P.: 'Fundamentals of computational swarm intelligence', John Wiley & Sons Ltd, The Artrium, Southern Gate, Chichester, West Sussex, England, 2005.

20 Al-Kazemi, B. and Mohan, C. K.: 'Multi-phase discrete particle swarm optimization', *Proceedings of the International Workshop on Frontiers in Evolutionary Algorithms*, 2002, pp. 622-625.

21 Al-Kazemi, B. and Mohan, C. K.: 'Multi-phase generalization of the particle swarm optimization algorithm', *Proceedings of the IEEE Congress on Evolutionary Computation,* 2002, pp. 489-494.

22 Yare, Y., Venayagamoorthy, G. K. and Aliyu, U. O.: ‘Optimal generator maintenance scheduling using a modified discrete PSO’, *Accepted for publication in IET Generation, Transmission & Distribution*, 2008.

23 Dahal, K. P., McDonald, J. R. and Burt, G. M.: ‘Modern heuristic techniques for scheduling generator maintenance in power systems’, *Transactions of Institute of Measurement and Control*, 2000, 22, pp. 179-194.

24 Wang, X. and McDonald, J. R.: ‘Modern power system planning’, McGraw-Hill, London, 1994, pp. 247-307.

APPENDIX

TABLE A.1

Typical Generator Maintenance Schedules Obtained by MDPSO and MS-MDPSO for the 21-Unit Test System

Week no.	Generating units scheduled for maintenance			Week no.	Generating units scheduled for maintenance	
	MDPSO	MS-MDPSO			MDPSO	MS-MDPSO
1	1	12,13		27	19	17,20
2	1	12,13		28	19,20	17,19
3	1	4,13		29	16	17,19
4	1	4		30	16	-
5	1	4		31	16	14
6	1	2,6		32	16	14
7	1,6	2,6		33	16	14
8	3,6,11	6		34	16	14
9	2,6,11	6		35	-	14
10	2,6	6,7,8		36	17	-
11	6	6,7		37	17	21
12	6	6,7		38	17	21
13	6,13	6,7,11		39	14	21
14	6,10,13	6,11		40	14	21
15	6,10,13	6		41	14	18
16	6,7,10	6		42	14	16
17	7,10	5		43	14	16
18	7,9,12	5,9		44	21	16
19	7,9,12	5,9		45	18,21	16
20	4	1		46	21	16
21	4	1		47	21	16
22	4	1,10		48	15	15
23	-	1,10		49	15	15
24	5	1,10		50	15	15
25	5	1,10		51	15	15
26	5,8	1		52	15	15

TABLE A.2

Typical Generator Maintenance Schedules Obtained by MDPSO-a and MS-MDPSO-a for the Nigerian Power System

Week no.	Generating units scheduled for maintenance			Week no.	Generating units scheduled for maintenance	
	MDPSO-a	MS-MDPSO-a			MDPSO-a	MS-MDPSO-a
1	1,9,11,17	1,4,15		27	26,31,32,33	20,22,27,29
2	1,9,11,14,16,17	1,4,15		28	26,32	20,22,27,34
3	1,3,14,16,17	1,4,15		29	22,26	20,22,27,34
4	1,3,16,17	1,4,15		30	22,26	34,35
5	1,3,10,16	1,4,16		31	19,22,24,38	32,34,35
6	3,4,10	3,5,16		32	19,22,24,38	32,37
7	3,4	3,5,16		33	19,24,27	32,37
8	2,4	3,5,16		34	19,24,27	25,33
9	2,4,7	3,5		35	27	25,33
10	2,4,7,8	3,5		36	27	25,33,40
11	2,6,8,12	2,8,10,11,14		37	35	25,33,40
12	2,6,12	2,8,10,11,14		38	21,30,35	36,40
13	5,6,15	2,6		39	21,30	36,40
14	5,6,15	2,6,17		40	21,25,30,34	23,26,40
15	5,6,15	2,6,17		41	21,25,34	23,26
16	5,13,15	6,7,9,12,13,17		42	25,34,37	23,26
17	5,13	6,7,9,12,13,17		43	25,34,37	23,26
18	20,23,29,39	18,19,21,39		44	48,49	47,48
19	20,23,29,39	18,19,21,39		45	44,48,49	44,47,48
20	18,20,23,29,39	18,19,21,39		46	44,48,49	44,47,48
21	18,20,23,28,39	18,19,21,30,39		47	41,48,49	41,47,48
22	18,28,36,39,40	24,30,39		48	41,43	41,42
23	18,28,36,40	24,28,30,38		49	43,45,46,47	42,45,46,49
24	28,33,40	24,28,31,38		50	45,46,47	45,46,49
25	31,33,40	24,28,29,31		51	42,45,46,47	43,45,46,49
26	31,32,33,40	20,22,27,28,29,31		52	42,45,46,47	43,45,46,49

TABLE A.3

Typical Generator Maintenance Schedules Obtained by MDPSO-b and MS-MDPSO-b for the Nigerian Power System

Week no.	Generating units scheduled for maintenance			Week no.	Generating units scheduled for maintenance	
	MDPSO-b	MS-MDPSO-b			MDPSO-b	MS-MDPSO-b
1	3,11,12,16	3,7,9,13,16		27	18,26,39	21,26,27,29,30
2	3,9,11,12,16	3,7,9,13,16		28	18,26,39	19,26,27,29,30
3	3,6,9,15,16	3,5,12,13,16		29	18,23,29	19,26,29,30
4	3,6,15,16	3,5,12,13,16		30	23,29,40	19,24,36
5	1,3,15	3,6		31	23,27,29,40	19,24,28,36
6	1,7,8,13,15	1,6		32	22,23,27,40	24,28,36
7	1,7,8,13,14	1,8,10		33	22,27,40	24,28,31,36
8	1,2,13,14	1,8,10		34	22,40	31,36,37
9	1,2,13,14	1,2		35	22,34,36,38	18,31,37,38
10	2,10,14	1,2,14,15		36	34,36,38	18,31,37,38
11	2,10	2,11,14,15		37	32,36,38	18,37,38
12	2,5	2,11,14,15		38	32,36,38	18,37,38
13	4,5	2,4,14,15		39	20,25,36,37	39,40
14	4,17	4,17		40	20,24,25,37	39,40
15	4,17	4,17		41	20,24,25,37	35,39,40
16	4,17	4,17		42	20,24,25,37	35,39,40
17	4,17	4,17		43	24,37	39,40
18	19,30,35	22,25,32		44	47,49	42,43,48
19	19,30,35	22,25,32		45	47,49	42,43,46,48
20	19,21,28,30,31	20,22,23,25		46	47,49	46,48
21	19,21,28,30,31	20,22,23,25		47	43,47,49	41,46,48
22	21,28,31,33	20,23		48	42,43,46	41,44,46
23	21,33	20,23		49	42,45,46,48	44,45,46,47,49
24	39	21,33		50	45,46,48	45,47,49
25	39	21,33,34		51	41,44,45,46,48	45,47,49
26	18,26,39	21,27,30,34		52	41,44,45,48	45,47,49

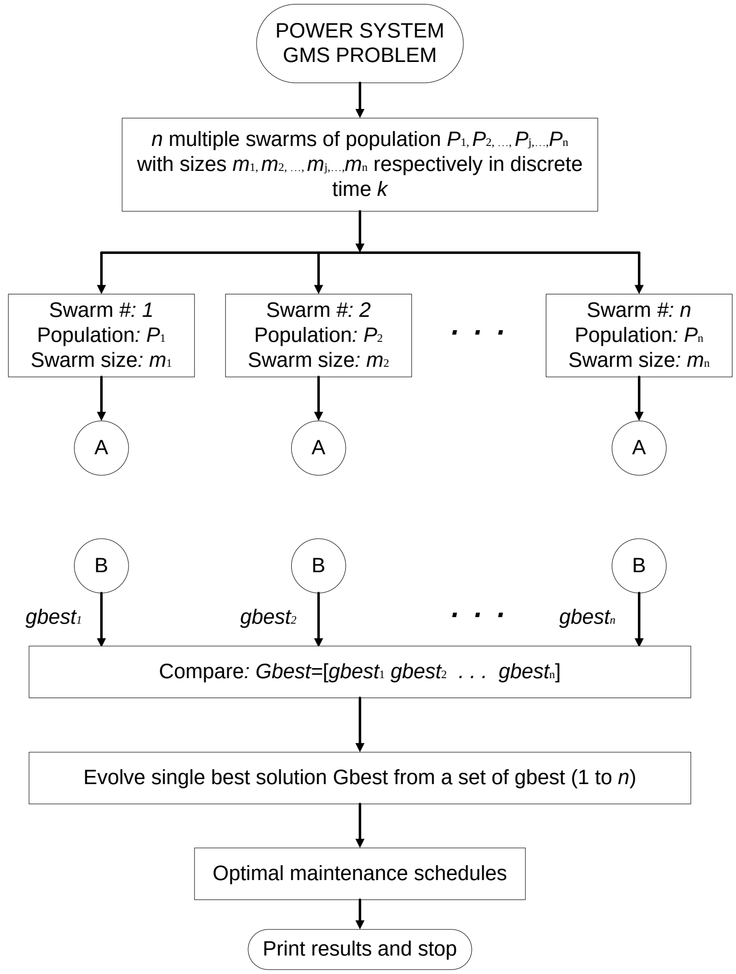

(a) *n* Multiple Swarms-MDPSO

Fig. 1. MS-MDPSO Algorithm Framework for Power System GMS Problem

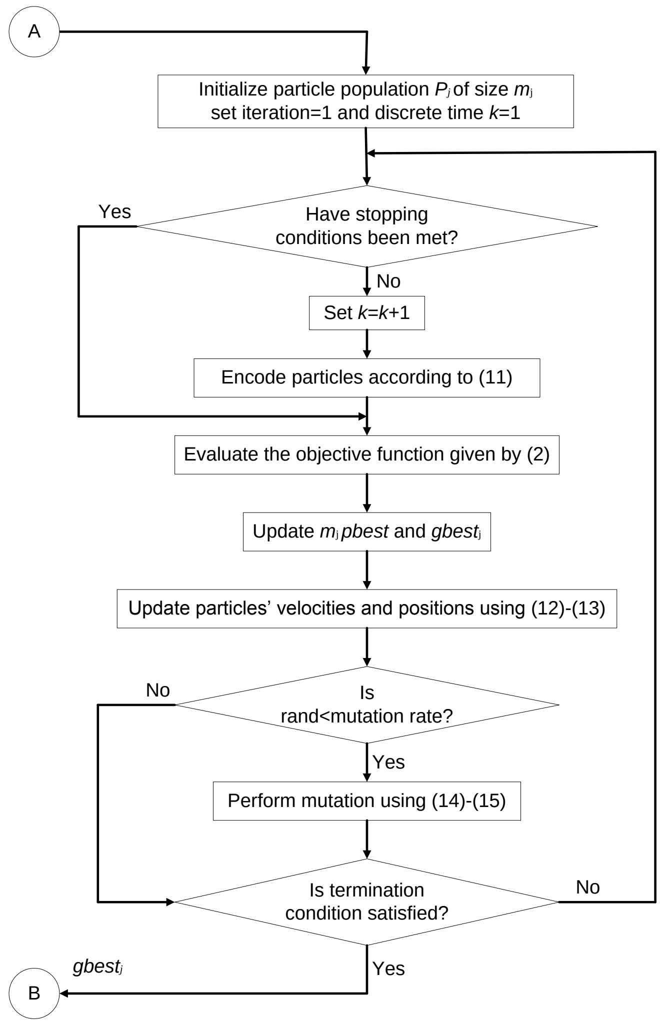

(b) MDPSO Implementation for Multiple Swarms Application

Fig. 1. MS-MDPSO Algorithm Framework for Power System GMS Problem (cont.)

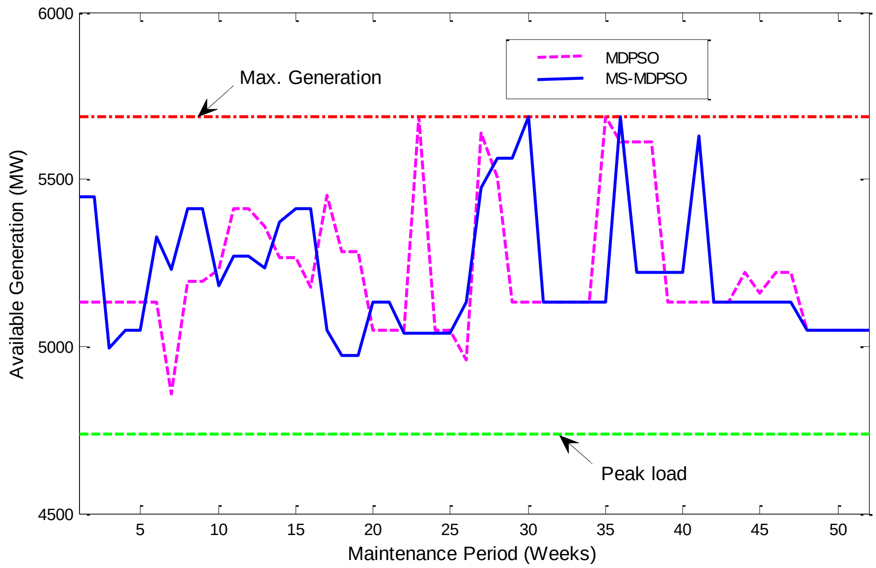

(a) Available Generation versus Maintenance Period for MDPSO and MS-DPSO

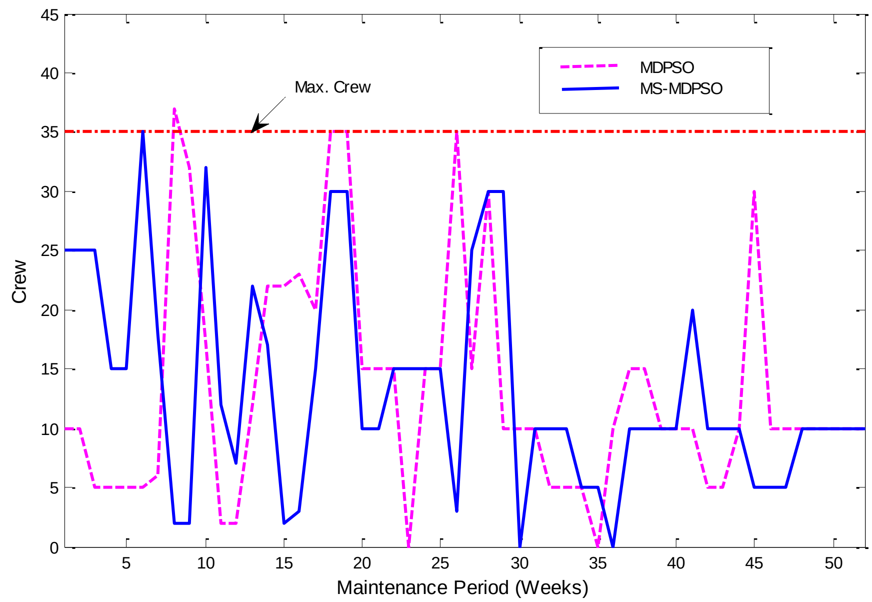

(b) Crew Requirement versus Maintenance Period for MDPSO and MS-MDPSO

Fig. 2. Generation, Technical Crew, Typical Convergence, Five Multiple Swarms and Gbest Plots for the 21-Unit Test System using MDPSO and MS-MDPSO Algorithms

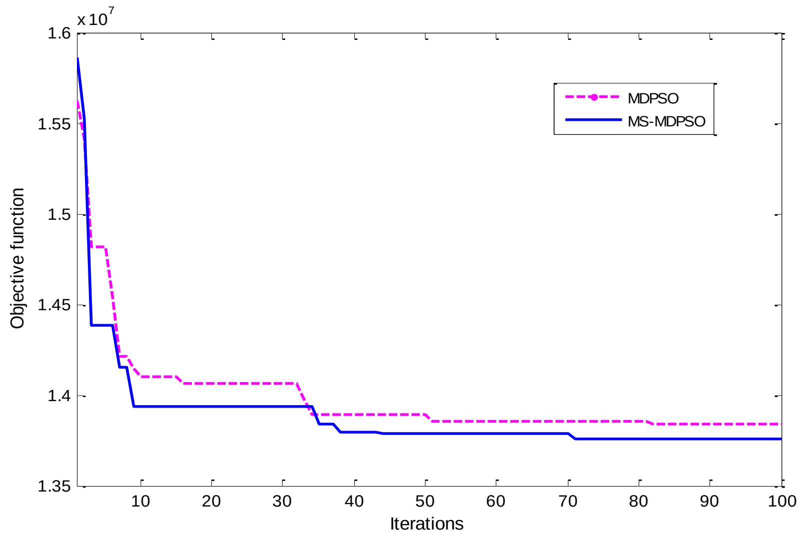

(c) Typical Convergence of the Objective Function given by (2)

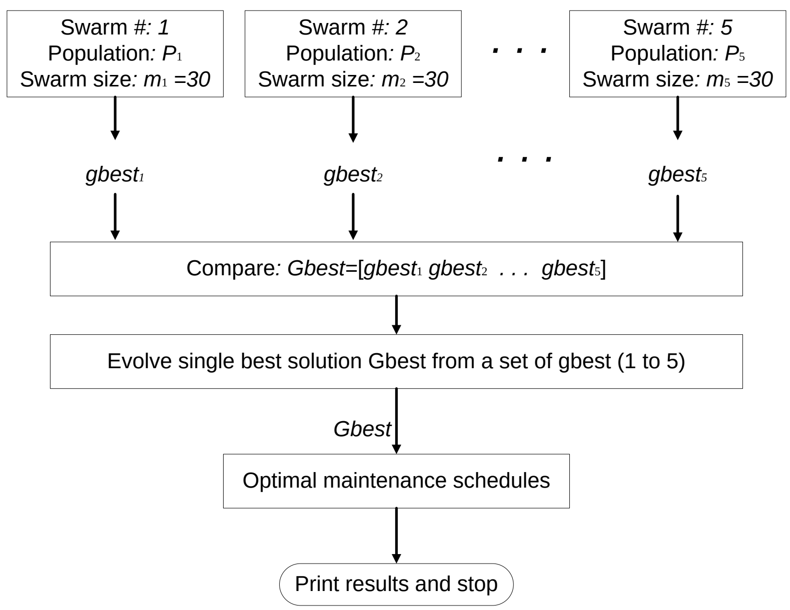

(d) Five Multiple Swarms-MDPSO

Fig. 2. Generation, Technical Crew, Typical Convergence, Five Multiple Swarms and Gbest Plots for the 21-Unit Test System using MDPSO and MS-MDPSO Algorithms (cont.)

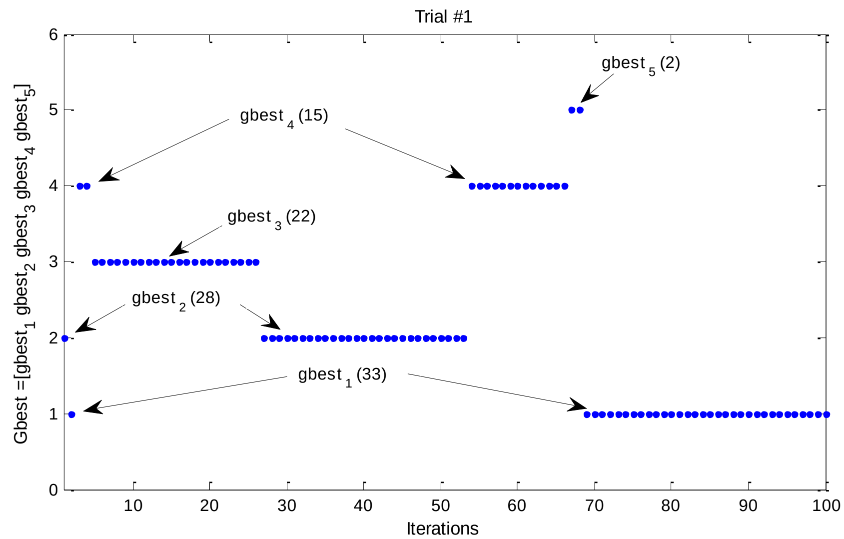

(e) Gbest versus Iterations for Five Multiple Swarms (Trial #1)

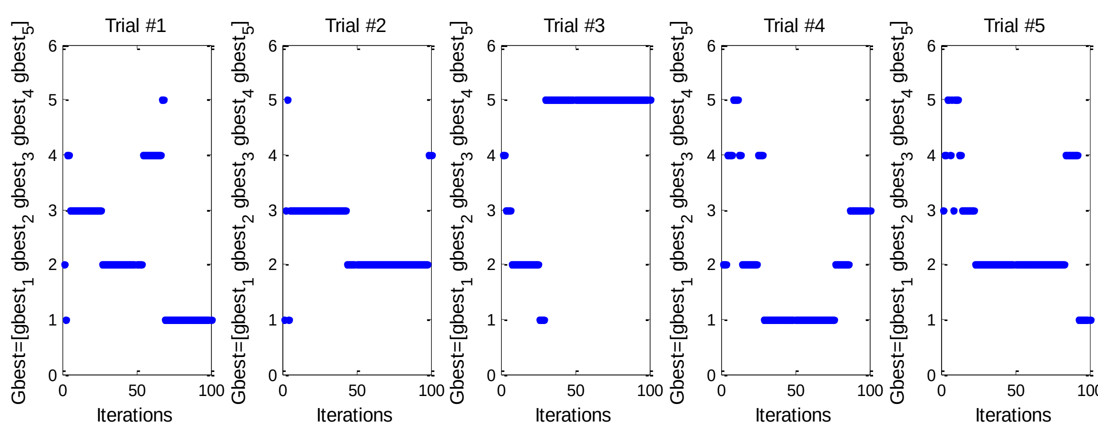

(f) Gbest versus Iterations for Five Multiple Swarms (Five Different Trials)

Fig. 2. Generation, Technical Crew, Typical Convergence, Five Multiple Swarms and Gbest Plots for the 21-Unit Test System using MDPSO and MS-MDPSO Algorithms (cont.)

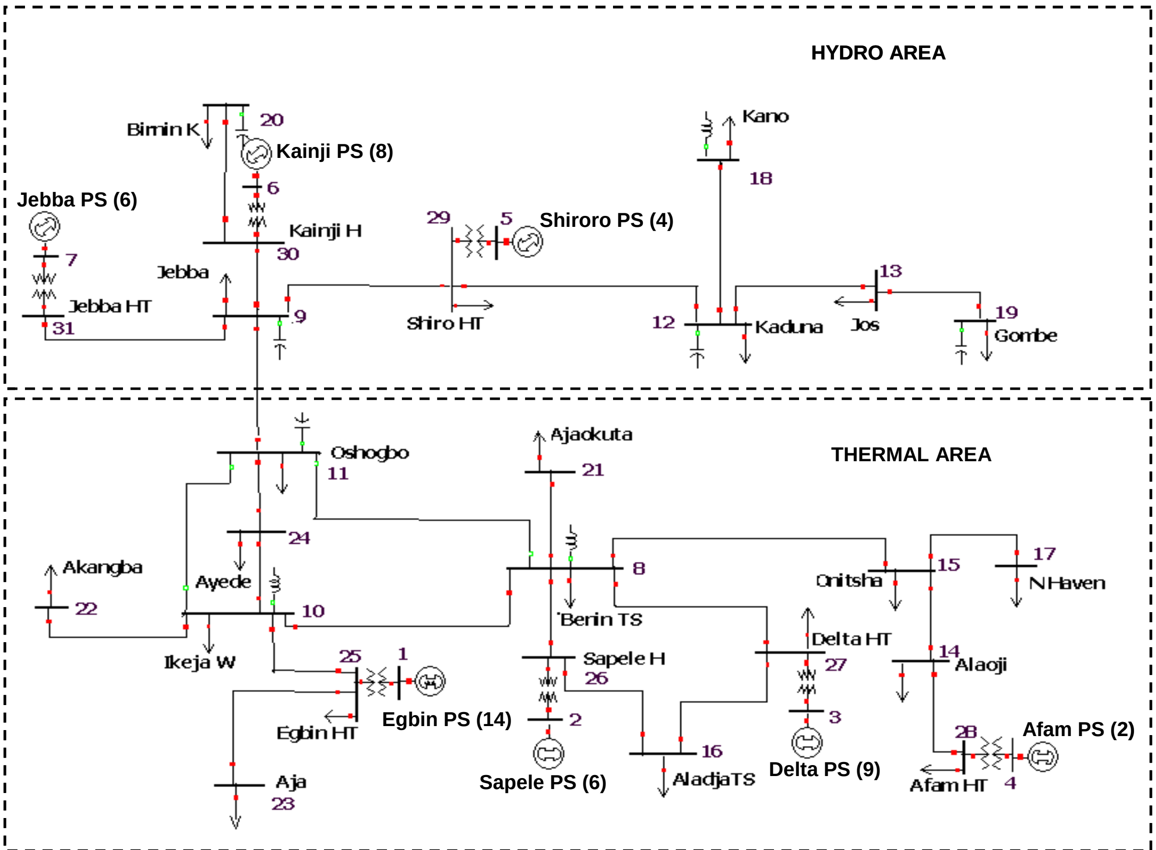

Fig. 3. Nigerian 330KV Grid showing 7 Power Generating Stations

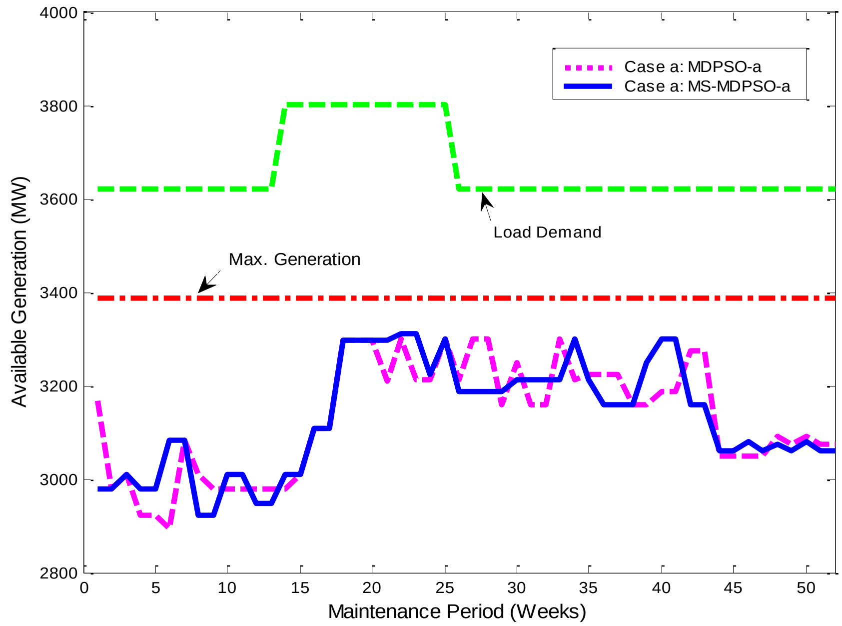

(a) Available Generation versus Maintenance Period for Case a: MDPSO-a and MS-MDPSO-a

Fig. 4. Generation and Crew Plots during Maintenance Period

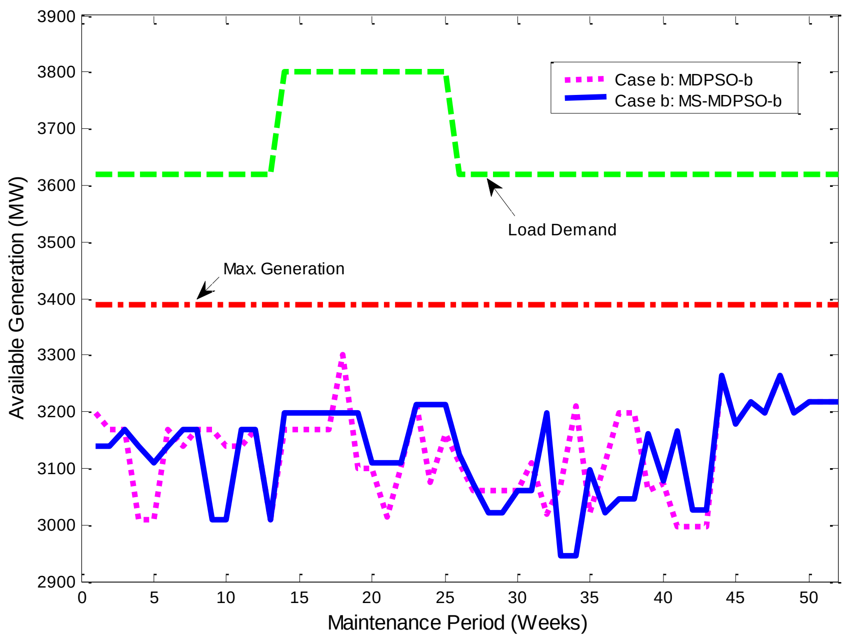

(b) Available Generation versus Maintenance Period for Case b: MDPSO-b and MS-MDPSO-b

Fig. 4. Generation and Crew Plots during Maintenance Period (cont.)

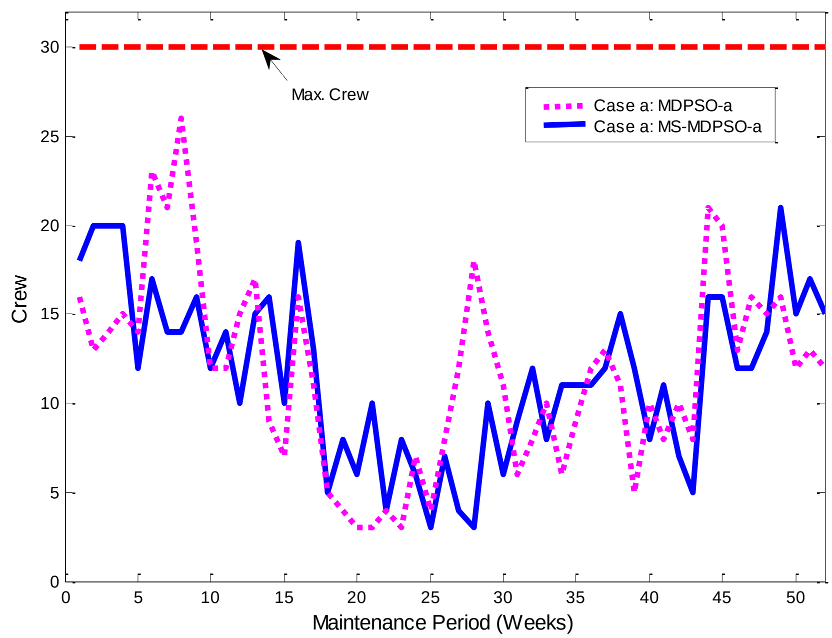

(c) Crew Requirement versus Maintenance Period for Case a: MDPSO-a and MS-MDPSO-a

Fig. 4. Generation and Crew Plots during Maintenance Period (cont.)

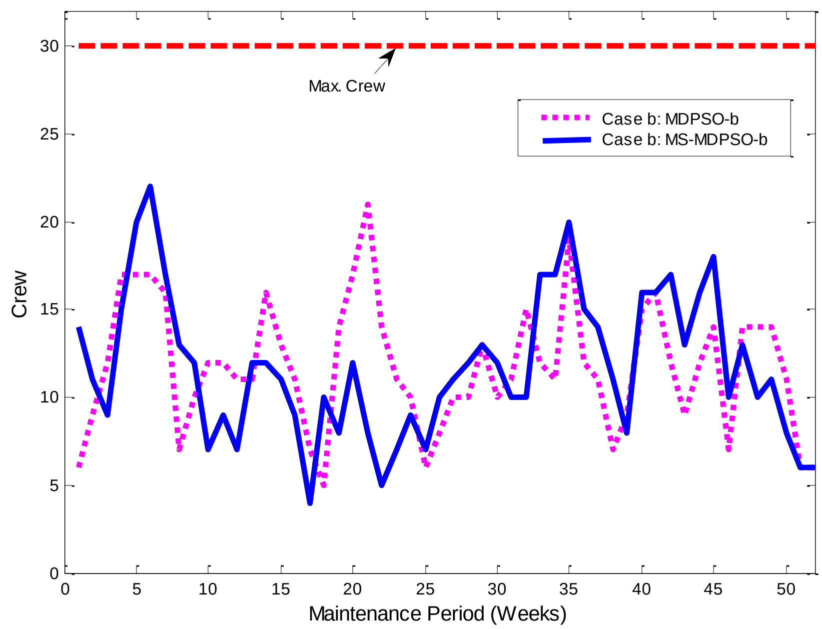

(d) Crew Requirement versus Maintenance Period for Case b: MDPSO-b and MS-MDPSO-b

Fig. 4. Generation and Crew Plots during Maintenance Period (cont.)

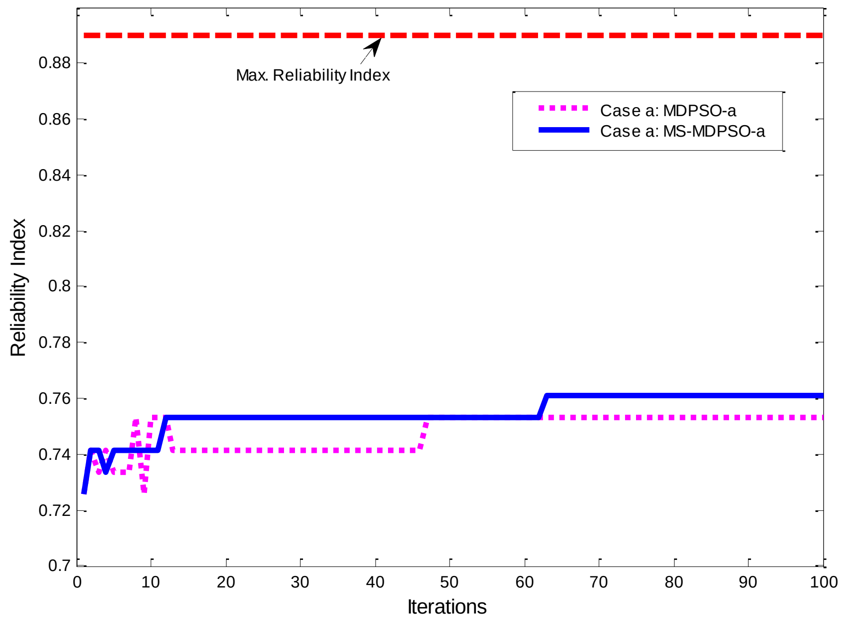

(a) Reliability Index versus Iterations for Case a: MDPSO-a and MS-MDPSO-a

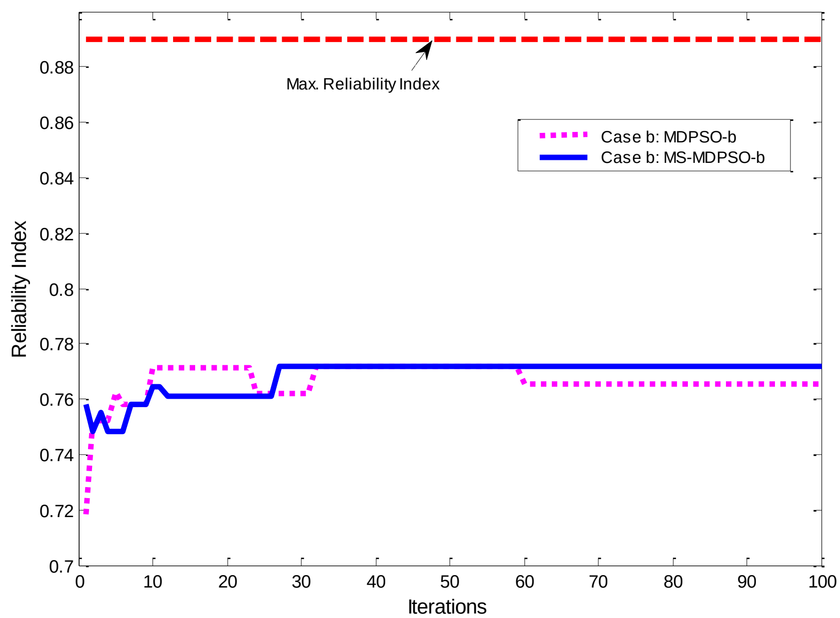

(b) Reliability Index versus Iterations for Case b: MDPSO-b and MS-MDPSO-b

Fig. 5. Reliability Index and Cost of Energy Plots

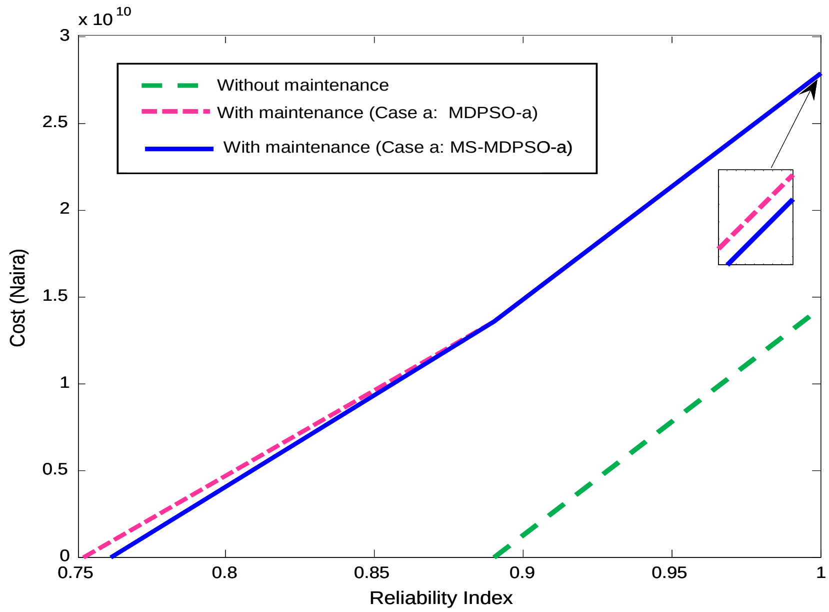

(c) Cost requirement versus Reliability Index for Case a: MDPSO-a and MS-MDPSO-a

Fig. 5. Reliability Index and Cost of Energy Plots (cont.)

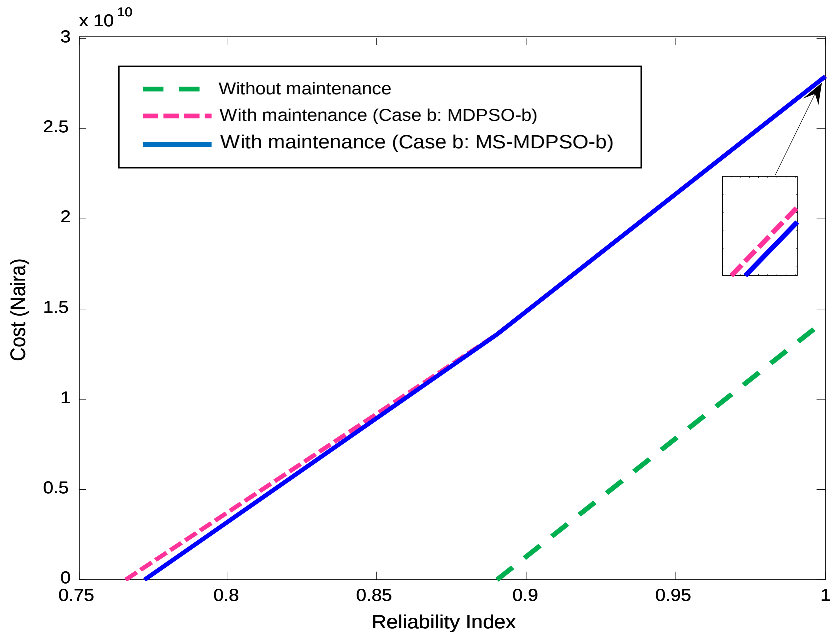

(d) Cost Requirement versus Reliability Index Plots for Case b: MDPSO-b and MS-MDPSO-b

Fig. 5. Reliability Index and Cost of Energy Plots (cont.)

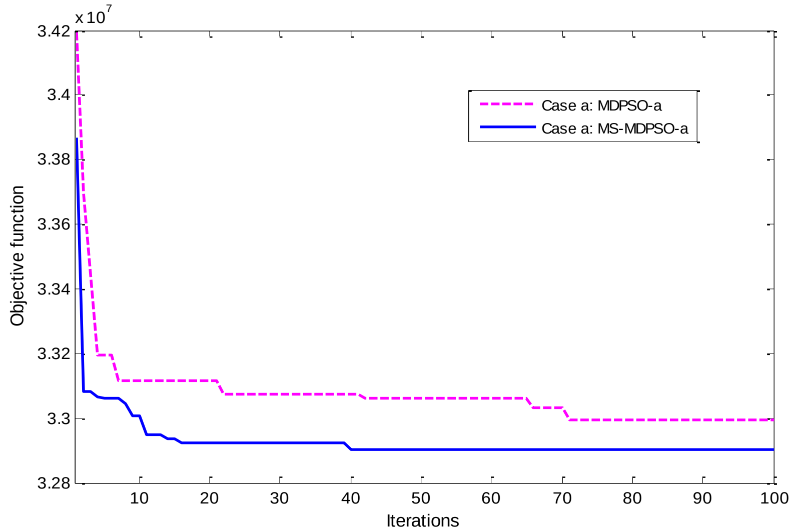

(a) Typical Convergence of the Objective Function given by (2) for Case a: MDPSO-a and MS-MDPSO-a

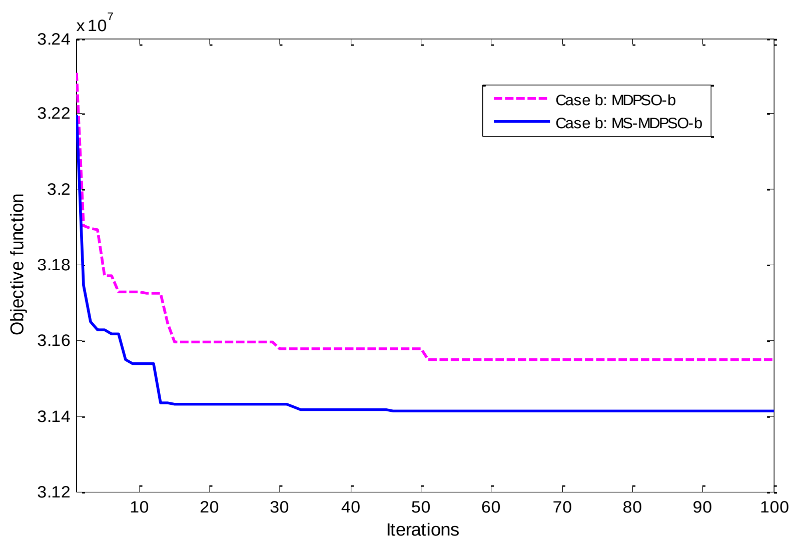

(b) Typical Convergence of the Objective Function given by (2) for Case b: MDPSO-b and MS-MDPSO-b

Fig. 6. Typical Convergence of the Objective Function given by (2) and Gbest Plots for the 49-Unit Nigerian Power System using MDPSO and MS-MDPSO Algorithms

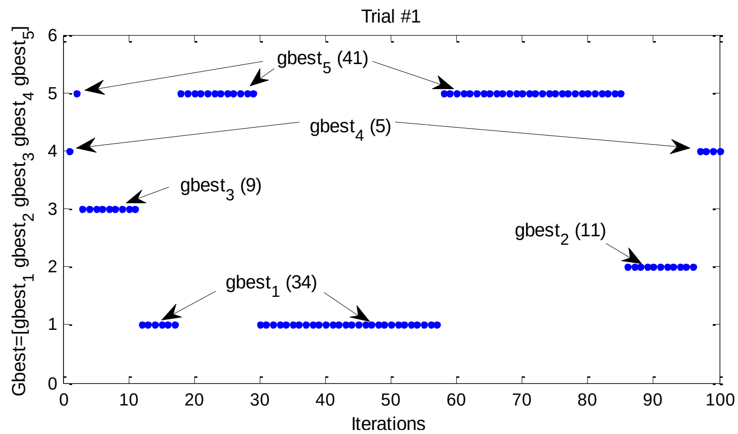

(c) Gbest versus Iterations for Five Multiple Swarms (Trial #1)

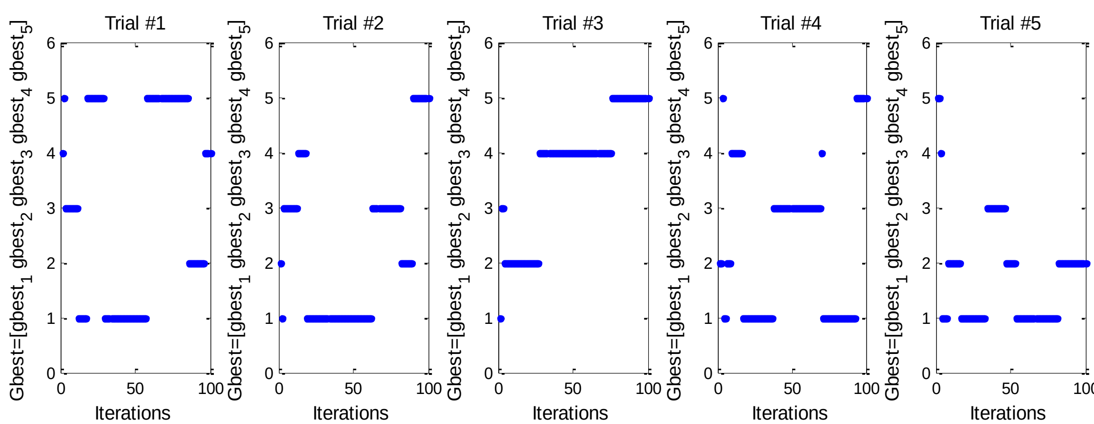

(d) Gbest versus Iterations for Five Multiple Swarms (Five Different Trials)

Fig. 6. Typical Convergence of the Objective Function given by (2) and Gbest Plots for the 49-Unit Nigerian Power System using MDPSO and MS-MDPSO Algorithms (cont.)

III. HEURISTIC METHODS FOR STATIC AND DYNAMIC ECONOMIC DISPATCH WITH PRACTICAL GENERATOR CONSTRAINTS

Y. Yare, G. K. Venayagamoorthy and A. Y. Saber

Real-Time Power and Intelligent Systems Laboratory, Department of Electrical and Computer Engineering, Missouri University of Science and Technology,
Rolla, MO 65409-0249 USA
E-mail: yyqh3@ieee.org, gkumar@ieee.org & aysaber@ieee.org

ABSTRACT: Static economic dispatch (SED) problem is solved in order to economically determine output powers of generating units in such a manner that the total generation (fuel) cost is minimized while load demand and all practical operating constraints are satisfied. Dynamic economic dispatch (DED) is an enhancement of SED and has the objective of dynamically determining the optimal outputs of generating units with predicted load demand over a certain period of time. Classical optimization methods assume generator cost curves to be continuous and monotonically increasing, whereas practical generators have a variety of nonlinearities in their cost curves making this assumption inaccurate. Hence, heuristic methods are proposed in this paper to circumvent the problems of imposed non-smooth assumptions. This paper presents three heuristic methods, namely, genetic algorithm (GA), differential evolution (DE) and modified particle swarm optimization (MPSO) for solving both the SED and DED problems for three test systems. Results and convergence performances of these three heuristic methods are presented and compared as a way of validating such methods in solving SED and DED problem characterized by practical and non-smooth generator constraints.

INDEX TERMS: Computational intelligence; Economic dispatch; Generation cost; Prohibited operating zone; Ramp-rate limit.

NOMENCLATURE

a_i, b_i & c_i Fuel cost coefficients for unit i

β_{gb} Global best strategic learning parameter

c_1 & c_2	Cognitive and social acceleration constants respectively
C_R	Crossover constant
d	Particle's dimension
D_i	Decimal integer value of binary string of the ith generating unit
e_i & f_i	Fuel cost coefficients for unit i considering valve-point loading effect
F	Scaling factor for mutation
G	Generation
i	Index of running generating units
$Iter$ & $Iter_{max}$	Current and maximum iteration number
t	Continuous time step
K_{pb}	Penalty factor coefficient for ED real power balance constraint
l	lth particle
M_R	Mutation rate
n	Number of bits representing each unit power output
np	Number of population in a generation
N	Total number of generating units
P_{gd}	Swarm's best position for dimension d
P_{lbd}	lth Particle best position for dimension d
P_{ld}	Position vector of the particle l in dimension d
P_i	Generating capacity of unit i
P_{loss}	System loss
P^D	Total real load demand
r, $rand$, $rand_1$ & $rand_2$	Random numbers with uniform distribution in the range of [0, 1]
$randn$	Gaussian distributed random number with a zero mean and a variance of 1
V_{ld}	lth particle velocity in dimension d
w_{iner}, w_{max} and w_{min}	Current, final and initial inertia weights
X^o	Initial random population
$X_{1,G}$, $X_{2,G}$ & $X_{3,G}$	Randomly selected parent population vectors

$X_{i,G}$, $X_{t,G+1}$ & $X_{i,G+1}$ Target vector, trial vector and best fit vector for the next generation respectively

1. INTRODUCTION

Economic dispatch (ED) of generating units is an important optimization task and is performed in order to supply electricity economically while minimizing the total generation cost. Modern power system is experiencing increased demand for electricity with related expansions in system size, which has resulted in higher number of generators and lower reserve margins making the ED problem more challenging and complicated [1]. Conventional dispatch methods employ Lagrangian multipliers and require monotonically increasing cost curve approximations. Unfortunately, the input-output characteristics of modern generating units are inherently highly nonlinear due to valve-point loading effects, ramp-rate limits, prohibited operating zones and so on, which tend to generate multiple local minima points in the cost function [2, 3]. Classical dispatch methods require that these characteristics be approximated. However, such approximations may lead to suboptimal operation of the generator and results in heavy revenue losses.

One of the options available to the utilities in order to maximize economic benefits through minimization of total generation cost is the ED. The ED allocates total power demand among the online generating units in order to minimize the cost of generation while satisfying important system constraints. Some factors that influence ED of a power system are operating efficiency of generating units, fuel and operating costs, and transmission losses [1, 2].

Dynamic economic dispatch (DED) is a method of scheduling generator outputs to meet anticipated and predicted load demand over a certain period of time in order to operate the power system most economically [4]. It is therefore the most accurate formulation of the economic dispatch problem and also the most difficult to solve. The DED is a dynamic optimization problem taking into account the constraints imposed on system operation by generator ramping-rate limits. The DED is normally solved by dividing the entire dispatch period into a number of small time intervals, then a static economic dispatch (SED) which is generally referred to as the ED, is employed to solve the dispatch problem in each interval [4].

The ED problem is in general non-smooth optimization problem with many local minima. Numerous classical techniques such as Lagrange based methods, linear programming, non-linear programming, quadratic programming and dynamic programming methods have been reported in the literature [5, 6].

Most of the power system optimization problems, including ED, have complex and non-linear characteristics with stringent equality and inequality constraints to be satisfied. Different optimization techniques applied so far for solving these problems can be classified according to the type of the search space and/or the objective function [5 - 7]. Depending on the problem formulation, the objective function could be minimization of the units' generation and maintenance costs, or some pre-defined reliability risks subject to some constraints, resulting in non-linear optimization as proposed in [5 - 7]. Solving such non-linear optimization problems for most cases may not be feasible because their numerical solutions require extensive computational efforts, which increase exponentially with the problem complexities. Even though deterministic optimization problems are formulated with known parameters, real world problems almost invariably include some unknown parameters [7, 8].

In this paper, genetic algorithm (GA), differential evolution (DE) and modified particle swarm optimization (MPSO) heuristic methods are applied to solve this challenging ED problem of three test systems, whose generating units are characterized by smooth and non-smooth operational features. Solving this practical optimization problem leads to a minimized total generation cost of operating the respective power systems in the presence of generator constraints.

The main contributions of this paper are:

- Application of heuristic methods to solve the static economic dispatch (for smooth and non-smooth fuel cost functions) and dynamic economic dispatch (for non-smooth fuel cost function with valve-point loading effects) problems on three test systems.
- Demonstrate the capability of heuristic methods for solving the non-smooth ED problem where the classical Lagrange based method cannot be directly applied.

- Solving ED problem considering practical generator constraints, namely, load balance, generator ramp-rate limits, prohibited operating zones and spinning reserve using heuristic methods.
- Comparison of performances of three heuristic methods (GA, DE and MPSO) for minimization of economic cost objective function.

2. ECONOMIC DISPATCH PROBLEM FORMULATION

The ED problem is to find the optimal combination of power generations that minimizes the total generation cost while satisfying some constraints. The ED problem is commonly formulated as costs optimization problem, with the aim of minimizing the total generation cost of the power system but still satisfying equality and inequality constraints. The inclusion of ramp-rate limits, prohibited operating zones, and other practical constraints results in non-smooth ED of generating units.

The problem objective is to minimize the economic cost function expressed as second order function of each unit's output P_i subject to satisfying practical generator constraints, and can be expressed as

$$\text{Min } f = F + K_{pb}\left(\sum_{i=1}^{N} P_i - P^D - P_{loss}\right)^2 \tag{1}$$

where,

$$F = \sum_{i=1}^{N} a_i + b_i P_i + c_i P_i^2 + \alpha \left| e_i \sin(f_i (P_i^{\min} - P_i)) \right| \tag{2}$$

where α =1 if valve-point loading effect is taken into account (for non-smooth fuel cost functions), otherwise α=0 (for smooth fuel cost functions).

The minimization of (1) is subject to the following constraints:

- *Load balance*

The generated power from all the running units must satisfy the load demand and system losses given by (3). The loading constraint in (3) is incorporated and enforced once in the objective function.

$$\sum_{i=1}^{N} P_i = P^D + P_{loss} \tag{3}$$

To calculate system losses, methods based on penalty factors and constant loss formula coefficients or the B-coefficients are in use [1, 9]. System loss expression based on the B-coefficients is used in this paper, and is given by (4).

$$P_{loss} = \sum_{i=1}^{N}\sum_{j=1}^{N} P_i B_{ij} P_j + \sum_{i=1}^{N} B_{oi} P_i + B_{oo} \tag{4}$$

- *Generator ramp-rate limits*

The power output of a practical generator cannot be adjusted instantaneously without limits. The operating range of all online units is restricted by the unit's ramp-rate limits during each dispatch period. Therefore, subsequent dispatch output of a generator should be limited between its up and down ramp-rate limits constraint [1, 2, 9]. Hence the generator operating limits given by (5) are modified according to (6).

$$P_i^{\min} \le P_i \le P_i^{\max} \tag{5}$$

$$\max(P_i^{\min}, P_i^{pre} - DR_i) \le P_i \le \min(P_i^{\max}, P_i^{pre} + UR_i) \tag{6}$$

- *Prohibited operating zone*

Each generator has its generation capacity, which cannot be exceeded at any time. It is common for a typical thermal unit to have a steam valve in operation, or a vibration in shaft bearing, which may result in interference and discontinuous input-output performance curve sections [1], known as the prohibited operating zones. Practically, adjusting the power output of a unit must avoid all capacity limits and unit's operation in prohibited zones [9]. The acceptable operating zones of a generating unit can be formulated as shown in (7).

$$\left.\begin{array}{ll} P_i^{\min} \le P_i \le P_{i,1}^{lower} & \\ P_{i,j-1}^{upper} \le P_i \le P_{i,j}^{lower} & j = 2,3,\ldots,pz_i \\ P_{i,pz_i}^{upper} \le P_i \le P_i^{\max} & \end{array}\right\} \tag{7}$$

- *Spinning reserve constraint*

Sufficient spinning reserve is required from all running units to maximize and maintain system reliability.

$$\sum_{i=1}^{N} P_i^{\max} \ge P^D + R \tag{8}$$

3. HEURISTIC METHOD BASED ED

The load demand is distributed among the running units in ED. The generation output of each unit should lie between the minimum and maximum power limits for good ED [1]. While minimizing the total generation cost, the total generation from running units should be equal to the total system demand plus the transmission network loss. The ED consists of finding the optimum operating policy and distribution of power among the running units while satisfying constraints (3) - (7) [1].

The evaluation function *f* (which is also called the fitness function in evolutionary and swarm intelligence), is defined for evaluating the fitness of each individual (or particle) in a generation (or swarm). The penalty function method uses functions to penalize the objective function or the fitness of the individual (or particle) in proportion to the magnitude of the constraint violation [1]. The penalty function parameter is selected to distinguish between infeasible and feasible solutions.

In order to emphasize the 'best' solution and speed up convergence of the iterative procedure, the evaluation function *f* is defined to minimize the economic cost function given by (1) for a specified load demand P^D while satisfying the constraints in (3) - (8).

In order to limit the evaluation value of a potential solution within a feasible range, the generators' real output power operating limits constraint in (5) - (7) should be satisfied. If a potential solution satisfies this constraint, then it is a feasible solution and f has a relatively minimal evaluation value. Otherwise, the f value of this potential solution is penalized.

Flowchart illustrating the implementation of GA, DE and MPSO based ED methods is shown in Fig. 1.

3.1. GA Based Economic Dispatch

Genetic algorithm is a search method based on the modeling of natural genetics and natural selection [6]. In GA, solutions to the problem are coded to mimic the genetic make-up of biological organisms. Each chromosome in the population represents a possible solution to the problem. A "fitness" value, derived from the problem's objective function is assigned to each member of the population. The GA searches for better solutions by letting the fitter chromosomes take over the population through a combined stochastic process of selection and recombination. Recombination is an operation whereby an old chromosome is copied into "mating pool" according to its fitness value. More highly fitted chromosomes (i.e. with better values of the objective function) receive a higher number of copies in the next generation. Copying chromosomes according to their fitness values have a higher probability of contributing one or more offspring in the next generation. Crossover is a structured recombination operation. This operation is similar to two scientists exchanging information. Although, reproduction and crossover effectively search and recombine existing chromosomes, they do not create any new genetic material in the population. Mutation is capable of overcoming this shortcoming. Mutation is a random alternation of a chromosome position that provides variation and occasionally introduces beneficial materials into the population.

Implementation of a problem in GA starts from the parameter encoding (that is, the representation of the problem). The encoding must be carefully designed to utilize the GA's ability to efficiently transfer information between chromosome strings and objective function of the problem. The GA for this ED problem is encoded by grouping the on-line units for ED according to Fig. 2. Each chromosome consists of maximum number of units called genes, with each gene encoded as n bits. As shown in Fig. 2, each generating unit power output is concatenated and encoded in a binary based string normalized over its operating range. Each generating unit string is assigned by n bits, thus a string individual has $n \times N$ bits [10].

Evaluation of a chromosome is accomplished by decoding the encoded chromosome string and computing the chromosome's fitness value using the decoded parameter. To obtain the actual power output of each generating unit for fitness evaluation, each string is decoded to the decimal value using (9) [10].

$$P_i = P_i^{\min} + \frac{D_i \times \left(P_i^{\max} - P_i^{\min}\right)}{2^n - 1}, \quad \text{for } i=1, 2, \ldots, N \tag{9}$$

In this paper, the number of bits (n) representing each unit power output is 16. The more the number of bits per unit power output the better the resolution.

The following steps outline the GA implementation process for solving the ED problem presented in this paper:

Step 1: Read in data (unit data, load demand, …)

Step 2: Initialize a population of chromosomes using the approach shown in Fig. 2

Step 3: Evaluate each chromosome in the population using (9)

Step 4: Compute fitness f of each chromosome using (1)

Step 5: Rank chromosomes according to their fitness f values

Step 6: Select the "best" parents for reproduction

Step 7: Apply crossover and mutation

Step 8: Evaluate new chromosomes and insert best into population displacing weaker chromosomes

Step 9: Stop and output results if convergence occurred (or maximum number of iterations is reached), otherwise go to Step 3 and repeat the process.

3.2. DE Based Economic Dispatch

Differential evolution is an optimization method that solves real-valued problems based on the principles of natural evolution [6]. Like other evolutionary algorithms, DE also relies on initial random population generation, which is then improved using selection, mutation, and crossover operations, repeated through generations until the convergence criterion is met [6].

Although the canonical form of differential evolution solves optimization problems over continuous spaces, minor adjustments to the code allow DE to solve mixed integer optimization problems [6]. This is achieved with the use of operator that rounds the variable to the nearest integer value, when the value lies between two integers.

An initial population composed of vectors, $X^{o}_{i,G}$, $i=1,2,\ldots np$, is randomly generated within the parameter space. In each generation, *np* competitions are held to determine the composition of the next generation. Every pair of randomly chosen vectors $X_{1,G}$ and $X_{2,G}$ defines a vector differential ($X_{1,G}$ - $X_{2,G}$). Their weighted differential is used to perturb another randomly chosen vector $X_{3,G}$ according to (10).

$$X'_{3,G+1} = X_{3,G} + F \cdot (X_{1,G} - X_{2,G}) \tag{10}$$

Typically, F lies within the range ($0 \leq F \leq 1.0$), and it controls the speed and robustness of the search; a lower value increases the rate of convergence but also the risk of being stuck at the local optimum. The crossover is a complimentary process for DE. It aims at reinforcing the prior successes by generating the offspring vectors. In every generation, each primary array vector $X_{i,G}$, is targeted for crossover with a vector like $X'_{3,G+1}$ to produce a trial vector $X_{t,G+1}$ according to (11).

$$X_{t,G+1} = \begin{cases} X'_{3,G+1} & \text{if } rand < C_R \\ X_{i,G} & \text{otherwise} \end{cases} \tag{11}$$

Typically, C_R is in the range ($0 \leq C_R \leq 1.0$). The newly created vector is evaluated by the objective function and the corresponding value is compared with the target vector. The best fit vector is kept for the next generation as determined by (12). The best parameter vector is evaluated for every generation in order to track the progress made throughout the minimization process; thus making the DE elitist method.

$$X_{i,G+1} = \begin{cases} X_{t,G+1} & if \ \ fit(X_{t,G+1}) \le fit(X_{i,G}) \\ X_{i,G} & otherwise \end{cases} \tag{12}$$

The DE implementation process in this paper is as follows: The control or the decision variables for the ED problem are real power outputs of all committed generations, and are therefore used to form the individuals in the population. A population of individuals is initialized using the approach shown in Fig. 2 and each individual is decoded and evaluated in the population using (9). An initial population composed of vectors $X^{o}_{i,G} = \left[P_{i,1}, P_{i,2}, ..., P_{i,j}, ..., P_{i,N}\right]$ is randomly generated within the parameter space (where $i=1,2,...np$, j is index of generating units in this DE formulation and N is number of committed generating units). In each generation, np competitions are held to determine the composition of the next generation. Randomly chosen vectors (individuals) $X_{1,G}$, $X_{2,G}$ and $X_{3,G}$ drawn from the population are defined by $X_{1,G} = \left[P_{1,1}, P_{1,2}, ..., P_{1,j}, ..., P_{1,N}\right]$, $X_{2,G} = \left[P_{2,1}, P_{2,2}, ..., P_{2,j}, ..., P_{2,N}\right]$ and $X_{3,G} = \left[P_{3,1}, P_{3,2}, ..., P_{3,j}, ..., P_{3,N}\right]$. The elements of $X_{1,G}$, $X_{2,G}$ and $X_{3,G}$ are real power outputs of the committed N generating units, which are subjected to the capacity constraints in (5) - (6). For N generators, an individual is represented as a vector of length N. Each element of the population is initialized randomly within the effective real power operating limits. The initialization is either based on (5) for generators without ramp-rate limits, or on (6) for generators with ramp-rate limits. The DE step by step process in evaluating the best parameter vector $X_{i,G+1}$ in (12) for every generation in order to track the progress made throughout the minimization process is accomplished by executing (10) - (12). The best parameter vector evaluated for the latest generation produces the optimal economic dispatch generation with the minimum generation cost.

The most common method used to select control parameters is parameter tuning. Parameter tuning adjusts the control parameters through experimentation until the best settings are determined. To avoid premature convergence of the DE algorithm, it is crucial that F be of sufficient magnitude. On the other hand, the scaling factor F should not be chosen too large, since the number of function evaluations increases as F

increases. F is made adaptive in this paper. The crossover constant C_R controls the diversity of the population. Relatively high values of C_R result in higher diversity and improved convergence speed. However, beyond certain threshold value, the convergence rate may decrease or the population may converge prematurely. On the other hand, small values of C_R increase the possibility that the algorithm stagnates in local minima. The population size plays an important role in the algorithm convergence rate. Small population may cause a poor searching performance and stagnations in local minima. Large populations increase the possibility for finding optimal solutions at the expense of a large number of function evaluations.

3.3. MPSO Based Economic Dispatch

The modified PSO is a combination of PSO and an evolutionary strategy enhancing the method to perform optimal search under complex environments [12]. This version of MPSO is a variant of the original formulation of the continuous particle swarm optimization (CPSO) to solve continuous optimization problems such as the ED problem considered in this paper.

Let X and V denote a particle's position and its corresponding flight speed or velocity respectively in a search space. Therefore, the lth particle is represented as X_{ld} = (X_{l1}, X_{l2},…, X_{lN}) in the d-dimensional space. The best previous position of the lth particle is recorded and represented as P_{lbd} =(P_{lb1}, P_{lb2},…, P_{lbN}). The index of the best particle among all the particles in a group is represented by P_{gd}. The rate of the velocity for lth particle is represented as V_{ld} = (V_{l1}, V_{l2},…, V_{lN}). In this version of PSO, the velocity is limited to a certain range [-V_{max}, V_{max}], such that V_{ld} always lies within this range [12]. The new velocity and position for each particle i in dimension d are determined according to the velocity and position update equations given by (13) and (14), while the inertia weight is updated according to (15).

$$V_{ld}(t) = wV_{ld}(t-1) + c_1 \cdot rand_1 \cdot (P_{lbd}(t-1) - X_{ld}(t-1)) + c_2 \cdot rand_2 \cdot (P^*_{gb}(t-1) - X_{ld}(t-1)) \qquad (13)$$

$$X_{ld}(t) = X_{ld}(t-1) + V_{ld}(t) \qquad (14)$$

$$w = w_{\max} - \left(\frac{w_{\max} - w_{\min}}{iter_{\max}} \right) \times iter \qquad (15)$$

Supposing P_{gd} is the swarm's global best particle chosen with a random number less than a predefined mutation rate (for $0 < M_R < 0.2$), then the mutation result of this particle is given by (16).

$$If\ rand < M_r$$

$$P^{*}_{gd}(t-1) = P_{gd}(t-1) + ceil(randn \times P_{gd}(t-1)/\beta_{gb}) \tag{16}$$

$$else$$

$$P^{*}_{gd}(t-1) = P_{gd}(t-1)` \tag{17}$$

$$end$$

$$d=1, 2, \ldots, N$$

Where β_{gb} is global best strategic learning parameter for mutation that can be either dynamically changing or fixed, and controls the mutation process introduced in this MPSO method. The main goal is to increase the diversity of the population by preventing the particles from moving too close to each other, thus converging prematurely to local optima. This eventually improves the CPSO's search performance.

The MPSO implementation process for solving the ED problem in this paper is as follows: The control or the decision variables for the ED problem are real power generations, and are therefore used to form the swarm. The real power outputs of all on-line generators are represented as the positions of the particles in the swarm [13 - 17]. For N generators, the particle's position is represented as a vector of length N. If there are N_{par} particles in the swarm, the lth particle in the swarm can be represented as a matrix shown in (18).

$$P_{ld} = \left[P_{l1}, P_{l2}, \ldots, P_{li}, \ldots, P_{lN}\right] \tag{18}$$

$$d=1, 2, \ldots, i, \ldots, N$$

Where P_{ld} is the position vector of the particle l in dimension d, and a feasible P_{ld} represents a potential solution to the optimization problem. The element P_{li} of the vector

P_{ld} is the lth position component of particle l, and it represents the real power generation of on-line generator i of the possible solution.

Each element of the swarm matrix is initialized randomly within the effective real power operating limits. The initialization is either based on (5) for generators without ramp-rate limits, or on (6) for generators with ramp-rate limits.

The ith dimension of the lth particle is assigned a value of P_{li} determined by (19) while satisfying the constraints given by (5) or (6) depending on whether ramp-rate limits are considered or not. Constraint (7) should also be satisfied if the units' prohibited operating zones are known.

$$P_{li} = P_{li}^{\min} + r \cdot (P_{li}^{\max} - P_{li}^{\min}) \tag{19}$$

The fitness values obtained from (1) for the initial particles of the swarm are set as the initial *pbest* values of the particles. The best value among all the *pbest* values becomes the *gbest*. Mutation operator is introduced into the method using (16).

The new velocity is computed using (13). To control excessive roaming of the particles, the velocity is limited to a certain range [-V_{max}, V_{max}], such that V_{ld} always lies only within this range. The maximum velocity is limited to between 10% - 20% of the dynamic range of the variable on each dimension.

The swarm is updated by updating the particle's position vector using (14). The *pbest* and *gbest* values are subsequently updated. The latest *gbest* position produces the optimal economic dispatch generation with the minimum generation cost.

4. CASE STUDIES, NUMERICAL RESULTS AND ANALYSIS

4.1. Case Studies

Three case studies are presented in this paper. Solving the static economic dispatch problem using heuristic methods for smooth and non-smooth fuel cost functions are demonstrated in Cases I and II, while Case III applies heuristic methods to solve the dynamic economic dispatch problem for a non-smooth fuel cost function with valve-point loading effects.

4.1.1. Case I

The test system in this case study consists of 6 thermal units, 26 buses and 46 transmission lines [16 - 18]. The generation limits, smooth fuel cost coefficients (α =0), ramp-rates limits and prohibited operating zones of these thermal units are shown in Tables A.1 and A.2 of the Appendix. The system real power loss is also considered in this case. The loss coefficients on 100MVA base capacity are presented in (20) - (22). The total load demand is 1263MW. There is 207MW of total spinning reserve accruable from the 6 thermal units, amounting to 14.08% of total generation, thus satisfying the constraint in (8).

Using the data presented in Tables A and B, the total generation cost resulting from the online units can be evaluated based on their economic dispatch generation after minimization of the objective function in (1) subject to satisfying constraints (3) - (8).

$$B_{ij} = \begin{bmatrix} 0.0017 & 0.0012 & 0.0007 & -0.0001 & -0.0005 & -0.0005 \\ 0.0012 & 0.0014 & 0.0009 & 0.0001 & -0.0006 & -0.0001 \\ 0.0007 & 0.0009 & 0.0031 & 0.0000 & -0.0010 & -0.0006 \\ -0.0001 & 0.0001 & 0.0000 & 0.0024 & -0.0006 & -0.0008 \\ -0.0005 & -0.0006 & -0.0010 & -0.0006 & 0.0129 & -0.0002 \\ -0.0005 & -0.0001 & -0.0006 & -0.0008 & -0.0002 & 0.0150 \end{bmatrix} \tag{20}$$

$$B_{oi} = 1.0e^{-03} * \begin{bmatrix} -0.3908 & -0.1297 & 0.7047 & 0.0591 & 0.2161 & -0.6635 \end{bmatrix} \tag{21}$$

$$B_{oo} = 0.0056 \tag{22}$$

4.1.2. Case II

The test data for this case is taken from a real power system consisting of 19 generating units characterized by smooth fuel cost coefficients (α =0), drawn from two industrial parks located in Bintan and Batam in Indonesia [19]. Table A.3 of the Appendix presents the output power ratings and fuel cost coefficients of the 19 generating units, from which the total generation cost is evaluated as described under Case I.

4.1.3. Case III

The test system for this case is a 10-unit system with valve-point loading effects (α =1) whose data is shown in Table A.4 of the Appendix. The hourly and dynamic load demand is divided into 24-hour intervals [4], and presented in Table A.5 of the Appendix.

4.2. Numerical Results and Analysis

All numerical results are obtained based on Matlab programs ran on PC with 2.2GHZ CPU speed and 1.5GB of RAM. The parameters shown in Table A.6 of the Appendix are used by the three heuristic methods and described as follows: 50 chromosomes, 50 individuals and 30 particles corresponding to the population sizes for the GA, DE and MPSO methods respectively are empirically determined values to produce the best convergence rates and computation times for Cases I, II and III. The population size plays an important role in the algorithms' convergence rates, in the sense that small population may cause a poor searching performance and stagnations in local minima. Large populations on the other hand, increase the possibility for finding optimal solutions at the expense of a large number of function evaluations and computation time. Maximum generations/iterations of 150, 500 and 500 for Cases I, II and III, respectively, are used for fair comparison among the three algorithms (GA, DE and MPSO). Figs 3 - 4 and 6 on pages 26 and 28, respectively, shows that the three algorithms converged before their maximum generations/iterations are reached. For Case III (10-unit test system), due to partly the ramping rate limits and valve-point loading effects imposed on the generating units, there are additional complexities and computations which incurred relatively more number of generations/iterations compared with Case I (6-unit test system) to converge to the best solution. Crossover rates of 0.7 and 0.8 for the GA and DE respectively are empirically determined to yield the best results. The GA method is adaptive with the mutation rate linearly varied from 0.07 to 0.01. This range produces the best result for the problems presented and solved in this paper. The MPSO's mutation rate of 0.15 is empirically determined during simulation to result in the best solutions. Higher values resulted in over exploration of the search space by the particles and consequent non-optimal solutions. The DE is adaptive with the scaling factor for mutation F linearly varied from 0.08 to 0.02. The best results are obtained within this range for the problems presented in this paper. MPSO's β_{gb} is dynamically varied but did yield good results. A fixed value of 2 however, is empirically determined to produce the best result. K_{pb} of 1000 is experimentally determined power balance weighting coefficients which serves as penalty for power balance constraint violation. A suitable value of 1000 is empirically determined to enforce the power balance constraint and produce best results for the three cases considered in this paper. The MPSO is adaptive with the inertia weight linear varied from 0.9 to 0.4. These are experimentally determined best limits during simulation. MPSO's c_1 and c_2 with values of 2 each, so that their total sum is 4 are empirically determined standard values to produce the best result. MPSO's V_{max} of 20% of the dynamic range of the variables on each dimension is empirically determined standard value to produce the best result. It controls the excessive roaming of the particles, and ensures that the particles are confined within some predetermined boundaries based on the problem dimension. Too large V_{max} may cause some particle's velocities to be too high and affects convergence rate.

Results of the three cases are presented below.

4.2.1. Case I

Table 1 shows the ED schedules generated by each of the six thermal units. The table also presents the total generation, total power loss and total generation costs produced by GA, DE and MPSO based ED methods. The table shows the amount of power generation economically dispatched to meet the load demand of 1263 MW while satisfying constraints (3) - (8). Total minimum generation costs in meeting load demand, as produced by GA, DE and MPSO based ED methods are \$15445, \$15445 and \$15444 respectively. Dispatch result from MPSO based ED method is seen to result in the best minimum generation cost and real power loss compared with the GA and DE based ED methods. This result demonstrate MPSO based ED method better capability in solving the ED problem compared with the GA and DE based ED methods for units characterized by ramp-rate limits and prohibited operating zones.

Table 2 shows the comparison of the generation costs among all the ED methods considered in this paper. The table shows that MPSO performs better than the GA and DE based ED methods in terms of the best minimum generation costs and standard deviations.

TABLE 1

Power Generation and Generation Costs Data for Case I (6-Unit Test System)

Generating units	Methods							
	100 Trials (Proposed)			50 Trials [16]		100 Trials [17]	50 Trials [18]	
	GA	DE	MPSO	GA [16]	PSO [16]	NPSO-LRS [17]	PSO [18]	MPSO [18]
P_1	439.7774	440.3697	438.9866	474.8066	447.4970	446.9600	451.2741	444.8882
P_2	179.6234	190.2445	162.9011	178.6363	173.3221	173.3944	162.4633	168.1455
P_3	261.5945	299.4663	267.0032	262.2089	263.4745	262.3436	262.6419	265.0000
P_4	133.5927	108.4497	138.7787	134.2826	139.0594	139.5120	130.3146	129.4751
P_5	151.3102	130.5306	158.3033	151.9039	165.4761	164.7089	173.8361	173.0299
P_6	109.4452	106.3589	109.0412	74.1812	87.1280	89.0162	95.1188	95.0435
Total generation over an hour (MW)	1275.3434	1275.4197	1275.0141	1276.0300	1276.0100	1275.9351	1275.6488	1275.5823
Load supplied over an hour (MW)	1263.0000	1263.0000	1263.0000	1263.0000	1263.0000	1263.0000	1263.0000	1263.0000
P_{loss} over an hour (MW)	12.3434	12.4197	12.0141	13.0217	12.9584	12.9361	12.6448	12.6411
Total min. generation cost over an hour ($)	15450	15445	15444	15459	15450	15450	15446	15444

The results presented in Tables 1 and 2 shows a reduction in both the total minimum generation costs and transmission losses produced by GA, DE and MPSO (after 150 iterations of 100 trials) in this paper compared with the results obtained in [16 - 18] on the same test system using GA and PSO (after 50 and 100 trials). The significant power loss reductions with the MPSO presented in this paper has the potential benefits of energy saving, fuel cost curtailment and CO_2 emission reduction. The loss reductions are reflections of improvements in the performances of the GA, DE and MPSO presented in this paper.

Table 3 shows the statistical comparison of computation efficiency for the GA, DE and MPSO methods considered in this paper. The MDPSO based ED method demonstrates faster computation time in finding the minimum generation cost compared with GA and DE based ED methods, as numerically shown in Table 3 for various scenarios of maximum generations/iterations. The GA however, converged to global solutions at faster rates than the DE under similar operating conditions as shown in Table 3.

TABLE 2

Statistical Comparison of Generation Costs for Case I (6-Unit Test System)

Methods		Total generation cost over an hour			
		Min. ($)	Max. ($)	Ave. ($)	Std
100 Trials (Proposed)	GA	15450	15498	15478	25.2104
	DE	15445	15500	15480	26.1426
	MPSO	15444	15496	15457	24.8425
50 Trials [16]	GA [16]	15459	15524	15469	-
	PSO [16]	15450	15492	15454	-
100 Trials [17]	NPSO-LRS [17]	15450	-	-	-
50 Trials [18]	PSO [18]	15446	15538	15477	-
	MPSO [18]	15444	15504	15460	-

TABLE 3

Comparison of Computation Efficiency for Case I (6-Unit Test System)

Description	Methods	Generations/Iterations				
		150	500	1000	3000	5000
Total CPU time (sec)	GA	3.82	11.58	23.88	84.85	175.32
	DE	13.78	44.71	92.11	284.96	510.68
	MPSO	0.89	1.63	3.05	8.55	14.29

Figure 3 shows the convergence of the minimum generation costs for GA, DE and MPSO based ED methods over 150 iterations. The figure shows converged minimum generation costs of $15445, $15445 and $15444 for GA, DE and MPSO methods respectively. The converged result also conforms to the minimum generation costs presented in Tables 1 and 2.

4.2.2. Case II

The ED schedules generated by each of the 19 online generating units using GA, DE and MPSO based ED methods are presented in Table 4. The table shows the units' generations economically dispatched to balance up the supplied load as shown in Table 4, while meeting the system constraints. The result shows that the DE and MPSO performed comparably well in terms of finding the most economical dispatch generation, total generation and minimum generation costs. Percent deviation errors in perfectly matching the supplied load of 70.2 MW produced by GA, DE and MPSO based ED methods are 0.062%, 0.066% and 0.00% respectively.

TABLE 4

Power Generation and Generation Costs Data for
Case II (19-Unit Test System)

Generating units	Generation (MW)		
	GA	DE	MPSO
P_1	5.8720	2.6138	4.1000
P_2	1.7407	1.7425	3.6000
P_3	5.8214	3.4850	6.1000
P_4	4.5662	4.3563	3.1000
P_5	4.9589	4.2275	3.1000
P_6	4.7991	4.3830	6.1000
P_7	2.8216	5.2787	6.1000
P_8	1.9510	3.4860	5.1000
P_9	3.8598	3.6570	2.1000
P_{10}	5.9470	5.1998	3.4000
P_{11}	2.6318	4.5713	2.4000
P_{12}	1.7762	2.7428	4.4000
P_{13}	4.8375	6.9993	5.1000

Generating units	Generation (MW)		
	GA	DE	MPSO
P_{14}	7.1800	6.8565	6.0000
P_{15}	2.5943	1.7425	2.1000
P_{16}	1.0058	1.3018	1.1000
P_{17}	1.7053	1.2026	2.1000
P_{18}	0.8738	1.3009	2.1000
P_{19}	5.3010	5.0987	2.1000
Total gen. over a week (MW)	70.2434	70.2460	70.2000
Load supplied over a week (MW)	70.2000	70.2000	70.2000
Total generation cost over a week ($)	242220	242240	242210

Table 5 shows the statistical comparison of the generation costs among all the ED methods considered in this paper. The table shows DE and MPSO methods performing fairly better than the GA method in terms of the statistical variation of the generation costs arrived at, and its corresponding standard deviations.

TABLE 5

Statistical Comparison of Generation Costs for
Case II (19-Unit Test System)

Methods	Total generation cost over a week			
	Min. ($)	Max. ($)	Ave. ($)	Std
GA	242220	242310	242300	28.4032
DE	242240	242350	242330	40.6283
MPSO	242210	242350	242280	40.0371

Table 6 shows the statistical comparison of computation efficiency for the GA, DE and MPSO based ED methods for the 19 units test system for different maximum generations/iterations. The MPSO method is shown to possess faster computation time compared with the GA and DE. In the contrary, the DE method exhibits the slowest computation time as presented in Table 5.

TABLE 6

Comparison of Computation Efficiency for Case II (19-Unit Test System)

Description	Methods	Generations/Iterations				
		150	500	1000	3000	5000
Total CPU time (sec)	GA	52.41	87.63	136.52	509.10	999.32
	DE	105.76	199.29	330.2	815.31	1363.96
	MPSO	3.42	7.57	14.33	39.72	67.66

The convergence performances over 500 iterations of the GA, DE and MPSO based ED methods for the 19-unit test system are presented in Fig. 4. The figure shows the minimum generation costs convergence behavior for each of the three methods considered in this paper, which simply corresponds to the best generation costs desired, and conforms to the result presented in Tables 4 and 5. The MPSO generated better minimum generation costs of $242210 compared with $242220 and $242240 generated by the GA and DE methods respectively as shown in Fig. 4 and Tables 4 and 5.

4.2.3. Case III

Figure 5 shows the best DED schedules for the 10-unit test system using the GA, DE and MPSO methods. The generating units' outputs are adapting to the hourly real power demand. The units' output are dynamically adjusted and allocated to meet the hourly dynamic load changes whose demand pattern is shown in Table A.5 of the Appendix, while satisfying the up and down ramp-rate limits constraint in (6) and presented in Table A.4 of the Appendix for Case III (10-unit system), as well as meeting other DED constraints. The best results depicted in Fig. 5 indicate that GA, DE and MPSO are all capable of solving the DED of a power system.

Figure 6 shows the DED convergence performances over 500 iterations using the GA, DE and MPSO methods for the 10-unit test system. The figure shows the minimum generation costs convergence behavior in hour 1 for each of the three methods considered in this paper. The GA, DE and MPSO methods generated in hour 1 the minimum generation costs of $29998, $29996 and $29995 respectively as shown in Fig. 6. These minimum generation costs represent the best DED generation costs obtained in hour 1. Similar convergence performance analysis can be made for the entire 24-hour dispatch period.

Table 7 shows the statistical comparison of the total daily generation costs among GA, DE and MPSO methods applied to solving the DED problem for the 10-unit test system obtained over 500 iterations of 100 trials. The MPSO result shows better performance in terms of the minimum (best) total daily generation cost of $103520 compared with total daily generation costs of $104530 and $104540 produced by GA and DE respectively. A minimum total daily generation cost of $103520 produced by the MPSO is also seen to outperform the $1035748 obtained in [4].

TABLE 7

Statistical Comparison of Total Daily Generation Costs
for the DED of Case III (10-Unit Test System)

Methods	Total daily generation cost			
	Min. ($)	Max. ($)	Ave. ($)	Std
GA	104530	104820	104720	200.9821
DE	104540	105050	104800	226.3501
MPSO	103520	104730	104140	201.1200

Table 8 shows the comparison of computation efficiencies of GA, DE and MPSO methods in solving the DED for Case III (10-unit test system) over 24-hour dispatch period obtained in 500 iterations. The table shows that MPSO method has faster computation time than GA and DE methods. The MPSO is 6.85 and 28.30 times faster than the GA and DE respectively, while the GA is 4.13 times faster than the DE for the DED problem of the 10-unit test system presented in this paper as deduced from Table 8. The GA and DE are slower than MPSO mainly because the number of bits (n) representing each unit power output used in this paper is 16. The more the number of bits per unit power output the better the quality and resolution of result, though at the expense of more computation time.

TABLE 8

Comparison of Computation Efficiency for the DED of Case III (10-Unit Test System) over 500 Iterations

	Dispatch period	GA	DE	MPSO		Dispatch period	GA	DE	MPSO
		Methods					Methods		
CPU time (sec)	Hour 1	19.26	77.64	2.78	CPU time (sec)	Hour 13	18.57	77.86	2.72
	Hour 2	19.00	77.83	2.81		Hour 14	18.90	77.48	2.76
	Hour 3	18.83	78.19	2.75		Hour 15	19.01	77.72	2.73
	Hour 4	18.69	77.69	2.75		Hour 16	19.01	78.02	2.75
	Hour 5	18.69	77.22	2.72		Hour 17	18.81	78.39	2.77
	Hour 6	18.78	78.32	2.77		Hour 18	18.76	78.50	2.76
	Hour 7	18.84	78.09	2.75		Hour 19	19.13	78.55	2.77
	Hour 8	18.66	77.16	2.73		Hour 20	18.95	78.28	2.78
	Hour 9	18.73	78.06	2.73		Hour 21	18.79	77.82	2.73
	Hour 10	18.87	77.79	2.73		Hour 22	18.92	77.73	2.76
	Hour 11	18.85	77.51	2.79		Hour 23	18.81	78.14	2.74
	Hour 12	19.00	77.66	2.72		Hour 24	18.84	78.50	2.75
CPU time over 24-hour (sec)						Total	452.69	1870.20	66.06
						Mean	18.86	77.92	2.75
						Std	±0.16	±0.39	±0.02

5. CONCLUSIONS

The power system challenges of efficiently and economically solving the static economic dispatch and dynamic economic dispatch problems for generators exhibiting practical and non-smooth characteristic behavior with heuristic methods have been presented. System losses have been incorporated to test the robustness of the heuristic methods. The heuristic methods for solving the static economic dispatch and dynamic economic dispatch problems have been compared on three test systems. The modified particle swarm optimization method shows better performance in terms of the quality of results, loss reduction and computational efficiency in locating optimal solution when compared with the genetic algorithm and differential evolution methods under similar operating conditions. Curse of dimensionality is seen not to have limitation on the methods' performances and in the quality of results obtained for the three power systems considered in this paper. The results offer good alternative for power system operation, control and planning activities in control centers desiring optimized energy management, generation costs curtailment and transmission loss reduction, in the face of continuously increasing global fuel costs and the irreplaceable depletion of conventional raw fuel resources.

Future work will investigate if results from re-coding purely real-valued GA and DE have comparable performances with the already real-coded MPSO method (especially in their computation times, ability to satisfy all constraints and quality of results) on similar test systems. Also, dynamic economic dispatch for a conventional power system integrating wind power is also planned for future work.

ACKNOWLEDGMENT

The financial support from the National Science Foundation (NSF), USA under the grant ECCS # 0348221 is gratefully acknowledged by the authors.

REFERENCES

1 Wood, A. J. and Wollenberg, B. F.: 'Power generation operation and control', John Wiley and Sons, New York, 2004.

2 Wang, C. and Shahidehpour, S. M.: 'Effects of ramp-rate limits on unit commitment and economic dispatch', *IEEE Trans. on Power Syst.*, 1993, 8, (3), pp. 1341-1349.

3 Victoire, T. A. A. and Jeyakumar, A. E.: 'Reserve constraint dynamic dispatch of units with valve-point effects', *IEEE Trans. on Power Syst.*, 2005, 20, (3), pp.1273-1282.

4 Attaviriyanupap, P., Kita, H., Tanaka, E. and Hasegawa, J.: 'A hybrid EP and SQP for dynamic economic dispatch with non-smooth fuel cost function', *IEEE Trans. on Power Syst.*, 2002, 17, (2), pp. 411-416.

5 Firma, H. T. and Legey, L. F. L.: 'Generation expansion: an iterative genetic algorithm approach', *IEEE Trans. on Power Syst.*, 2002, 17, (3), pp. 901-906.

6 Engelbrecht, A. P.: 'Fundamentals of computational swarm intelligence', John Wiley & Sons Ltd, West Sussex, England, 2005.

7 Damousis, I. G., Bakirtzis, A. G. and Dokopolous, P. S.: 'Network-constrained economic dispatch using real-coded genetic algorithm', *IEEE Trans. on Power Syst.*, 2003, 18, (1), pp. 198-205.

8 Chen, P.-H. and Chang, H.- C.: 'Large-scale economic dispatch by genetic algorithm', IEEE *Trans. on Power Syst.*, 1995, 10, (4), pp. 1919-1926.

9 Pereira-Neto, A. and Savedra, O. R.: 'Efficient evolutionary strategy optimization procedure to solve the nonconvex economic dispatch problem with generator constraints', *IET Gen. Trans. Dist.*, 2005, 152, (5), pp. 653-660.

10 Tippayachai, J., Ongsakul, W. and Ngamroo, I.: 'Parallel micro genetic algorithm for constrained economic dispatch', *IEEE Trans. on Power Syst.*, 2002, 17, (3), pp. 790-797.

11 Sinha, N., Chakarabarti, R. and Chattopadhyay, P. K.: ‘Evolutionary programming techniques for economic load dispatch’, *IEEE Trans. on Evol. Comp.*, 2003, 7, (1), pp. 83-94.

12 del Valle, Y., Venayagamoorthy, G. K., Mohagheghi, S., Hernandez, J. and Harley, R. G.: ‘Particle swarm optimization: Basic concepts, variants and applications in power system’, IEEE *Trans. on Evol. Comp.*, 2008, 12, (2), pp. 171-195.

13 Kuo, C.-C.: ‘A novel coding scheme for practical economic dispatch by modified particle swarm approach’, *IEEE Trans. on Power Syst.* 2008, 23, (4), pp. 1825-1835.

14 Park, J.-B., Lee, K.-S. , Shin, J.-R. and Lee, K. W.: ‘A particle swarm optimization for economic dispatch with nonsmooth cost functions’, *IEEE Trans. on Power Syst.*, 2005, 20, (1), pp. 34-42.

15 Chaturvedi, K. T., Pandit, M. and Srivastava, L.: ‘Self-organizing hierarchical particle swarm optimization for nonconvex economic dispatch’, *IEEE Trans. on Power Syst.*, 23, (3), pp. 1079-1087.

16 Gaing, Z.-L.: ‘Particle swarm optimization to solving the economic dispatch considering the generator constraints’, *IEEE Trans. on Power Sys.*, 2003, 18, (3), pp. 1187-1195. Closure to discussion of, ‘Particle swarm optimization to solving the economic dispatch considering the generator constraints’, *IEEE Trans. on Power Syst.*, 2004, 19, (4), pp. 2122-2123.

17 Selvakumar, A. I. and Thanushkodi, K.: ‘A new particle swarm optimization solution to nonconvex economic dispatch problems’, *IEEE Trans. on Power Syst.*, 2007, 22, (1), pp. 42-51.

18 Neyestani, M., Farsangi, M. M., Nezamabadi-pour, H. and Lee, K. Y.: ‘A modified particle swarm optimization for economic dispatch with nonsmooth cost functions’, *IFAC Symposium on Power Plants and Power syst. Contr.* Tampere Hall, Finland, 2009.

19 Lee, K. Y. and El-Sharkawi, M. A.: ‘Modern heuristic optimization techniques: theory and applications to power systems’, IEEE Press, 445 Hoes Lane, Piscataway, New Jersey, 2008.

APPENDIX

TABLE A.1

Generating Units Data for Case I (6-Unit Test System)

Generating unit	Power limits (MW)		Fuel cost coefficients		
	P_i^{min}	P_i^{max}	a_i (\$)	b_i (\$/MW)	c_i (\$/MW^2)
P_1	100	500	240	7.0	0.0070
P_2	50	200	200	10.0	0.0095
P_3	80	300	220	8.5	0.0090
P_4	50	150	200	11.0	0.0090
P_5	50	200	220	10.5	0.0080
P_6	50	120	190	12.0	0.0075

TABLE A.2

Ramp-Rate Limits and Prohibited Zones of Generating Units for Case I (6-Unit Test System)

Generating unit	P_i^{pre} (MW)	UR_i (MW/h)	DR_i (MW/h)	Prohibited zones (MW)
P_1	440	80	120	[210 240] [350 380]
P_2	170	50	90	[90 110] [140 160]
P_3	200	65	100	[150 170] [210 240]
P_4	150	50	90	[80 90] [110 120]
P_5	190	50	90	[90 110] [140 150]
P_6	110	50	90	[75 85] [100 105]

TABLE A.3

Generating Units Data for Case II (19-Unit Test System)

Generating unit	Generating units' maximum output power (MW)	Fuel cost coefficients		
		a_i (\$)	b_i (\$/MW)	c_i (\$/MW^2)
P_1	6.1	52.6	5.44	0.0038
P_2	6.1	52.6	5.44	0.0038
P_3	6.1	52.6	5.44	0.0038
P_4	6.1	52.6	5.44	0.0038
P_5	6.1	52.6	5.44	0.0038
P_6	6.1	52.6	5.44	0.0038
P_7	6.1	52.6	5.44	0.0038
P_8	6.1	53.7	6.34	0.0046
P_9	6.1	51.5	5.34	0.005
P_{10}	6.4	51.5	5.34	0.005
P_{11}	6.4	52.5	5.34	0.0057
P_{12}	6.4	52.5	5.34	0.0057
P_{13}	8	76.5	8.06	0.0346
P_{14}	8	76.5	8.06	0.0346
P_{15}	2.1	55.4	7.1	0.0076
P_{16}	2.1	55.4	7.1	0.0076
P_{17}	2.1	55.4	6.95	0.0076
P_{18}	2.1	55.4	7.3	0.0076
P_{19}	6.1	59.3	7.1	0.0079

TABLE A.4

Generating Units Data for Case III (10-Unit Test System)

Gen. Unit	Power limits (MW)		Fuel cost coefficients					UR_i (MW/h)	DR_i (MW/h)
	P^{min}	P^{max}	a_i ($)	b_i ($/MW)	c_i ($/MW^2)	e_i ($)	f_i (rad/MW)		
P_1	150	470	958.20	21.60	0.00043	450	0.041	80	80
P_2	135	460	1313.60	21.05	0.00063	600	0.036	80	80
P_3	73	340	604.97	20.81	0.00039	320	0.028	80	80
P_4	60	300	471.60	23.90	0.00070	260	0.052	50	50
P_5	73	243	480.29	21.62	0.00079	280	0.063	50	50
P_6	57	160	601.75	17.87	0.00056	310	0.048	50	50
P_7	20	130	502.70	16.51	0.00211	300	0.086	30	30
P_8	47	120	639.40	23.23	0.00480	340	0.082	30	30
P_9	20	80	455.60	19.58	0.10908	270	0.098	30	30
P_{10}	55	55	692.40	22.54	0.00951	380	0.094	30	30

TABLE A.5

24-Hour Dynamic Load Demand for Case III (10-Unit Test System)

Time (Hour)	1	2	3	4	5	6	7	8	9	10	11	12
Load demand (MW)	1036	1110	1258	1406	1480	1628	1702	1776	1924	2072	2146	2220

Time (Hour)	13	14	15	16	17	18	19	20	21	22	23	24
Load demand (MW)	2072	1924	1776	1554	1480	1628	1776	2072	1924	1628	1332	1184

TABLE A.6

Parameters for GA, DE and MPSO Methods

	GA	DE	MPSO
Population size	50 chromosomes	50 individuals	30 particles
Max. generation/ max. iteration	150 (Case I), 500 (Case II) and 500 (Case III)	150(Case I), 500 (Case II) and 500 (Case III)	150(Case I), 500 (Case II) and 500 (Case III)
C_R	0.7	0.8	-
M_R	Adaptive mutation (linearly decreasing from 0.07 to 0.01)	-	0.15
F	-	Adaptive scaling factor (linearly decreasing from 0.08 to 0.02)	-
β_{gb}	-	-	2
K_{pb}	1000	1000	1000
w_{iner}	-	-	Adaptive inertia weight (linearly decreasing from 0.9 & 0.4)
c_1 & c_2	-	-	2 (each)
V_{max}	-	-	20% of the dynamic range of the variable on each dimension

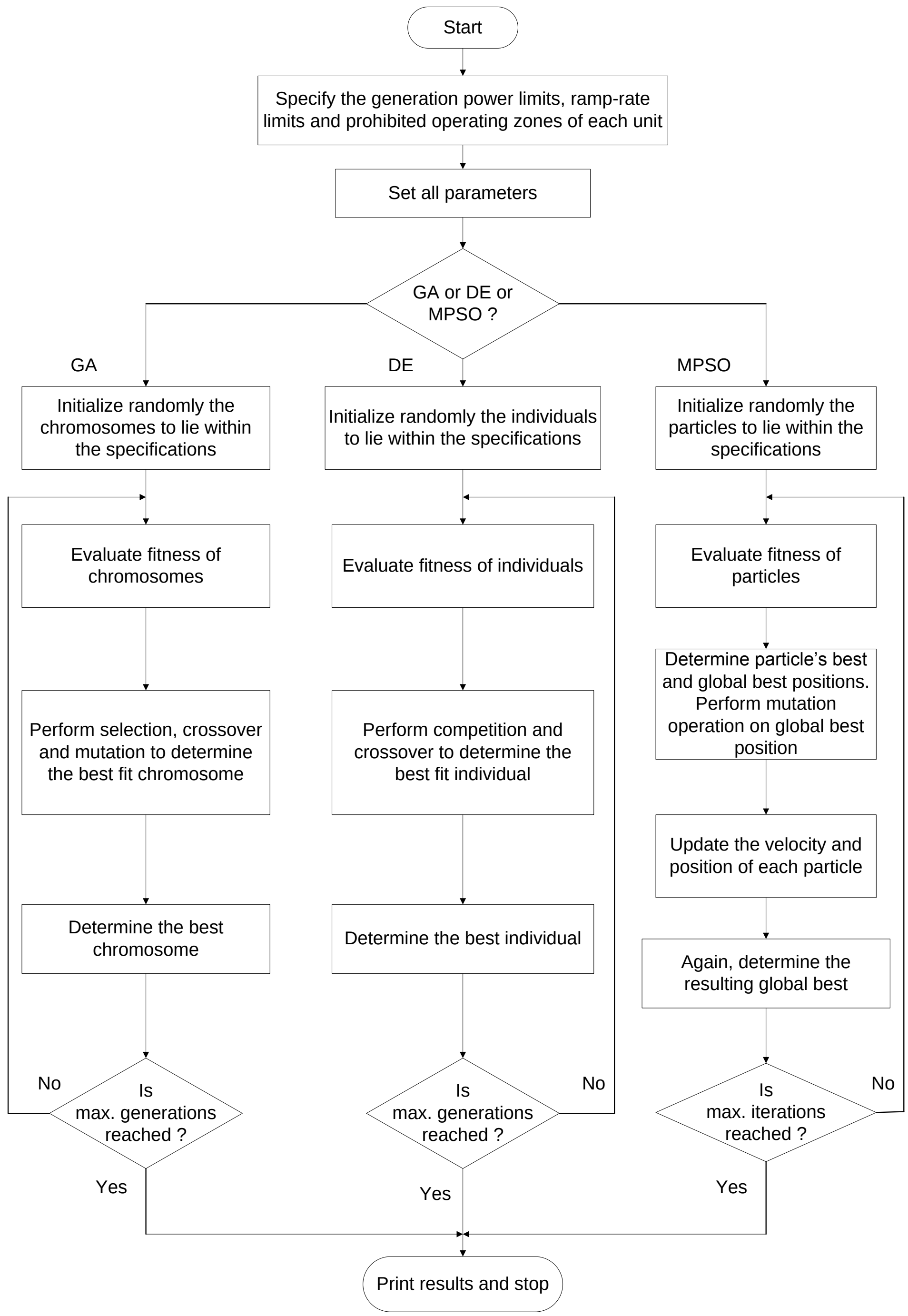

Fig. 1. A Flowchart Illustrating GA, DE and MPSO Based ED Methods

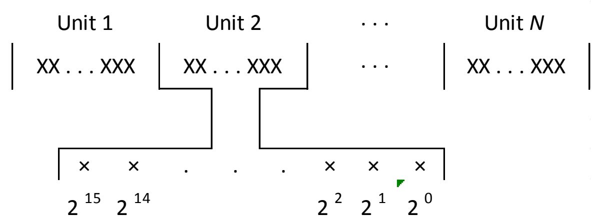

Fig. 2. The 16 × *N* bits Concatenated Binary Coding Scheme

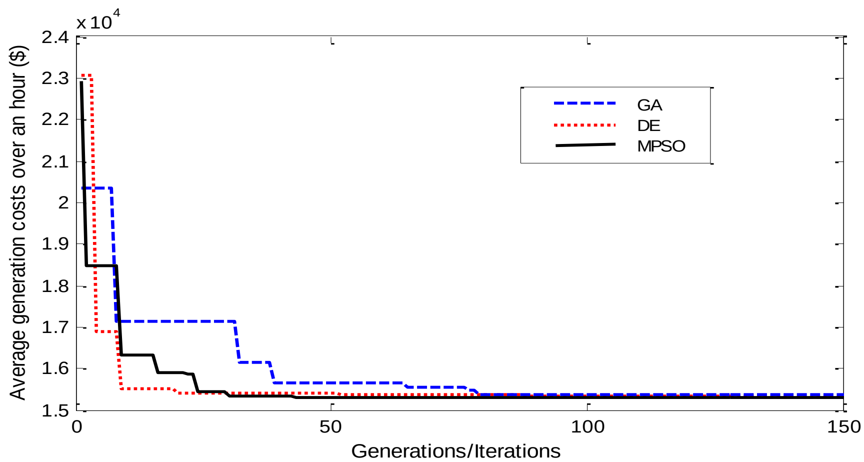

Fig. 3. Average Generation Cost Plots for Case I (6-Unit Test System)

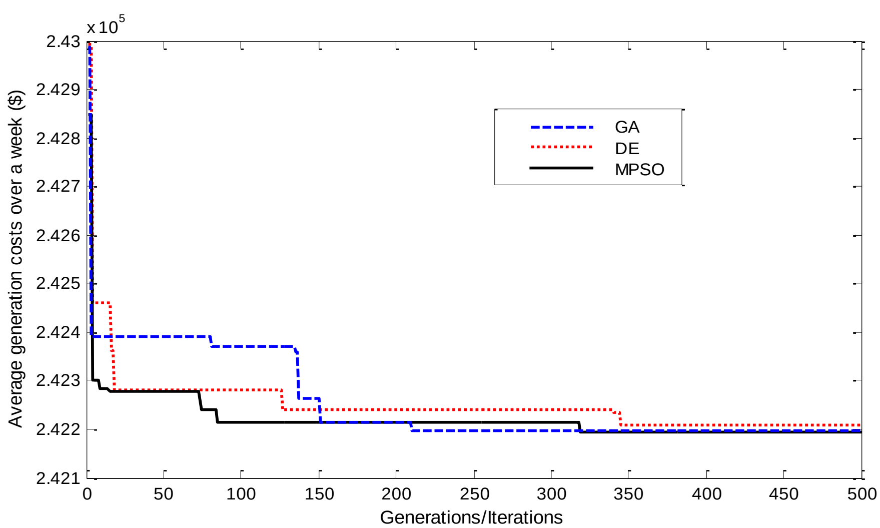

Fig. 4. Average Generation Cost plots for the Case II (19-Unit Test System)

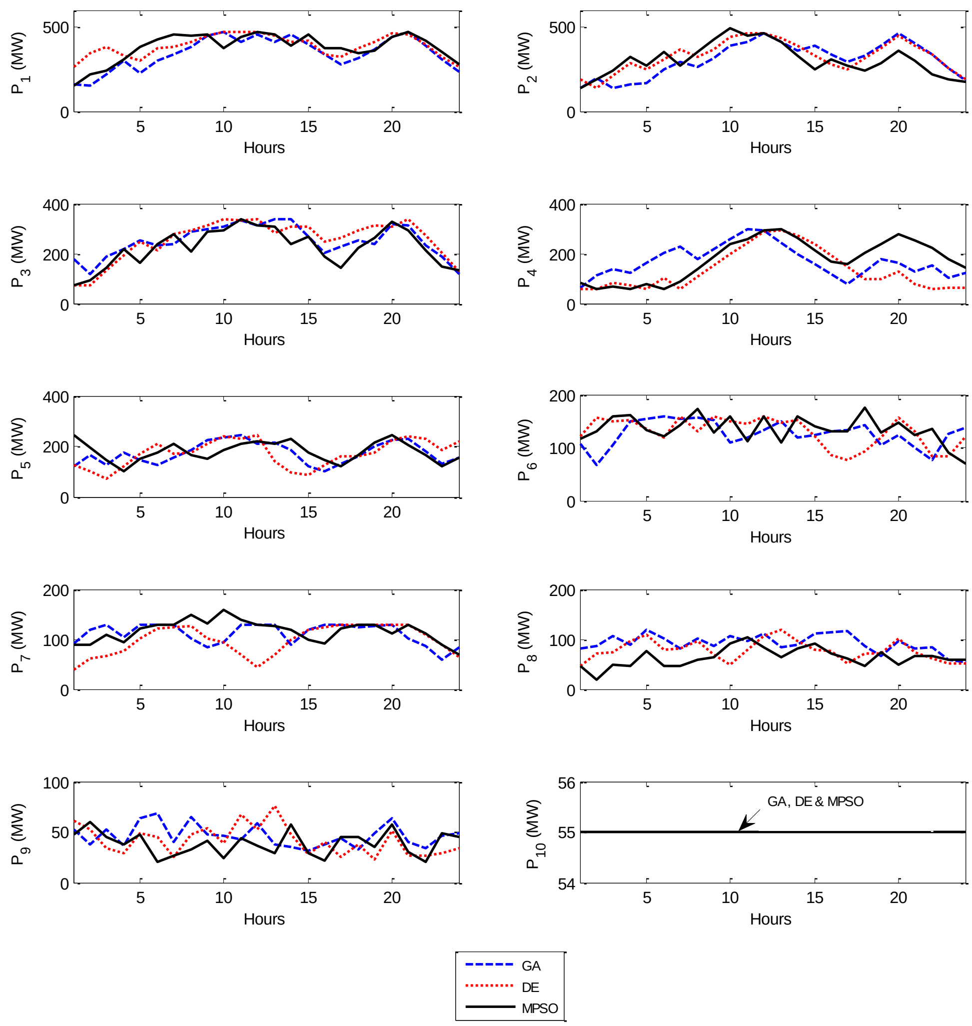

Fig. 5. Dynamic Economic Dispatch Schedules Plots for Case III (10-Unit Test System)

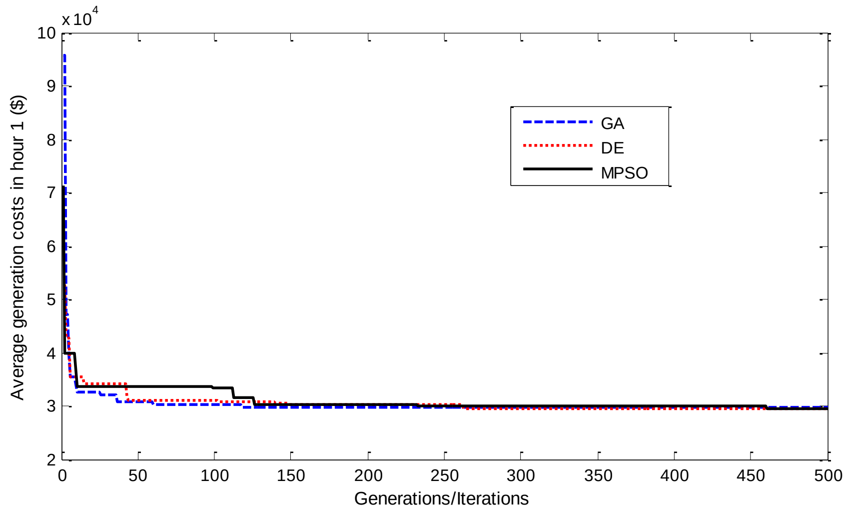

Fig. 6. Average Generation Cost Plots in Hour 1 for Case III (10-Unit Test System)

IV. MULTI-OBJECTIVE COMBINED ECONOMIC AND EMISSION DISPATCH WITH UNCERTAINTY IN WIND POWER FOR A WIND-HYDROTHERMAL SYSTEM

Y. Yare and G. K. Venayagamoorthy

Real-Time Power and Intelligent Systems Laboratory,
Missouri University of Science and Technology Rolla, MO 65409-0249 USA
(E-mail: yyare@ieee.org & gkumar@ieee.org)

ABSTRACT: This paper presents multi-objective combined economic and emission dispatch (MO-CEED) optimization problem for a wind-hydrothermal power system. This MO-CEED problem formulation becomes a challenging problem because of the presence of uncertainty in wind power (due to uncertain wind speed). Another aspect of the challenge is the integration/mixing of the wind power with the hydrothermal grid system for the purposes of economically meeting dynamic load demand while minimizing emission. The MO-CEED optimization process for this wind-hydrothermal power system while satisfying practical constraints, must also find trade-off solutions between multiple objectives (minimizing both fuel cost and emission simultaneously). A modified particle swarm optimization (MPSO) algorithm is used to solve this MO-CEED problem. Results are presented to show the benefits from integrating wind power with conventional hydrothermal power system including cost saving, emission reduction and the positive impact of capacity credit of wind power. A family of distributed optimal Pareto fronts for the MO-CEED problem has been generated for different scenarios of capacity credit of wind power. The potential for practical application of this approach in dispatch centers of wind-hydrothermal power system is demonstrated. A platform for achieving increased integration of renewable/sustainable energy is presented.

INDEX TERMS: Combined economic and emission dispatch, cost saving, emission reduction, multi-objective function, uncertainty in wind power.

NOMENCLATURE

A_w Swept area of the wind turbine's blade

a_i, b_i & c_i Fuel cost coefficients (coeffs) of the ith thermal unit

α_i, β_i, ζ_i, σ_i & λ_i Emission coeffs of the ith thermal unit

β_{gb} Global best strategic learning parameter for mutation

c_1 & c_2 Cognitive and social acceleration constants respectively

$C_{D,w}$ & $C_{E,w}$ Penalty cost coeffs for calling reserves to cover for deficit wind-generated power and for not using all available wind power respectively from wth wind plant

C_h & C_w Cost functions for hth hydro unit and wth wind plant respectively

C_p Performance coeff

d Particle's dimension

e_i & f_i Fuel cost coeffs of the ith thermal unit with valve-point effect

E_T Total CO_2 emission (tCO_2/h)

F_T, F_H & F_W Total costs derived from thermal, hydro and wind plants respectively ($/h)

F_{Total} Multi-objective function

$Iter$ & $Iter_{max}$ Current and maximum iteration number respectively

l lth particle

LF_k Apparent power flow (MVA) in line k

$LF_k^{\max}$ Maximum limit for apparent power flow

M_r Mutation rate

N Number of dimensions

η_i Price penalty factor for the ith thermal unit ($/$tCO_2$)

N_c Total number of constraints

n_d & N_{prob} Index and total number of discrete probability step of a normal distribution respectively

N_H & N_T Total number of running (or on-line) hydro and thermal units respectively

N_W Total number of wind-powered plants (or wind farms)

NB Total number of PQ buses

NE Total number of transmission lines

$P_{reference,wt}$ Actual production of wind power from the wth wind-powered plant (wind farm) in period t

P_{error,n_d} Probability of error ($Error_{n_d}$) at each n_dth discrete probability step of a normal distribution

$P_{exp,wt}$ Expected wind power from the wth wind-powered plant (wind farm) in period t

$P_{forecast,nd}$ Wind power forecast at each n_dth discrete probability step of a normal distribution

P_{gd} Swarm's best position for dimension d

P_{ht} & P_{it} Scheduled generations from the hth hydro and ith thermal units respectively in period t

$P_i^{\min}$ & $P_i^{\max}$ Minimum and maximum power limits respectively for thermal unit i

P_{loss} System loss

P_{lbd} lth particle best position for dimension d

P_{ld} Position vector of the particle l in dimension d

P_t^D Total real load demand for period t

P_w Wind turbine output power

R System reserve

ρ Density of air

r, $rand$, $rand_1$ & $rand_2$ Random numbers with uniform distribution in the range of [0, 1]

$randn$ Gaussian distributed random number with a zero mean and a variance of 1

t Index of period

T Set of indices of periods in dispatching horizon

U_{ht} & U_{it} On-line status of hth hydro and ith thermal units respectively in time t

V_i Voltage magnitude at bus i

$V_i^{\min}$ & $V_i^{\max}$ Minimum and maximum voltage limits at bus i

V_w Wind speed

V_{ld} & V_{max} lth particle velocity in dimension d and maximum particle velocity respectively

ω Weighting factor for multi-objective function

w_{iner}, $w_{iner}^{\min}$ & $w_{iner}^{\max}$ Current, initial and final inertia weights respectively

1. INTRODUCTION

Economic load dispatch (ELD) of generating units is an important optimization task and is performed in order to supply electricity economically to meet demand while minimizing the total generation cost and satisfying system constraints [1 - 3]. Modern power system is experiencing increased demand for electricity with related expansions in system size, which has resulted in higher number of generators and lower reserve margins making the ELD problem more challenging and complicated [1 - 3].

Utilities have been forced to modify their design and operational strategies to enhance de-carbonization as a consequence of increased public awareness of the relevant environmental protection laws and the passage of the Clean Air Act Amendments of 1990. To this effect, many strategies have been proposed, such as, installation of pollutant cleaning equipment, switching to low emission fuels, replacement of the aged fuel-burners with cleaner ones, and emission dispatching [4]. The first three strategies involve considerable long-term investment in the form of modification of existing equipment or simply installation of new equipment. The latter option of emission dispatching is a short-term approach in which a bi-objective fuel cost and emission functions are minimized simultaneously. A number of methods have been reported in the literature regarding economic and emission dispatch problem. One such work reduces this multi-objective problem to a single objective problem by converting the emission into constraint to be met while minimizing the economic cost function [4 - 7]. This approach however exposes weakness in establishing trade-off relations between the two conflicting objectives. Another optimization technique minimizes the economic and emission objectives alternately at different stages of the optimization process [4 - 7].

Worldwide interest in reducing environmental pollution and the increasing concern over possible energy shortage has led to fruitful increasing interest in generation of renewable electrical energy. Wind power has become the fastest growing energy sources in the world and the leading source among various renewable energy sources in the power industry. New concepts for cluster management include the aggregation of geographically dispersed wind farms according to various criteria, for the purpose of an optimized network management, maintenance and generation scheduling. These clusters are operated and controlled like large conventional power plants [8 - 14].

This paper addresses the stochastic multi-objective combined economic and emission dispatch (MO-CEED) optimization problem for a wind-hydrothermal power system with uncertainty in wind power. A modified particle swarm optimization (MPSO) algorithm that is suitable for large scale optimization [15] is applied to solve this MO-CEED problem. Further challenges imposed on this MO-CEED optimization problem is the uncertainty in wind power factored into the problem formulation to effectively and practically represent integration issues of a practical wind-hydrothermal power system.

The main contributions of this paper are:

- Formulation of a stochastic MO-CEED optimization problem for a wind-hydrothermal power system.
- Handling of uncertainty in wind power.
- Solving the stochastic MO-CEED problem for wind-hydrothermal power system using a family of optimal Pareto fronts.
- Demonstration of potential for increased daily cost saving and emission reduction for a practical Nigerian power system.

2. PROBLEM FORMULATION

2.1. Objective Functions

Normally, a wind turbine creates mechanical torque on a rotational shaft, while an electrical generator on the same rotating shaft is controlled to produce an opposing electromagnetic torque. In steady operation, the magnitude of the mechanical torque is converted to the real power given by (1) and is delivered to the grid [8].

$$P_w = \frac{1}{2}\rho A_w C_p V_w^3 \tag{1}$$

Multiple wind turbines in the wind farm are required to generate aggregated MW for bulk delivery to the power grid system. From the simulation point of view, an aggregated model is sufficient to represent the entire wind farm at the point of common coupling [8].

F_T expresses the traditional sum of the fuel costs of the conventional thermal generators to be minimized, expressed by quadratic function with sine component for each unit's output P_{it} as given by (3). The emission dispatch problem is formulated as atmospheric pollutants emission minimization problem, with the aim of minimizing the total emission of the system. The problem is formulated as a quadratic polynomial with the total emission E_T given by (4). From (6) - (8), C_h and C_w are the direct costs for the power derived from the hydro units and wind farms (wind-powered plants) respectively. The existence and size of these terms will depend on the ownership of the hydro units and wind-powered plants. If the hydro generators and wind-powered plants are owned by the system operator (or utility owned, such as in vertically integrated power networks), these terms may not even exist if it accounts only for the incremental fuel cost, which is zero for the hydro and wind. The penalty cost $C_{E,w}$ for not using all available wind may be set to zero. The last term in (7) relates to the price that must be paid for overestimation of the available wind power. Without regard to ownership of the wind-powered plants, the model must account for the possibility that a reserve would need to be drawn on if all the available wind power is inadequate to cover the amount of the wind power schedule in a given time period.

To model the uncertainty in wind power, the expected wind farm power output $P_{exp,wt}$ is formulated as a probabilistic function of the wind forecast as expressed by (8). The error ($Error_{n_d}$) of wind power forecast at each discrete step n_d of a normal distribution of wind power forecast is taken to be within the range ±10%. This probability of occurrence of the error in wind power forecast (P_{error,n_d}) is in the range ($0 \leq P_{error,n_d} \leq 1$). The reference wind power generation ($P_{reference,wt}$) is the amount of wind power demanded by the network operator from the wind farm operator. It is the "firm" capacity of a wind farm power output that can be counted on as a reliable contribution to the sum of all grid capacity for the wind-hydrothermal power system to meet the load demand and losses. The expected wind farm power output ($P_{exp,wt}$) must therefore seek to balance the reference wind power ($P_{reference,wt}$), otherwise penalty cost is placed according to (9). Active power balancing comes at a cost. The capacity credit of wind power refers to the capability of wind power to increase the available capacity and hence increase reliability of the power system [8]. If wind power is introduced into the system, the available capacity is increased. This amount of wind power results in a decrease in the number of hours with a capacity deficit, thus increasing the reliability of the power system as a result of the wind power integration. Therefore to implicitly represent the capacity credit of wind power and to further handle the uncertainty of wind power, probability of unavailability of wind power γ is defined and added to the objective function in (2) using (7) - (9). This probability of unavailability of wind power lies within the range ($0 \le \gamma \le 1$). Probability of unavailability of wind power γ=1 signifies there is no wind power from the wind farm (this can represent a scenario with insufficient wind speed to turn the turbine blades in the wind farm as wind may not be available all the time and hence insignificant capacity credit of wind power), while γ=0 indicates that there is significant wind power from the wind farm (this can represent a scenario with maximum wind speed to turn the turbine blades in the wind farm and hence significant capacity credit of wind power is added to the grid).

$$F_{Total} = \sum_{t=1}^{T} \left[\omega F_T + (1-\omega)\eta_i E_T + F_H + F_W \right] \tag{2}$$

i=1, 2, …, N_T

where,

$$F_T = \sum_{i=1}^{N_T} U_{it} \left(a_i + b_i P_{it} + c_i P_{it}^2 + \tau \left| e_i \sin\left(f_i \left(P_{it}^{\min} - P_{it} \right) \right) \right| \right) \tag{3}$$

$$E_T = \sum_{i=1}^{N_T} U_{it} \left(\alpha_i + \beta_i P_{it} + \zeta_i P_{it}^2 + \sigma_i e^{\lambda_i P_{it}} \right) \tag{4}$$

$$\eta_i = \frac{F_T \left(P_i^{\max} \right)}{E_T \left(P_i^{\max} \right)}, \quad i=1, 2, \ldots, N_T \tag{5}$$

$$F_H = \sum_{h=1}^{N_H} U_{ht} \left(C_h \left(P_{ht} \right) \right) \tag{6}$$

$$F_W = (1-\gamma) \sum_{w=1}^{N_W} \left[C_w (P_{\exp,wt}) + C_{E,w} \left(P_{\exp,wt} - P_{reference,wt} \right) + C_{D,w} \left(P_{reference,wt} - P_{\exp,wt} \right) \right] \tag{7}$$

$$P_{\exp,wt} = \sum_{n_d}^{N_{prob}} \left[\left(P_{forecast,n_d} \pm Error_{n_d} \right) \times P_{Error\,n_d} \right] \tag{8}$$

$$If \begin{cases} P_{\exp,wt} > P_{reference,wt}, then\, C_{E,w} > 0\ and\ C_{D,w} = 0 \\ P_{\exp,wt} = P_{reference,wt}, then\, C_{E,w} = 0\ and\ C_{D,w} = 0 \\ P_{\exp,wt} < P_{reference,wt}, then\, C_{E,w} = 0\ and\ C_{D,w} > 0 \end{cases} \tag{9}$$

where τ = 1 if valve-point loading is taken into account (for nonconvex fuel cost functions), otherwise $\tau = 0$ (for convex fuel cost functions). U_{it} and U_{ht} can take values of 0 or 1 (0: if the thermal or hydro unit is off-line, 1: if the thermal or hydro unit is on-line). In this paper, however, U_{it} and U_{ht} are given the value of 1.

2.2. Constraints

The multi-objective function in (2) is minimized to satisfy the MO-CEED constraints (10) - (18).

- *Load balance constraint*

The generated power from all the running units must satisfy the load demand and the system losses.

$$\sum_{i=1}^{N_T} U_{it} P_{it} + \sum_{h=1}^{N_H} U_{ht} P_{ht} + (1-\gamma) \sum_{w=1}^{N_W} P_{\exp,wt} = P_t^{\,D} + P_{loss}\text{ , for all } t \in T \tag{10}$$

P_{loss} calculation: A common approach to model transmission losses in the system is to use Kron's approximated loss formula in terms of *B*-coefficients [1] given by (11).

$$P_{loss} = \sum_{i=1}^{N_T+N_H} \sum_{j=1}^{N_T+N_H} P_i B_{ij} P_j + \sum_{i=1}^{N_T+N_H} B_{io} P_i + B_{oo} \tag{11}$$

- *Thermal units generation and ramp-rate limits*

The operating range of all online units is restricted by the unit's ramp-rate limits during each dispatch period [1 - 3]. Hence the generator operating limits is given by (12) and modified according to (13).

$$P_i^{\min} \le P_{it} \le P_i^{\max}, \quad \text{for all } t \in T \tag{12}$$

$$\max(P_i^{\min}, P_i^{pre} - DR_i) \le P_{it} \le \min(P_i^{\max}, P_i^{pre} + UR_i) \tag{13}$$

• *Thermal units' prohibited operating zone*

Practically, adjusting the power output of a unit must avoid all capacity limits and unit's operation in prohibited zones [1 - 3]. The acceptable operating zones of a generating unit can be formulated as shown in (14).

$$\left.\begin{array}{ll} P_i^{\min} \le P_{it} \le P_{i,1}^{lower} & \\ P_{i,j-1}^{upper} \le P_{it} \le P_{i,j}^{lower} & j = 2,3,\ldots,pz_i \\ P_{i,pz_i}^{upper} \le P_{it} \le P_i^{\max} & \end{array}\right\} \tag{14}$$

$(i = 1, 2, \ldots, N_T)$

• *Hydro units generation and ramp-rate*

Each thermal generating unit must not exceed lower and upper generation limits. Hence the generator operating limits are given by (15).

$$P_h^{\min} \le P_{ht} \le P_h^{\max}, \quad (h = 1, 2, \ldots, N_H) \quad \text{for all } t \in T \tag{15}$$

• *Spinning reserve constraint*

Sufficient spinning reserve is required from all running units to maximize and maintain system reliability.

$$\sum_{i=1}^{N_T} U_{it} P_i^{\max} + \sum_{h=1}^{N_H} U_{ht} P_h^{\max} \ge P_t^D + P_{loss} + R, \quad \text{for all } t \in T \tag{16}$$

• *Security constraints*

These comprise the inequality constraints of voltages at load buses (17) and transmission line loadings (18).

$$V_i^{\min} \le V_i \le V_i^{\max}, \quad \text{for all } i \in NB \tag{17}$$

$$\left|PF_k\right| \le PF_k^{\max}, \quad \text{for all } k \in NE \tag{18}$$

3. MULTI-OBJECTIVE OPTIMIZATION

Generally, simultaneous optimization of several objective functions is explicitly associated with lots of engineering and real-world problems. This type of optimization process leads to set of optimal solutions rather than a single optimal solution, since no one solution can be presumed to be of superior quality than any other with respect to all the objective functions. The purpose is to determine a trade-off surface, which is a set of non-dominated optimal solutions points known as *Pareto-optimal* solutions [4 - 7].

- *Weighted-sum method*

  In this approach, the generation (fuel) cost function F_T in (3) and the total emission function E_T in (4) are aggregated using a weight coefficient ω ($0 \leq \omega \leq 1$), whose value varies according to the relative importance of the two objective functions F_T and E_T expressed in (19).

$$\text{Minimize} \quad f_{\omega} = \omega F_T + (1 - \omega)_i E_T \tag{19}$$

  ω = 1.0 implies minimum fuel cost, and ω = 0.0 implies minimum emission. Using (19) the trade-off between the fuel cost and the emission can be evaluated and their *Pareto-optimal front* established over the range of admissible values of ω.

- *Non-linear constrained multi-objective optimization method*

  The MO-CEED problem seeks to minimize two objective functions, generation (fuel) cost F_T and emission E_T simultaneously, while meeting the constraints shown in (21) and (22). By aggregating the objectives and constraints, the problem can be formulated mathematically as a nonlinear constrained multi-objective optimization problem expressed in (20) - (22).

$$\text{Minimize} \qquad [F_T, E_T] \tag{20}$$

$$\text{Subject to:} \quad g(P_i) = 0 \tag{21}$$

$$h(P_i) \leq 0 \tag{22}$$

Mathematically, a general multi-objective function can be formulated to consist of a number of objective functions simultaneously optimized to satisfy certain number of equality and inequality constraints as presented in (23) - (25).

$$\text{Minimize} \quad F_i(x) \qquad i=1, 2, \ldots, N_{obj} \tag{23}$$

$$\text{Subject to:} \quad g_j(x) = 0 \qquad j=1, 2, \ldots, M \tag{24}$$

$$h_k(x) \leq 0 \qquad k=1, 2, \ldots, M \tag{25}$$

Any two optimal solutions to a multi-objective optimization problem represented by x^1 and x^2 can be classified into two possibilities, one dominates/covers the other or none dominates the other. Mathematically, a solution x^1 dominates/covers x^2 if the conditions expressed by (26) - (27) are satisfied.

$$F_i(x^1) \leq F_i(x^2) \qquad \forall i \in \{1, 2, \ldots, N_{obj}\} \tag{26}$$

$$F_j(x^1) < F_j(x^2) \qquad \exists j \in \{1, 2, \ldots, N_{obj}\} \tag{27}$$

Conditions (26) and (27) must be met for solution x^1 to dominate/cover x^2. If this happens, then x^1 and x^2 are called the non-dominant and dominated solutions respectively. The non-dominated solutions within the problem space are the *Pareto-optimal* solutions and can be referred to as *Pareto-optimal set/front* [4 - 6].

4. MPSO FOR SOLVING THE MO-CEED PROBLEM

Bio-inspired and evolutionary techniques have been shown to be very effective optimization tools in solving power system problems [15, 16]. Hence their application in solving the MO-CEED problem for a wind-hydrothermal power system presented in this paper.

The modified PSO is a combination of PSO and an evolutionary strategy enhancing the method to perform optimal search under complex environments [15, 16]. This version of MPSO is a variant of the original formulation of the continuous particle swarm optimization (CPSO) to solve continuous optimization problems such as the one considered in this paper.

The new velocity and position for each particle i in dimension d is determined according to the velocity and position update equations given by (28) and (29) respectively [15]. The inertia weight w_{iner} is updated according to (30).

$$V_{ld}(t) = w_{iner} \cdot V_{ld}(t-1) + c_1 \cdot rand_1 \cdot (P_{lbd}(t-1) - X_{ld}(t-1)) + c_2 \cdot rand_2 \cdot (P^*_{gb}(t-1) - X_{ld}(t-1)) \quad (28)$$

$$X_{ld}(t) = X_{ld}(t-1) + V_{ld}(t) \quad (29)$$

$$w_{iner} = w_{iner}^{\max} - \left(\frac{w_{iner}^{\max} - w_{iner}^{\min}}{iter_{\max}} \right) \times iter \quad (30)$$

A mutation operator is introduced into the MPSO algorithm, so that the swarm's best position in dimension d is updated according to (31).

$If\ rand < M_r$

$$P^*_{gd}(t-1) = P_{gd}(t-1) + ceil\ (randn \times P_{gd}(t-1) / \beta_{gb}) \quad (31)$$

$else$

$$P^*_{gd}(t-1) = P_{gd}(t-1)` \quad (32)$$

end

$d = 1, 2, \ldots, N$

The control or the decision variables for the MO-CEED problem are real power generations, and are therefore used to form the swarm. The real power outputs of all on-line generators are represented as the positions of the particles in the swarm [6, 16]. For N generators, the particle's position is represented as a vector of length N. If there are N_{par} particles in the swarm, the lth particle in the swarm can be represented as a matrix shown in (33).

$$P_{ld} = [P_{l1}, P_{l2}, \ldots, P_{li}, \ldots, P_{lN}] \quad (33)$$

d=1, 2, …, i, …, N

The element P_{li} of the vector P_{ld} is the lth position component of particle l, and it represents the real power generation of on-line generator i of the possible solution. A feasible P_{ld} represents a potential solution to the optimization problem. Each element of the swarm matrix is initialized randomly within the effective real power operating limits. The initialization is either based on (12) and (15) for generators without ramp-rate limits, or on (13) and (16) for generators with ramp-rate limits. The *i*th dimension of the *l*th particle is assigned a value of P_{li} determined by (34) while satisfying the constraints given by (12) and (15) or (13) and (16) depending on whether ramp-rate limits are considered or not. Constraint (14) should also be satisfied if the units' prohibited operating zones are known.

$$P_{li} = P_{li}^{\min} + r \cdot (P_{li}^{\max} - P_{li}^{\min}) \tag{34}$$

The fitness values obtained from (2) for the initial particles of the swarm are set as the initial *pbest* values of the particles. The best value among all the *pbest* values becomes the *gbest*. Mutation operator is introduced into the method using (31).

The new velocity is computed using (28). To control excessive roaming of the particles, the velocity is limited to a certain range [-V_{max}, V_{max}], such that V_{ld} always lies only within this range. The maximum velocity is limited to between 10% - 20% of the dynamic range of the variable on each dimension.

The swarm is updated by updating the particle's position vector using (29). The *pbest* and *gbest* values are subsequently updated.

5. CASE STUDY AND DISCUSSION

5.1. The Nigerian Wind-Hydrothermal Power System

The test data for this case is taken from a real power system whose thermal generating units are characterized with convex fuel cost coefficients (τ = 0, σ_i = 0 & λ_i = 0 in (3) - (4)) for simplicity. The Nigerian conventional grid system comprises a total of 49 functional generating units spread across 7 generating stations located at: AFAM, DELTA, EGBIN, SAPELE, JEBBA, KAINJI and SHIRORO [15] as shown in Fig. 1. Table A.1 of the Appendix presents Nigeria's power stations data, units' minimum and maximum power outputs limits, and is a modification of the data presented in [15]. A 9% spinning reserve is used to improve the system reliability and provide sufficient ramping capacity for balancing wind power variability in addition to existing load variations. Table A.2 of the Appendix presents the Nigerian thermal stations' fuel cost and emission coefficients. All the generating units at AFAM and DELTA stations as well as 8 generating units at EGBIN station are gas turbines (GTs), while all generating units at SAPELE station and other 6 generating units at EGBIN station are steam turbines (STs). Also the four thermal plants utilize natural gas supplied from the Nigerian Gas Company (NGC) as their raw material input. The three hydro stations (Hs) namely JEBBA, KAINJI and SHIRORO are located in Northwestern Nigeria. The anticipated wind farm/plant for integration with the hydrothermal power system is located at Ikeja-Lagos in Area 1 of Fig. 1.

Forecasted hourly load demand for Nigeria [16] presented in Table A.3 of the Appendix is considered and used to illustrate the implementation and potential benefits in solving the MO-CEED optimization problem for a wind-hydrothermal power system.

The transmission losses (P_{loss}) for the Nigerian grid system is computed using (11), with the loss coefficients obtained via parametric estimation based on several power flow scenarios [18, 19] for its largely radial network structure. The estimated loss formula coefficients for the thermal and hydro generating stations are given in matrix form in [18, 19]. Equations (17) and (18) are relaxed in the solution due to line data unavailability. But can be easily incorporated with line data availability by solving the optimal power flow (OPF) and checking for violation in network constraints.

5.2. Numerical Results and Analysis

All numerical results are obtained based on programs developed in the matlab environment on a PC with 2.2GHz CPU speed and 1.5GB of RAM.

The following MPSO and wind-powered plant parameters are used in this paper: population size of 30, $w_{iner}^{\min}$ and $w_{iner}^{\max}$ of 0.4 and 0.9, respectively, c_1 and c_2 of 2, V_{max} is 20% of the dynamic range of the variable on each dimension, M_r of 0.15, $Iter_{max}$ of 100, β_{gb} of 2, ρ of 1.2kgm^{-2}, A_w of 5024m^{-2}, and C_p of 0.59 [8]. The penalty cost coefficients, $C_{E,w}$ and $C_{D,w}$ are empirically tuned to values between 0 and 1000 according to (9), to effectively enforce the constraints in (9). The values are also in accordance with maximum wind power available. The costs C_h and C_w paid to hydro and wind plants owners respectively for the generated power actually used from hydro units and wind units are each set to 0, since both are owned by common utility operator (Nigerian government holds ownership of both plants).

The electricity generated by a utility-scale wind turbine is normally collected and fed into utility power lines, where it is mixed with electricity from other power plants and delivered to utility customers. The output of a wind turbine depends on the turbine's size and the wind's speed through the rotor. Most manufacturers of utility-scale wind turbines offer machines in the 700KW to 2.5MW range [8].

A daily wind average output power of 130.12MW in Lagos-Nigeria [20, 21] represents only about 13.01% capacity factor for a wind farm facility of 500 wind turbines, each rated at 2MW. A wind plant is "fueled" by the wind, which blows steadily at times and not at all at other times. Although modern utility-scale wind turbines typically operate 65% to 90% of the time, they often run at less than full capacity [8]. Therefore, a capacity factor of less than 40% is common, although they may achieve higher capacity factors during windy periods. A capacity factor of 40% to 80% is typical for conventional plants. The forecasted wind farm power output ($P_{forecast}$) is drawn from the wind speed data shown in Table A.4 of the Appendix [20, 21]. To handle the uncertainty in wind energy at each hour of generation, the expected wind farm power output ($P_{exp,wt}$) is a probabilistic function of the forecasted wind farm power output ($P_{forecast}$) and the forecast error ($Error_{n_d}$) as expressed by (8), and is used for illustrating the MO-CEED optimization problem for the wind–hydrothermal power system presented in this paper. The reference wind power generation $P_{reference,wt}$ anticipated from the wind farm for the power system to meet load demand must balance the expected generation $P_{exp,wt}$ given by (8), otherwise penalty cost is incurred in the objective function in (2) using (9).

The MO-CEED problem is handled as a multi-objective optimization problem where both generation cost and carbon dioxide (CO_2) emission are optimized simultaneously using MPSO. Convergence of the combined multi-objective function given by (2) is shown in Fig. 2, where the total cost F_{Total} is seen to converged to 275490.00Naira/h. Typical convergence plots of generation cost and CO_2 emission objectives are presented in Fig. 3 using MO-CEED weight factor (ω) of 0.6 under the probability of uncertainty in wind power (γ) of 0.8 for illustration. From Fig 3, it can be seen that the generation cost and CO_2 emission converged to 270.57Naira/h and 16.29tCO_2/h respectively, as shown in Table 1 when the MO-CEED weight factor (ω) is 0.6. Similar analyses using eleven different MO-CEED weight factors (ω) of 0.1 intervals for simplicity in the range [0, 1] under probability of uncertainty in wind power (γ) of 0.8 are shown in Table 1. It is also worth noting that 101, 1001 or 10001 different MO-CEED weight factors (ω) of 0.01, 0.001 or 0.0001 intervals respectively in the range [0, 1] will also work, though at the expense of more number of multi-objective function evaluations and more computation time.

To generate the eleven non-dominated solutions, the MPSO algorithm is applied eleven times over the range of admissible values of MO-CEED weight factors (ω), under probability of uncertainty in wind power (γ) of 0.8 for illustration as presented in Table 1 during hour 1. The table also shows the best solutions in hour 1 for optimized units' dispatch and total generation output, load demand, power loss, generation cost and CO_2 emission. A similar table can be obtained and drawn for each of the 24-hour dispatch periods. Only one type of pollutant (CO_2) is considered for simplicity. The CO_2 emission conversion factors according to reference values of the fuel characteristics are shown in Table A.5 of the Appendix [22, 23]. The CO_2 emission is generally taken to be proportional to the generator's fuel consumption using similar form of the fuel cost function with appropriately derived CO_2 emission coefficients from Tables A.2 and A.5 of the Appendix [22, 23].

The diversity of the Pareto optimal fronts over the trade-off surfaces under different levels of capacity credits of wind power (with probabilities of uncertainty in wind power (γ) of 0.8, 0.6, 0.4 and 0.2) are shown in Fig. 4. Each Pareto optimal set has 11 non-dominated solutions. The Pareto optimal front produced under γ = 0.2 presents the best trade-off surface while minimizing the generation cost and emission, compared with the Pareto optimal fronts generated under γ = 0.8, 0.6 and 0.4. This indicates that with increased capacity credit of wind power, the generation cost and CO_2 emission can be effectively curtailed and reduced respectively. This consequently increases the total cost savings.

TABLE 1

The Best Solutions of Optimized Generation Cost and CO_2 Emission Considering Uncertainty in Wind Power during Hour 1

Probability of uncertainty in wind power γ=0.8												
weight factors (ω)		ω =1	ω =0.9	ω =0.8	ω =0.7	ω =0.6	ω =0.5	ω =0.4	ω =0.3	ω =0.2	ω =0.1	ω =0
Thermal units generation in hour 1 (MW)	P_1	80.00	80.00	80.00	80.00	80.00	80.00	80.00	80.00	80.00	80.00	80.00
	P_2	80.00	80.00	80.00	80.00	80.00	80.00	144.00	80.00	80.00	190.00	80.00
	P_3	80.00	80.00	128.02	80.00	80.00	119.00	80.00	184.00	122.00	80.00	80.00
	P_4	80.00	80.00	80.00	110.00	80.00	80.00	80.00	80.00	80.00	80.00	190.00
	P_5	80.00	80.00	80.00	80.00	80.00	80.00	80.00	80.00	80.00	80.00	80.00
	P_6	80.00	80.00	80.00	82.00	80.00	80.00	80.00	80.00	80.00	80.00	80.00
	P_7	160.00	160.00	160.00	160.00	160.00	160.00	140.43	133.08	160.00	160.00	167.00
	P_8	20.00	20.00	20.00	20.00	30.00	20.00	30.00	20.00	30.00	20.00	20.00
	P_9	20.00	20.00	25.00	20.00	20.00	20.00	20.00	26.00	20.00	30.00	30.00
	P_{10}	20.00	30.00	20.00	21.00	20.00	30.00	20.00	20.00	21.00	30.00	20.00
	P_{11}	20.00	30.00	30.00	21.00	30.00	20.00	20.00	24.00	30.00	30.00	20.00
	P_{12}	20.00	30.00	20.00	30.00	20.00	20.00	25.00	20.00	27.00	30.00	30.00
	P_{13}	30.00	30.00	20.00	20.00	28.00	30.00	30.00	28.00	20.00	22.00	21.00
	P_{14}	20.00	28.00	20.00	20.00	30.00	20.00	30.00	20.00	20.00	23.00	30.00
	P_{15}	10.00	10.00	10.00	6.00	10.00	5.00	5.00	7.00	10.00	10.00	5.00
	P_{16}	5.00	5.00	5.00	5.00	10.00	10.00	9.00	10.00	10.00	5.00	5.00
	P_{17}	10.00	5.00	6.00	5.00	5.00	5.00	5.00	9.70	5.00	10.00	5.00
	P_{18}	10.00	5.00	9.00	7.00	5.00	10.00	5.00	10.00	9.00	6.00	7.00
	P_{19}	6.00	5.00	5.00	5.00	5.00	5.00	5.00	5.00	7.00	8.00	5.00
	P_{20}	85.30	50.00	40.92	81.30	85.30	85.30	85.30	64.30	83.30	41.33	40.00
	P_{21}	115.85	97.80	138.00	90.85	137.00	104.00	90.85	90.85	100.85	90.85	115.85
	P_{22}	100.00	90.85	115.85	85.00	115.85	115.85	85.00	90.00	85.00	85.00	109.92
	P_{23}	10.00	10.00	10.00	19.60	10.00	10.00	10.00	19.60	19.60	10.00	19.60
	P_{24}	10.00	10.00	10.00	19.60	10.00	19.60	19.60	10.00	17.00	10.00	12.00
	P_{25}	10.00	19.60	19.60	19.60	10.00	15.00	10.00	10.00	13.00	10.00	10.00
	P_{26}	18.60	10.00	10.00	10.00	10.00	19.64	10.00	19.60	19.60	10.00	13.00
	P_{27}	5.00	5.00	10.00	5.00	5.00	10.00	5.00	5.00	5.00	5.00	5.00
	P_{28}	52.50	85.00	40.00	85.00	40.00	85.00	71.00	40.00	85.00	40.00	40.00
	P_{29}	85.00	79.00	85.00	85.00	40.00	58.00	40.00	44.00	40.00	40.00	40.00
	P_{30}	65.00	40.00	40.00	48.00	40.00	40.00	40.00	85.00	40.00	85.00	40.00
	P_{31}	52.00	85.00	43.00	40.00	85.00	4.00	85.00	40.00	42.00	40.00	40.00
Hydro units generation in hour 1 (MW)	P_{32}	88.30	88.30	88.30	88.30	88.30	88.30	88.30	88.30	88.30	88.30	88.30
	P_{33}	88.30	88.30	88.30	88.30	88.30	88.30	88.30	88.30	88.30	88.30	88.30
	P_{34}	88.30	88.30	88.30	88.30	88.30	88.30	88.30	88.30	88.30	88.30	88.30
	P_{35}	88.30	88.30	88.30	88.30	88.30	88.30	88.30	88.30	88.30	88.30	88.30
	P_{36}	88.30	88.30	88.30	88.30	88.30	88.30	88.30	88.30	88.30	88.30	88.30
	P_{37}	88.30	88.30	88.30	88.30	88.30	88.30	88.30	88.30	88.30	88.30	88.30
	P_{38}	112.51	112.50	112.50	112.50	112.50	112.50	112.50	112.50	112.50	112.50	112.50
	P_{39}	10.00	10.00	10.00	10.00	10.00	10.00	10.00	10.00	10.00	10.00	10.00
	P_{40}	10.00	10.00	10.00	10.00	10.00	10.00	10.00	10.00	10.00	10.00	10.00
	P_{41}	10.00	10.00	10.00	10.00	10.00	10.00	10.00	10.00	10.00	10.00	10.00
	P_{42}	10.00	10.00	10.00	10.00	10.00	10.00	10.00	10.00	10.00	10.00	10.00
	P_{43}	76.50	76.50	76.50	76.50	76.50	76.50	76.50	76.50	76.50	76.50	76.50
	P_{44}	90.00	90.00	90.00	90.00	90.00	90.00	90.00	90.00	90.00	90.00	90.00
	P_{45}	10.00	10.00	10.00	10.00	10.00	10.00	10.00	10.00	10.00	10.00	10.00
	P_{46}	140.00	140.00	140.00	140.00	140.00	140.00	140.00	140.00	140.00	140.00	140.00
	P_{47}	140.00	140.00	140.00	140.00	140.00	140.00	140.00	140.00	140.00	140.00	140.00
	P_{48}	140.00	140.00	140.00	140.00	140.00	140.00	140.00	140.00	140.00	140.00	140.00
	P_{49}	10.00	10.00	10.00	10.00	10.00	10.00	10.00	10.00	10.00	10.00	10.00
Wind power gen. in hour 1 (MW)		27.92	27.92	27.92	27.92	27.92	27.92	27.92	27.92	27.92	27.92	27.92
Total generation in hour 1 (MW)		2756.98	2756.97	2757.11	2757.67	2757.87	2757.11	2756.90	2751.85	2758.07	2757.90	2757.09
Power demand, P^D in hour 1 (MW)		2750.00	2750.00	2750.00	2750.00	2750.00	2750.00	2750.00	2750.00	2750.00	2750.00	2750.00
Power loss, P_{loss} in hour 1 (MW)		6.98	6.97	7.11	7.67	7.87	7.11	6.90	6.85	8.07	7.90	7.09
Gen. cost, F_T ($\times 10^3$ Naira/h)		266.93	267.85	268.38	268.50	270.57	271.80	272.49	273.04	273.44	274.99	277.81
CO_2 emission, E_T (tCO_2/h)		16.64	16.51	16.46	16.45	16.29	16.26	16.18	16.15	16.13	16.07	15.99

Table 2 shows the statistical comparison of total generation cost and CO_2 emission over a 24-hour dispatch period. The table further explores the impact of capacity credit of wind power (modeled as probability of uncertainty in wind power) on the total generation cost and CO_2 emission over a 24-hour dispatch period. The statistical results are obtained after 100 iterations of 100 trials over the entire 24-hour dispatch period. The results show relative daily generation cost reductions of 8600.00Naira (0.13%), 6100.00Naira (0.09%) and 6500.00Naira (0.10%) for MO-CEED weight factors (ω) of 0.8, 0.5 and 0.2 respectively under MO-CEED #2 (γ=0.6) scenario compared with MO-CEED #2 (γ=0.6) scenario. The best reduction in the relative daily generation cost is, therefore, obtained when MO-CEED weight factor (ω) is 0.8 under the MO-CEED #2 (γ=0.6) scenario. Similarly, under the MO-CEED #3 (γ=0.4) and MO-CEED #4 (γ=0.2) scenarios, the best reductions in the relative daily generation cost obtained are 11300.00Naira (0.17%) and 24800.00Naira (0.38%) respectively, corresponding to MO-CEED weight factors (ω) of 0.2 and 0.5 respectively. The result shows corresponding reductions in the relative daily CO_2 emission of 0.443tCO_2 (0.11%), 0.620tCO_2 (0.16%), and 0.890tCO_2 (0.23%) under the MO-CEED #2 (γ=0.6), MO-CEED #3 (γ=0.6) and MO-CEED #4 (γ=0.2) scenarios respectively.

Table 3 shows the total daily cost savings derived from the relative daily generation and CO_2 emission cost savings for MO-CEED #2, #3 and #4 compared with MO-CEED #1. A maximum total daily cost savings of 41733Naira is obtained under MO-CEED #4 (γ=0.2) scenario while a minimum total daily cost saving of 16383.333Naira is obtained under MO-CEED #2 (γ=0.6) scenario. This result shows that with further increases in capacity credit of wind power, the total daily cost savings can be significantly improved. With this approach, the total daily cost savings can be predicted (or extrapolated) into the future in the case of long-term planning of wind-hydrothermal power system. The result also shows how the capacity credit (modeled as probability of uncertainty in wind power) can positively impact decision making through proper evaluation of amount of total daily cost savings accruable from reductions in both fuel consumption and CO_2 emission.

TABLE 2

Statistical Comparison of Optimized Daily Generation Cost (F_T) and CO_2 Emission (E_T) Considering Uncertainty in Wind Power

	MO-CEED weight factors (ω)	ω=0.8				ω=0.5				ω=0.2			
		min	max	mean	std	min	max	mean	std	min	max	mean	std
MO-CEED #1: Probability of uncertainty in wind power γ=0.8	Total generation cost, F_T over 24hrs (x10^3 Naira)	6495.500	6530.300	6503.200	±13.654	6487.700	6511.400	6493.500	±13.921	6478.600	6505.200	6483.700	±13.670
	Total CO_2 emission, E_T over 24hrs (tCO_2)	388.518	391.112	389.419	±1.020	388.662	391.684	389.610	±0.933	388.727	392.815	390.193	±0.881
MO-CEED #2: Probability of uncertainty in wind power γ=0.6	Total generation cost, F_T over 24hrs (x10^3 Naira)	6486.900	6521.200	6496.400	±13.823	6481.600	6515.000	6503.000	±13.744	6472.100	6511.000	6497.100	±13.305
	Relative generation cost reduction over 24hrs (x10^3 Naira)	8.600 (0.13%)	-	-	-	6.100 (0.09%)	-	-	-	6.500 (0.10%)	-	-	-
	Total CO_2 emission over 24hrs (tCO_2)	388.075	390.274	389.785	±1.069	388.195	390.901	390.182	±0.985	388.267	391.201	389.826	±1.058
	Relative CO_2 emission reduction over 24hrs (tCO_2)	0.443 (0.11%)	-	-	-	0.467 (0.12%)	-	-	-	0.46 (0.12%)	-	-	-
MO-CEED #3: Probability of uncertainty in wind power γ=0.4	Total generation cost, F_T over 24hrs (x10^3 Naira)	6485.100	6498.300	6490.400	±12.689	6477.200	6494.500	6484.500	±12.281	6467.300	6493.400	6484.100	±12.8122
	Relative generation cost reduction over 24hrs (x10^3 Naira)	10.000 (0.16%)	-	-	-	10.500 (0.16%)	-	-	-	11.300 (0.17%)	-	-	-
	Total CO_2 emission over 24hrs (tCO_2)	387.84	390.103	389.646	±0.909	388.035	390.150	389.767	±0.857	388.107	391.000	389.800	±0.915
	Relative CO_2 emission reduction over 24hrs (tCO_2)	0.678 (0.17%)	-	-	-	0.627 (0.16%)	-	-	-	0.620 (0.16%)	-	-	-
MO-CEED #4: Probability of uncertainty in wind power γ=0.2	Total generation cost, F_T over 24hrs (x10^3 Naira)	6475.500	6488.500	6483.100	±12.509	6462.900	6486.100	6482.600	±12.032	6456.400	6485.900	6481.500	±12.993
	Relative generation cost reduction over 24hrs (x10^3 Naira)	20.000 (0.31%)	-	-	-	24.800 (0.38%)	-	-	-	22.200 (0.34%)	-	-	-
	Total CO_2 emission over 24hrs (tCO_2)	387.502	390.072	388.793	±1.039	387.772	390.086	388.959	±1.021	387.900	390.472	389.306	±0.991
	Relative CO_2 emission reduction over 24hrs (tCO_2)	1.016 (0.26%)	-	-	-	0.890 (0.23%)	-	-	-	0.827 (0.21%)	-	-	-

TABLE 3

Total Daily Cost Saving Considering Uncertainty in Wind Power

S/N	Probability of uncertainty (γ) in wind power	Relative daily generation cost saving (Naira)	Relative daily CO_2 emission cost saving (Naira)	Total daily cost saving (Naira)
1	MO-CEED #2 with γ=0.6	8600.000	7783.333	16383.333
2	MO-CEED #3 with γ=0.4	11300.000	11300.000	22600.000
3	MO-CEED #4 with γ=0.2	24800.000	16933.333	41733.333

6. CONCLUSION

In this paper, the problem of multi-objective combined economic and emission dispatch (MO-CEED) for a wind-hydrothermal power system has been formulated and solved using a modified particle swarm optimization (MPSO) algorithm. Handling of uncertainty in wind power has been formulated as a stochastic optimization and part of the MO-CEED optimization problem formulation, and solved using a family of optimal Pareto fronts for different scenarios of capacity credit of wind power. Capacity credit of wind power is demonstrated to impact the generation cost curtailment, carbon dioxide (CO_2) emission reduction and the total daily cost savings. Results show that further increases in capacity credit of wind power have potential of substantially improving long-term total cost savings. It is shown that an important benefit related to the wind power integration is the additional MW capacity added to the hydrothermal power system. It is demonstrated that the wind power displaces portions of electricity produced from thermal units, thus the quantity of fuel burnt by the thermal units is reduced and the wind power provides a fuel saving, and also enhances CO_2 emission reduction. The MO-CEED optimization result presented in this paper provides enabling platforms and potential for optimizing short and long term system planning, operations and energy management.

Limitations are not imposed on the number of trade-off objectives that can be optimized, hence further work could flexibly incorporate more objectives (such as stability, security or system losses etc).

ACKNOWLEDGMENT

The financial support from the National Science Foundation (NSF), USA under the grant ECCS # 0348221 is gratefully acknowledged by the authors. The Authors are also grateful to Prof. U. O. Aliyu from Abubakar Tafawa Balewa University, Bauchi, Nigeria for providing some relevant data for the studies carried out.

REFERENCES

1 Wood, A. J. and Wollenberg, B. F.: ‘Power generation operation and control’, ISBN 9814-12-664-0, John Wiley and Sons, New York, NY, 2004

2 Wang, C. and Shahidehpour, S. M.: 'Effects of ramp-rate limits on unit commitment and economic dispatch', *IEEE Transactions on Power Systems,* August 1993, 8, (3), pp. 1341-1349

3 Victoire, T. A. A. and Jeyakumar, A. E.: 'Reserve constraint dynamic dispatch of units with valve-point effects', *IEEE Transactions on Power Systems,* August 2005, 20, (3), pp. 1273-1282

4 Abido, M. A.: 'Environmental/economic power dispatch using multiobjective evolutionary algorithms', *IEEE Transactions on Power Systems,* November 2003, 18, (4), pp. 1529-1537

5 Coello Coello, C. A., Pulido, G. T. and Lechuga, M. S.: 'Handling multiple objectives with particle swarm optimization', *IEEE Transactions on Evolutionary Computation,* June 2004, 8, (3), pp. 256-279

6 Lee, K. Y. and El-Sharkawi, M. A.: 'Modern heuristic optimization techniques: theory and applications to power systems', ISBN 978-0471-45711-4, IEEE Press, 445 Hoes Lane, Piscataway, New Jersey, 2008

7 Momoh, J. A.: 'Electric Power system applications of optimization', ISBN 0-8247-9105-3, Marcel Dekker, Inc, 270 Madison Avenue, New York, NY 10016, 2001

8 Ackermann, T.: 'Wind Power in Power Systems', ISBN 10: 0-470-85508-8 (H/B), John Wiley & Sons Ltd, The Atrium, Southern Gate, Chichester, West Sussex PO19 8SQ, England, 2005.

9 Li, Shuhui and Wunsch, D. C.: 'Using neural networks to estimate wind turbine power generation', *IEEE Transactions on Energy Conversion,* September 2001, 16, (3), pp. 276-282

10 Denny, E. and O'Malley, M.: 'Quantifying the total net benefits of grid integrated wind', *IEEE Transactions on Power Systems,* May 2007, 22, (2), pp. 605-615

11 Jabr, R. A. and Pal, B. C.: 'Intermittent wind generation in optimal power flow dispatching', *IET Generation, Transmission & Distribution,* 2008, 3, (1), pp. 66-74

12 Chompoo-inwai, C., Yingvivatanapong, C., Methaprayoon, K. and Lee, W.: 'Reactive compensation techniques to improve the ride-through capability of wind turbine during disturbance', *IEEE Transactions on Industry Applications,* May/June 2005, 41, (3), pp. 666-672

13 Chompoo-inwai, C., Lee, W., Fuangfoo, P., Williams, M. and Liao, J. R.: 'System impact study for the interconnection of wind generation and utility system', *IEEE Transactions on Industry Applications,* January/February 2005, 41, (1), pp. 163-168

14 Chen, C.-L.: 'Simulated annealing-based optimal wind-thermal coordination scheduling', *IET Generation, Transmission & Distribution,* 2007, 1, (3), pp. 447-455

15 Yare, Y., Venayagamoorthy, G. K. and Aliyu, U. O.: 'Optimal generator maintenance scheduling using a modified discrete PSO', *IET Generation, Transmission & Distribution,* November 2008, 2, (6), pp. 834-846

16 del Valle, Y., Venayagamoorthy, G. K., Mohagheghi, S., Hernandez, J. and Harley, R. G.: 'Particle swarm optimization: Basic concepts, variants and applications in power system', *IEEE Transactions on Evolutionary Computation*, April 2008, 12, (2), pp. 171-195

17 Adepoju, G. A., Ogunjuyigbe, S.O. A. and Alawode, K. O.: 'Application of neural network to load forecasting in Nigeria electrical power system', *The Pacific Journal of Science and Technology*, May 2007, 8, (1), pp. 68-72

18 Wudil, T. S. G., Ajiboye, I. O., Jiya, J. D. and Aliyu, U. O.: 'Development of transmission loss formula for Nigerian electric power system', *6th International Conference on Power Systems Operation and Planning – VI (ICPSOP),* Universidade Jean Piaget, Praia, Cape Verde, South Africa, May 2005, pp. 93-97

19 Bakare, G. A., Aliyu, U.O., Venayagamoorthy, G. K. and Shu'aibu, Y. K.: 'Genetic algorithms based economic dispatch with application to coordination of Nigerian thermal power plants', *IEEE PES General Meeting*, June 2005, 1, pp. 551-556

20 Okoro, O. I. and Chikuni, E.: 'Prospects of wind energy in Nigeria', *International Conference on the Domestic Use of Energy*, Cape Peninsula University of Technology, Cape Town, South Africa, April 2007

21 http://www.timeanddate.com/weather/nigeria/lagos/hourly, accessed March 2010

22 Simopoulos, D. N., Giannakopoulos, Y. S., Kavatza, S. D. and Vournas, C. D.: 'Effects of emission constraints on short-term unit commitment', *IEEE Mediterranean Electrotechnical Conference Melecon 2006*, Benalmadena (Malaga), Spain, May 2006

23 http://vlex.com/vid/guidelines-reporting-greenhouse-emissions-36467981, accessed August 2007

APPENDIX

TABLE A.1

Nigerian Hydrothermal Units' Data

Type of power station	Power station					Power limits (MW)		Ramp rate limits		
	Name of power station	S/N	Plant number	Name of turbine unit	Type of turbine	P^{min}	P^{max}	P^{pre} (MW)	UR (MW/h)	DR (MW/h)
Thermal	Egbin PS	1	3	EGBINST1	ST	80.0	190.0	120.0	50.0	90.0
		2	3	EGBINST2	ST	80.0	190.0	120.0	50.0	90.0
		3	3	EGBINST3	ST	80.0	190.0	120.0	50.0	90.0
		4	3	EGBINST4	ST	80.0	190.0	120.0	50.0	90.0
		5	3	EGBINST5	ST	80.0	190.0	120.0	50.0	90.0
		6	3	EGBINST6	ST	80.0	190.0	120.0	50.0	90.0
		7	4	EGBINGT1	GT	90.0	220.0	200.0	60.0	100.0
		8	4	EGBINGT2	GT	20.0	30.0	25.0	20.0	25.0
		9	4	EGBINGT3	GT	20.0	30.0	25.0	20.0	25.0
		10	4	EGBINGT4	GT	20.0	30.0	25.0	20.0	25.0
		11	4	EGBINGT5	GT	20.0	30.0	25.0	20.0	25.0
		12	4	EGBINGT6	GT	20.0	30.0	25.0	20.0	25.0
		13	4	EGBINGT7	GT	20.0	30.0	25.0	20.0	25.0
		14	4	EGBINGT8	GT	20.0	30.0	25.0	20.0	25.0
	Sapele PS	15	5	SAPELST1	ST	5.0	10.0	7.0	5.0	6.0
		16	5	SAPELST2	ST	5.0	10.0	7.0	5.0	6.0
		17	5	SAPELST3	ST	5.0	10.0	7.0	5.0	6.0
		18	5	SAPELST4	ST	5.0	10.0	7.0	5.0	6.0
		19	5	SAPELST5	ST	5.0	10.0	7.0	5.0	6.0
		20	5	SAPELST6	ST	40.0	85.3	70.0	40.0	60.0
	Afam PS	21	1	AFAMGT19	GT	60.0	138.0	100.0	60.0	70.0
		22	1	AFAMGT20	GT	60.0	138.0	100.0	60.0	70.0
	Delta PS	23	2	DELTAG03	GT	10.0	19.6	15.0	10.0	12.0
		24	2	DELTAG04	GT	10.0	19.6	15.0	10.0	12.0
		25	2	DELTAG06	GT	10.0	19.6	15.0	10.0	12.0
		26	2	DELTAG07	GT	10.0	19.6	15.0	10.0	12.0
		27	2	DELTAG08	GT	5.0	10.0	7.0	5.0	6.0
		28	2	DELTAG15	GT	40.0	85.0	70.0	40.0	60.0
		29	2	DELTAG16	GT	40.0	85.0	70.0	40.0	60.0
		30	2	DELTAG17	GT	40.0	85.0	70.0	40.0	60.0
		31	2	DELTAG18	GT	40.0	85.0	70.0	40.0	60.0
Hydro	Jebba PS	32	6	JEBBGH1	H	50.0	88.3	-	-	-
		33	6	JEBBGH2	H	50.0	88.3	-	-	-
		34	6	JEBBGH3	H	50.0	88.3	-	-	-
		35	6	JEBBGH4	H	50.0	88.3	-	-	-
		36	6	JEBBGH5	H	50.0	88.3	-	-	-
		37	6	JEBBGH6	H	50.0	88.3	-	-	-
	Kainji PS	38	7	KAING05	H	55.0	112.5	-	-	-
		39	7	KAING06	H	5.0	10.0	-	-	-
		40	7	KAING07	H	5.0	10.0	-	-	-
		41	7	KAING08	H	5.0	10.0	-	-	-
		42	7	KAING09	H	5.0	10.0	-	-	-
		43	7	KAING10	H	35.0	76.5	-	-	-
		44	7	KAING11	H	55.0	90.0	-	-	-
		45	7	KAING12	H	5.0	10.0	-	-	-
	Shiroro PS	46	8	SHIRGH1	H	50.0	140.0	-	-	-
		47	8	SHIRGH2	H	50.0	140.0	-	-	-
		48	8	SHIRGH3	H	50.0	140.0	-	-	-
		49	8	SHIRGH4	H	5.0	10.0	-	-	-

*GT - Gas turbine, ST - Steam turbine and H - Hydro.
Nigerian Naira=0.008US$ at 2003

TABLE A.2

Nigerian Thermal Stations' Fuel Cost and Emission Coefficients

Power station	Fuel cost coefficients			Emission coefficients		
	a_i (Naira/h)	b_i (Naira/MWh)	c_i (Naira/MW^{2}h)	α_i (tCO$_2$/h)	β_i (tCO$_2$/MWh)	ζ_i (tCO$_2$/MW^{2}h)
Sapele	6929.000	7.840	0.130	0.416	0.000470	0.0000078
Delta	525.740	6.130	1.200	0.032	0.000368	0.0000720
Afam	1998.000	56.000	0.092	0.120	0.003360	0.0000055
Egbin	12787.000	13.100	0.031	0.767	0.000786	0.0000019

TABLE A.3

Nigerian Hourly Load Demand Forecast [17]

Time (Hour)	1	2	3	4	5	6	7	8	9	10	11	12
Load demand (MW)	2750	2700	2700	2600	2650	2840	2950	3050	2930	2810	2710	2690

Time (Hour)	13	14	15	16	17	18	19	20	21	22	23	24
Load demand (MW)	2680	2675	2670	2672	2676	2750	2950	3096	3094	3093	3000	2960

TABLE A.4

Hourly Wind Speed in Nigeria - Lagos [20, 21]

Time (Hour)	1	2	3	4	5	6	7	8	9	10	11	12
Wind speed (mph)	12	11	10	10	9	8	7	8	8	8	8	8

Time (Hour)	13	14	15	16	17	18	19	20	21	22	23	24
Wind speed (mph)	8	8	9	9	10	11	12	12	12	11	11	11

TABLE A.5

Emission Conversion Factors [22, 23]

Unit type	Net calorific value (KJ/m^3)	Emission factor (tCO$_2$/TJ)	Oxidation factor (%)	Fuel supply cost (\$/m^3)	Emission conversion factor	
					(tCO$_2$/\$)	(tCO$_2$/Naira)
Oil	41031	77.4	0.995	157.00	0.02013	0.00016
Gas	31736	56.1	0.995	0.23	0.00800	0.00006
Coal	29308	98.3	0.990	51.30	0.05560	0.00045

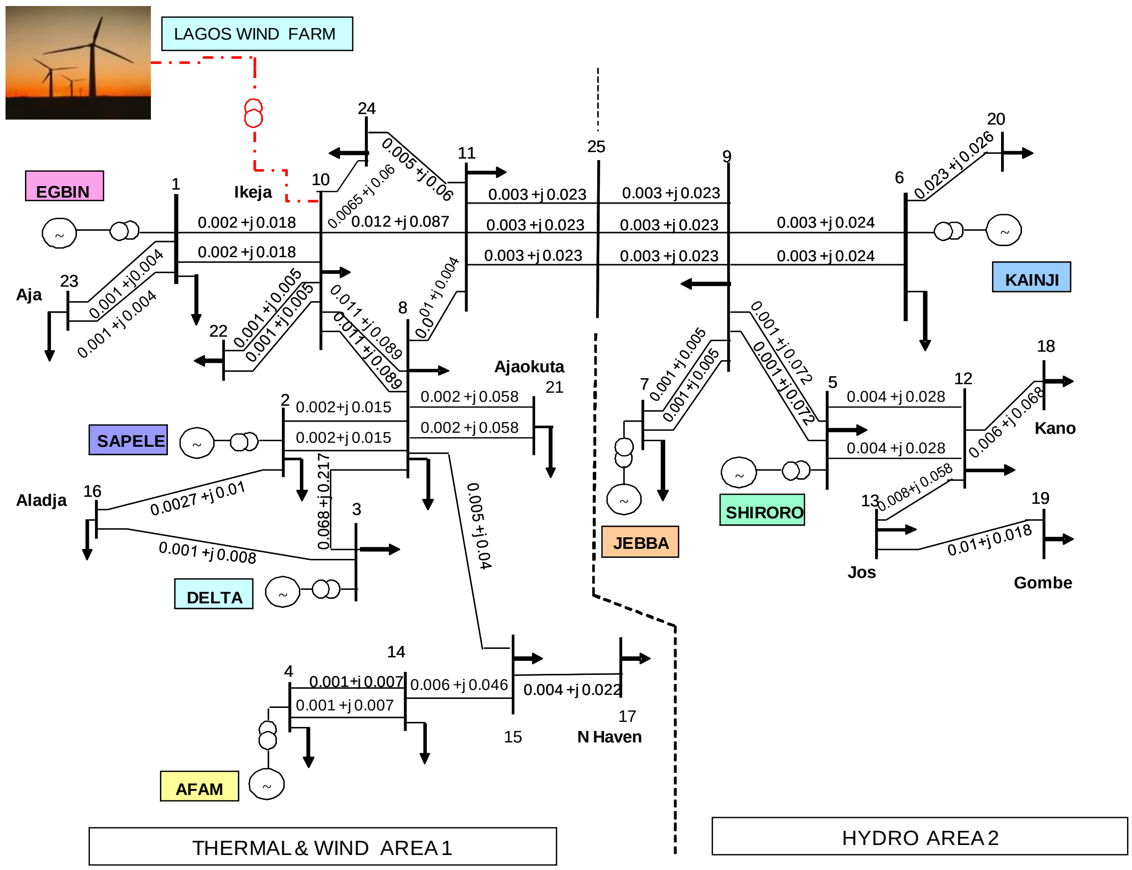

Fig. 1. Nigerian Wind-Hydrothermal 330-KV, 25-Bus Grid System

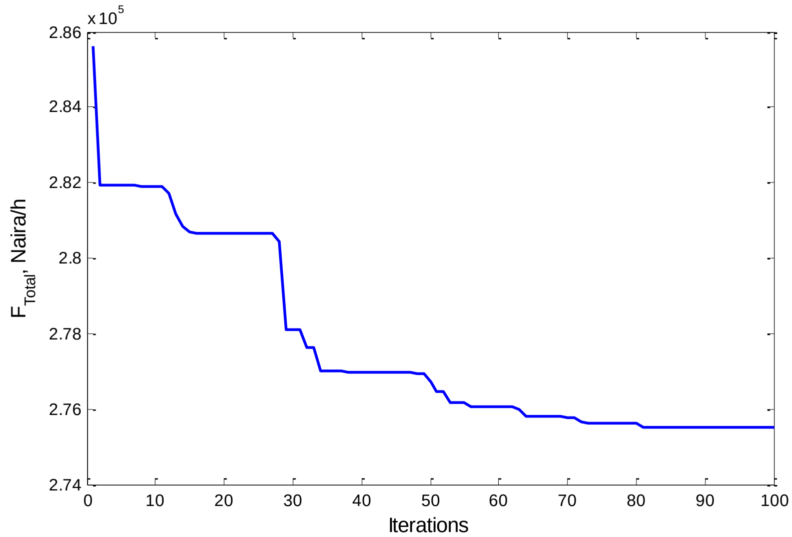

Fig. 2. Convergence of the Multi-Objective Function (F_{Total}) given by (2) with γ=0.8 and ω=0.6

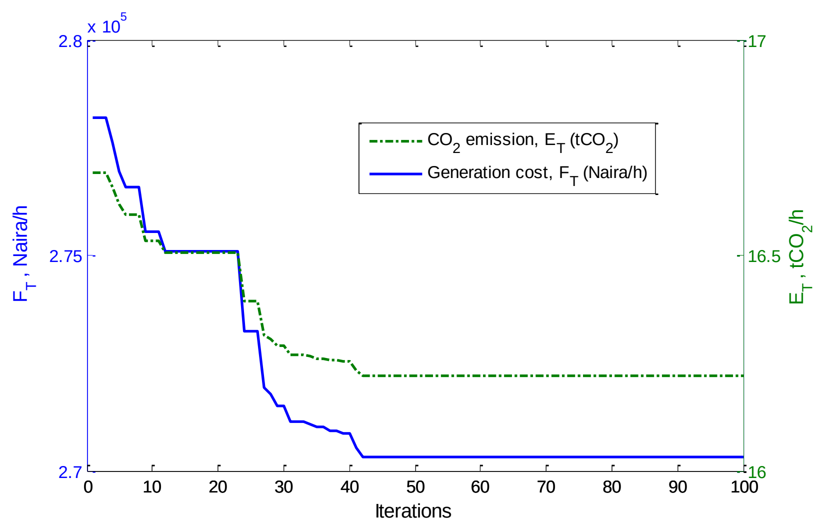

Fig. 3. Convergence of Generation Cost (F_T) and CO_2 Emission (E_T) Objective Functions with γ=0.8 and ω=0.6

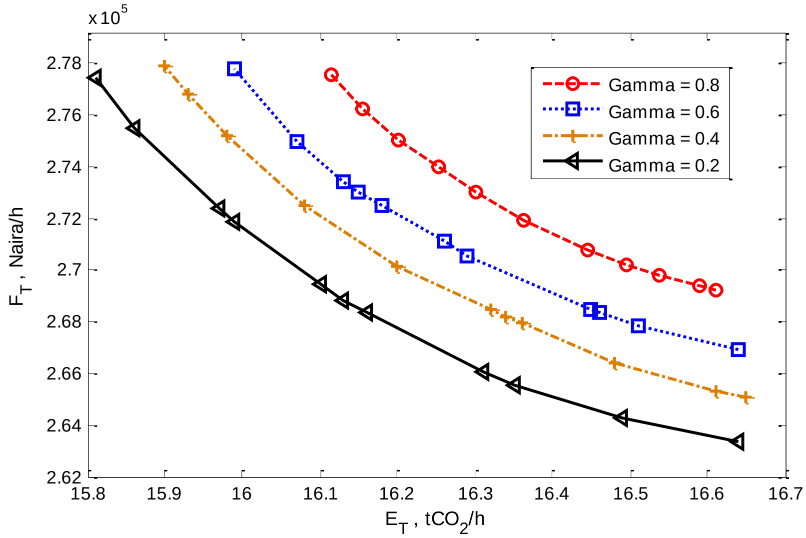

Fig. 4. Family of Pareto Optimal Fronts of the MO-CEED Problem with γ=0.8, 0.6, 0.4 and 0.2

V. GENERATOR MAINTENANCE SCHEDULING FOR A WIND-HYDROTHERMAL POWER SYSTEM WITH UNCERTAINTY IN WIND POWER GENERATION

Y. Yare, *Student Member, IEEE*, G. K. Venayagamoorthy, *Senior Member, IEEE*, and A. Y. Saber, *Member, IEEE*

ABSTRACT— Smart grid delivers electricity from suppliers to consumers using intelligent technology to save energy, reduce cost, accommodate variety of generation options, increase reliability, efficiency and transparency etc. In pursuance of the smart grid initiative, this paper presents an optimal preventive generator maintenance scheduling (GMS) for a wind-hydrothermal power system. GMS problem is solved with the aim of maximizing economic benefits subject to satisfying system constraints. This GMS formulation becomes a stochastic problem because of the uncertainty in wind power and its incorporation into the hydrothermal power system. The objective is to perform GMS in such a manner that the annual cost saving is increased, annual generation cost is minimal and the potential for carbon dioxide (CO_2) emission reduction is enhanced, while all operating constraints are satisfied in the presence of uncertainty in wind generation. A modified discrete particle swarm optimization (MDPSO) algorithm is used to solve this GMS problem. Results are presented to show the benefits accruable from integrating wind power into conventional hydrothermal power system even for the purpose of GMS and the positive impact of increasing wind penetration.

INDEX TERMS—Cost saving, economic cost function, CO_2 emission, generator maintenance scheduling, smart grid, uncertainty in wind power.

NOMENCLATURE

A_w Swept area of the wind turbine's blade

a_i, b_i & c_i Fuel cost coefficients for unit i

AM_t Available crew/labor at period t

β_{gb} Global best strategic learning parameter for mutation

c_1 & c_2 Cognitive and social acceleration constants respectively

$C_{D,w}$ & $C_{E,w}$ Penalty cost coefficients (coeffs) for calling reserves to cover for deficit wind-generated power and for not using all available wind power respectively from *w*th wind plant

C_h & C_w Cost functions for *h*th hydro unit and *w*th wind plant respectively

C_{jk} Technical crew/labor needed by unit j at week k

C_p Performance coeff

d Particle's dimension

d_{jk} Maintenance start indicator and state of unit j in week k

D_{jt} Maintenance downtime for unit j in period t

ep_j Earliest period for maintenance of unit j to begin

γ Probability of unavailability of wind power and lies in the range of [0, 1]

$Iter$ & $Iter_{max}$ Current and maximum iteration number respectively

k Discrete time step

l *l*th particle

l_j Latest period for maintenance of unit j to end

M_r Mutation rate

MR_{jk} & TMR_t Maintenance resources/budgets needed by unit j at week k and producer's total available resources/budgets at period t respectively

N Number of dimensions

n_d & N_{prob} Index and total number of discrete probability step of a normal distribution respectively

N_H & N_T Total number of running (or on-line) hydro and thermal units respectively

N_m Total number of generating units in maintenance

N_W Total number of wind-powered plants (or wind farms)

$P_{reference,wt}$ Actual production of wind power from the *w*th wind-powered plant (wind farm) in period t

P_{error,n_d} Probability of error ($Error_{n_d}$) at each n_dth discrete probability step of a normal distribution

$P_{exp,wt}$ Expected wind power from the *w*th wind-powered plant (wind farm) in period t

$P_{forecast,nd}$ Wind power forecast at each n_dth discrete probability step of a normal distribution

P_{gd} Swarm's best position for dimension d

P_{ht} & P_{it} Scheduled generations from the hth hydro and ith thermal units respectively in period t

$P_i^{\min}$ & $P_i^{\max}$ Minimum and maximum power limits respectively for thermal unit i

P_{loss} System loss

P_{lbd} lth particle best position for dimension d

P_{ld} Position vector of the particle l in dimension d

P_t^D Total real load demand for period t

P_w Wind turbine output power

PF_t^l & $PF_{\max}^l$ Power flow and maximum power flow limit in transmission line l respectively

R System reserve

ρ Density of air

r, $rand$, $rand_1$ & $rand_2$ Random numbers with uniform distribution in the range of [0, 1]

$randn$ Gaussian distributed random number with a zero mean and a variance of 1

t Index of period

T Set of indices of periods in planning horizon

U_{ht} & U_{it} Scheduled maintenance state of hth hydro and ith thermal units respectively in time t

V_w Wind speed

V_{ld} & V_{max} lth particle velocity in dimension d and maximum particle velocity respectively

V_{jt} Unit's maintenance cost per week

w_{iner} , $w_{iner}^{\min}$ & $w_{iner}^{\max}$ Current, initial and final inertia weights respectively

I. INTRODUCTION

Vision of the smart grid is presented by the U.S. Department of Energy's (DOE's) National Energy Technology Laboratory in "A vision for the Modern Grid" [1]. A smart grid delivers electricity from suppliers to consumers using intelligent technology to provide high quality power that save energy, reduce cost, accommodate wide variety of generation options, increase reliability and transparency, be able to heal itself, resist attack, run more efficiently, and enable electricity market to flourish [1]. Such a modernized electricity network is being promoted as a way of addressing energy independence, global warming and emergency resilience issues. One of the visions of the smart grid is that it optimizes assets and operates efficiently. Today's grid has minimal integration of limited operational data with asset management processes and technologies. Grid technologies that are effectively integrated with asset management processes leads to effectively managed assets and costs [1]. Maintenance scheduling is part of asset management functions. Hence, this paper presents and solves the GMS problem for a wind-hydrothermal (accommodating multiple generation options) power system in accordance with the functions of the smart grid.

Maintenance scheduling of generating units is an important task in power system and plays important role in the operation and planning activities of the electric power utility. The simultaneous solution of all aspects of the operation, planning and scheduling problems in the presence of system complexity at different time-scales, different order of uncertainties and problem's dimensionality is required for the efficient economic operation of the utility system [2]-[4]. Power system equipment are made to remain in good operating conditions by regular preventive maintenance. Modern power system is experiencing increased demand for electricity with related expansions in system size, which has resulted in higher number of generators and lower reserve margins making the generator maintenance scheduling (GMS) problem more complicated. The aim of maintenance scheduling is to determine the optimized timing and duration for scheduled planned maintenance overhauls for generating units while maintaining high system reliability, reducing production cost, prolonging generator life time subject to some unit and system constraints [2]-[4].

A new approach for establishing power systems scheduled generators outages for maintenance purposes in short-term operations planning horizon is presented in [5]. This paper focused on modeling grid operation constraints and the resulting large-scale optimization problem is solved by mixed-integer programming techniques aided by Benders decomposition strategy. Maintenance scheduling problem that solved several uncertainties associated with it is presented in [6]. Fuzzy model for the integrated generation and transmission maintenance scheduling problem accounts for such uncertainties and introduces a solution technique to solve for the optimal schedule [6]. A new approach to maintenance scheduling of generating units in competitive electricity markets is presented in [7]. This paper focused on modeling a game-theoretic framework for the maintenance scheduling units' problem to analyze strategic behaviors of generating companies. An analytic foundation to assess the maintenance needs in a competitive environment is discussed in and presented in [8]. A stochastic optimization model is proposed in [8] that consider the trade-off among short and long-term objectives to determine the optimal maintenance profile for generating units over the life of the assets. A method designated as the maintenance coordination technique to coordinate composite system maintenance scheduling in a deregulated utility system is proposed in [9]. A technically sound coordinating mechanism based on incentives /disincentives among producers and the operator is presented in [10]. This mechanism allows producers to maximize their respective profits while the operator ensures an appropriate level of reliability. A new approach to security coordinated maintenance scheduling in deregulation is presented in [11], wherein the independent system operator (ISO) does not generate a maintenance schedule by itself, but calls for maintenance scheduling plans from individual generation companies (GENCOs). Stochastic mid-term risk-constrained hydrothermal scheduling algorithm in a generation company is proposed in [12] as the schedule is used by the GENCO for bidding purposes to the ISO. The optimization method in [12] is based on stochastic price-based unit commitment. A stochastic model for the optimal risk-based generation maintenance outage scheduling based on hourly price-based unit commitment in a GENCO is present in [13], wherein the maintenance outage schedules is submitted by GENCOs to the ISO for approval before implementation. A unit maintenance scheduling problem formulation for a generation producer is presented in [14], to maximize its benefit while thoroughly considering the risk associated with unexpected unit failures. A mechanism for unit maintenance scheduling in the deregulated environment, based on the different functions of power producers and ISO is proposed in [15]. The proposed scheme aims to achieve a trade-off between ensuring the producers' benefits and maintaining the system reliability, providing satisfactory maintenance windows and cost-reflective reward/charge to individual producers.

Worldwide interest in reducing environmental pollution and the increasing concern over possible energy shortage has led to fruitful increasing interest in generation of renewable electrical energy. Wind power has become the fastest growing energy sources in the world and the leading source among various renewable energy sources in the power industry.

Wind turbines are usually placed in clusters (wind farms), with sizes ranging from a few MW up to several MW. Therefore, a large wind farm typically consists of hundreds of individual WTGs running simultaneously. The pooling of several large wind farms into clusters (in the GW range) will make new options feasible for an optimized integration of variable-output generation into electricity supply systems. Wind power fluctuates over time, mainly under the influence of meteorological fluctuations. The variations occur on all time scales: seconds, minutes, hours, days, months, seasons and years. Understanding these variations and their predictability is of key importance. New concepts for cluster management include the aggregation of geographically dispersed wind farms according to various criteria, for the purpose of an optimized network management, maintenance and generation scheduling. These clusters are operated and controlled like large conventional power plants [16]-[22].

Capabilities of discrete particle swarm optimization (DPSO) algorithm have been enhanced with evolutionary strategies (ESs) to produce a modified discrete particle swarm optimization (MDPSO) in [23]. Detail comparison of three algorithms – DPSO, MDPSO and GA and their application to solving a hydrothermal power system GMS problem are also presented in [23], which showed that MDPSO produced better results compared with DPSO and GA on a benchmark test system and practical power system.

The main contributions of this paper are:

- Formulation of GMS as a stochastic optimization problem for a wind-hydrothermal power system.
- Solving a stochastic GMS problem for a wind-hydrothermal power system.
- Handling of uncertainty in wind power generation over the entire maintenance horizon.
- Increased annual cost saving in a stochastic GMS.
- Enhanced CO_2 emission reduction in a stochastic GMS.

II. PROBLEM FORMULATION

The societal benefits of wind generation include the capacity value of wind generation, the emissions savings and the reduction in the fuel bill resulting from reduction in outputs of combustion plants in the system. Normally, a wind turbine creates mechanical torque on a rotational shaft, while an electrical generator on the same rotating shaft is controlled to produce an opposing electromagnetic torque. In steady operation, the magnitude of the mechanical torque is converted to the real power given by (1) and is delivered to the grid [16].

$$P_w = \frac{1}{2}\rho A_w C_p V_w^3 \tag{1}$$

Multiple wind turbines in the wind farm are required to generate aggregated MW for bulk delivery to the power grid system. From the simulation point of view, an aggregated model is sufficient to represent the entire wind farm at the point of common coupling [16]. The control value of wind power considers the capability of wind power to participate in balancing production and consumption in the power system. Since electric power cannot be stored it is necessary to produce exactly as much power as is consumed, all the time. The balancing problem is handled differently depending on the time frame. The availability of balancing solutions (generation capabilities, load management, energy storage) in power systems is an important factor for the integration of wind power in power systems. Even though power system balancing is not a new problem, wind power does provide a number of new challenges which needs to be addressed if the amount of wind power increases above certain levels [16]-[24]. With increasing wind power penetration the demands of the grid operators are changing. In response to these demands, besides energy generation, modern wind turbines and wind farms are developing towards the concept of so-called WEPP (wind energy power plant) [16].

In general, there are two main categories of objective functions in GMS, namely, based on reliability and economic cost [4], [23]. The economic cost function is considered in this paper. The costs that need to be minimized for this optimal maintenance scheduling of generators are the generation and maintenance costs, while penalty cost is added to the objective function for violation of any of the constraints [4], [23].

Suppose $T_j \subset T$ is the set of periods when maintenance of unit j may start, $T_j = \{t \in T : ep_j \le t \le l_j - D_{jt} + 1\}$ for each j. Define maintenance start indicator of unit j in period k represented by d_{jk} as 0 or 1 (0: if unit j starts maintenance at week k, 1: if unit j is on-line in week k). Let S_{jt} be the set of start time periods k such that if the maintenance of unit j starts at period k that unit will be in maintenance at period t, $S_{jt} = \{k \in T_j : t - D_{jt} + 1 \le k \le t\}$.

The GMS problem is commonly formulated as costs optimization problem, with the aim of minimizing the total maintenance cost of the power system but still satisfying some equality and inequality constraints. The input-output characteristics of a generator are approximated using quadratic or piecewise quadratic functions with the assumption that the incremental cost curves of the units are monotonically increasing piecewise-linear functions [3], [4]. However, real input-output characteristics display higher-order nonlinearities and discontinuities due to valve-point loading effect which is modeled as a recurring rectified sinusoidal function [3], [4]. The valve-point loading effects introduce ripples in the heat-rate curves and make the objective function nonsmooth (nonconvex) with multiple minima [3], [4]. However, the valve-point loading has little or no effect on the system performance when considering long-term generation scheduling. Hence it can be neglected with reasonable accuracy for the long-term GMS problem presented in this paper.

The objective function given in (2) is for the minimization of the economic cost function which consists of the generation (thermal, hydro and wind) and maintenance costs. The generation cost of a thermal unit is expressed as second order function of each unit output P_{it} . Since the equations for the generation cost of units are expressed on a per hour basis, a multiplier of 168 is used to get the total cost for generation in one week. F_1 defines the traditional sum of the fuel costs of the conventional thermal generators as given by (3), while F_2 defines the cost for generating hydro power as expressed by (4). C_h and C_w are the direct costs for the power derived from the hydro units and wind farms (wind-powered plants) respectively as shown in (4) and (5). The existence and size of these terms will depend on the ownership of the hydro units and wind-powered plants. If the hydro generators and wind-powered plants are owned by the system operator (or utility owned, such as in vertically integrated power networks), these terms may not even exist if it accounts only for the incremental fuel cost, which is zero for the hydro and wind. The penalty cost $C_{E,w}$ for not using all available wind may be set to zero. The last term in (5) relates to the price that must be paid for overestimation of the available wind power. Without regard to ownership of the wind-powered plants, the model must account for the possibility that a reserve would need to be drawn on if all the available wind power is inadequate to cover the amount of the wind power schedule in a given time period.

To model the uncertainty in wind power, the expected wind farm power output $P_{exp,wt}$ is formulated as a probabilistic function of the wind forecast as expressed by (6). The error ($Error_{n_d}$) of wind power forecast at each discrete step n_d of a normal distribution of wind power forecast is taken to be within the range ±10%. This probability of occurrence of the error in wind power forecast (P_{error,n_d}) is in the range ($0 \leq P_{error,n_d} \leq 1$). The reference wind power generation ($P_{reference,wt}$) is the amount of wind power demanded by the network operator from the wind farm operator. It is the "firm" capacity of a wind farm power output that can be counted on as a reliable contribution to the sum of all grid capacity for the wind-hydrothermal power system to meet the load demand and losses. The expected wind farm power output ($P_{exp,wt}$) must therefore seek to balance the reference wind power ($P_{reference,wt}$), otherwise penalty cost is placed according to (7). Active power balancing comes at a cost. The capacity credit of wind power refers to the capability of wind power to increase the available capacity and hence increase reliability of the power system [16]. If wind power is introduced into the system, the available capacity is increased. This amount of wind power results in a decrease in the number of hours with a capacity deficit (especially during GMS), thus increasing the reliability of the power system as a result of the wind power integration. Therefore to implicitly represent the capacity credit of wind power and to further handle the uncertainty of wind power, probability of unavailability of wind power γ is defined and added to the objective function in (2) using (5) - (8). This probability of unavailability of wind power lies within the range ($0 \leq \gamma \leq 1$). Probability of unavailability of wind power γ=1 signifies there is no wind power from the wind farm (this can represent a scenario with insufficient wind speed to turn the turbine blades in the wind farm as wind may not be available all the time and hence insignificant capacity credit of wind power), while γ=0 indicates that there is significant wind power from the wind farm (this can represent a scenario with maximum wind speed to turn the turbine blades in the wind farm and hence significant capacity credit of wind power is added to the grid).

The maintenance cost for all units in maintenance is represented by each unit's fixed maintenance cost per week V_{jt} times the downtime D_{jt} of each unit on maintenance as expressed by (8).

From (2) - (8), the input variables are: P_{it}, P_{ht}, $P_{forecast,\ n_d}$, V_{jt} and D_{jt}, output variable are: U_{it}, U_{ht}, F_1, F_4 and objective function (2), while the decision variables are: γ, $P_{reference}$, $Error_{\ n_d}$ and $P_{error,\ n_d}$.

$$\min \left(\sum_{t=1}^{T} \left[F_1(P_{it}) + F_2(P_{ht}) + F_3(P_{forecast,n_d}) + F_4(V_{jt}, D_{jt}) \right] \right) \tag{2}$$

where,

$$F_1 = \sum_{i=1}^{N_T} U_{it} \left[168 \left(a_i + b_i P_{it} + c_i P_{it}^2 \right) \right] \tag{3}$$

$$F_2 = \sum_{h=1}^{N_H} U_{ht} \left[C_h \left(P_{ht} \right) \right] \tag{4}$$

$$F_3 = (1-\gamma)\sum_{w=1}^{N_W} \left[C_w(P_{\exp,wt}) + C_{E,w}\left(P_{\exp,wt} - P_{reference,wt}\right) + C_{D,w}\left(P_{reference,wt} - P_{\exp,wt}\right) \right] \quad (5)$$

$$P_{\exp,wt} = \sum_{n_d}^{N_{prob}} \left[\left(P_{forecast,n_d} \pm Error_{n_d}\right) \times P_{Error\ n_d} \right] \quad (6)$$

$$If \begin{cases} P_{\exp,wt} > P_{reference,wt}, then\, C_{E,w} > 0\ and\ C_{D,w} = 0 \\ P_{\exp,wt} = P_{reference,wt}, then\, C_{E,w} = 0\ and\ C_{D,w} = 0 \\ P_{\exp,wt} < P_{reference,wt}, then\, C_{E,w} = 0\ and\ C_{D,w} > 0 \end{cases} \quad (7)$$

$$F_4 = \sum_{j=1}^{N_m} V_{jt} D_{jt} \quad (8)$$

U_{it} and U_{ht} take values of 0 or 1 (0: if the thermal or hydro unit is scheduled for maintenance, 1: if the thermal or hydro unit is running/on-line) depending on the generated schedule.

The objective function in (2) is minimized to satisfy the GMS constraints (9) - (20).

- *Technical crew/labor constraint*

This defines the crew/labor availability for maintenance task. The number of people required to perform maintenance task cannot exceed the available crew/labor within each period.

$$\sum_{j \in N_m} \sum_{k \in S_{jt}} C_{jk}(1 - d_{jk}) \le AM_t, \qquad \text{for all } t \in T \quad (9)$$

- *Maintenance window and duration constraint*

This defines the possible times and duration of maintenance for each generating unit. It specifies the starting of maintenance at the beginning of an interval and finishing at the end of the same interval. With commencement of maintenance task, the maintenance start indicator d_{jk} is 0, and remains 0 for the entire duration of maintenance represented by D_{jt} as expressed by (10).

$$\sum_{j \in N_m} \sum_{k \in S_{jt}} (1 - d_{jk}) = D_{jt}, \qquad \text{for all } t \in T \quad (10)$$

- *Continuous maintenance constraint*

The following constraint in (11) ensures that the maintenance of each unit should not be interrupted once it begins.

$$(1-d_{j,k})-(1-d_{j,k-1})\le(1-d_{j,t+(D_{j,t}-1)}), \quad \text{for all } j\in N_m,\ k\in S_{jt},\ t\in T \qquad (11)$$

- *Maintenance resource and budget constraint*

Due to limitations on total resources/budgets available to units for maintenance, several units should not be scheduled to be on maintenance simultaneously beyond allowable total resources/budgets.

$$\sum_{j\in N_m}\sum_{k\in S_{jt}} MR_{jk}(1-d_{jk})\le TMR_t, \qquad \text{for all } t\in T \qquad (12)$$

- *Load balance constraint*

The generated power from all the running units must satisfy the load demand and the transmission losses expressed by (13).

$$\sum_{i=1}^{N_T} U_{it}P_{it}+\sum_{h=1}^{N_H} U_{ht}P_{ht}+(1-\gamma)\sum_{w=1}^{N_W} P_{\exp,wt}=P_t^D+P_{loss}, \text{ for all } t\in T \qquad (13)$$

P_{loss} calculation: A common approach to model transmission losses in the system is to use Kron's approximated loss formula in terms of *B*-coefficients [3] given by (14).

$$P_{loss}=\sum_{i=1}^{N_T+N_H}\sum_{j=1}^{N_T+N_H} P_i B_{ij} P_j+\sum_{i=1}^{N_T+N_H} B_{io}P_i+B_{oo} \qquad (14)$$

- *Thermal units generation and ramp-rate limits*

Each thermal generating unit must not exceed lower and upper generation limits. The operating range of all online units is restricted by the unit's ramp-rate limits during each dispatch period.

Therefore, subsequent dispatch output of a generator should be limited between its up and down ramp-rate limits constraint [3]. Hence the generator operating limits given by (15) are modified according to (16).

$$P_i^{\min} \le P_{it} \le P_i^{\max}, \ (i = 1, 2, \ldots, N_T) \quad \text{for all } t \in T \tag{15}$$

$$\max(P_i^{\min}, P_i^{pre} - DR_i) \le P_{it} \le \min(P_i^{\max}, P_i^{pre} + UR_i) \tag{16}$$

- *Thermal units' prohibited operating zones*

Each thermal generator has its generation capacity, which cannot be exceeded at any time. It is common for a typical thermal unit to have a steam valve in operation, or a vibration in shaft bearing, which may result in interference and discontinuous input-output performance curve sections [3], known as prohibited operating zones. Practically, adjusting the power output of a unit must avoid all capacity limits and unit's operation in prohibited zones [3]. The acceptable operating zones of a generating unit can be formulated as shown in (17).

$$\left.\begin{array}{ll} P_i^{\min} \le P_{it} \le P_{i,1}^{lower} & \\ P_{i,j-1}^{upper} \le P_{it} \le P_{i,j}^{lower} & j = 2,3,\ldots,pz_i \\ P_{i,pz_i}^{upper} \le P_{it} \le P_i^{\max} & \end{array}\right\} \tag{17}$$

$$(i = 1, 2, \ldots, N_T)$$

- *Hydro units generation limits*

Constraint (18) limits power scheduling from hydro generating units depending on water availability in the reservoir over a given period of time. It is a simpler representation that avoids detailed reservoir balance constraints for simplicity.

$$P_h^{\min} \le P_{ht} \le P_h^{\max}, \ (h = 1, 2, \ldots, N_H) \text{ for all } t \in T \tag{18}$$

- *Spinning reserve constraint*

Sufficient spinning reserve margin is required from all running units to ensure high level of system reliability.

$$\sum_{i=1}^{N_T} U_{it} P_i^{\max} + \sum_{h=1}^{N_H} U_{ht} P_h^{\max} - P_t^D \geq R, \quad \text{for all } t \in T \tag{19}$$

- *Line capacity constraint*

The power flows on transmission lines are constrained by line capacities which depend on the transmission line voltage.

$$PF_t^l \leq PF_{\max}^l, \quad \text{for all } t \in T \tag{20}$$

III. MDPSO FOR SOLVING THE GMS PROBLEM

Bio-inspired and evolutionary techniques have been shown to be very effective optimization tools in solving maintenance scheduling problems [4], [24]. Hence their application in solving the wind integrated-hydrothermal GMS problem presented in this paper.

The general concepts behind optimization techniques initially developed for problems defined over real-valued vector spaces, such as PSO, can also be applied to discrete-valued search spaces where either binary or integer variables are used [24]. When integer solutions (not necessarily 0 or 1) are needed, the real values of the particles' velocity or position are truncated to the nearest integer values [24]. Results obtained using integer PSO indicate that the performance of the method is not affected when the real values of the particles' velocity or position are truncated [24].

MDPSO is a combination of DPSO and an evolutionary strategy to enhance the standard DPSO algorithm to perform better search for optimal solutions under complex environments. The MDPSO is a newer variant of the original formulation of the DPSO to solve discrete optimization problems as explained below [23], [24]. A mutation operator is introduced into the MDPSO algorithm. The main goal is to increase the diversity of the population. In DPSO, the particles tend to cluster into local region after few iterations of search, emphasizing on exploitation rather than exploration of the entire search space. Increased diversity brings about a balance in exploitation as well as exploration. This leads to a better search performance by MDPSO compared with DPSO. In addition, the inertia weight is dynamically adjusted.

Let X and V denote a particle's coordinates (position) and its corresponding flight speed (velocity) in a search space, respectively. Therefore, the lth particle is represented as $X_{ld} = (X_{l1}, X_{l2}, \ldots, X_{lN})$ in the d-dimensional space. The best previous position of the lth particle, referred to as *pbest*, is recorded and represented as $P_{lbd} = (P_{lb1}, P_{lb2}, \ldots, P_{lbN})$. The index of the best particle among all the *pbest* in the swarm is referred to as the *gbest* and is represented by P_{gd}. The rate of the velocity for particle lth is represented as $V_{ld} = (V_{l1}, V_{l2}, \ldots, V_{lN})$. In this version of PSO, the velocity is limited to a certain range [- V_{max}, V_{max}] such that V_{ld} always lies in that range. The new velocity and position for each particle i in dimension d are determined according to the velocity and position update equations given by (21) and (22) respectively. The inertia weight w_{iner} is updated according to (23).

$$\begin{aligned} V_{ld}(k) = round\ (w_{iner} \cdot V_{ld}(k-1) + c_1 \cdot rand_1 \cdot (P_{lbd}(k-1) - X_{ld}(k-1)) \\ + c_2 \cdot rand_2 \cdot (P^*_{gb}(k-1) - X_{ld}(k-1))) \end{aligned} \quad (21)$$

$$X_{ld}(k) = X_{ld}(k-1) + V_{ld}(k) \quad (22)$$

$$w_{iner} = w^{\max}_{iner} - \left(\frac{w^{\max}_{iner} - w^{\min}_{iner}}{iter_{\max}} \right) \times iter \quad (23)$$

A mutation operator is introduced into the MDPSO algorithm, so that the swarm's best position in dimension d is updated according to (24).

$If\ rand < M_r$

$$P^*_{gd}(k-1) = P_{gd}(k-1) + ceil\ (randn \times P_{gd}(k-1) / \beta_{gb}) \quad (24)$$

$else$

$$P^*_{gd}(k-1) = P_{gd}(k-1)` \quad (25)$$

end

where $d = 1, 2, \ldots, N$ and β_{gb} can be either dynamically changing or fixed.

The pseudocode for GMS implementation using the MDPSO is given below:

Step 1: Initialize randomly a population of particles to lie within specified maintenance window of each unit over entire maintenance period.

Step 2: Set all parameters c_1, c_2, $w_{iner}^{\min}$, $w_{iner}^{\max}$, $Iter_{max}$ and V_{max}.

Step 3: Evaluate the fitness value of each particle using (2).

Step 4: Determine *pbest* and *gbest.*

Step 5: Update velocity and position of each particle using (21) and (22) respectively.

Step 6: Perform mutation using (24) if a random number < M_r and then output resulting optimal maintenance schedule. Otherwise simply output optimal maintenance schedule.

Step 7: Terminate and print results if GMS's maximum number of trials is reached. Otherwise go to *Step* 3 and repeat.

IV. CASE STUDY AND DISCUSSIONS

A. Nigerian Grid System

The test data for this case is taken from a real power system whose thermal generating units are characterized with convex fuel cost coefficients for simplicity. In addition, valve-point loading effect is not considered for long-term generation scheduling. The Nigerian conventional grid system comprises a total of 49 functional generating units spread across seven generating stations located at: AFAM, DELTA, EGBIN, SAPELE, JEBBA, KAINJI and SHIRORO [15] as shown in Fig. 1. Table A of the Appendix is a modification of similar table in [23] to accommodate the weekly maintenance cost (Naira) for each generating unit which participates in maintenance for the entire maintenance horizon of 52 weeks. The table presents generating units' minimum and maximum power outputs (with a total maximum generation of 4145.5MW), technical crew/manpower requirement during maintenance, allowed maintenance duration and downtime. A 12% spinning reserve is used to improve the system reliability and provide sufficient ramping capacity for balancing wind power variability and generation lost from units' shutdown/undergoing maintenance, in addition to balancing existing load variations. Table B of the Appendix presents the Nigerian thermal stations fuel cost coefficients. All the generating units at AFAM and DELTA stations as well as 8 generating units at EGBIN station are gas turbines (GTs), while all generating units at SAPELE station and other 6 generating units at EGBIN station are steam turbines (STs). Also the four thermal plants utilize natural gas supplied from the Nigerian Gas Company (NGC) as their raw material input. The three hydro stations (Hs) namely JEBBA, KAINJI and SHIRORO are located in Northwestern Nigeria. The anticipate wind farm/plant for integration with the hydrothermal power system is located in wind farm Area 3 as shown in Fig. 1.

Well over two decades of operational experience and available historical data on hydrological conditions reveal that inflow variation profile at each hydro station location, by and large affects the generated power output of each hydro plant [23]. The maintenance window and sequence constraints of the three hydro plants are greatly influenced by the trend of the inflow into these hydrological areas.

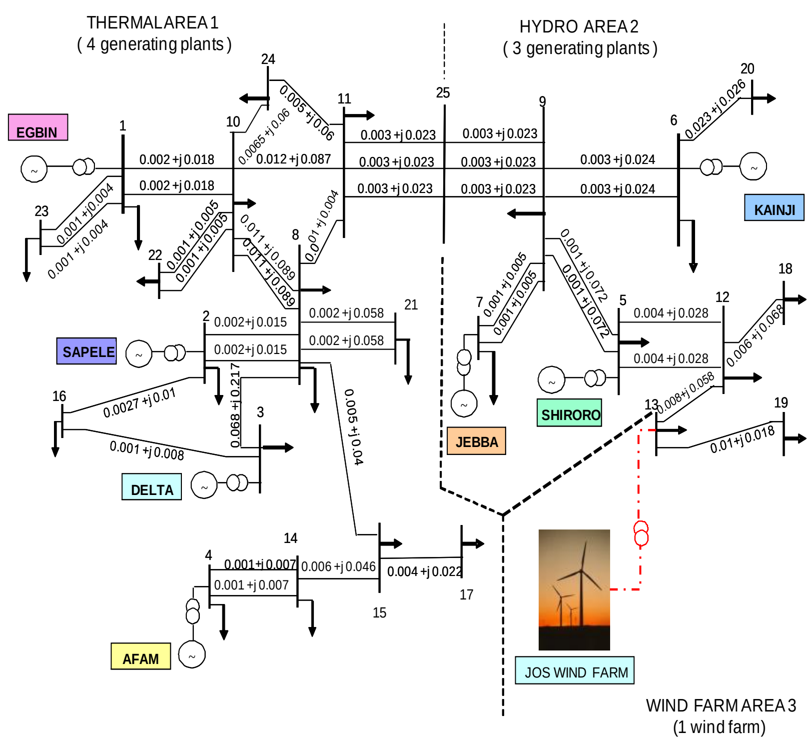

Fig. 1. Nigerian Wind Integrated-Hydrothermal 330-KV, 24-Bus Grid System

Available historical studies indicate that Nigeria experiences a seasonal load variation profile. To model this load variation, a weekly peak load demand of 3625MW [23] plus a 5% load increase is considered during the seasonally hot period (March to July annually) in Nigeria which also associates with the peak demand period as depicted in Fig. 2. Weekly peak demand for periods outside of the March to July is relatively constant due to the predominantly residential-based electricity consumers in Nigeria. On the other hand, substantial industrial loads are supplied with electricity from distributed generation (DG).

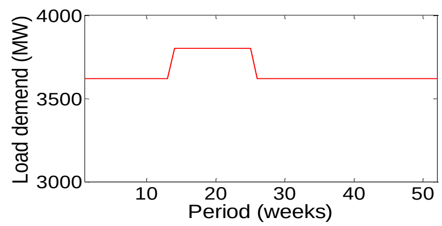

Fig. 2. Annual Load Demand Pattern

The transmission losses (P_{loss}) for the Nigerian grid system is computed using (14), with the loss coefficients obtained via parameter estimation based on several power flow scenarios [25], [26] for its largely radial network structure. The estimated loss formula coefficients for the thermal and hydro generating stations are given in matrix form in [25], [26]. Equation (20) is relaxed in the solution due to line data unavailability. But can be easily incorporated with line data availability by solving the optimal power flow (OPF) and checking for violation in network constraints.

B. Numerical Results and Analysis

All numerical results are obtained based on programs developed in the Matlab environment on a PC with 2.2GHz CPU speed and 1.5GB of RAM.

The following MDPSO and wind-powered plant parameters are used for GMS calculation: population size of 30, $w_{iner}^{\min}$ and $w_{iner}^{\max}$ of 0.4 and 0.9 respectively, c_1 and c_2 of 2, V_{max} is 20% of the dynamic range of the variable on each dimension, M_r of 0.15, $Iter_{max}$ of 500, β_{gb} of 2, ρ of 1.2kgm^{-2}, A_w of 5024m^{-2}, and C_p of 0.59 [16]. The penalty cost coefficients, $C_{E,w}$ and $C_{D,w}$ are empirically tuned to values between 0 and 1000 according to (7), to effectively enforce the penalty conditions in (5). The values are also in accordance with maximum wind power available. The costs C_h and C_w paid to hydro and wind plants owners respectively for the generated power actually used from hydro units and wind units are each set to 0, since both are owned by common utility operator (Nigerian government holds ownership of both plants).

The electricity generated by a utility-scale wind turbine is normally collected and fed into utility power lines, where it is mixed with electricity from other power plants and delivered to utility customers. The output of a wind turbine depends on the turbine's size and the wind's speed through the rotor.

Figure 3 shows the seven Nigerian forecasted wind farms' generation patterns [27], while Table I presents the statistical variation of these seven forecasted wind farms' power outputs used for illustration in this paper. The seven wind farms are geographically dispersed across various regions of Nigeria, representing areas with significant amount of wind gusts and speed. From Fig. 3 and Table I it can be seen that wind farm cited in Jos area projects the highest wind power output with a relatively low standard deviation and hence low level of wind variability and intermittency, compared with the remaining six wind farms. The Jos wind farm located in wind farm area 3 of Fig. 1 is therefore used as the only viable wind generation source that can effectively participate in the wind integrated-hydrothermal maintenance scheduling. An annual mean output power of 408.34MW represents about 40.83% capacity factor for a wind farm facility of 500 wind turbines, each rated at 2MW. The Jos wind turbine's actual maximum power output is 1.585MW, while the wind farm's total actual maximum power generation is 792.474MW, assuming all the turbines are operating at their actual maximum power output capabilities. A wind plant is "fueled" by the wind, which blows steadily at times and not at all at other times. Although modern utility-scale wind turbines typically operate 65% to 90% of the time, they often run at less than full capacity [16]. Therefore, a capacity factor of 25% to 40% is common, although they may achieve higher capacity factors during windy weeks or months. A capacity factor of 40% to 80% is typical for conventional plants. The 52 weeks forecasted wind farm generation pattern for Jos, shown in Fig. 3 represents the wind farm power output forecast $P_{forecast}$ used for illustrating the GMS problem for wind integrated–hydrothermal power system. The reference wind power generation $P_{reference,wt}$ anticipated from Jos wind farm for the power system to meet load demand must balance the expected generation $P_{exp,wt}$ given by (6), otherwise penalty cost is incurred in the objective function in (2) using (5).

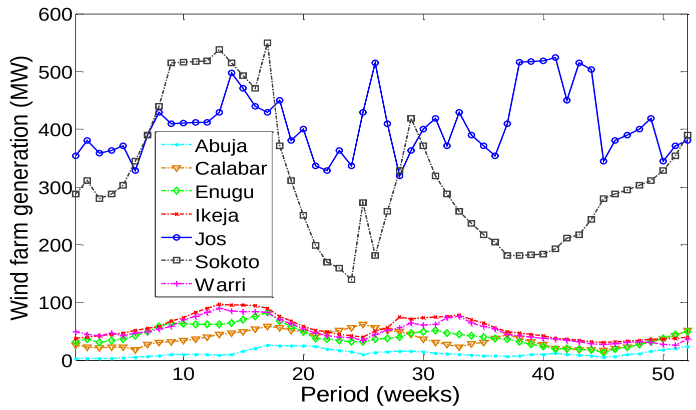

Fig. 3. Wind Farms' Generation Forecasts [27]

TABLE I

Statistical Variation of Seven
Wind farms Power Output Forecasts [27]

Wind farm		Wind farm output power (MW)	
No.	Location	Annual mean	Standard deviation
1	Abuja	12.03	6.22
2	Calabar	36.05	12.96
3	Enugu	41.97	16.97
4	Ikeja	56.54	19.96
5	Jos	408.34	56.55
6	Sokoto	309.86	115.04
7	Warri	51.4	18.11

Figure 4 shows the convergence of annual generation costs presented in Table II for four different GMS and corresponding probabilities of unavailability of wind power for 100 iterations of 100 trials using the MDPSO algorithm. The converged annual generation costs are 1068000000Naira, 1055800000Naira, 1046100000Naira and 1036700000Naira corresponding to GMS #1 (γ=0.8), GMS #2 (γ=0.6), GMS #3 (γ=0.4) and GMS #4 (γ=0.2) respectively as shown in Table II. The result indicates that relative reduction in fuel consumption cost is obtained with increasing capacity credit of wind power.

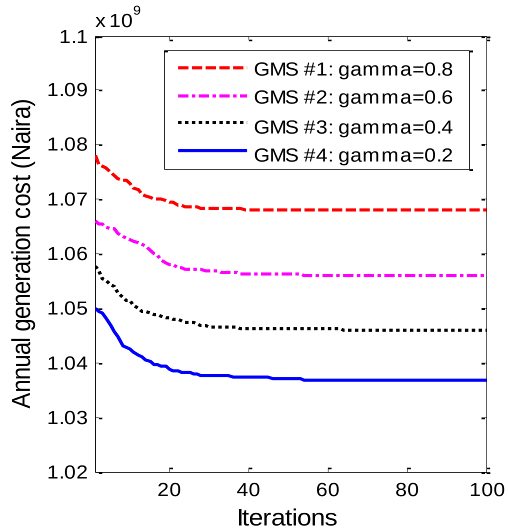

Fig. 4. Convergence of Annual Generation Cost for Different GMS Scenarios

Table II shows maintenance schedules generated by MDPSO algorithm for the 49 generating units over a period of 52 weeks obtained over 100 trials. The results are obtained for four different probabilities of unavailability of wind power γ. The table shows the units scheduled for maintenance on weekly basis over 52 weeks and also presents the weekly maintenance costs, with an annual maintenance cost of 41120000 Naira over the entire maintenance horizon. A unit's maintenance cost in Naira/week is provided as a fixed quantity for each of the 49 generating units presented in Table A of the Appendix. The maintenance cost is calculated by multiplying the fixed maintenance cost per week times the maintenance downtime of each unit in maintenance. Once a unit's maintenance is started it cannot be aborted, and each unit must undergo scheduled maintenance once per year. Table II also shows the annual transmission losses, annual generation, annual generation costs and annual carbon dioxide (CO_2) emission concentrations under different probabilities of unavailability of wind power. The annual generation cost (fuel consumption cost) and the annual CO_2 emission decreases with decreasing probability of unavailability of wind power. Only one type of pollutant (CO_2) is considered for simplicity. The CO_2 emission conversion factors according to reference values of the fuel characteristics are shown in Table C of the Appendix. The CO_2 emission is generally taken to be proportional to the generator's fuel consumption using similar form of the fuel cost function with appropriately derived CO_2 emission coefficients from Tables B and C of the Appendix [28], [29].

Figure 5 shows the system reliability indices (RIs) plots during generator maintenance under GMS #1 (γ=0.8), GMS #2 (γ=0.6), GMS #3 (γ=0.4) and GMS #4 (γ=0.2) scenarios. The converged results are obtained after 100 iterations of 100 trials using the MDPSO algorithm. The converged RIs are 0.934, 0.936, 0.939 and 0.951 corresponding to GMS #1 (γ=0.8), GMS #2 (γ=0.6), GMS #3 (γ=0.4) and GMS #4 (γ=0.2) respectively. The high RI value of 0.951 is obtained at the expense of significant capacity credit of wind power introduced into the grid (when probability of unavailability of wind power is γ=0.2). The RI shows an increasing trend as the contribution of the capacity credit of wind power to the grid increases. The result also shows the capability of introducing wind power to increase reliability of the power system since the available capacity is increased. If the reliability was acceptable before the installation/introduction of wind power, wind power integration will enable the power system to meet a higher demand (or offset capacity deficit due to GMS) at the same reliability level.

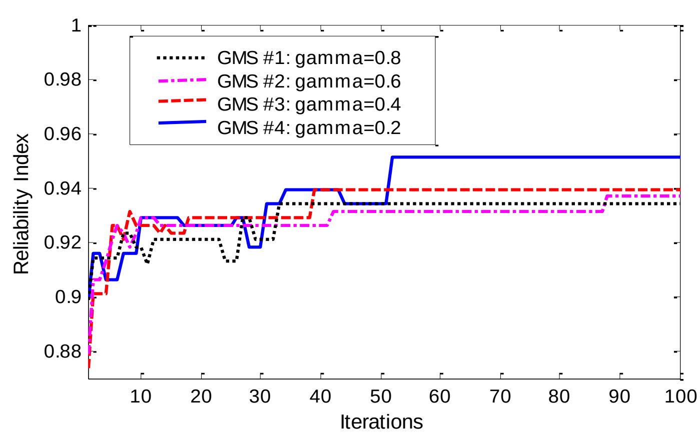

Fig. 5. Convergence of Reliability Indices for Different GMS Scenarios

TABLE II

Annual Maintenance Schedules, Transmission Losses, Maintenance, Generation Costs and CO_2 Emissions Considering Uncertainty in Wind Generation

Maintenance week	GMS #1: Probability of unavailability of wind power γ=0.8		GMS #2: Probability of unavailability of wind power γ=0.6		GMS #3: Probability of unavailability of wind power γ=0.4		GMS #4: Probability of unavailability of wind power γ=0.2	
	Generating units scheduled for maintenance	Weekly maintenance cost (Naira)	Generating units scheduled for maintenance	Weekly maintenance cost (Naira)	Generating units scheduled for maintenance	Weekly maintenance cost (Naira)	Generating units scheduled for maintenance	Weekly maintenance cost (Naira)
1	18	280000	-	0	8,11	280000.00	4,8	420000
2	18	280000	1	280000	8,11,20	560000.00	2,4,5,8	980000
3	18	280000	1,6,10	700000	16,18,19,20	1120000.00	2,4,5,13,18	1260000
4	2,3,8,18	980000	1,6,7,10	840000	16,18,19,20	1120000.00	2,4,5,13,18	1260000
5	2,3,8,12	840000	1,6,7,11,17	1120000	12,14,16,18,19,20	1400000.00	2,4,5,10,12,18,20	1680000
6	2,3,5,12	980000	1,6,11,17	980000	12,14,16,18,19	1120000.00	2,5,7,10,12,14,17,18,20	1960000
7	2,3,5,14,19	1260000	5,6,17,19,20	1400000	3,7	420000.00	7,14,17,19,20	1120000
8	2,3,5,14,15,19	1540000	5,15,17,19,20	1400000	2,3,7,13,15	1120000.00	3,15,17,19,20	1400000
9	4,5,7,15,19,20	1540000	3,5,8,12,15,19,20	1680000	2,3,6,13,15	1260000.00	3,11,15,17,19	1260000
10	4,5,7,9,13,15,19,20	1820000	3,4,5,8,12,15,19,20	1960000	1,2,3,6,9,15	1540000.00	3,11,15,19	980000
11	4,6,9,13,15,16,20	1680000	3,4,5,15	1120000	1,2,3,4,6,9,15	1820000.00	3,9,15	700000
12	1,4,6,11,16,17,20	1820000	2,3,4,13,16,18	1540000	1,2,4,5,6,17	1680000.00	1,3,6,9	980000
13	1,4,6,11,16,17	1540000	2,3,4,13,16,18	1540000	1,4,5,6,10,17	1540000.00	1,6,16	840000
14	1,6,16,17	1120000	2,4,16,18	1120000	1,4,5,10,17	1260000.00	1,6,16	840000
15	1,6,10,17	980000	2,9,14,16,18	1120000	4,5,17	840000.00	1,6,16	840000
16	1,10	420000	2,9,14	560000	5	280000.00	1,6	840000
17	-	0	-	0	-	0.00	-	0
18	36,40,41	690000	35,42,45	720000	48	200000.00	49	200000
19	36,40,41	690000	35,42,45	720000	43,48	420000.00	49	200000
20	36,40,41	690000	35,42,45	970000	34,43	470000.00	33	250000
21	36,37	500000	35,44,45	750000	34,43	470000.00	33,40	470000
22	37,42	470000	41,44	470000	34,39	500000.00	33,40	470000
23	37,42	470000	41,44	470000	34,39	500000.00	33,40	470000
24	37,42	470000	41,43	440000	39,44	500000.00	47	200000
25	45,48	450000	36,43	470000	35,39,44	750000.00	47	200000
26	43,45,48	670000	36,43	470000	35,42,44	720000.00	38,39,42	720000
27	32,34,43,45	970000	36,48	450000	35,42,44	720000.00	38,39,42	720000
28	32,34,43,45	970000	36,48	450000	32,35,42	720000.00	38,39,42,44	970000
29	32,34	500000	46	200000	32,38	500000.00	38,39,44	750000
30	32,34	500000	46	200000	32,38	500000.00	34,44	500000
31	47	200000	47	200000	32,38	500000.00	34,44	500000
32	47	200000	47	200000	38	250000.00	32,34	500000
33	46	200000	32,33	500000	46	200000.00	32,34,41,43	940000
34	39,46	450000	32,33,38	750000	46	200000.00	32,41,43	690000
35	39,44	500000	32,33,38	750000	49	200000.00	32,41,43	690000
36	35,39,44	750000	32,33,38	750000	49	200000.00	48	450000
37	33,35,39,44	1000000	38,39,40	720000	33,37	500000.00	36,48	450000
38	33,35,44	750000	34,37,39,40	970000	33,36,37	750000.00	35,36	500000
39	33,35	500000	34,37,39,40	970000	33,36,37	750000.00	35,36	500000
40	33,38	500000	34,37,39	750000	33,36,37,45	1000000.00	35,36,37,45	750000
41	38,41	450000	34,37	500000	36,40,41,45	940000.00	35,37,45	750000
42	38,41	450000	49	200000	40,41,45,47	890000.00	37,45,46	700000
43	38	250000	49	200000	40,41,45,47	890000.00	37,45,46	700000
44	24,29	420000	22	280000	31	280000.00	24,26	280000
45	22,24,25,29	840000	22,27,29,31	1120000	26,28,30,31	980000.00	24,26,28	560000
46	22,25,26,28,29,31	1400000	22,26,27,29,31	1260000	26,27,28,29,30,31	1540000.00	21,22,27,28,29	1400000
47	21,22,26,28,29,30,31	1820000	21,22,26,27,28,29,31	1820000	21,22,27,28,29,30,31	1960000.00	21,22,27,28,29	1400000
48	21,22,27,28,30,31	1680000	21,22,25,27,28,29,30,31	2100000	21,22,27,28,29,30	1680000.00	21,22,23,27,28,29,30,31	2100000
49	21,22,27,28,30,31	1680000	21,24,25,28,30	1120000	21,22,25,27,29	1260000.00	21,22,23,27,29,30,31	1820000
50	21,23,27,30	980000	21,23,24,28,30	1120000	21,22,23,24,25	980000.00	21,22,25,30,31	1260000
51	21,23,27	700000	21,23,30	700000	21,22,23,24	840000.00	25,30,31	700000
52	-	0	-	0	-	0.00	-	0
Annual maintenance cost (Naira)		41120000	-	41120000	-	41120000	-	41120000
Annual power loss (MW)		241.944	-	227.592	-	212.004	-	198.588
Annual load demand (MW)		190675.000	-	190675.000	-	190675.000	-	190675.000
Annual power generation (MW)		190916.944	-	190902.592	-	190887.004	-	190873.588
Annual generation cost from thermal units only (Naira)		1068000000	-	1055800000	-	1046100000	-	1036700000
Annual CO_2 emission (tCO_2)		61818	-	61662	-	61350	-	61110

Figures 6 and 7 show typical maintenance cost and maintenance crew plots respectively for the 49-unit Nigerian hydrothermal system using the MDPSO algorithm. It can be deduced from these figures that weeks 5, 14, 50-51 indicate periods with heavy maintenance work resulting in large maintenance costs, compared with weeks 18-19, 32-33 and 43 representing periods with relatively low maintenance tasks. The weekly manpower requirement depicted in Fig. 7 clearly satisfies the crew/labor constraint in (9), and shows a mean and standard deviation of 12±6.20.

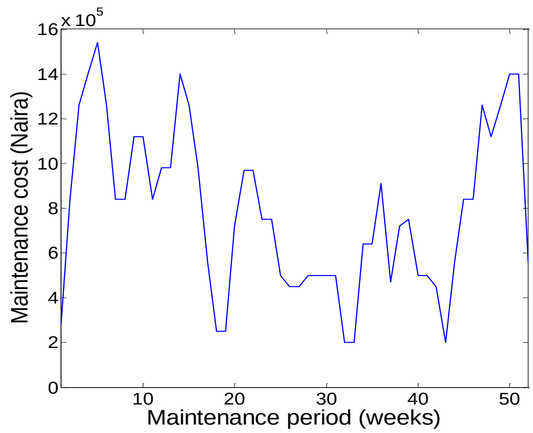

Fig. 6. Typical Maintenance Cost Plot for the 49-Unit Nigerian Hydrothermal System with MDPSO Solution

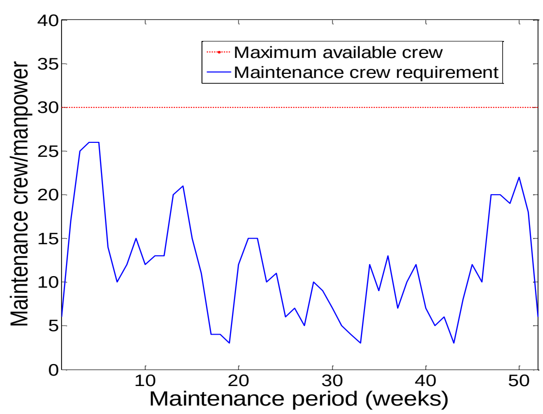

Fig. 7. Typical Maintenance Crew/Labor Plot for the 49-Unit Nigerian Hydrothermal System with MDPSO Solution

Figure 8 shows at a glance the impact of capacity credit of wind power on the annual generation cost and annual generation cost saving. As wind power from the wind farm becomes more available to increase the capacity credit of wind power, compensate and effectively displace portions of thermal generation supplying load, the generation from more expensive thermal-based units ramps down and results in lowering the overall annual cost of generation. The four different GMS scenarios (with their probabilities of unavailability of wind power) drawn from Table II are shown plotted in Fig. 8. It is seen from the figure that decreasing the probability of unavailability of wind power translates to significant fuel cost savings, since the capacity credit of wind power will be increased as well. This can help the utility operators in making qualitative and logical long-term planning that ensures cost effective system operation.

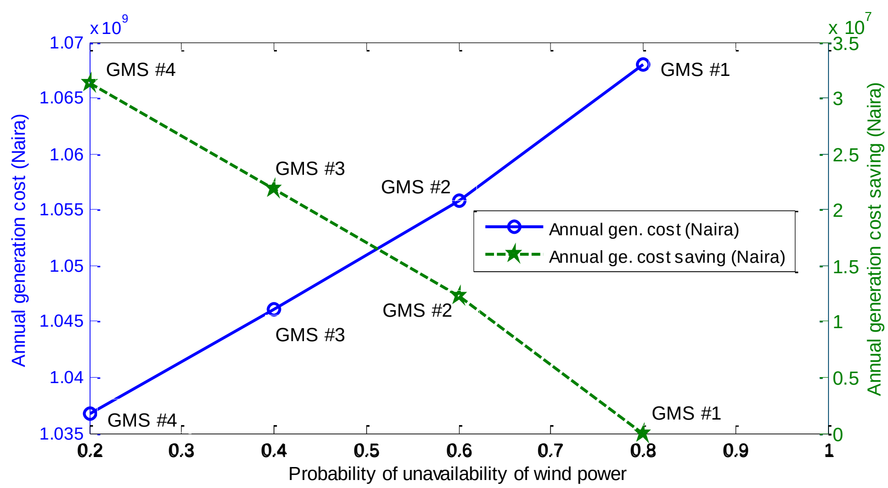

Fig. 8. Annual Generation Cost and Saving for Different GMS and Probabilities of Unavailability of Wind Power

Figure 9 shows the annual CO_2 emission concentrations plotted against the annual generation costs for four GMS scenarios considered in this paper. Implementation of GMS #1 (γ=0.8), GMS #2 (γ=0.6), GMS #3 (γ=0.4) and GMS #4 (γ=0.2) produce 61818tCO_2, 61662tCO_2, 61350tCO_2 and 61110tCO_2 respectively in annual CO_2 emission, which translates to 0%, 0.25%, 0.76% and 1.15% respectively in annual CO_2 emission reduction benefits. These annual CO_2 emission reduction benefits can be significantly improved with increased capacity credit of wind power through vigorous wind penetration initiatives.

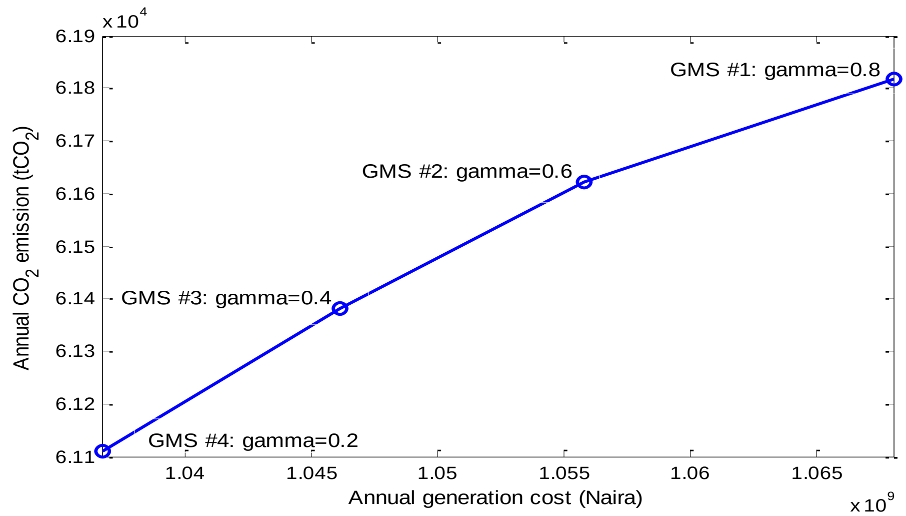

Fig. 9. Annual CO_2 Emission versus Annual Generation Cost for Different GMS and Probabilities of Unavailability of Wind Power

Table III presents the statistical comparison of the annual generation cost and annual CO_2 emission cost for different probabilities of unavailability of wind power. The results are obtained after 100 iterations of 500 trials over the entire maintenance period of 52 weeks. The results show minimum, maximum and average percent in annual energy cost savings of 2.93%, 3.01% and 2.73% respectively, while the minimum, maximum and average percent in annual CO_2 emission cost savings are 1.15%, 1.05% and 1.09% respectively. These results are achieved by choosing to implement GMS #4 (γ=0.2) compared with GMS #1 (γ=0.8). Similar analysis can be made for GMS #2 (γ=0.6) and GMS #3 (γ=0.4) compared with GMS #1 (γ=0.8). The best annual generation cost and annual CO_2 emission cost obtained are 1036700000Naira and 1018500000Naira respectively corresponding to GMS #4 (γ=0.2) as shown in Table III.

Table IV shows the minimum and maximum limits of the total relative annual cost savings derived from the relative annual generation cost and relative annual CO_2 emission cost savings that can be obtained when implementing GMS #1, #2, #3 or #4 for the different probabilities of unavailability of wind power considered in this paper. A maximum total relative annual cost saving of 47800000 Naira is achievable using GMS #4 (γ=0.2) compared with GMS #1 (γ=0.8), while a minimum total relative annual cost saving of 14800000 Naira is obtainable using GMS #2 (γ=0.6) compared with GMS #1 (γ=0.8). The result also shows how the capacity credit of wind power can be translated into knowing the amount of total annual cost savings accruable from both reductions in fuel consumption and CO_2 emission.

TABLE III

Statistical Comparison of Annual Generation and CO_2 Emission Costs Considering Probability of Unavailability of Wind Power

S/N	Probability of unavailability of wind power (γ)	Annual generation cost (x100000)				Annual CO_2 emission cost (x100000)			
		Minimum (Naira)	Maximum (Naira)	Mean (Naira)	Standard deviation	Minimum (Naira)	Maximum (Naira)	Mean (Naira)	Standard deviation
1	GMS #1: γ=0.8	10680	10787	10701	±15.567	10303	10344	10316	±10.508
2	GMS #2: γ=0.6	10558	10627	10590	±13.907	10277	10308	10289	±13.380
3	GMS #3: γ=0.4	10461	10566	10501	±14.142	10225	10258	10238	±12.837
4	GMS #4: γ=0.2	10367	10429	10409	±14.330	10185	10224	10204	±14.860
Percent of annual cost saving between implementing GMS #1 (γ=0.8) and GMS #4 (γ=0.2)		2.93%	3.01%	2.73%	-	1.15%	1.05%	1.09%	-

TABLE IV

Total Relative Annual Cost Saving Considering Probability of Unavailability of Wind Power

S/N	Probability of unavailability of wind power (γ)	Relative annual generation cost saving (x100000 Naira)		Relative annual CO_2 emission cost saving (x100000 Naira)		Total relative annual cost saving (x100000 Naira)	
		Minimum	Maximum	Minimum	Maximum	Minimum	Maximum
1	GMS #2: γ=0.6	122	177	26	36	148	213
2	GMS #3: γ=0.4	219	221	78	86	297	307
3	GMS #4: γ=0.2	313	358	118	120	431	478

V. CONCLUSIONS

One of the smart grid visions of effectively integrating asset management processes into the grid which leads to effectively managed assets and costs have been demonstrated and presented. The problem of optimal preventive generator maintenance scheduling (GMS) for a wind-hydrothermal power system has been shown and solved using a modified discrete particle swarm optimization (MDPSO) algorithm. Handling uncertainty in wind power associated with solving the stochastic GMS problem has been formulated and demonstrated using probabilistic method. One of the key benefits associated with the wind power integration is the capacity credit of wind power added to the wind-hydrothermal power system. It is demonstrated that the wind generation displaces electricity produced from thermal units (that is, ramps down thermal generation), thus the quantity of fuel burnt by the thermal units is reduced and the wind generation provides a fuel saving, and also enhances carbon dioxide (CO_2) emission reduction. Even though CO_2 emission reduction is not explicitly modeled into the cost function, the proposed model results in CO_2 emission reduction benefits with increased capacity credit of wind power. This GMS stochastic optimization result present useful platforms for long-term planning and optimized energy management in the presence of uncertainty in wind power generation.

Future work will incorporate short-term planning schemes such as unit commitment and economic dispatch on smaller time-frames (minutes to hours). This multi-period (short and long-term) generation scheduling problem for wind-hydrothermal power system is carried out in future work. Future work will also explicitly incorporate environmental pollution (CO_2 emission) in the objective function and the problem solved as multi-objective constrained optimization. Also, to re-optimize the maintenance schedules in an event of forced generator outage during a normal preventive maintenance, a dynamic optimization technique such as adaptive dynamic programming can be used to automatically generate optimal GMS. Otherwise, one has to manually trigger an MDPSO based GMS whenever needed.

VI. APPENDIX

TABLE A

Nigerian Hydrothermal Units' and Maintenance Data

Type of power station	Power station					Power limits		Ramp rate limits			Maintenance data			
	Name of power station	S/N	Plant number	Name of turbine unit	Type of turbine	P^{min}	P^{max}	P^{pre} (MW)	UR (MW/h)	DR (MW/h)	Allowed maint. Period	Maint. duration (Weeks)	Manpower required for each week	Maint. cost per week (Naira)
Thermal	Egbin PS	1	3	EGBINST1	ST	80.0	190.0	120.0	50.0	90.0	January - April (1 - 17 weeks)	5	6+5+5+4+2	280000
		2	3	EGBINST2	ST	80.0	190.0	120.0	50.0	90.0		5	6+5+5+4+2	280000
		3	3	EGBINST3	ST	80.0	190.0	120.0	50.0	90.0		5	6+5+5+4+2	280000
		4	3	EGBINST4	ST	80.0	190.0	120.0	50.0	90.0		5	6+5+5+4+2	280000
		5	3	EGBINST5	ST	80.0	190.0	120.0	50.0	90.0		5	6+5+5+4+2	280000
		6	3	EGBINST6	ST	80.0	190.0	120.0	50.0	90.0		5	6+5+5+4+2	280000
		7	4	EGBINGT1	GT	90.0	220.0	200.0	60.0	100.0		2	4+3	140000
		8	4	EGBINGT2	GT	20.0	30.0	25.0	20.0	25.0		2	4+3	140000
		9	4	EGBINGT3	GT	20.0	30.0	25.0	20.0	25.0		2	4+3	140000
		10	4	EGBINGT4	GT	20.0	30.0	25.0	20.0	25.0		2	4+3	140000
		11	4	EGBINGT5	GT	20.0	30.0	25.0	20.0	25.0		2	4+3	140000
		12	4	EGBINGT6	GT	20.0	30.0	25.0	20.0	25.0		2	4+3	140000
		13	4	EGBINGT7	GT	20.0	30.0	25.0	20.0	25.0		2	4+3	140000
		14	4	EGBINGT8	GT	20.0	30.0	25.0	20.0	25.0		2	4+3	140000
	Sapele PS	15	5	SAPELST1	ST	5.0	10.0	7.0	5.0	6.0		4	4+3+3+2	280000
		16	5	SAPELST2	ST	5.0	10.0	7.0	5.0	6.0		4	4+3+3+2	280000
		17	5	SAPELST3	ST	5.0	10.0	7.0	5.0	6.0		4	4+3+3+2	280000
		18	5	SAPELST4	ST	5.0	10.0	7.0	5.0	6.0		4	4+3+3+2	280000
		19	5	SAPELST5	ST	5.0	10.0	7.0	5.0	6.0		4	4+3+3+2	280000
		20	5	SAPELST6	ST	40.0	85.3	70.0	40.0	60.0		4	4+3+3+2	280000
	Afam PS	21	1	AFAMGT19	GT	60.0	138.0	100.0	60.0	70.0	November - December (44 - 52 weeks)	5	5+5+4+3+3	280000
		22	1	AFAMGT20	GT	60.0	138.0	100.0	60.0	70.0		5	5+5+4+3+3	280000
	Delta PS	23	2	DELTAG03	GT	10.0	19.6	15.0	10.0	12.0		2	4+3	140000
		24	2	DELTAG04	GT	10.0	19.6	15.0	10.0	12.0		2	4+3	140000
		25	2	DELTAG06	GT	10.0	19.6	15.0	10.0	12.0		2	4+3	140000
		26	2	DELTAG07	GT	10.0	19.6	15.0	10.0	12.0		2	4+3	140000
		27	2	DELTAG08	GT	5.0	10.0	7.0	5.0	6.0		4	4+4+3+3	280000
		28	2	DELTAG15	GT	40.0	85.0	70.0	40.0	60.0		4	4+4+3+3	280000
		29	2	DELTAG16	GT	40.0	85.0	70.0	40.0	60.0		4	4+4+3+3	280000
		30	2	DELTAG17	GT	40.0	85.0	70.0	40.0	60.0		4	4+4+3+3	280000
		31	2	DELTAG18	GT	40.0	85.0	70.0	40.0	60.0		4	4+4+3+3	280000
Hydro	Jebba PS	32	6	JEBBGH1	H	50.0	88.3	-	-	-	May - October (18 - 43 weeks)	4	5+4+3+2	250000
		33	6	JEBBGH2	H	50.0	88.3	-	-	-		4	5+4+3+2	250000
		34	6	JEBBGH3	H	50.0	88.3	-	-	-		4	5+4+3+2	250000
		35	6	JEBBGH4	H	50.0	88.3	-	-	-		4	5+4+3+2	250000
		36	6	JEBBGH5	H	50.0	88.3	-	-	-		4	5+4+3+2	250000
		37	6	JEBBGH6	H	50.0	88.3	-	-	-		4	5+4+3+2	250000
	Kainji PS	38	7	KAING05	H	55.0	112.5	-	-	-		4	5+5+4+3	250000
		39	7	KAING06	H	5.0	10.0	-	-	-		4	5+5+4+3	250000
		40	7	KAING07	H	5.0	10.0	-	-	-		3	4+3+2	220000
		41	7	KAING08	H	5.0	10.0	-	-	-		3	4+3+2	220000
		42	7	KAING09	H	5.0	10.0	-	-	-		3	4+3+2	220000
		43	7	KAING10	H	35.0	76.5	-	-	-		3	4+3+2	220000
		44	7	KAING11	H	55.0	90.0	-	-	-		4	5+4+3+3	250000
		45	7	KAING12	H	5.0	10.0	-	-	-		4	5+4+3+3	250000
	Shiroro PS	46	8	SHIRGH1	H	100.0	249.0	-	-	-		2	4+3	200000
		47	8	SHIRGH2	H	100.0	249.0	-	-	-		2	4+3	200000
		48	8	SHIRGH3	H	75.0	140.0	-	-	-		2	4+3	200000
		49	8	SHIRGH4	H	100.0	249.0	-	-	-		2	4+3	200000

*GT - Gas turbine, ST - Steam turbine and H - Hydro. Most units requiring higher number of manpower and longer duration are typically aged. Nigerian Naira=0.008US$ at 2003.

TABLE B

Nigerian Thermal Stations' Fuel Cost coefficients

Power station	Fuel cost coefficients		
	a_i (Naira/h)	b_i (Naira/MWh)	c_i (Naira/MW^2h)
Sapele	6929.000	7.840	0.130
Delta	525.740	6.130	1.200
Afam	1998.000	56.000	0.092
Egbin	12787.000	13.100	0.031

TABLE C

Emission Conversion Factors [28], [29]

Unit type	Net calorific value	Emission factor	Oxidation factor	Fuel supply cost	Emission conversion factor	
	(KJ/m^3)	(tCO_2/TJ)	(%)	(\$/m^3)	(tCO_2/\$)	(tCO_2/Naira)
Oil	41031	77.4	0.995	157.00	0.02013	0.00016
Gas	31736	56.1	0.995	0.23	0.00800	0.00006
Coal	29308	98.3	0.990	51.30	0.05560	0.00045

VII. ACKNOWLEDGMENT

This work was supported by the National Science Foundation, USA under Grant ECCS #0348221.

VIII. REFERENCES

[1] S. E. Collier, "Ten steps to a smarter grid," *IEEE Industry Applications Magazine*, pp. 62-68, March/April 2010.

[2] M. Shahidehpour and M. Marwali, *Maintenance scheduling in restructured power system*. ISBN 0-7923-7872-5, Kluver Academic Publishers, Norwell, Massachusetts, 2000.

[3] A. J. Wood and B. F. Wollenberg, *Power generation operation and control*. ISBN 9814-12-664-0, John Wiley and Sons, New York, NY, 2004.

[4] K. Y. Lee and M. A. El-Sharkawi, *Modern heuristic optimization techniques: theory and applications to power systems*. ISBN 978-0471-45711-4, IEEE Press, 445 Hoes Lane, Piscataway, New Jersey, 2008.

[5] E. L. da Silva, M. Th. Schilling and M. C. Rafael, "Generation maintenance scheduling considering transmission constraints," *IEEE Transactions on Power Systems*, vol. 15, no. 2, pp. 838-843, May 2000.

[6] M. Y. El-Sharkh and A. A. El-Keib, "Maintenance scheduling of generation and transmission systems using fuzzy evolution programming ," *IEEE Transactions on Power Systems*, vol. 18, no. 2, pp. 862-866, May 2003.

[7] J.-H. Kim, J.-B. Park, J.-K. Park and B. H. Kim, "A new game-theoretic framework for maintenance strategy analysis," *IEEE Transactions on Power Systems,* vol. 18, no. 2, pp. 698-706, May 2003.

[8] D. Chattopadhyay, "Life-cycle maintenance management of generating units in a competitive environment," *IEEE Transactions on Power Systems,* vol. 19, no. 2, pp. 1181-1189, May 2004.

[9] R. Billinton and R. Mo, "Composite system maintenance coordination in a deregulated environment," *IEEE Transactions on Power Systems,* vol. 20, no. 1, pp. 485-492, February 2005.

[10] A. J. Conejo, R. Garcia-Bertrand and M. Diaz-Salazar, "Generation maintenance scheduling in restructured power systems," *IEEE Transactions on Power Systems,* vol. 20, no. 2, pp. 984-992, May 2005.

[11] H. Barot and K. Bhattacharya, "Security coordinated maintenance scheduling in deregulation based on genco contribution to unserved energy," *IEEE Transactions on Power Systems,* vol. 23, no. 4, pp. 1871-1882, November 2008.

[12] L. Wu, M. Shahidehpour and Z. Li, "Genco's risk-constrained hydrothermal scheduling," *IEEE Transactions on Power Systems,* vol. 23, no. 4, pp. 1847-1858, February 2008.

[13] L. Wu, M. Shahidehpour and T. Li, "Genco's risk-based maintenance outage scheduling," *IEEE Transactions on Power Systems,* vol. 23, no. 1, pp. 127-136, February 2008.

[14] C. Feng, X. Wang and F. Li, "Optimal maintenance scheduling of power producers considering unexpected unit failure," *IET Generation, Transmission & Distribution,* vol. 3, no. 5, pp. 460-471, 2009.

[15] C. Feng and X. Wang, "A competitive mechanism of unit maintenance scheduling in a deregulated environment," *IEEE Transactions on Power Systems,* vol. 25, no. 1, pp. 351-359, February 2010.

[16] T. Ackermann, *Wind Power in Power Systems*. ISBN 10: 0-470-85508-8 (H/B), John Wiley & Sons Ltd, The Atrium, Southern Gate, Chichester, West Sussex PO19 8SQ, England, 2005.

[17] S. Li and D. C. Wunsch, "Using neural networks to estimate wind turbine power generation," *IEEE Transactions on Energy Conversion,* vol. 16, Issue 3, pp. 276-282, September 2001.

[18] E. Denny and M. O'Malley, "Quantifying the total net benefits of grid integrated wind," *IEEE Transactions on Power Systems,* vol. 22, no. 2, pp. 605-615, May 2007.

[19] R. A. Jabr and B. C. Pal, "Intermittent wind generation in optimal power flow dispatching," *IET Generation, Transmission & Distribution,* vol. 3, no. 1, pp. 66-74, 2008.

[20] C. Chompoo-inwai, C. Yingvivatanapong, K. Methaprayoon and W. Lee, "Reactive compensation techniques to improve the ride-through capability of wind turbine

during disturbance," *IEEE Transactions on Industry Applications,* vol. 41, no. 3, pp. 666-672, May/June 2005.

[21] C. Chompoo-inwai, W. Lee, P. Fuangfoo, M. Williams and J. R. Liao, "System impact study for the interconnection of wind generation and utility system," *IEEE Transactions on Industry Applications,* vol. 41, no. 1, pp. 163-168, January/February 2005.

[22] C. L. Chen, "Simulated annealing-based optimal wind-thermal coordination scheduling," *IET Generation, Transmission & Distribution,* vol. 1, no. 3, pp. 447-455, 2007.

[23] Y. Yare, G. K. Venayagamoorthy and U. O. Aliyu, "Optimal generator maintenance scheduling using a modified discrete PSO," *IET Generation, Transmission & Distribution,* vol. 2, no. 6, pp. 834-846, November 2008.

[24] Y. del Valle, G. K. Venayagamoorthy, S. Mohagheghi, J. Hernandez and R. G. Harley, "Particle swarm optimization: Basic concepts, variants and applications in power system," *IEEE Transactions on Evolutionary Computation*, vol. 12, no. 2, pp. 171-195, April 2008.

[25] T. S. G. Wudil, I. O. Ajiboye, J. D. Jiya and U. O. Aliyu, "Development of transmission loss formula for Nigerian electric power system," *6th International Conference on Power Systems Operation and Planning – VI (ICPSOP),* Universidade Jean Piaget, Praia, Cape Verde, South Africa, pp. 93-97, 22-26 May 2005.

[26] G. A. Bakare, U.O. Aliyu, G. K. Venayagamoorthy and Y. K. Shu'aibu, "Genetic algorithms based economic dispatch with application to coordination of Nigerian thermal power plants," *IEEE PES General Meeting,* vol. 1, pp. 551-556, June 2005.

[27] O. I. Okoro and E. Chikuni, "Prospects of wind energy in Nigeria," in *International Conference on the Domestic Use of Energy,* Cape Peninsula University of Technology, Cape Town, South Africa, 10-13 April 2007.

[28] D. N. Simopoulos, Y. S. Giannakopoulos, S. D. Kavatza and C. D. Vournas, "Effects of emission constraints on short-term unit commitment," in *IEEE Mediterranean Electrotechnical Conference Melecon 2006,* Benalmadena (Malaga), Spain, 16-19 May 2006.

[29] (Journal of the European Union) August 2007. Commission Decision of 18 July 2007 establishing guidelines for the monitoring and reporting of greenhouse gas emissions pursuant to Directive 2003/87/EC of the European Parliament and of the Council (notified under document number C(2007) 3416) (1). Available: http://vlex.com/vid/guidelines-reporting-greenhouse-emissions-36467981, accessed August 2007.

VI. REAL-TIME STABILITY ASSESSMENT OF A POWER SYSTEM

Y. Yare, *Student Member, IEEE*, and G. K. Venayagamoorthy, *Senior Member, IEEE*

ABSTRACT— The real-time (RT) stability assessment (SA) is to determine a power system's ability to continue to provide service (electric energy) in a RT manner in case of an unforeseen catastrophic contingency. Credible contingencies are analyzed using non real-time (NRT) and RT stability assessment indices (SAIs). Cascading stages of fuzzy inference system is applied to combine the different NRT and RT SAIs to determine the network status. The network status reflects the effect that each credible contingency has on the system and the distance to stability/security limit. In this paper, a practical Nigerian power system modeled on the real-time digital simulator (RTDS) platform is used as case study to implement and simulate in RT generator maintenance scheduling (GMS). GMS reflects power generation loss due to scheduled shutdown maintenance. Under the implementation of the GMS, the system is subject to load shedding, three-phase short circuit fault on the tie-line and permanent transmission line outage (*N-1* contingency and topology change). Results show that the network status has potential for use by system operators to take preventive real-time decisions.

INDEX TERMS — Electromechanical oscillations, energy management, generator maintenance scheduling, real-time stability assessment.

I. INTRODUCTION

Real-time stability assessment (RT-SA) deals with the analysis of a power system assuming credible system contingencies or sequence of events had occurred in RT. To assess the level of system strength or weakness relative to the occurrence of an undesired event, a quantitative measure based on stability index is often considered. If the analysis indicates that a system is unstable, the stability control should provide preventive strategies by changing system operating conditions to a more viable status, hence forestalling the possibility of cascading outages. A power system is said to be stable if it can withstand all credible contingencies without violating any of the system constraints.

If there is at least one contingency, or sequence of probable events, which violates the system constraints, the system is judged to be unstable or insecure [1], [2]. An interconnected power system, depending on its size, has hundreds to thousands of modes of oscillations. In the analysis and control of system stability, two distinct types of system oscillations are usually recognized [1], [2]. One type is associated with units at a generating station swinging with respect to the rest of the power system. Such oscillations are referred to as “local plant mode” oscillations. The frequencies of these oscillations are typically in the range 0.8 to 2.0 Hz. The second type of oscillations is associated with the swinging of many machines in one part of the system against machines in other parts. These are referred to as “inter-area mode” oscillations, and have frequencies in the range 0.1 to 0.7 Hz [1], [2].

In a deregulated environment, increased interconnections and unforeseen changes in the system topology and load can cause system instability [1], [2] which needs to be addressed in RT. In monopolistic environment, however, utilities could afford increased security margins, which is no longer probable under the smart grid environment. Because of this and the limited investments in the construction of new power plants, the system is required to operate closer to its stability boundary. This, in turn, requires the industry to develop better methods of quantifying the RT stability status of their systems. The reason for undertaking a stability assessment therefore is to determine the ability of the power system to continue providing service in case of an unforeseen, but probable, catastrophic contingency. A power system can become unstable for various reasons such as, major component failures, communication interruptions, human errors, unfavorable weather conditions, and sometimes sabotage.

Some key challenges associated with RT-SA are [1], [2]: the large numbers of contingencies and sequence of events that are typically needed to provide accurate SA, the wide range of operating conditions and topology of the power system makes the operating space very complex, the speed by which the SA can be assessed in real-time, the large number of measurements available in the power system, and the lack of methods to enhance the correlations between measurements and SA, and the lack of effective assessment index.

A development in the area of contingency screening for static security analysis is presented in [3]. Neural networks application to dynamic security contingency screening and ranking is summarized in [4]. The paper presents the use of information on the prevailing operating condition and directly provides contingency screening and ranking using a trained neural network. Several indices are proposed in [5] for contingency screening in an on-line dynamic security assessment. These indices are based on the concepts of coherency, transient energy conversion between kinetic energy and potential energy, and three dot products of system variables. An integrated scheme to study power system vulnerability considering protection system failures is proposed in [6]. The paper establishes a new protection system reliability model including two major failure modes to demonstrate their effects on power system reliability. Application of trajectory sensitivity analysis of power systems containing FACTS compensators is discussed in [7]. The paper presents the effect of the use of various FACTS devices on the system transient stability by applying trajectory sensitivity analysis. A new model describing the uncertainty of fault clearing time for probabilistic transient stability assessment of power systems is presented in [8]. The paper uses a corrected transient energy function-based strategy to evaluate the probabilistic instability index of systems. In [9], the concept of angle radius is developed to introduce projection energy function, which in turn allows for the assessment of critical clearing time and generation limit of system.

This paper addresses the real-time stability assessment of a power system during energy generation as a smart grid initiative toward achieving better energy stability and security, efficiency and emergency resilience in the presence of generator maintenance scheduling (generator outages reflecting *N-1*, *N-2*, ..., *N-k* contingencies), load shedding (load outage), three-phase short circuit fault on the tie-line (major system perturbation) and permanent transmission line outage (*N-1* contingency and topology change). In the smart grid sense, the case studies of generation outages can also viewed as generation additions when going from *N-2* generation sources to *N-1* generation sources.

The main contributions of this paper can be summarized as:

- Formulation of a power system stability index, also known as the network status, based on real-time and non-RT analysis of the system parameters and operating condition.

- Implementation of the network status index in real-time.
- Illustration of the usefulness of network status index on a practical Nigerian power system implemented on a real-time digital simulator. Case studies presented include *N-k* generator outages resulting from generator maintenance scheduling, and *N-1* permanent transmission line outage (topology change).

II. POWER SYSTEM STABILITY ASSESSMENT

The following subsections describe the non real-time (NRT) and RT stability assessment indexes (SAIs) used in the development of a network stability index for a power system.

A. NRT-SAI

A methodology to be added to the power system dispatch problem in order to evaluate and improve voltage stability margin by optimizing generators and synchronous condensers reactive power injection is presented in [10]. Contingency screening and ranking method for voltage stability assessment is discussed and presented in [11], wherein the method is capable of selecting contingencies that lead to voltage insecurities. A new Hilbert-Huang based approach for on-line modal identification from power system measurements compared with the Prony analysis has been presented in [12].

The NRT-SAI presented in this paper comprises of the Prony and transient energy function (TEF) methods for investigating and carrying out quasi-RT stability assessment (SA) of a power system modeled on the real-time digital simulator (RTDS) platform.

1. Prony Analysis

Prony analysis is a technique of analyzing a signal obtained from power system simulation programs for the purpose of extracting (determining) the modal content in that signal. The content may include mode, damping, phase and magnitude information contained in the signal [13]. In this paper, eigenvalue indexes (*EVIs*) presented in Section III are used in the composition of NRT-SAI and are based on normalized damping ratios that lie in the range [0, 1]. These damping ratios derived from the Prony analysis are used because they explicitly relate to the dynamic behavior of the system and are useful for investigating and determining how the system damping affects its stability and hence network status, in addition to the transient energy of the system.

2. Transient Energy Function

The primary purpose for the application of the TEF method is for the analysis of power system stability. Initially the system is operating at a stable equilibrium point. If a fault occurs, the equilibrium is disturbed and the synchronous machines accelerate. To avoid instability, the system must be capable of absorbing the kinetic energy at a time when the forces on the generators tend to bring them toward new equilibrium positions [14]. With the operation of power systems closer to limits, SA of the power system is becoming increasingly important. An inherent advantage of the TEF method is the availability of the degree of stability (or instability) in terms of the transient energy margin in (1) [14]. Transient energy indexes (*TEIs*) presented in Section III are used in the composition of NRT-SAI and are obtained after normalizing the total transient energies derived from the TEF analysis, to lie in the range [0, 1].

$$TE_G = \sum_{t_s}^{t_f} 0.5 \cdot H_G \cdot \Delta\omega_G^2 \tag{1}$$

where G is the generator; H_G is the inertia constant of generator G; and $\Delta\omega_G$ is the speed deviation of generator G.

B. RT-SAI

The RT-SAIs presented in this paper encompasses six useful indexes for real-time assessment of power system undergoing scheduled shutdown generator maintenance, while subjected to credible contingencies. The RT-SAIs quantifies the magnitude or degree in which power system parameters are affected by each credible contingency on a given operating state. They will also reflect the effect that each individual credible contingency causes to parameters of the system, and in addition will indicate the distance to the security limit taking into consideration the specific criterion of evaluation that may be defined [1], [2], [15]. In this paper, credible contingencies are simulated in real-time and the dynamic states of the power system captured immediately following each contingency, while the stability assessment indexes are evaluated in real-time. Each contingency can be screened to be either secure or insecure.

The criterion to define the RT-SAIs is based on two important aspects related to the post-disturbance transition: i) an unacceptable performance is related to large variations of system parameters, particularly voltage and frequency and ii) the resultant post-disturbance system trajectory will converge to an acceptable steady-state condition. The RT-SAIs given by (2) - (7) are implemented on the RTDS platform for the purpose of carrying out RT-SA. These RT-SAIs are combined in Section III into a new index, called a real-time stability assessment index (*RTSAI*), which satisfies the definition and classification of power system stability presented in [1], [2].

1. Angle index (AI)

Generators usually have protection to avoid asynchronous operation. The maximum slip of the load angle offers a suitable security margin since, in case this is not exceeded, the generator may regain its synchronism. The *AI* is defined by (2) [1], [2], [15].

$$AI = \min\left\{1, \quad \max_{i=1 \ldots NG}\left(\frac{\delta_{c,i,\max}}{\delta_{c,\max,adm}}\right)\right\} \tag{2}$$

where $\delta_{c,i,max}$ is the maximum deviation of the load angle of *i*th generator during the simulation time, $\delta_{c,max,adm}$ is the maximum admissible load angle given by the protection relay, and *NG* is the number of generators operating in the system.

2. Maximum frequency deviation index (MFDI)

The maximum frequency deviation from its nominal value is an indication of dynamic effect produced by the contingency analyzed on the system. The higher the maximum frequency deviation, the bigger the disturbing effect produced by the contingency and vice versa. The *MFDI* is defined by (3) [1], [2], [15].

$$MFDI = \min\left\{1, \quad \max_{i=1...NG}\left[\frac{|\Delta f_{i,\max}|}{\Delta f_{i,\max,adm}}\right]\right\} \tag{3}$$

where NG is the number of generators operating on the system, $\Delta f_{i,\max}$ is the maximum frequency deviation and $\Delta f_{i,\max,adm}$ is the maximum admissible frequency deviation.

3. Dynamic voltage index (DVI)

An important requirement that must be satisfied for voltage transients is that at no point in the power system except during application of the fault in the case of short circuit analysis should the voltage level remain below certain limit [3]. The *DVI* is defined by (4) [2], [15].

$$DVI = \min\left\{1, \quad \max_{i=1...N}\left[\frac{|V_n - v_{i,\min}|}{V_n - v_{i,\min,adm}}\right]\right\} \tag{4}$$

where $v_{i,min}$ is the minimum instantaneous voltage on *i*th node during the transient, $v_{i,min,adm}$ is the minimum admissible voltage value (0.7pu used in [20]), N is the number of nodes of the system and V_n is the rated voltage.

4. Quasi-stationary voltage index (QSVI)

This index takes into account the recovery and control of the node voltage at the end of the transient period following the contingency. The *QSVI* is defined by (5) [2], [15].

$$QSVI = \min\left\{1, \quad \max_{i=1...N}\left[\frac{|\Delta v_{i,aft}|}{|\Delta v_{i,\lim}|}\right]\right\} \tag{5}$$

where $\Delta v_{i,\lim}$ is a percentage of the rated voltage (3%V_n for 500kv nodes and 5%V_n for 220kv nodes), $\Delta v_{i,aft}$ is the post-contingency voltage deviation on the *i*th node at the end of the transient period and $\Delta v_{i,\lim}$ is the maximum voltage deviation limit.

5. Power flow index (PFI)

Transmission lines (*TLs*) power flow after contingency should not exceed the maximum admissible value since an excess of power flow through the *TLs* in the post-contingency steady-state may activate lines protections, thus impairing the system security. The *PFI* is defined by (6) [2], [15].

$$PFI = \begin{cases} \dfrac{1}{NL}\sum_{i=1}^{NL} w_i \left(\dfrac{P_{i,aft}}{P_{i,\lim}}\right)^n & if\ P_{i,aft} < P_{i,\lim} \\ 1 & if\ P_{i,aft} \geq P_{i,\lim} \end{cases} \tag{6}$$

where $P_{i,aft}$ is the power flow through the *i*th line at the end of the transient period following the contingency, $P_{i,lim}$ is the power flow limit taking into account the strictest restriction (thermal, voltage, or stability limits), n is the norm (used to reduce the contribution to the *PFI* of *TLs* that have not reached their limits or to amplify the contribution of *TLs* that have exceeded their limits), w_i is a weight factor (which stands for the relative importance of the *TLs* in the system) and *NL* stands for the number of *TLs* in the power system.

6. Load shedding index (LSI)

When an unexpected generator outage occurs, or a generation area is lost due to an unexpected line outage, in order to compensate the unbalance between the generated power and the load demand, in some extreme cases it is necessary to disconnect load so that the system integrity may be kept. The *LSI* is defined by (7) [2], [15].

$$LSI = \frac{P_{shed}}{P_{total}} \tag{7}$$

where P_{shed} is the total disconnected load and P_{total} is the total demand of the system before the contingency.

III. NETWORK STABILITY INDEX COMPOSITION

In this section, the NRT-SAIs and RT-SAIs are composed to generate a single stability index for the power network. The combination of these stability indices shown in Fig. 1, adheres to the definition and classification of power system stability defined by the IEEE/CIGRE Joint Task Force on Stability Terms and Definitions [2].

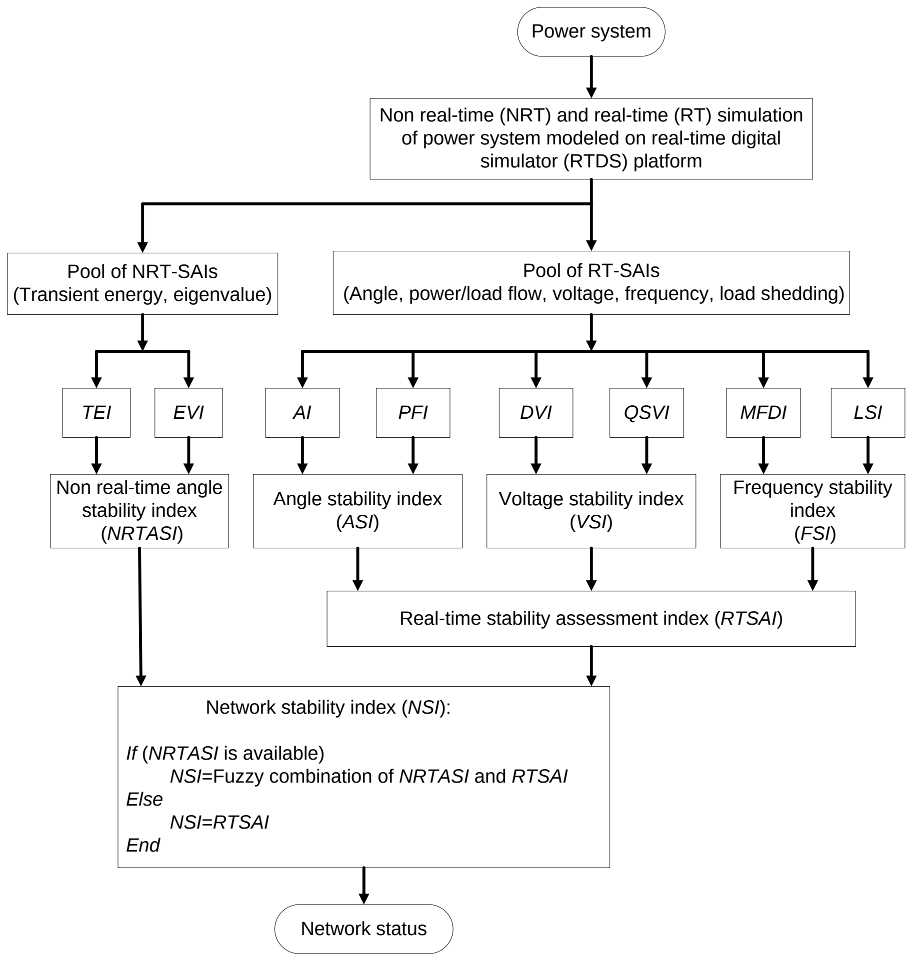

Fig. 1. Cascading Stages for Obtaining Network Status (Network Stability Index)

Use of fuzzy inference system is adopted in this paper to provide mathematical framework for modeling the uncertainty associated with models of power system parameters used and for inferring information from a given set of numerical NRT-SAIs and RT-SAIs. Fig. 1 shows cascading stages of fuzzy inference system applied to capture the different effects of the power system parameters, in order to reflect the impact that each credible contingency have on the system parameters and indicates the distance to security/stability limit taking into consideration the specific criterion of evaluation for each assessment indices. It also presents the overall network status that could easily be used by power system operators.

A. Non Real-Time Angle Stability Index (NRTASI)

The effect of the considered contingency on the angle stability in NRT scenario is represented through the non real-time angle stability index (*NRTASI*), which is generated from the composition of the transient energy index (*TEI*) and eigenvalue index (*EVI*). The universe of the input and output variables has been partitioned into three linguistic values of LOW, MEDIUM and HIGH. Each variable is equally distributed along the interval [0, 1]. Triangular fuzzy sets are used for modeling each linguistic value for simplicity [16]. Fig. 2 shows the term set and membership functions for the inputs and for the output. The rule base for the *TEI*, *EVI* and *NRTASI* are shown in Table I. Each rule has two fuzzy inputs (*TEI* and *EVI*) and one fuzzy output (*NRTASI*). The closer the normalized *TEI* or *EVI* is to one, the greater its influence on the *NRTASI*. Conversely, the closer the normalized *TEI* or *EVI* is to zero, the smaller its influence on the *NRTASI*.

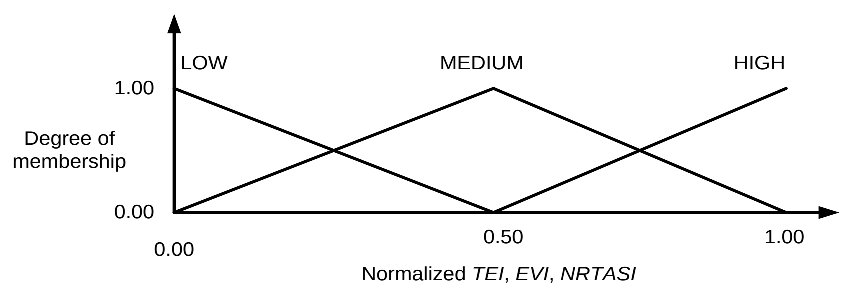

Fig. 2. Fuzzy Sets Characterizing *TEI*, *EVI* and *NRTASI*

TABLE I

Rule Base of *TEI*, *EVI* and *NRTASI*

Rule No.	Fuzzy Inputs		Fuzzy output
	TEI	*EVI*	*NRTASI*
1	LOW	LOW	LOW
2	LOW	MEDIUM	MEDIUM
3	LOW	HIGH	HIGH
4	MEDIUM	LOW	MEDIUM
5	MEDIUM	MEDIUM	MEDIUM
6	MEDIUM	HIGH	HIGH
7	HIGH	LOW	HIGH
8	HIGH	MEDIUM	HIGH
9	HIGH	HIGH	HIGH

B. Angle Stability Index (ASI)

The effect of the considered contingency on the angle index (*AI*) and power flow index (*PFI*) is represented through the angle stability index (*ASI*), which is generated from the fuzzy composition of the *AI* and *PFI*. The fuzzy composition and rule base for *ASI* are similar to the one for the *NRTASI*, explained above.

C. Voltage Stability Index (VSI)

The effect of the considered contingency on the system voltage is represented through the voltage stability index (*VSI*), which is generated from the fuzzy composition of the dynamic voltage index (*DVI*) and quasi-stationary voltage index (*QSVI*). The fuzzy composition and rule base for *VSI* are similar to the one for the *NRTASI*, explained above.

D. Frequency Stability Index (FSI)

The effect of the considered contingency on the maximum frequency deviation index (*MFDI*) and load shedding index (*LSI*) is represented through the frequency stability index (*FSI*), which is generated from the fuzzy composition of the *MFDI* and *LSI*. The fuzzy composition and rule base for *FSI* are similar to the one for the *NRTASI*, explained above.

E. Real-Time Stability Index (RTSI)

The effects of the angle stability index (*ASI*), voltage stability index (*VSI*) and frequency stability index (*FSI*) are combined to generate the *RTSAI*. The universe of the fuzzy input and output variables has been partitioned into three linguistic values of LOW, MEDIUM and HIGH. Each variable is equally distributed along the interval [0, 1]. The form of the fuzzy set characterizing *ASI*, *VSI*, *FSI* and *RTSI* are similar to the ones presented in Fig. 2. The rule base for the *ASI*, *VSI*, *FSI* and *RTSAI* are shown in Table II.

TABLE II

Rule Base of *ASI*, *VSI*, *FSI* and *RTSAI*

Rule No.	Fuzzy Inputs			Fuzzy output
	ASI	*VSI*	*FSI*	*RTSAI*
1	LOW	LOW	LOW	LOW
2	LOW	LOW	MEDIUM	MEDIUM
3	LOW	LOW	HIGH	HIGH
4	LOW	MEDIUM	LOW	MEDIUM
5	LOW	MEDIUM	MEDIUM	MEDIUM
6	LOW	MEDIUM	HIGH	HIGH
7	LOW	HIGH	LOW	HIGH
8	LOW	HIGH	MEDIUM	HIGH
9	LOW	HIGH	HIGH	HIGH
10	MEDIUM	LOW	LOW	MEDIUM
11	MEDIUM	LOW	MEDIUM	MEDIUM
12	MEDIUM	LOW	HIGH	HIGH
13	MEDIUM	MEDIUM	LOW	MEDIUM
14	MEDIUM	MEDIUM	MEDIUM	MEDIUM
15	MEDIUM	MEDIUM	HIGH	HIGH
16	MEDIUM	HIGH	LOW	HIGH
17	MEDIUM	HIGH	MEDIUM	HIGH
18	MEDIUM	HIGH	HIGH	HIGH
19	HIGH	LOW	LOW	HIGH
20	HIGH	LOW	MEDIUM	HIGH
21	HIGH	LOW	HIGH	HIGH
22	HIGH	MEDIUM	LOW	HIGH
23	HIGH	MEDIUM	MEDIUM	HIGH
24	HIGH	MEDIUM	HIGH	HIGH
25	HIGH	HIGH	LOW	HIGH
26	HIGH	HIGH	MEDIUM	HIGH
27	HIGH	HIGH	HIGH	HIGH

F. Network Stability Index (NSI)

The effects of the non real-time angle stability index (*NRTASI*) and *RTSAI* are composed together to obtain the network stability index (*NSI*). If the non real-time data (that is *NRTASI*) is not available or the system can significantly changed, the *NSI* takes only the assessment from real-time simulation (that is *RTSAI*) until NRTASI is computed and available for use. The universe of the fuzzy input variables has been partitioned into three linguistic values similar to the ones shown in Fig. 2, while the fuzzy output variable has been partitioned into five linguistic values of LOW, MEDIUM-LOW, MEDIUM, MEDIUM-HIGH and HIGH. Each variable is equally distributed along the interval [0, 1].

Fig. 3 shows the fuzzy set characterizing the *NSI*. The rule base for the *NRTASI*, *RTSI* and *NSI* are shown in Table III.

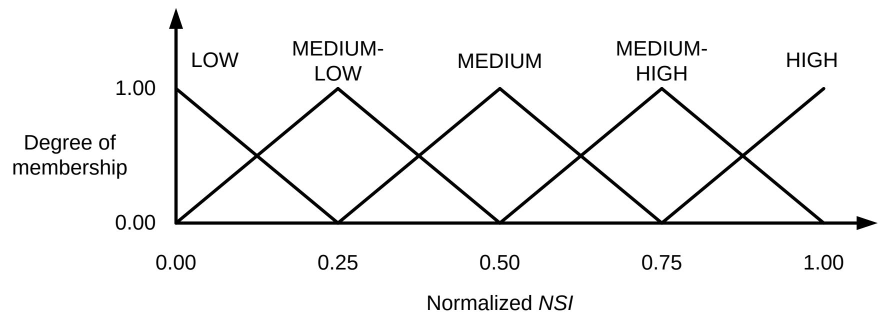

Fig. 3. Fuzzy Sets Characterizing *NSI*

TABLE III

Rule Base of *NRTASI*, *RTSAI* and *NSI*

Rule No.	Fuzzy Inputs		Fuzzy output
	NRTASI	*RTSAI*	*NSI*
1	LOW	LOW	LOW
2	LOW	MEDIUM	MEDIUM-LOW
3	LOW	HIGH	MEDIUM
4	MEDIUM	LOW	MEDIUM-LOW
5	MEDIUM	MEDIUM	MEDIUM
6	MEDIUM	HIGH	MEDIUM-HIGH
7	HIGH	LOW	MEDIUM
8	HIGH	MEDIUM	MEDIUM-HIGH
9	HIGH	HIGH	HIGH

IV. CASE STUDY: GMS OF THE NIGERIAN POWER SYSTEM

The aim of generator maintenance scheduling is to determine the optimized timing and duration for scheduled planned maintenance overhauls for generating units while maintaining high system reliability, reducing production cost, prolonging generator life time subject to some unit and system constraints [11]. In this section, GMS is carried out on a practical Nigerian power system and the *NSI* is implemented to evaluate the system status during the weeks of maintenance and disturbance.

A. The Nigerian Power System

The Nigerian 330-KV, 25-bus grid power system presented in Fig. 4 is modeled on five Racks of the real-time digital simulator (RTDS) [17]. It consists of 49 units positioned in 7 generating plants (AFAM, DELTA, EGBIN, SAPELE, JEBBA, KAINJI and SHIRORO plants) located in 2 distinct areas as shown in Fig. 4. The generating units' data with a total generation of 3718.50MW (excluding spinning reserve) and total load demand of 3627.00MW are presented in [18]. A 9% spinning reserve is used to improve the system reliability during implementation of the scheduled generator maintenance. Table IV shows the load buses with their connected load demand (MW). AFAM, DELTA and 8 units of EGBIN thermal plants are gas fired, while SAPELE and 6 units of EGBIN thermal plants are steam driven. JEBBA, KAINJI and SHIRORO hydro plants are water driven [18].

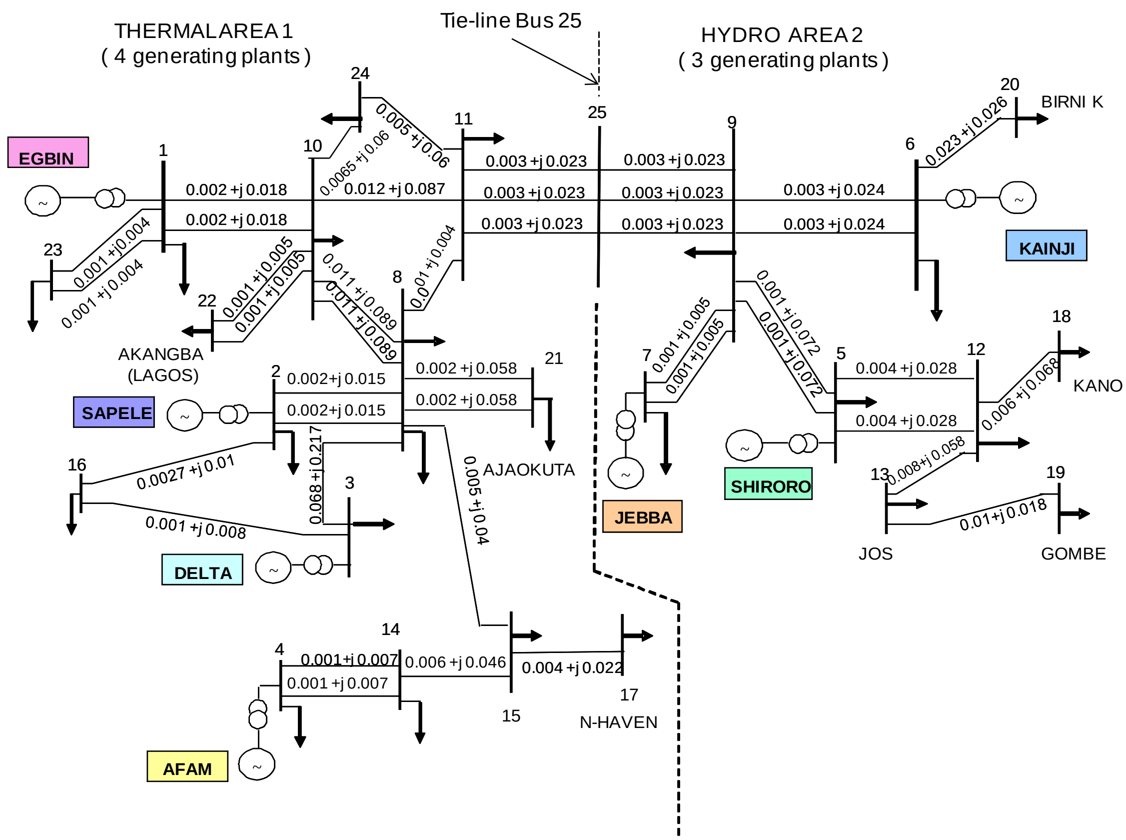

Fig. 4. Nigerian Hydrothermal 330-KV, 25-Bus Grid System

TABLE IV

Load Buses With Connected Load Demand (MW)

Bus number	1	2	3	4	5	6	7	8	9	10	11	12	13	14	15	16	17	18	19	20	21	22	23	24	25	Total supplied load (MW)
Load supplied (MW)	147.00	-	95.00	156.00	63.00	-	-	198.00	12.00	585.00	294.00	224.00	72.00	199.00	131.00	106.00	135.00	204.00	106.00	120.00	31.00	337.00	246.00	166.00	-	3627.00

B. NRT-SA of Nigerian Power System

All numerical results are obtained based on 50μs real-time simulation carried out on the RTDS platform, in conjunction with Prony and TEF programs developed using matlab environment and ran on PC with 2.2GHz CPU speed and 3.0GB of RAM.

Table V shows five cases with different maintenance schedules drawn from the optimal solutions presented in [18]. Cases I to V are feasible generator maintenance implementation scenarios selected from [18] to investigate and carry out the SA of the Nigerian power system. The five cases are arranged in increasing order of generation loss due to GMS tasks carried out on maintenance weeks 6, 47, 4 and 2 corresponding to (*N-3*), (*N-4*), (*N-6*) and (*N-5*) contingencies respectively. The Table also presents the loads that must be shedded in the course of maintenance tasks to ensure reliable system operation through reasonable generation and demand power balance. A 9% spinning reserve is used to improve the system reliability as shown in Table V.

In this paper, three-phase short circuit fault considered as a severe credible contingency is applied at the tie-line Bus 25 of Fig. 4. The fault is clear after 200ms.

Two case studies are presented below namely: with PSS and no SVC, and with PSS and SVC.

1. Case study 1: system with PSS and no SVC

Studies have shown that the Nigerian system is potentially unstable when experiencing major system perturbations according to the results presented in [19], there is therefore the need for two PSSs to be located in both Areas 1 and 2 for purpose of implementing Cases I to V in order to effectively damp out the inter-area and local mode oscillations of the system under consideration without compromising the stability of other modes in the system.

TABLE V

Five Cases Considering Scheduled Maintenance, Generation Loss and Shedded Load for the 49-Unit Nigerian Power System

		Cases	Maintenance week	Units scheduled for maintenance	Generation loss due to scheduled maintenance (MW)	Load shedded		Total available generation including 9% spinning reserve (MW)	Supplied load demand (MW)
						Bus number	Toatal load loss (MW)		
Without maintenance		I	-	-	0.00	-	-	4044.93	3627.00
With maintenance	No load shedding	II	Week 6	6,7,18 (*N-3*)	220.00	-	-	3824.93	3627.00
		III	Week 47	40,44,46,49 (*N-4*)	327.00	-	-	3717.93	3627.00
	With load shedding	IV	Week 4	2,3,10,14,15,17 (*N-6*)	440.00	8,23	117.00	3604.93	3510.00
		V	Week 2	2,3,8,15,17 (*N-5*)	600.00	10,21	289.00	3444.93	3338.00

PSSs were tuned using the procedure described in [19]. The PSS parameters for Egbin (thermal Area 1) and Shiroro (hydro Area 2) plants are K_{STAB}=25.830, T_1=0.380s, T_2=0.990s, T_3=0.35s and T_4=0.005s, and K_{STAB}=28.210, T_1=0.690s, T_2=0.770s, T_3=0.230s and T_4=0.005s respectively. The stabilizer outputs are limited between -0.05 and 0.2 to ensure the maximum contribution of the stabilizer. TE and modal analysis are used for screening generators on which to add PSS in Areas 1 and 2. The influence of simultaneous location of PSS each in Areas 1 and 2, their effects on the local and inter-area modes, as well as on the overall TE of the system are summarized in Table VI under Case I scenario.

The main observations from Table 11 are given below. PSS each located at Egbin and Shiroro plants results in:

- Improved damping of the local modes in Areas 1 and 2 (frequency and damping ratio in Areas 1 and 2 are 1.644Hz and 0.164, and 1.630Hz and 0.126 respectively).
- Improved damping of the inter-area mode (frequency and damping ratio of 0.406Hz and 0.252 respectively).
- Enhanced overall TE of the system of 32.67KJ (indicates a 14.86% reduction in TE of the system).

TABLE VI

Effect of PSS at Various Locations on Transient Energies, Eigenvalues, Frequencies and Damping Ratios for the Nigerian Power System under Case I Scenario

PSS location	Area 1 Local mode	Area 2 Local mode	Inter-area mode	Transient energy (TE)		
	Eigenvalue (frequency-Hz, damping ratio)	Eigenvalue (frequency-Hz, damping ratio)	Eigenvalue (frequency-Hz, damping ratio)	Unit	Units' TE (KJ)	Total system TE (KJ)
No PSS	-0.5798 ±9.9480i (1.586, 0.058)	-0.9214±10.0373i (1.604, 0.090)	-0.5181 ± 2.4728i (0.402, 0.205)	Afam Delta Egbin Sapele Jebba Kainji Shiroro	10.79 5.66 4.95 6.13 2.89 3.18 4.77	38.37
Area 1: Afam Area 2: Jebba	-0.8223 ± 10.2304i (1.634, 0.080)	-1.1569± 10.9950i (1.759, 0.105)	-0.5570 ± 2.3745i (0.388, 0.228)	Afam Delta Egbin Sapele Jebba Kainji Shiroro	10.40 5.21 4.86 5.70 3.53 2.72 4.15	36.57
Area 1: Afam Area 2: Kainji	-1.5830 ±9.9513i (1.604, 0.157)	-1.2541 ± 10.2156i (1.638, 0.122)	-0.5036 ±2.3871i (0.388, 0.206)	Afam Delta Egbin Sapele Jebba Kainji Shiroro	9.21 5.28 4.61 5.67 2.62 2.95 4.42	34.76
Area 1: Afam Area 2: Shiroro	-1.4695 ± 9.9621i (1.603, 0.146)	-1.2754 ± 10.2143i (1.638, 0.124)	-0.5046 ±2.3916i (0.389, 0.207)	Afam Delta Egbin Sapele Jebba Kainji Shiroro	9.05 5.22 4.56 5.63 2.59 2.90 4.37	34.32
Area 1: Delta Area 2: Jebba	-0.6571± 10.2710i (1.638, 0.064)	-0.9392 ± 10.2198i (1.633, 0.092)	-0.5468 ± 2.4342i (0.397, 0.219)	Afam Delta Egbin Sapele Jebba Kainji Shiroro	10.10 5.20 4.62 5.70 2.55 2.97 4.45	35.59
Area 1: Delta Area 2: Kainji	-0.9403 ± 10.2251i (1.634, 0.092)	-1.2276 ± 10.2952i (1.650, 0.118)	-0.4904± 2.1911i (0.357, 0.218)	Afam Delta Egbin Sapele Jebba Kainji Shiroro	10.80 5.10 4.86 6.09 2.78 3.18 4.68	37.49
Area 1: Delta Area 2: Shiroro	-0.5987± 10.0262i (1.599, 0.060)	-1.1522± 10.0636i (1.612, 0.114)	-0.4879 ± 2.2213i (0.362,0.214)	Afam Delta Egbin Sapele Jebba Kainji Shiroro	10.40 5.08 4.74 6.12 2.78 3.13 3.66	35.91
Area 1: Egbin Area 2: Jebba	-1.4198± 10.0320i (1.613, 0.140)	-0.9765± 10.2367i (1.637, 0.095)	-0.5697 ± 2.4674i (0.403, 0.225)	Afam Delta Egbin Sapele Jebba Kainji Shiroro	9.89 5.16 4.20 5.58 2.50 2.92 4.40	34.65
Area 1: Egbin Area 2: Kainji	-1.2078 ±10.0613i (1.613, 0.119)	-1.2651± 10.1963i (1.635, 0.123)	-0.4934 ± 2.2394i (0.365, 0.215)	Afam Delta Egbin Sapele Jebba Kainji Shiroro	9.80 5.00 3.28 5.46 2.50 2.89 4.38	33.31
Area 1: Egbin Area 2: Shiroro	-1.6969± 10.1919i (1.644, 0.164)	-1.2944± 10.1581i (1.630, 0.126)	-0.6426 ± 2.4658i (0.406, 0.252)	Afam Delta Egbin Sapele Jebba Kainji Shiroro	8.64 5.02 4.02 5.42 2.50 2.80 4.27	32.67
Area 1: Sapele Area 2: Jebba	-1.4404 ± 10.2477i (1.647, 0.139)	-0.9176± 10.2260i (1.634, 0.090)	-0.5417 ± 2.4336i (0.397, 0.217)	Afam Delta Egbin Sapele Jebba Kainji Shiroro	9.66 5.29 5.03 4.36 2.57 2.96 4.41	34.28
Area 1: Sapele Area 2: Kainji	-1.0572 ± 10.1434i (1.623, 0.104)	-1.2418 ± 10.2036i (1.636, 0.121)	-0.4910± 2.1985i (0.359, 0.218)	Afam Delta Egbin Sapele Jebba Kainji Shiroro	10.30 5.67 4.80 4.69 2.79 3.13 4.66	36.04
Area 1: Sapele Area 2: Shiroro	-1.0483 ± 10.0869i (1.614, 0.103)	-1.2393±10.2313i (1.640, 0.120)	-0.4743± 2.1880i (0.356, 0.212)	Afam Delta Egbin Sapele Jebba Kainji Shiroro	10.10 5.50 4.66 4.52 2.71 3.05 4.62	35.16

Further, the TE for Cases I to V with and without PSS are presented in Table 12. Table 13 also shows the percent reductions in total system TE for Cases I to V after stability enhancement with PSS located each at Egbin and Shiroro plants. A maximum of 66.58% in total system TE reduction is obtained for Case V compared with a minimum of 14.86% for Case I.

TABLE VII

Effect of PSS each at Egbin and Shiroro on Transient Energy Reductions for Cases I to V

Generating unit	Case I		Case II		Case III		Case IV		Case V	
	Transient energy (KJ)		Transient energy (KJ)		Transient energy (KJ)		Transient energy (KJ)		Transient energy (KJ)	
	No PSS	With PSS	No PSS	With PSS	No PSS	With PSS	No PSS	With PSS	No PSS	With PSS
Jebba (G21 - G26)	2.89	2.50	4.36	3.44	6.24	4.81	3.59	2.62	14.83	4.00
Kainji (G27 - G34)	3.18	2.80	4.69	3.82	6.54	5.17	3.91	2.73	15.05	4.39
Shiroro (G35 - G38)	4.77	4.27	6.46	5.49	8.15	6.70	5.49	4.91	16.18	5.92
Sapele (G15 - G20)	6.13	5.42	9.40	7.67	14.05	11.11	7.72	5.87	16.48	8.77
Egbin (G1 - G14)	4.95	4.02	8.46	6.48	12.65	9.34	7.35	6.14	29.06	8.28
Delta (G41 - G49)	5.66	5.02	8.92	7.26	12.74	10.13	7.40	6.22	29.97	8.57
Afam (G39 - G40)	10.79	8.64	14.97	12.89	25.75	21.97	12.39	10.21	43.37	15.19
Total TE (KJ)	38.37	32.67	57.26	47.05	86.13	69.23	47.86	38.70	164.94	55.12
Percent reduction in TE using PSS (%)	14.86		17.83		19.62		19.14		66.58	

Table VIII on the other hand, shows the modal analysis with and without the PSS. The table presents the effect of PSS on the system eigenvalues, frequencies and damping ratios for Cases I to V. With PSS located each at Egbin and Shiroro plants, it is seen from Table VIII that the system damping is improved for Cases I to V compared with the scenario without the PSS. The inter-area and local mode frequencies of Table VIII for Cases I to V shows that the stability of other modes in the system is not compromised. A number of time domain simulations were performed to confirm the results of the TE and modal analysis with and without PSS.

TABLE VIII

Effect of PSS each at Egbin and Shiroro on Eigenvalue, Frequency and Damping Ratio for Cases I to V

Generating unit	Mode	3-Phase short circuit fault applied for 200ms at Tie-line Bus 25									
		No maintenance		With scheduled shutdown generator maintenance							
		Case I		Case II		Case III		Case IV		Case V	
		Eigenvalue (frequency-Hz, damping ratio)		Eigenvalue (frequency-Hz, damping ratio)		Eigenvalue (frequency-Hz, damping ratio)		Eigenvalue (frequency-Hz, damping ratio)		Eigenvalue (frequency-Hz, damping ratio)	
		No PSS	With PSS	No PSS	With PSS	No PSS	With PSS	No PSS	With PSS	No PSS	With PSS
	Inter-area	-0.5181 ± 2.4728i (0.402, 0.205)	-0.6426 ± 2.4658i (0.406, 0.252)	-0.4790 ±2.4646i (0.400, 0.191)	-0.6134 ±2.4483i (0.402, 0.243)	-0.5348 ± 2.3606i (0.385, 0.221)	-0.6036± 2.2159i (0.366, 0.263)	-0.5467 ±2.5373i (0.413, 0.211)	-0.6087 ±2.3979i (0.394, 0.246)	-0.5927 ±2.6258i (0.428, 0.220)	-0.5487 ±2.3034i (0.377, 0.232)
Thermal area 1 (G1 - G20, G39 - G40)	Intra-area	-1.1815 ± 9.9312i (1.592, 0.118)	-1.6969 ± 10.1919i (1.644, 0.164)	-1.0939 ±10.2049i (1.634, 0.107)	-1.3429 ±9.6606i (1.552, 0.138)	-0.5579 ± 9.7682i (1.557, 0.057)	-1.3290 ± 9.6817i (1.555, 0.136)	-0.5893 ±10.1317i (1.615, 0.058)	-1.1777 ±10.9545i (1.753, 0.107)	-0.6132 ±10.6069i (1.691, 0.058)	-1.3758 ±10.2388i (1.644, 0.133)
Hydro area 2 (G21 - G38)	Intra-area	-0.9118 ±10.0197i (1.601, 0.091)	-1.2944±10.1581i (1.630, 0.126)	-1.0234 ± 8.1119i (1.301, 0.125)	-1.1421± 8.1704i (1.313, 0.138)	-0.6983 ± 9.6206i (1.535, 0.072)	-1.1820 ± 9.9735i (1.598, 0.118)	-0.9695 ± 8.3763i (1.342, 0.115)	-1.1601± 8.3917i (1.348, 0.137)	-0.8003 ± 10.0458i (1.604, 0.079)	-1.3584 ± 10.2497i (1.645, 0.131)

A permanent transmission line outage (*N-1* contingency) is applied between buses 8 and 11 in Fig. 4, in addition to the (*N*-*5*) generation loss contingency of Case V which results in (*N*-*6*) credible contingencies simulated on the system. The permanent transmission line outage is a major system perturbation where the transmission line between buses 8 and 11 is permanently removed. Again, the speed deviations of Afam and hydro plants been the worst affected plants in Areas 1 and 2 respectively following this type of major system upset are shown in Fig. 5 with and without the PSS. Without the PSS, the system instability grows leading to loss of synchronism and eventual system collapse compared with the case having PSS installed each at Egbin and Shiroro plants. Similar analysis can be carried out for (*N*-*7*), (*N*-*8*)… contingencies to investigate the effect of PSS in stabilizing a system subjected to multiple topology changes.

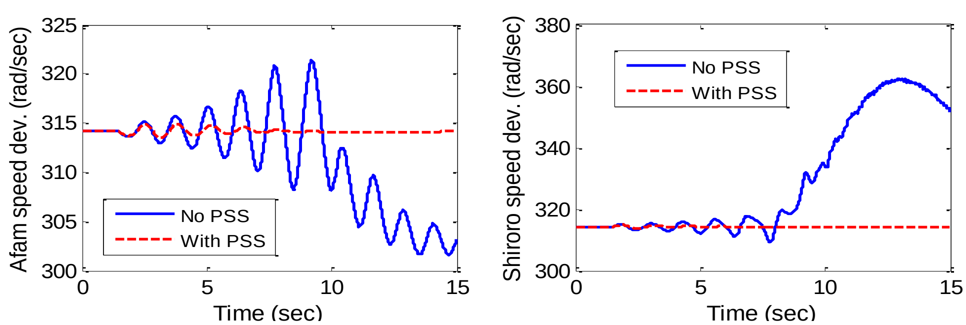

Fig. 5. Afam and Shiroro Speed Deviations for Topology Change

2. Case study 2: system with PSS and SVC

It is a known fact that the steady-state transmittable power can be increased and the voltage profile along the line controlled by appropriate reactive shunt compensation [1], [20]. It is obvious that for a radial line, the end of the line, where the largest voltage variation occurs is the best location for the reactive compensator [1], [20]. In order to investigate the impact on the power system to SVC placement, bus voltage profiles were obtained after simulating maintenance Cases II to V as shown in Table IX. For all the cases considered, Bus 18 exhibits the largest voltage variations of 0.0997 pu, 0.0996 pu, 0.0995 pu and 0.0993 pu for Cases II, III, IV and V respectively. To further investigate, the SVC is alternately sited at two different system buses that exhibit the largest voltage deviation from nominal value; namely, Buses 18 (with voltage deviation > 0.05 pu) and 19 (with voltage deviation approximately 0.05 pu) in Area 2 of Fig. 4. Buses 18 and 19 are high-tension buses located at the end of transmission lines that feed loads of 204 MW and 106 MW respectively as shown in Table IV. Locating SVC at 18 and 19 is motivated by the fact that reactive support is considerably needed for voltage profile improvement drawing from the results in Table IX under no SVC scenario. The system voltage deviation metric is used to evaluate the voltage deviation of the entire power system. The system voltage deviation metrics obtained after alternately siting SVC of size 100MVar at Buses 18 and 19 under Case III maintenance scenario are presented in Table IX. Placing SVC at Bus 18 produced system voltage deviation metric of 0.0781 pu compared with SVC at Bus 19 which generated a higher system voltage deviation metric of 0.0805 pu.

Further analyses reveal that locating SVC at Bus 18 yields the minimal voltage deviation for all GMS cases presented in [18]. Bus 18 is therefore the best location for placing the SVC for the Nigerian grid system shown in Fig. 4 planned for yearly GMS.

TABLE IX

Effect of SVC at Various Locations on System Voltage Deviation Metric

Bus number	System bus voltages under maintenance scenario (pu)					
	Case II (No SVC)	Case III (No SVC)	Case IV (No SVC)	Case V (No SVC)	Case III (SVC at Bus 18)	Case III (SVC at Bus 19)
1	0.9912	0.9921	0.9923	0.9940	0.9926	0.9929
2	0.9992	0.9971	1.0050	1.0050	1.0010	1.0010
3	0.9976	0.9958	1.0010	1.0000	0.9987	0.9987
4	1.0060	0.9857	1.0070	1.0070	1.0070	1.0070
5	1.0200	1.0200	1.0210	1.0210	1.0330	1.0320
6	1.0210	1.0200	1.0210	1.0210	1.0220	1.0220
7	1.0060	1.0060	1.0070	1.0070	1.0070	1.0070
8	0.9986	0.9964	1.0060	1.0050	1.0010	1.0010
9	1.0080	1.0080	1.0090	1.0090	1.0100	1.0100
10	0.9704	0.9734	0.9717	0.9919	0.9751	0.9750
11	0.9981	0.9980	1.0030	1.0040	1.0010	1.0010
12	0.9851	0.9850	0.9854	0.9854	1.0180	1.0170
13	0.9620	0.9620	0.9623	0.9623	0.9939	1.0070
14	1.0020	0.9829	1.0040	1.0030	1.0030	1.0030
15	0.9889	0.9760	0.9932	0.9930	0.9902	0.9903
16	0.9960	0.9942	1.0010	1.0000	0.9980	0.9973
17	0.9754	0.9626	0.9796	0.9794	0.9766	0.9766
18	0.9003	0.9004	0.9005	0.9007	1.0000	0.9735
19	0.9502	0.9502	0.9505	0.9505	0.9825	1.0000
20	0.9888	0.9886	0.9894	0.9894	0.9906	0.9905
21	1.0170	1.0150	1.0240	1.0270	1.0200	1.0200
22	0.9590	0.9620	0.9603	0.9803	0.9659	0.9655
23	0.9883	0.9893	0.9924	0.9911	0.9900	0.9900
24	0.9724	0.9759	0.9746	0.9858	0.9770	0.9763
25	1.0050	1.0050	1.0080	1.0090	1.0070	1.0070
System voltage deviation metric (pu)	0.1407	0.1442	0.1396	0.1313	0.0781	0.0805

C. RT-SA of Nigerian Power System

Figure 6 shows the real-time plots of *AI*, *MFDI*, *DVI*, *QSVI*, *PFI* and *LSI* for Cases I to V. *AI* and *MFDI* are compared for scenarios with and without PSS, while *DVI*, *QSVI* and *PFI* are compared for scenarios with and without SVC installed in the system. The presented RT-SAIs in Fig. 6 are evaluated in real-time for a power system during energy generation shortfall (maintenance scheduling/generator outage), subjected to load shedding (load outage) and three-phase short circuit fault (severe disturbance) applied at the tie-line Bus 25 of Fig. 4. In order to compensate the imbalance between the generated power and the load demand in Cases IV and V, 117MW and 289MW loads are disconnected respectively resulting in *LSI* greater than zero as shown in Fig. 6.

Table X shows the RT-SAI matrix for the Nigerian power system obtained from real-time simulations on the RTDS platform. The states of the power system security are deduced from the real-time simulation results shown in Fig. 6 and the RT-SAIs definitions presented in Section II. It can be emphasized that the addition of PSS and SVC impacted positively in enhancing and improving stability, voltage profile and transmittable power, based on the RT-SAIs plots of Fig. 6 and the RT-SAI matrix shown in Table X.

TABLE X

NRT-SAI and RT-SAI Matrix of Nigerian Power System Incorporating PSS and SVC

		Cases	NRT-SAI				RT-SAI										
			Total TE (KJ)		*Eigenvalue*		*AI*		*MFDI*		*DVI*		*QSVI*		*PFI*		*LSI*
			No PSS	With PSS	No PSS	With PSS	No PSS	With PSS	No PSS	With PSS	No SVC	With SVC	No SVC	With SVC	No SVC	With SVC	
Without maint.		I	38.370	32.670	0.205	0.252	0.166	0.165	0.453	0.430	1.000	1.000	0.106	0.104	0.525	0.513	0.000
With maint.	No load shedding	II	57.260	47.050	0.191	0.243	0.179	0.178	0.455	0.447	1.000	1.000	0.119	0.116	0.533	0.514	0.000
		III	86.130	69.230	0.221	0.263	0.171	0.170	0.459	0.448	1.000	1.000	0.137	0.122	0.539	0.515	0.000
	With load shedding	IV	47.860	38.700	0.211	0.246	0.182	0.181	0.467	0.459	1.000	1.000	0.168	0.147	0.544	0.519	0.030
		V	164.940	55.120	0.220	0.232	0.209	0.208	0.469	0.465	1.000	1.000	0.196	0.165	0.549	0.524	0.080

In order to obtain numeric values from the fuzzy sets as a result of the fuzzy inferences presented in Section III, the fuzzy centroid method is used for defuzzification [16] and is not repeated here for reason of space limitation. However, Tables XI and XII show the results of defuzification for two scenarios, viz; No PSS and SVC, and another With PSS and SVC. The numeric values present the impacts of introducing PSS and SVC into the system to improve security and stability.

TABLE XI

Indices with No PSS and SVC for Cases I to V

			Fuzzy inputs (Normalized indices)								Fuzzy outputs						Network status: security/stability assessment
		Cases	*TEI*	*EVI*	*AI*	*PFI*	*DVI*	*QSVI*	*MFDI*	*LSI*	*NRTASI*	*ASI*	*VSI*	*FSI*	*RTSAI*	*NSI*	
Without maint.		I	0.233	0.932	0.794	0.956	1.000	0.541	0.966	0.000	0.537	0.619	0.517	0.501	0.441	0.499	1 (Least insecured/unstable)
With maint.	No load shedding	II	0.347	1.000	0.856	0.970	1.000	0.607	0.970	0.000	0.575	0.669	0.590	0.620	0.564	0.570	2
		III	0.522	0.864	0.818	0.981	1.000	0.699	0.979	0.000	0.586	0.721	0.679	0.698	0.692	0.642	3
	With load shedding	IV	0.290	0.905	0.871	0.990	1.000	0.857	0.995	0.375	0.598	0.767	0.752	0.876	0.784	0.713	4
		V	1.000	0.868	1.000	1.000	1.000	1.000	1.000	1.000	0.650	0.837	0.837	0.937	0.897	0.821	5 (Most insecured/unstable)

TABLE XII

Indices With PSS and SVC for Cases I to V

			Fuzzy inputs (Normalized indices)								Fuzzy outputs						Network status: security/stability assessment
		Cases	*TEI*	*EVI*	*AI*	*PFI*	*DVI*	*QSVI*	*MFDI*	*LSI*	*NRTASI*	*ASI*	*VSI*	*FSI*	*RTSAI*	*NSI*	
Without maint.		I	0.233	0.932	0.794	0.956	1.000	0.541	0.966	0.000	0.537	0.619	0.517	0.501	0.441	0.499	1 (Least insecured/unstable)
With maint.	No load shedding	II	0.347	1.000	0.856	0.970	1.000	0.607	0.970	0.000	0.575	0.669	0.590	0.620	0.564	0.570	2
		III	0.522	0.864	0.818	0.981	1.000	0.699	0.979	0.000	0.586	0.721	0.679	0.698	0.692	0.642	3
	With load shedding	IV	0.290	0.905	0.871	0.990	1.000	0.857	0.995	0.375	0.598	0.767	0.752	0.876	0.784	0.713	4
		V	1.000	0.868	1.000	1.000	1.000	1.000	1.000	1.000	0.650	0.837	0.837	0.937	0.897	0.821	5 (Most insecured/unstable)

In each of the five GMS cases considered in this paper, Case I is observed to be the least insecure/unstable compared with Cases II, III, IV or V. Case I has *NSIs* of 0.499 (with No PSS and SVC) and 0.386 (With PSS and SVC). Conversely, Case V is the most insecure/unstable case with *NSIs* of 0.821 (with No PSS and SVC) and 0.764 (With PSS and SVC). The order of security/stability ranking and hence the network status can easily be seen and drawn from Tables XI and XII.

V. CONCLUSION

In this paper, the non real-time (NRT) and real-time (RT) stability assessment (SA) of a power system are demonstrated on a real-time digital simulator (RTDS) platform. A practical Nigerian power system modeled on the RTDS platform is used as case study to implement and simulate in RT generator maintenance scheduling (GMS) which is a reflection of power generation loss due to scheduled shutdown maintenance (*N-1*, *N-2*, ..., *N-k* contingencies) while subjecting the system to load shedding (load outage), three-phase short circuit fault on the tie-line (major disturbance) and permanent transmission line outage (*N-1* contingency and topology change). Five GMS cases of the Nigerian power system have been illustrated for simplicity. Cascading stages of fuzzy inference system is used to compose the different effects of the NRT and RT power system parameters, in order to reflect the effect that each credible contingency have on the system parameters and indicates the distance to stability/security limit. The NRT and RT stability assessment indexes (SAIs) presented in this paper are demonstrated to be effective tools in assessing the overall stability of a power system under different and most probable practical operating conditions.

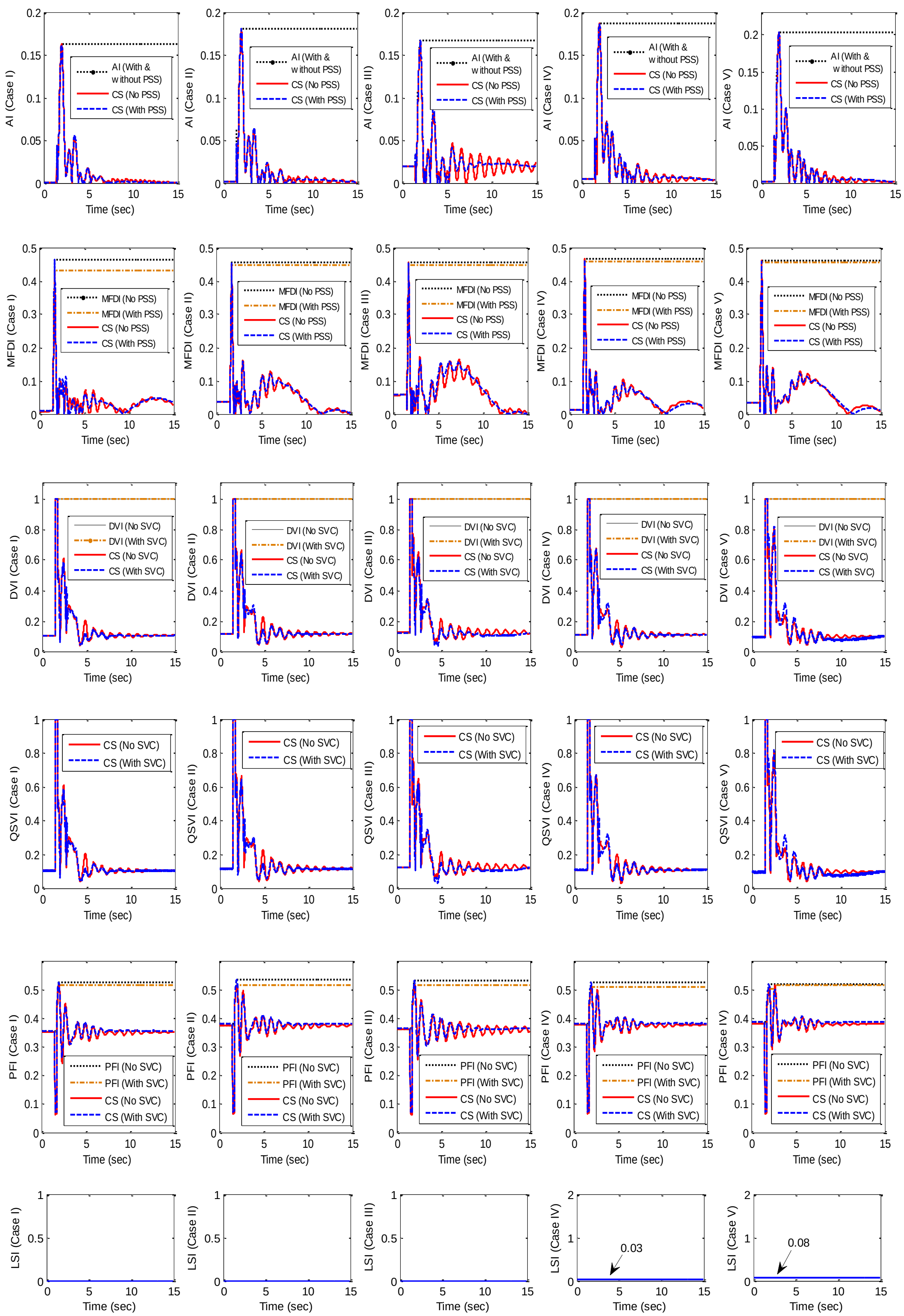

Fig. 6. Plots of Real-Time *AI*, *MFDI*, *DVI*, *QSVI*, *PFI*, and *PFI* for Cases I to V for the Nigerian Power System

They also show great potential for use as tools for energy management. This overall network status information can easily be used by power system operators and energy control centers. Many utilities are currently adding synchrophasor measurement capability to their systems. This capability can provide real-time information about the system current state and used to improve the accuracy of state estimation.

VI. ACKNOWLEDGMENT

This work was supported by the National Science Foundation, USA under Grant ECCS #0348221.

VII. REFERENCES

[1] P. Kundur, *Power System Stability and Control*. USA: The EPRI Power System Engineering Series, McGraw-Hill, Inc, 1994.

[2] P. Kundur *et al.,* "“Definition and classification of power system stability," IEEE/CIGRE joint task force on stability terms and definitions," *IEEE Trans. on Power Systems,* vol. 19, no. 3, pp. 1387-1401, August 2004.

[3] V. Brandwajn, A. B. R. Kumar, A. Ipakchi, A. Bose and S. D. Kuo, "Severity indices for contingency screening in dynamic security assessment," *IEEE Transactions on Power Systems*, vol. 2, no. 3, pp. 1136-1142, August 1997.

[4] Y. Mansour, E. Vaahedi and M. A. El-Sharkawi, "Dynamic security contingency screening and ranking using neural networks," *IEEE Transactions on Power Systems*, vol. 8, no. 4, pp. 942-950, July 1997.

[5] C. Fu and A. Bose, "Contingency ranking based on severity indices in dynamic security analysis," *IEEE Transactions on Power Systems*, vol. 14, no. 3, pp. 980-986, August 1999.

[6] X. Yu and C. Singh, "A practical approach for integrated power system vulnerability analysis with protection failures," *IEEE Transactions on Power Systems*, vol. 19, no. 4, pp. 1811-1820, November 2004.

[7] D. Chatterjee and A. Ghosh, "Transient stability assessment of power systems containing series and shunt compensators," *IEEE Transactions on Power Systems*, vol. 22, no. 3, pp. 1210-1220, August 2007.

[8] D. Z. Fang, L. Jing and T. S. Chung, "Corrected transient energy function-based strategy for stability probability assessment of power system," *IET Gener. Transm. Distrib*. vol. 2, no. 3, pp. 424-432, 2008.

[9] D. Z. Fang, J. G. Yang, W. Sun, Z. Y. Xue and S. Q. Yuan, "Transient stability assessment using projection formulations," *IET Gener. Transm. Distrib*. vol. 3, no. 6, pp. 596-603, 2009.

[10] T. V. Menezes, L. C. P. da Silva and V. F. da Costa, "Dynamic VAR Sources Scheduling for Improving Voltage Stability Margin," *IEEE Transactions on Power Systems*, vol. 18, no. 2, pp. 969-971, May 2003.

[11] R. D. de Moura and R. B. Prada, "Contingency screening and ranking method for voltage stability assessment," *IET Gener. Transm. Distrib*. vol. 152, no. 6, pp. 891-898, 2005.

[12] T. J. Browne, V. Vittal, G. T. Heydt and A. R. Messina, "A comparative assessment of two techniques for modal identification from power system measurements," *IEEE Transactions on Power Systems*, vol. 23, no. 3, pp. 1408-1415, August 2008.

[13] D. J. Trudnowski, J. R. Smith, T. A. Short and D. A. Pierre, "An application of prony methods in PSS design for multimachine systems," *IEEE Transactions on Power Systems*, vol. 6, no. 1, pp. 118-126, February 1991.

[14] A. A. Fouad and V. Vittal, *Power System Transient Stability Analysis using the Transient Energy Function Method*. Englewood Cliffs, NJ: Prentice-Hall, 1992.

[15] J. M. G. Alvarez and P. E. Mercado, "Online inference of the dynamic security levels of power systems using fuzzy techniques," *IEEE Transactions on Power Systems*, vol. 22, no. 2, pp. 717-726, May 2007.

[16] L. H. Tsoukalas and R. E. Uhrig, *Fuzzy and Neural Approach in Engineering.* 605 Third Avenue, New York, John Wiley & Sons, 1997.

[17] Manitoba HVDC Research Center Inc, RTDS/EMTDC *user's guide,* 244 Cree Crescent, Winnipeg, Manitoba, Canada R3J3W1.

[18] Y. Yare, G. K. Venayagamoorthy and U. O. Aliyu, "Optimal generator maintenance scheduling using a modified discrete PSO," *IET Gener. Transm. Distrib*. vol. 2, no. 1, pp. 834-846, 2008.

[19] T. K. Das, G. K. Venayagamoorthy and U. O. Aliyu, "Bio-inspired algorithms for the design of multiple optimal power system stabilizers: SPPSO and BFA," *IEEE Transactions on Industry Applications,* vol. 44, no. 5, pp. 1445-1457, September 2008.

[20] N. G. Hingorani and L. Gyugyi, *Understanding FACTS: Concepts and Technology of Flexible AC Transmission Systems.* 445 Hoes Lane, Piscataway, NJ 08855-1331, USA: IEEE Press, John Wiley & Sons Inc., 2000.

SECTION
2. CONCLUSIONS

2.1. INTRODUCTION

This section summarizes the work presented in this dissertation. It has been shown in this dissertation how to obtain a secured power system operation that has the following benefits desirable of a modern power system: secured maintenance schedules and generation dispatch, feasible maintenance schedules and dispatch for practical implementation, increased power system efficiency and reliability, optimal power system operation, efficient dynamic optimization, better power quality and reduction in transmission line losses, saving in fuel cost needed for power system operation and emission reduction.

2.2. DISSERTATION SUMMARIES

This dissertation presents six articles that have been published/submitted for journal publications as follows:

Paper I presents a modified discrete particle swarm optimization (MDPSO) algorithm for generating optimal preventive maintenance schedule of generating units for economical and reliable operation of a power system, while satisfying system load demand and crew constraints. Discrete particle swarm optimization (DPSO) is known to effectively solve large scale multi-objective optimization problems and has been widely applied in power system. Here, the MDPSO proposed for the generator maintenance scheduling (GMS) optimization problem generates optimal and feasible solutions and overcomes the limitations, of the conventional methods, such as extensive computational effort, which increases exponentially as the size of the problem increases. The efficacy of the proposed algorithm is illustrated and compared with the genetic algorithm (GA) and DPSO in two case studies – a 21-unit test system and a 49-unit system feeding the Nigerian national grid. The MDPSO algorithm is found to generate schedules with comparatively higher system reliability indices than those obtained with GA and DPSO.

In Paper II, a challenging power system problem of effectively scheduling generating units for maintenance is presented and solved. The problem of generator maintenance scheduling (GMS) is solved in order to generate optimal preventive maintenance schedules of generators that guarantee improved economic benefits and reliable operation of a power system, subject to satisfying system load demand, allowable maintenance window, and crew and resource constraints. Multiple swarms concept is incorporated into the MDPSO algorithm to form a robust multiple swarms-modified particle swarm optimization (MS-MDPSO) algorithm and is suitably applied to solve this GMS problem. The performance and effectiveness of the MS-MDPSO algorithm in solving the GMS problem is illustrated and compared with the MDPSO algorithm on two power systems, the 21-unit test system and 49-unit Nigerian hydrothermal power system. The GMS of the two power systems are considered and the results presented shows great potential for utility application in their area control centers for effective energy management, short and long term generation scheduling, system planning and operation.

The problem of static and dynamic economic dispatch are presented and solved in Paper III. Static economic dispatch (SED) problem is solved in order to economically determine output powers of generating units in such a manner that the total generation (fuel) cost is minimized while load demand and all practical operating constraints are satisfied. Dynamic economic dispatch (DED) is an enhancement of SED and has the objective of dynamically determining the optimal outputs of generating units with predicted load demand over a certain period of time. Classical optimization methods assume generator cost curves to be continuous and monotonically increasing, whereas practical generators have a variety of nonlinearities in their cost curves making this assumption inaccurate. Hence, heuristic methods are proposed in this paper to circumvent the problems of imposed non-smooth assumptions. This paper presents three heuristic methods, namely, GA, differential evolution (DE) and MPSO for solving both the SED and DED problems for three test systems. Results and convergence performances of these three heuristic methods are presented and compared as a way of validating such methods in solving SED and DED problem characterized by practical and non-smooth generator constraints.

Paper IV presents multi-objective combined economic and emission dispatch (MO-CEED) optimization problem for a wind-hydrothermal power system. This MO-CEED problem formulation becomes a challenging problem because of the presence of uncertainty in wind power (due to uncertain wind speed). Another aspect of the challenge is the integration/mixing of the wind power with the hydrothermal grid system for the purposes of economically meeting dynamic load demand while minimizing emission. The MO-CEED optimization process for this wind-hydrothermal power system while satisfying practical constraints, must also find trade-off solutions between multiple objectives (minimizing both fuel cost and emission simultaneously). A modified particle swarm optimization (MPSO) algorithm is used to solve this MO-CEED problem. Results are presented to show the benefits from integrating wind power with conventional hydrothermal power system including cost saving, emission reduction and the positive impact of capacity credit of wind power. A family of distributed optimal Pareto fronts for the MO-CEED problem has been generated for different scenarios of capacity credit of wind power. The potential for practical application of this approach in dispatch centers of wind-hydrothermal power system is demonstrated. A platform for achieving increased integration of renewable/sustainable energy is presented.

In pursuance of the smart grid initiative of delivering electricity from suppliers to consumers using intelligent technology to save energy, reduce cost, accommodate variety of generation options, increase reliability, efficiency and transparency etc, Paper V presents an optimal preventive generator maintenance scheduling (GMS) for a wind-hydrothermal power system. GMS problem is solved with the aim of maximizing economic benefits subject to satisfying system constraints. This GMS formulation becomes a stochastic problem because of the uncertainty in wind power and its incorporation into the hydrothermal power system. The objective is to perform GMS in such a manner that the annual cost saving is increased, annual generation cost is minimal and the potential for carbon dioxide (CO_2) emission reduction is enhanced, while all operating constraints are satisfied in the presence of uncertainty in wind generation. A modified discrete particle swarm optimization (MDPSO) algorithm is used to solve this GMS problem. Results are presented to show the benefits accruable from integrating wind power into conventional hydrothermal power system even for the purpose of GMS and the positive impact of increasing wind penetration.

Paper VI presents the real-time (RT) stability assessment (SA) of a power system. The real-time (RT) stability assessment (SA) is to determine a power system’s ability to continue to provide service (electric energy) in a RT manner in case of an unforeseen catastrophic contingency. Credible contingencies are analyzed using non real-time (NRT) and RT stability assessment indices (SAIs). Cascading stages of fuzzy inference system is applied to combine the different NRT and RT SAIs to determine the network status. The network status reflects the effect that each credible contingency has on the system and the distance to stability/security limit. In this paper, a practical Nigerian power system modeled on the real-time digital simulator (RTDS) platform is used as case study to implement and simulate in RT generator maintenance scheduling (GMS). GMS reflects power generation loss due to scheduled shutdown maintenance. Under the implementation of the GMS, the system is subject to load shedding, three-phase short circuit fault on the tie-line and permanent transmission line outage (*N-1* contingency and topology change). Results show that the network status has potential for use by system operators to take preventive real-time decisions.

2.3. MAIN CONCLUSION

The following are main conclusions of this dissertation:

- Developed modified particle swarm optimization (MDPSO) algorithm to achieve fast convergence and better quality solutions.
- Developed multiple-swarms MDPSO framework to achieve faster convergence and better quality solutions.
- Illustrated and applied the MDPSO to solve the reliability based GMS optimization problem of a practical hydrothermal power system.
- Illustrated and applied the multiple-swarms MDPSO framework to solve the reliability based GMS optimization problem of a hydrothermal power system.
- Illustrated the smooth and nonsmooth economic cost function formulation of the GMS optimization problem with practical generator constraints using both the classical and heuristic methods.
- Demonstrated and applied heuristic methods, namely, GA, DE and MDPSO to solve the static and dynamic ED for generators with smooth and nonsmooth economic cost functions with practical constraints and transmission line losses.
- Incorporated additional practical generator constraints such as the generator

prohibited zones and ramp-rate limits, system power loss and increased the dimensionality of the problem in solving the ED problem.

- Formulated stochastic MO-CEED optimization problem for a wind-hydrothermal power system [11]. Uncertainty in wind power was incorporated in this formulation.
- Solved the stochastic MO-CEED problem for wind-hydrothermal power system using a family of optimal Pareto fronts.
- Presented platforms for which optimized energy and generation cost management in the presence of wind energy penetration is made possible.
- Quantified emission reductions as a consequence of increased capacity credit of wind power during GMS, as well as after solving the MO-CEED.
- Demonstrated the potential for increased daily cost saving and emission reduction for a practical Nigerian power system.
- Formulated the network status index for a power system and implemented in real time platform.
- Demonstrated on the Nigerian hydrothermal power system for *N-1*, *N-2*, ..., *N-k* generator outages and *N-1* permanent transmission line outage (topology change).

2.4. FUTURE RESEARCH

The proposed optimization algorithms can be flexibly modified to accommodate the maintenance unit requirements of emerging independent power producers and future generation additions as well as network constraints not considered in this dissertation.

Future research can investigate if results from re-coding purely real-valued GA and DE have comparable performances with the real-coded MPSO algorithm (especially in their computation times, ability to satisfy all constraints and quality of solutions) on similar test systems. Also, dynamic economic dispatch for a conventional power system integrating wind power is another area for future work.

Limitations are not imposed on the number of trade-off objectives that can be optimized in the MO-CEED optimization problem, hence further work could flexibly incorporate more objectives (such as stability, security or system losses etc).

Future research can incorporate short-term planning schemes such as unit commitment and economic dispatch on smaller time-frames (minutes to hours) into the long-term power system optimization problem, such as the GMS. This multi-period (short and long-term) generation scheduling problem for wind-hydrothermal power system can be looked into in future work. Also, to re-optimize the maintenance schedules in an event of forced generator outage during a normal preventive maintenance, a dynamic optimization technique such as adaptive dynamic programming can be used in future research to automatically generate optimal GMS.

Real-time phasor measurement unit (PMU) data deployment in the power system network and the introduction of the flexible integrated phasor system (FIPS) technology in the future will provide a robust on-line platform for easy implementation of the RT-SA of a power system presented in this dissertation, which enhances smart grid development.

VITA

Yusuf Yare was born in Akwanga, Nasarawa State, Nigeria. In May 1994, he received his B.Eng. with honors in Electrical and Electronics Engineering from Abubakar Tafawa Balewa University Bauchi, Nigeria. He had one year training as Electrical/Production Engineer at the Shell Petroleum Development Company (SPDC) of Nigeria Ltd, Western Division from May 1994 to June 1995. In September 1997, he received his M.Eng. degree in Electronics Engineering from Abubakar Tafawa Balewa University Bauchi, Nigeria, where he also had teaching experience until March 1998. In March 1998, he joined Nigeria's National Electric power Authority (NEPA) as Assistant Manager (Technical Division) and later became Senior Manager (Operations and Maintenance) after working with NEPA for nearly ten years. He did his summer training (as a Ph.D. graduate student) at ABB Corporate Research Center, Vasteras, Sweden during the summer of 2007. In December 2010, he received his Ph.D. in Electrical Engineering from the Missouri University of Science and Technology, Rolla, Missouri, USA.

He has published conference and journal papers, some of which are listed with the references of this research. He has contributed to a book chapter. He has participated in several international Institute of Electrical and Electronics Engineers (IEEE) Power and Energy Society (PES) student poster contests and presented papers at international conferences. He served as peer reviewer of IEEE Transactions on Smart grid, European Transactions on Electrical Power, IEEE PES conference and IEEE Swarm intelligence Symposium (SIS) conference all in the USA. He was a grant recipient of the prestigious IEEE Computational Intelligence Society (CIS) Walter Karplus Summer Research Award in 2007, and was a recipient of SPDC Nigeria Ltd University Award.

Yusuf Yare has been a member of IEEE, The Institution of Engineering and Technology (IET), IEEE PES, IEEE CIS, the Council for the Regulation of Engineering in Nigeria (COREN), Nigerian Society of Engineer (NSE) and the Nigerian Institute of Management (NIM).